Mechanisms of anthracycline-induced dysfunction of Ca^{2+} handling proteins in the heart

by

Amy Dianne Hanna
BSc (Hons)

A thesis submitted for the degree of Doctor of Philosophy
of The Australian National University

September 2013

The John Curtin School of Medical Research
The Australian National University
Canberra
Australia

Australian
National
University

Statement

This thesis describes research conducted with the Cardiac and Skeletal Muscle Proteomics Group, Department of Molecular Bioscience, The John Curtin School of Medical Research, The Australian National University, Canberra, Australia between September 2009 and August 2013. The research conducted in this PhD was supported by grants from the National Health and Medical Research Council, an Australian Postgraduate Award and a John Curtin School of Medical Research supplementary scholarship.

The results and analyses presented in this thesis are my own original work, conducted under the supervision of Assistant Professor Nicole Beard and Professor Angela Dulhunty, except where otherwise acknowledged.

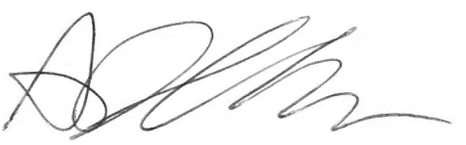

Amy Hanna

Cardiac and Skeletal Muscle Proteomics Group

Department of Molecular Bioscience

John Curtin School of Medical Research

The Australian National University

Acknowledgements

Completing this PhD has been extremely rewarding but also challenging and I could not have completed it without the immense support of my supervisors. I would firstly like to thank the Chair of my supervisory panel, Assistant Professor Nicole Beard who has and will continue to be a great role model to me through her hard work, dedication and high scientific standards. Nikki's guidance and encouragement in all aspects of my training have been essential in the completion of this project and in helping me reach my full potential. I would also like to extend my deepest thanks to my co-supervisor Professor Angela Dulhunty. Angela has been a wonderful teacher, always encouraging me to expand my knowledge and understanding of my subject area and beyond. Her expertise has been immeasurable and I am extremely grateful for the time she has spent helping me become a more independent researcher. Together Nikki and Angela have provided me with invaluable training as a scientist and I could not have asked for a better pair of supervisors. I am very proud to say that you are my mentors and will always value my time spent with you both.

I would like to thank my advisor, Dr Len Arnolda who has provided valuable guidance on the use of anthracyclines in clinical practise. I am also grateful to Dr Louise Tierney for serving as advisor during the early stages of my PhD. Our conversations discussing experimental design, data analysis and science in general were much appreciated.

This project would have been a lot more difficult without the technical support I have received from the following people: Suzy Pace and Joan Stivala, who have provided me with general support in the lab, in addition to countless tubes of SR vesicles and lipids over the years. Thanks also for helping me to extend my knowledge of opera, ancient history and classical music; Prof Esther Gallant whose single channel expertise has been invaluable. I am very grateful to Esther for providing me with drawers and shelves full of perfusion tubing, dissection tools and electrophysiology equipment. Your help and access to this equipment made it much easier to put together the Langendorff apparatus; Alex Lam, whose proficiency with single channel experiments was a great help in completing the luminal Ca^{2+} response project; Finally, Dr Peter Milburn in the Biomolecular Resource Facility whose technical expertise helped establish the thiol probe assay.

I would like to extent my gratitude to those who helped me with different aspects of the cardiomyocyte isolation protocol. Thank you to Dr Yi Zhang at Canberra Hospital who trained me in the dissection and cannulation procedures. I am very grateful to Dr Victoria Benson at Sydney University for giving advice on the working myocyte isolation protocol. Vicky's assistance has been very much appreciated and was instrumental in allowing us to set up this technique in our lab. I would like to sincerely thank Cathy Gillespie in the Microscopy and Cytometry Resource Facility who has been a wonderful help in training with the confocal microscope. Cathy's expertise and help with troubleshooting has been a great assistance in establishing Ca^{2+} imaging protocols and with getting equipment designed for these experiments. Finally, thank you to Stephen Holgate and all at the Research School of Physics and Engineering who helped with the design and construction of the myocyte stimulation chamber.

I would like to sincerely thank all past and present members of the Muscle Research Group for your support and friendship over the years. The long hours in the lab were made a lot more bearable having you all around. I'm grateful to everyone who has provided me with support over the years, whether that was by giving advice, helping out with a problem in the lab or by providing me with food and coffee. Thanks especially to my officemate, Hermia Willemse – your IT expertise was greatly appreciated in the final stages of thesis preparation!

Finally I would like to extend my utmost gratitude to my family, who I miss every day. First and foremost thanks must go to Mum and Dad - I could never express how grateful I am to my parents for their love and support and for being such fantastic role models to me. A huge thankyou to my siblings, James, Paul and Michelle and Kate and Charles and to my amazing nieces and nephews, Lavina, Luca, Lachlan and Mirna. They're always the first people I ring for advice, or when experiments have gone badly and I need cheering up. I know I can always count on them and feel very lucky to have them in my life. Thanks also to the many uncles, aunts and cousins who have called or visited me in Canberra during the last five years, and especially to those who have had me stay with them during my many trips to Sydney. Also, thanks to Paul, Michelle and Christine for being my fitness gurus over the last few years. Finally, a very sincere thankyou to my Canberra family - Doug, Susan and Jonathan Riding. The move to Canberra would have been so much harder without your friendship and I will always be grateful for your kindness, support and generosity.

Abstract

Anthracyclines, such as doxorubicin and daunorubicin, are powerful chemotherapy agents, whose use is limited due to the onset of potentially fatal cardiotoxic side effects. This cardiotoxicity is complex, manifesting as arrhythmogenesis and heart failure. Several proteins important in intracellular Ca^{2+} signalling have been identified as drug binding targets, including the cardiac ryanodine receptor Ca^{2+} release channel (RyR2), the Ca^{2+} binding protein calsequestrin (CSQ2) and the Sarco/Endoplasmic Reticulum Ca-ATPase (SERCA2A). The drug metabolites are believed to be important in the devastating cardiac effects of these drugs but their actions have been poorly characterized. Previous work showed that the anthracycline daunorubicin modulates RyR2 and that its effects were attributable to ligand binding and thiol oxidation.

The functional effect of doxorubicin and its metabolite, doxorubicinol on RyR2 was assessed by adding clinically relevant drug concentrations to single RyR2 channels in lipid bilayers. Both drugs caused biphasic modulation of RyR2 activity where there was an early increase in channel activity followed by an inhibitory phase which persisted for the lifetime of the experiment. RyR2 channel activation, but not inhibition, could be reversed by drug washout, typical of a ligand binding effect. This was supported by affinity chromatography experiments showing that doxorubicin and doxorubicinol bind to RyR2. Conversely, the irreversible nature of the inhibitory effect suggested a non-ligand binding effect. Treatment with doxorubicin/doxorubicinol reduced the number of thiols on RyR2, indicative of a drug-induced thiol-modification such as oxidation. Together, these results support the earlier hypothesis that initial activation of RyR2 by anthracyclines is due to ligand binding, while the inhibitory effect is due to direct thiol-oxidation.

In addition to modulating RyR2, doxorubicinol was found to alter other aspects of SR Ca^{2+} handling. For the first time, the effect of doxorubicinol on the luminal Ca^{2+} sensitivity of single RyR2 channels has been assessed. Doxorubicinol abolished the response of RyR2 to changes in luminal Ca^{2+}. Additional experiments revealed that the abolition of luminal Ca^{2+} sensing was due to an interaction between doxorubicinol and CSQ2. Furthermore, in intact SR vesicles, a decrease in the Ca^{2+} uptake rate showed that doxorubicinol inhibits the function of SERCA2A. This effect could be prevented by pre-treatment with the thiol protective agent dithiothreitol, indicating that

doxorubicinol's inhibition of SERCA2A was due to thiol oxidation. Hence doxorubicinol causes substantial dysfunction of SR Ca^{2+} handling proteins, affecting both Ca^{2+} release and Ca^{2+} uptake pathways.

To determine the effects of doxorubicinol in an intact cell, cardiomyocytes were isolated from adult mouse hearts and loaded with the Ca^{2+} indicator Fluo-4 AM. Pre-treatment with doxorubicinol reduced cytoplasmic Ca^{2+} transients, depleted SR load and inhibited SERCA2A and the Na^{+}- Ca^{2+} exchanger. Furthermore, doxorubicinol-treated myocytes exhibited more spontaneous Ca^{2+} release events and had a higher resting Ca^{2+} concentration. These effects resulted in an overall impairment in contractile function.

This project provides novel insight into the cellular mechanisms of anthracyclines and is the most thorough characterization of the effects of these drugs on cardiomyocyte Ca^{2+} handling to date. The results suggest that by targeting multiple Ca^{2+} handling proteins, anthracyclines severely disturb cardiomyocyte Ca^{2+} homeostasis and that these effects may have an important role in the onset of anthracycline-mediated arrhythmia and heart failure.

Publications

Dulhunty AF, Beard NA, **Hanna AD**. Regulation and dysregulation of cardiac ryanodine receptor (RyR2) open probability during diastole in health and disease. *Journal of General Physiology* 2012 Aug;140(2):87-92.

Dulhunty AF, Wium E, Li L, **Hanna AD**, Mirza S, Talukder S, Ghazali NAA, Beard NA. Factors inside the intracellular calcium store determine cardiac RyR channel activity and cardiac output. *Clinical and Experimental Pharmacology and Physiology*, May;39(5):477-84

Hanna AD, Janczura M, Cho E, Dulhunty AF, Beard NA (2011) Multiple actions of the anthracycline daunorubicin on cardiac ryanodine receptors. *Molecular Pharmacology* 11 Sep;80(3):538-49

Wei L, **Hanna AD**, Beard NA & Dulhunty AF (2009). Unique isoform-specific properties of calsequestrin in the heart and skeletal muscle. *Cell Calcium* May;45(5)474-84

Selected Conference Abstracts

Australian Society for Medical Research
Hanna, A.D., Lam, A., Dulhunty, A.F., Beard, N.A.
Anthracycline-induced dysfunction of cardiac SR Ca^{2+} handling: a potential pathway to anthracycline-induced cardiotoxicity. Sydney, Australia, 12/2012, Oral Presentation

Australian Physiological Society
Hanna, A.D., Lam, A., Dulhunty, A.F., Beard, N.A.
Anthracycline-induced dysfunction of cardiac SR Ca^{2+} handling: a potential pathway to anthracycline-induced cardiotoxicity. Sydney, Australia, 12/2012, Oral Presentation

Gordon Research Conference on Muscle Excitation-Contraction Coupling
Hanna, A.D., Janczura M, Dulhunty, A.F., and Beard N.A.
Anthracycline-induced dysfunction of cardiac SR Ca^{2+} handling: a potential pathway to anthracycline-induced cardiotoxicity
Les Diablerets, Switzerland, 06/2012. Poster presentation

Gage Muscle Conference
Hanna, A.D., Dulhunty, A.F. and Beard, N.A.
Anthracycline-induced dysfunction of cardiac SR Ca^{2+} handling: a potential pathway to anthracycline-induced cardiotoxicity
Canberra, Australia 04/2012. Oral presentation

Gage Conference on Ion Channels and Transporters,
Hanna, A.D., Dulhunty, A.F. and Beard, N.A.
Multiple effects of the anthracycline daunorubicin on cardiac ryanodine receptors",
Canberra, Australia 04/2011. Poster presentation

Joint meeting: Australian Society for Biophysics and the Australian Physiological Society
Hanna, A.D., Dulhunty, A.F. and Beard, N.A.
Multiple effects of the anthracycline daunorubicin on cardiac ryanodine receptors
Adelaide, Australia, 11/2010. Poster presentation

Gage Muscle Conference
Hanna A.D., Dulhunty, A.F. and Beard, N.A.
Multiple effects of the anthracycline daunorubicin on cardiac ryanodine receptors
Canberra, Australia, 04/2010. Poster presentation

Abbreviations

4,4'-DTDP	4,4'-dithiodipyridine
ATP	Adenosine-5'-triphosphate
BAPTA	1,2-bis(2-aminophenoxy)ethane-N,N,N,N-tetraacetic acid
BDM	2,3-butanedione monoxime
$CaCl_2$	Calcium chloride
CaM	Calmodulin
CaMKII	Calcium/calmodulin-dependent protein kinase II
CICR	Calcium-induced Calcium Release
CNBr	Cyanogen-bromide
CPVT	catecholaminergic polymorphic ventricular tachycardia
CsCl	Caesium chloride
CsMS	Caesium methane sulfonate
CSQ	Calsequestrin
DAD	Delayed afterdepolarization
daunOL	daunorubicinol
DHPR	Dihydropyridine Receptor
DoxOL	doxorubicinol
DTT	dithiothreitol
EADs	early afterdepolarizations
EC coupling	Excitation-contraction coupling
EDTA	Ethylenediaminetetraacetic acid
EGTA	ethylene glycol tetraacetic acid
FKBP	FK506 binding protein
F_o	Open Frequency
GSH	Glutathione
GSSG	Glutathione disulphide

H_2O_2	Hydrogen peroxide
HEPES	2-[4-(2-hydroxyethyl)piperazin-1-yl]ethanesulfonic acid
IP_3R	Inositol 1,4,5-triphosphate receptors
KCl	Potassium chloride
LTCC	L-type Ca^{2+} Channel
mRNA	Messenger RNA
NCX	Sodium-calcium exchangers
NEM	*N*-ethyl maleimide
NO	Nitric oxide
NOS	Nitric oxide synthase
O_2^-	Superoxide anion
$ONOO^-$	Peroxynitrate anion
PBS	Phosphate buffered saline
PKA	Protein kinase A
P_o	Open probability
P_o	Open probability
RNS	Reactive nitrogen species
ROS	Reactive oxygen species
RyR	Ryanodine receptor
SDS-PAGE	Sodium dodecyl sulfate polyacrylamide gel electrophoresis
SERCA	Sarcoplasmic/endoplasmic reticulum Ca^{2+}-ATPase
Sinoatrial node	SA node
SR	Sarcoplasmic reticulum
T_c	Mean closed time
TCEP	tris-(2-carboxyethyl)phosphine
TES	2-[[1,3-dihydroxy-2-(hydroxymethyl)propan-2-yl]amino]ethanesulfonic acid
T_o	Mean open time

Table of Contents

Chapter One

Introduction

1.1 Muscle function

There are 3 types of muscle, including skeletal, cardiac and smooth, which together make up approximately 50% of the body's total mass. The muscular system performs four core functions including 1) skeletal movement, 2) maintenance of posture and joint stabilization, 3) storage and movement of substances through the body and 4) heat generation. The ability of muscle tissue to perform these functions relies on several innate characteristics including excitability, contractility, extensibility and elasticity. Although all three muscle types share these core characteristics, they differ in their location, anatomy and in their control by the nervous and endocrine systems. Some of the defining characteristics and specific functions of the three muscle types are as follows:

Cardiac muscle: Cardiac muscle is striated and is located in the heart. The purpose of cardiac muscle is to allow the heart to effectively function as a pump, distributing oxygen-enriched blood to the systemic circulation. Cardiac muscle is not under voluntary control but rather contains a subset of specialized fibres that are autorhythmic and facilitate the rapid spread of excitation through the heart. This process can be influenced by neural and endocrine factors.

Skeletal Muscle: Like cardiac muscle, skeletal muscle is striated. It is primarily found attached to the bones of the skeleton, functioning in body movement, posture and joint stabilization. Skeletal muscle is voluntarily controlled via the somatic nervous system, though some fibres, for example those involved in posture and joint stabilization, are under subconscious control.

Smooth Muscle: Smooth muscle lacks striations. It is found in the lining of hollow organs and other structures like blood vessels and respiratory airways. Like cardiac muscle, smooth muscle is autorhythmic and is not under voluntary control. Smooth muscle is also regulated by various neural and endocrine factors.

The primary focus of this thesis will be cardiac muscle, although some aspects of skeletal muscle physiology, mainly at the cellular level, will be discussed occasionally.

1.2 Cardiac anatomy

The heart is located in the thoracic cavity (Figure 1.1A), enclosed within a double walled sac called the pericardium. The outer layer of the pericardium is the fibrous pericardium, a layer of dense connective tissue which anchors the heart in place, limiting its range of motion and preventing the heart from over filling. The inner layer, or serous pericardium, is itself composed of two layers, between which lies the pericardial cavity. The inner layer of the serous pericardium is continuous with the epicardium, which is the most superficial layer of the heart itself. Both the epicardium and endocardium, the inner most layer of the heart, are primarily composed of connective tissue. Sandwiched between them is the myocardium which constitutes the bulk of the heart and is the layer that actually contracts and relaxes during the heartbeat (Figure 1.1B). The myocardium is extensively vascularized by the coronary circulation, which provides the heart with the persistent blood supply it requires to function (Katz, 2006). The physiology and function of the contractile muscle that makes up the central myocardial layer of the heart is the subject of this thesis.

1.3 Cardiac physiology

1.3.1 The intrinsic cardiac conduction system

The anatomy of cardiac muscle favours rapid intercellular communication. Individual fibres are connected in series and in parallel by intercalated discs which provide a mechanical linkage between the cells. Gap junctions facilitate electrical coupling between cells by providing a low-resistance passage for ions. Electrical coupling allows the cells of a chamber to act as a syncytium, ensuring an entire chamber will contract at once rather than pockets of cells within a chamber responding at difference time points. This synchronicity is a vital aspect of cardiac function.

While the gap junctions permit coordinated contraction of the chambers, the sequence of contraction and the actual generation of excitation are attributable to the specialized fibres of the cardiac conduction system (Figure 1.2A). The action potential originates in the autoryhythmic cells of the sinoatrial node (SA node). These cells are termed autorhythmic because they are self-excitable, not requiring any external stimulus to undergo depolarization.

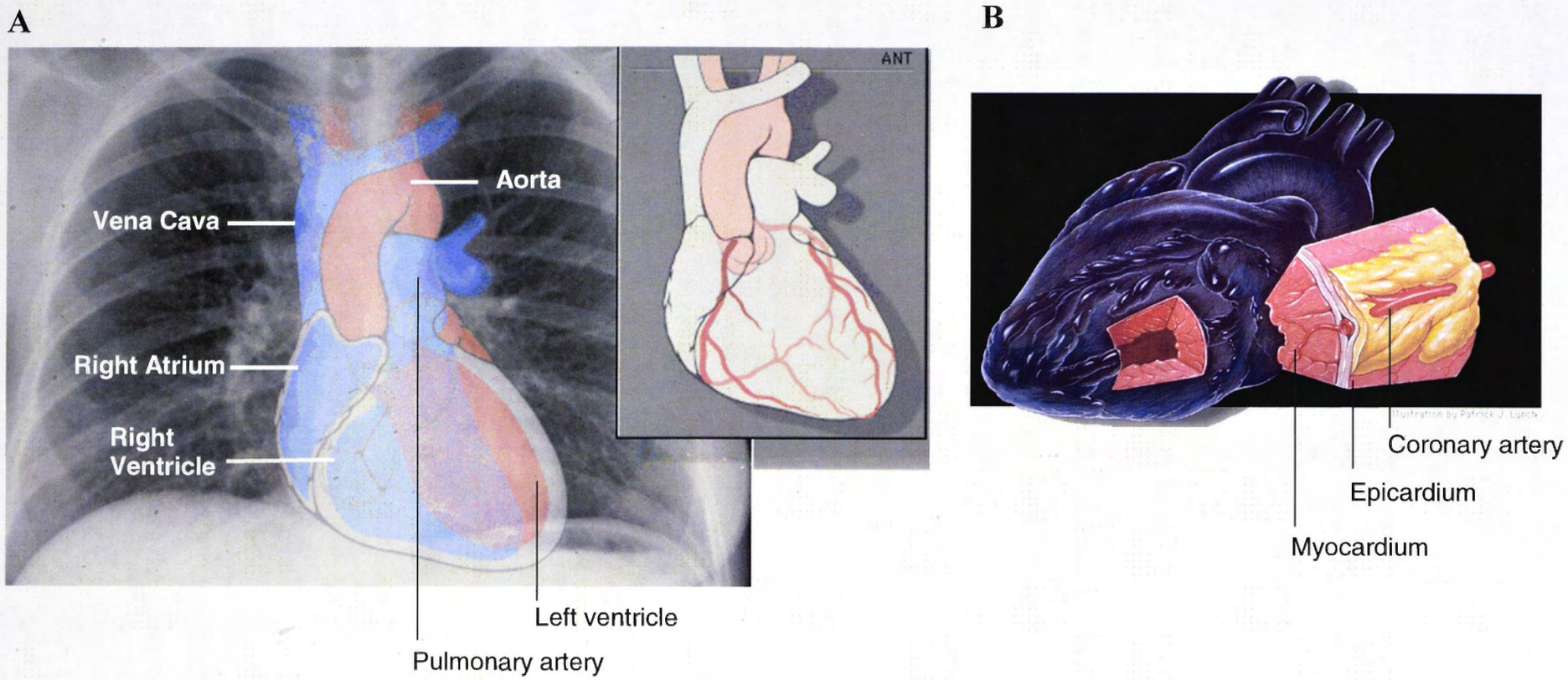

Figure 1.1 – Cardiac anatomy. **(A)** An x-ray showing the position of the heart in the thoracic cavity. Inset shows the position of the major coronary arteries. Vessels shaded red carry oxygenated blood, those carrying deoxygenated blood are shaded blue. **(B)** Schematic of layers of heart wall showing a coronary artery embedded in the epicardium. The myocardium constitutes the bulk of the heart wall and is extensively vascularized. Endocardium lines the chamber but is not distinct in this image. For simplicity only major features are depicted here. For full details see (Lynch and Jaffe, 2006).

While such cells exist in other regions of the heart, including the atrioventricular node (AV node), the SA node has the fastest rate of depolarization and therefore sets the frequency of excitation in the heart, or heart rate (Bers, 2001). The ionic currents contributing to SA node activity and other cardiac action potentials will be discussed in more detail in Section 1.3.3. From the SA node the depolarization travels throughout the atria before reaching the AV node. Due to the slower conduction speed of the AV node there is a brief pause here before the signal moves rapidly through the AV bundle, the right and left bundle branches and finally the Purkinje fibres from where it propagates through the ventricular contractile fibres causing contraction of the ventricles (Figure 1.2A).

1.3.2 Blood flow through the heart

The sequence of excitation set by the cardiac conduction system (Section 1.3.1) means that in a normal heart, immediately following SA node depolarization the atria are stimulated, followed rapidly by ventricular stimulation (Figure 1.2B). Atrial stimulation causes the two atria to contract, ejecting blood into the ventricles. The pause in signal conduction at the AV node, reportedly about 0.16 s, allows the atria to finish contracting before ventricular contraction is initiated (Hall, 2010). This is important since early ventricular stimulation would cause contraction of the ventricles before they are fully refilled. Coordinated ventricular contraction causes 1) from the right ventricle, deoxygenated blood to travel to the pulmonary circulation to be oxygenated and unload carbon dioxide and 2) from the left ventricle, oxygenated blood to travel through the systemic circulation where it delivers oxygen and collects carbon dioxide from all the tissues of the body. In essence then, the heart is actually composed of both an atrial syncytium and a ventricular syncytium. For the heart to effectively supply blood to the entire circulation it is essential that this coordinated and synchronous contraction is maintained. Abnormalities in the electrical signalling pathway can alter the rhythm and synchronicity of the heart, with severe consequences for cardiac function.

1.3.1 Cardiac action potentials

Cardiac action potentials result from the complex gating of many different types and subtypes of ion channels, principally involving the movement of Na^+, Ca^{2+} and K^+ ions across the sarcolemmal.

Figure 1.2 – Cardiac physiology (**A**) Cardiac conduction system. (1) The action potential originates in the sinoatrial node and propagates along the atrial muscle fibres, before arriving at the atrioventricular node (2). Here there is a brief pause, delaying signal conduction through the ventricles. From the AV node the signal moves through the atrioventricular bundle (3), along the right and left bundle branches (4) and finally the Purkinje fibres (5) before propagating along ventricular muscle fibres (Germann and Stanfield, 2004). **(B)** Blood flow in the cardiac cycle (i) Diastole – chambers are relaxed, deoxygenated blood returning from the body via the vena cava enters the right atrium. Oxygenated blood from the lungs enters the left atrium via the pulmonary veins. (ii) In systole, the atria contract first forcing the blood from the atria into the ventricles. (iii) Ventricles contract pumping blood through the pulmonary and systemic circulations via the pulmonary artery and aorta, respectively (OpenStax College).

A

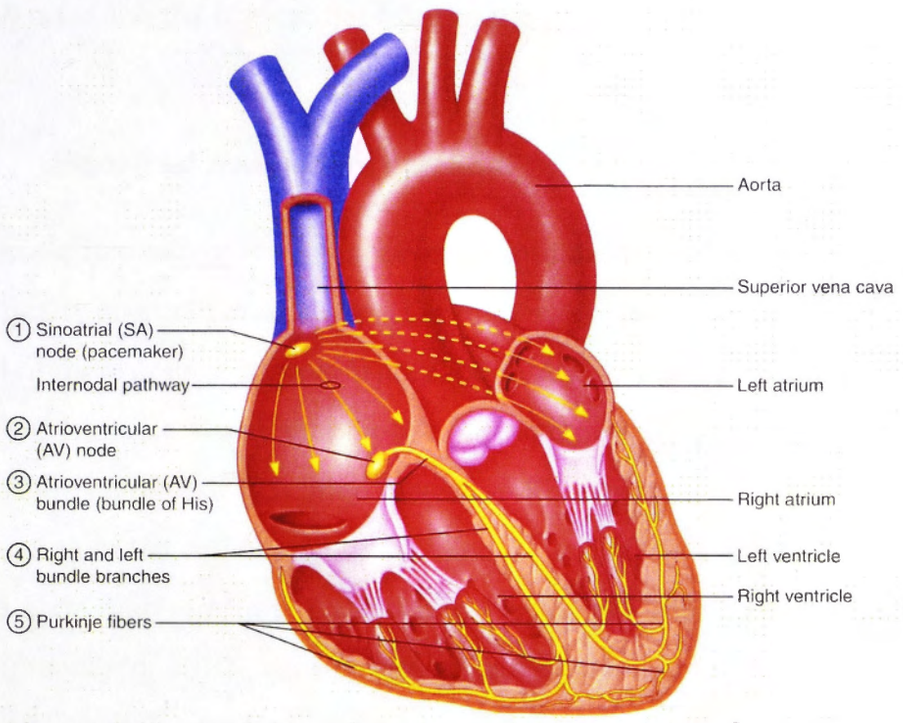
Aorta
Superior vena cava
1 Sinoatrial (SA) node (pacemaker)
Internodal pathway
Left atrium
2 Atrioventricular (AV) node
3 Atrioventricular (AV) bundle (bundle of His)
Right atrium
4 Right and left bundle branches
Left ventricle
Right ventricle
5 Purkinje fibers

B

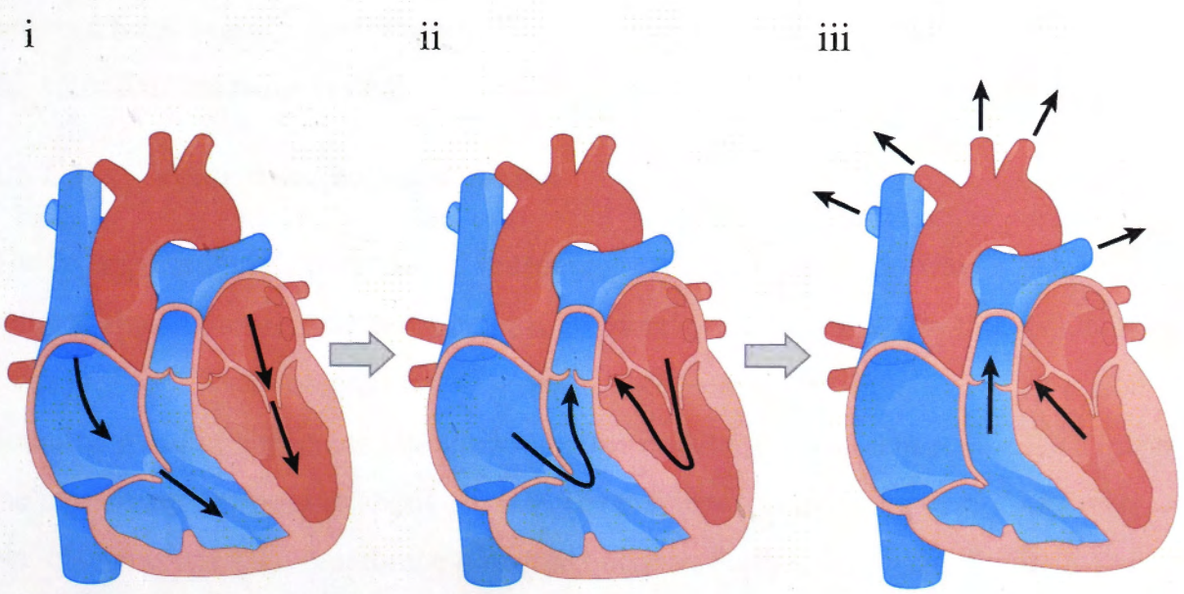
i
ii
iii

Any discussion of cardiac action potentials is complicated by the fact that the waveform of the action potential varies substantially, depending on the region of the heart being discussed (Figure 1.3). For simplicity, in this thesis only the action potential waveforms of the SA node and the myocardial layer of the ventricular muscle tissue will be discussed.

1.3.1.1 Sinoatrial node action potential

The principle function of the SA node is the initiation of the action potential, hence it has practically no contractile ability (DiFrancesco, 2010). The resting membrane potential of these cells is approximately -60 mV. However, unlike non-autorhythmic fibres of the heart (in ventricular muscle for example), SA node cells do not have a stable, resting membrane potential. Instead, following repolarization there is gradual depolarization of the cell caused by Na^+ and K^+ influx via a "funny" current (I_f). I_f is activated upon repolarization of the cell (reviewed in Hille, 2001; Baruscotti et al., 2010; DiFrancesco, 2010), causing slow depolarization until threshold is reached for the opening of firstly, T-type Ca^{2+} channels and secondly, L-type Ca^{2+} channels (LTCC). Upon activation of LTCC, the threshold for action potential generation is reached with a large influx of Ca^{2+} (phase 0) (Figure 1.3). Repolarization occurs when outward K^+ channels open and there is inactivation or reduced permeability of LTCC and I_f (Katz, 2006). Because the length of I_f sets the duration between action potentials, and therefore between heart beats, it is also referred to as the pacemaker current and it is regulated by the autonomic nervous system.

1.3.1.2 Ventricular action potential

The resting membrane potential of ventricular myocytes is more negative than SA node cells, at approximately -90 mV, due to K^+ channels being open at this time (-90mV is close to the reversal potential for K^+) (phase 4) (Figure 1.3B). Initiation of an action potential requires sufficient depolarization, most likely from an adjacent cell, to increase the membrane potential to about -70 mV, the threshold for opening of Na^+ channels. As Na^+ channels open the membrane potential becomes further depolarized, which activates more Na^+ channels in a positive feedback mechanism. At the same time, K^+ channels are shut off. Together, these effects cause the rapid upstroke of phase 0 of the ventricular action potential.

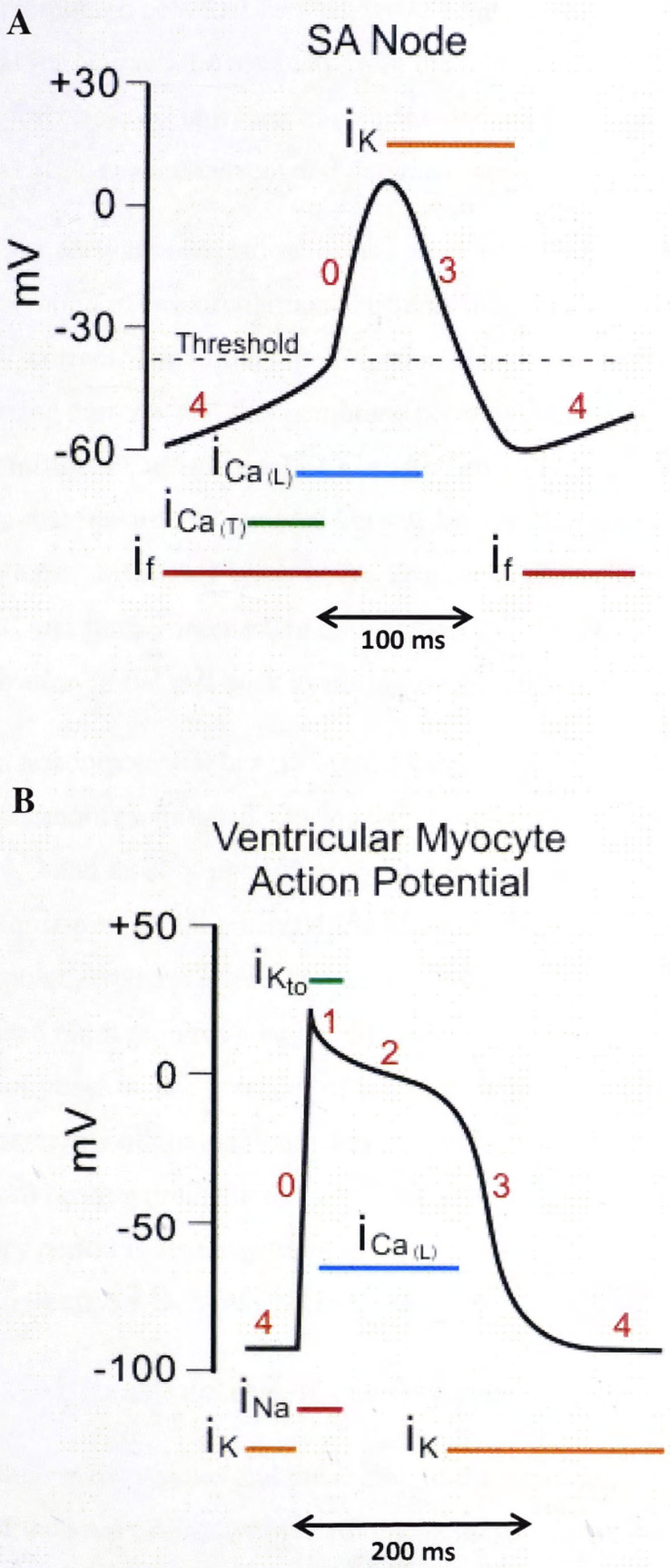

Figure 1.3 – Cardiac action potential waveforms. The contribution of major ion currents to the change in membrane potential (y-axis, mV) as a function of time is shown for a typical action potential in the (**A**) sinoatrial node and (**B**) ventricular myocytes. Time values are from (Katz, 2006). Images from (Klabunde, 2011).

As the membrane potential depolarizes to positive values, it approaches the reversal potential for Na^+ and moves away from the reversal potential for K^+, reducing the driving force for Na^+ entry and increasing the driving force for K^+ efflux. At the action potential peak, inward current and outward current are equal (Bers, 2001).

Phase 1, or early repolarization, occurs as more Na^+ channels are shut and there is a brief activation of two repolarising currents including a transient outward K^+ current and a Cl^- current. The initial repolarization phase ends with the inactivation of these repolarizing currents and the membrane potential plateaus (phase 2). During this time there is influx of Ca^{2+} via the LTCC and efflux of K^+ via delayed rectifier channels meaning that inward and outward current are approximately equal, causing the plateau in membrane potential (Figure 1.3B). Late repolarization occurs as there is deactivation of LTCC and further increase in outward current via the K^+ channels causing repolarization of the cell back to resting membrane potential.

Once an action potential has occurred there is a refractory period in which a new action potential cannot be initiated. During the absolute refractory period, which includes phases 1, 2 and most of phase 3 of the action potential, no stimulus of any magnitude is able to initiate an action potential. As phase 3 progresses and the membrane potential is more repolarized there is a relative refractory period. At this time an action potential can be initiated but it requires a larger stimulus to reach threshold then what is required at the end of phase 4. The presence of such a long refractory period, that exists for almost the entire period of contraction is likely to be a protective mechanism, preventing the heart from beating prematurely before the chambers have finished refilling. The refractory period is also important in preventing the propagation of aberrant electrical signals (re-entry) which may be arrhythmogenic.

1.4 Ultrastructure of cardiac muscle fibres

Depending on the species and the region of the heart, approximately 45-60 % (Bers, 2001) of the total cardiomyocyte volume consists of myofilaments, the contractile machinery of the cell. These proteins, including myosin (thick filaments) and actin (thin filaments) are what give skeletal and cardiac muscle their striated appearance. Filaments are arranged within a sarcomere, the functional contractile unit of striated muscle (Figure 1.4). A sarcomere extends the distance between two Z-discs, with the different shading within a sarcomere reflecting the arrangement of thin and thick filaments (Katz,

2006). The darker area is the anisotropic (A) band and corresponds to the length of the thick filaments. Within the A-band there are areas where the thick filament overlaps with the thin filaments, and a central area (H-zone) where there is no overlap (Figure 1.4B). The outer, lighter coloured area is the isotropic (I) band which is composed only of thin filaments (Jenkins et al., 2006). The M-line at the centre of each sarcomere contains various supporting proteins which connect neighbouring thick filaments. The structural protein titin, extends through the thick filament, from the M-line to the Z-line (Bers, 2001; Katz, 2006).

The next largest component of cardiomyocytes is mitochondria which occupy about 35% of the total cell volume (Bers, 2001; Katz, 2006), reflecting the fact that cardiac muscle relies almost exclusively on aerobic metabolism for its energy demands. Another prominent feature of the cardiomyocyte is the sarcoplasmic reticulum (SR). The SR is a muscle specific, Ca^{2+} storage organelle. This membrane bound compartment comes in close contact to, but is not continuous with, the surface and t-tubular membranes. The region of the SR which forms junctions with the t-tubule or, to a lesser extent, the sarcolemmal membrane is the junctional SR with the remainder mainly existing as extended or corbular SR (Jorgensen et al., 1993).

1.4.1 Mechanism of force generation in EC coupling

First described in 1954 (Huxley and Niedergerke, 1954; Huxley and Hanson, 1954) the sliding filament theory proposes that muscle tension is created when there is an increase in the overlap between thick and thin filaments, causing the sarcomeres to draw closer together and leading to cell shortening, or contraction. During this process the physical length of the filaments does not change, only the overlap between the two. This is facilitated by crossbridge formation between myosin and actin. During relaxation, the binding site on actin for myosin heads is obscured by the tropomyosin protein, which itself is bound to a complex of 3 troponin proteins (Katz, 2006). Ca^{2+} released from the SR, binds to troponin, altering its interaction with tropomyosin. This shifts tropomyosin from its site on actin, allowing myosin heads to access binding sites on actin. The interaction of actin and myosin permits crossbridge cycling, where the myosin heads rotate and pull the actin protein toward the M-line, causing the sarcomere to shorten (Figure 1.4B) (Huxley, 2004).

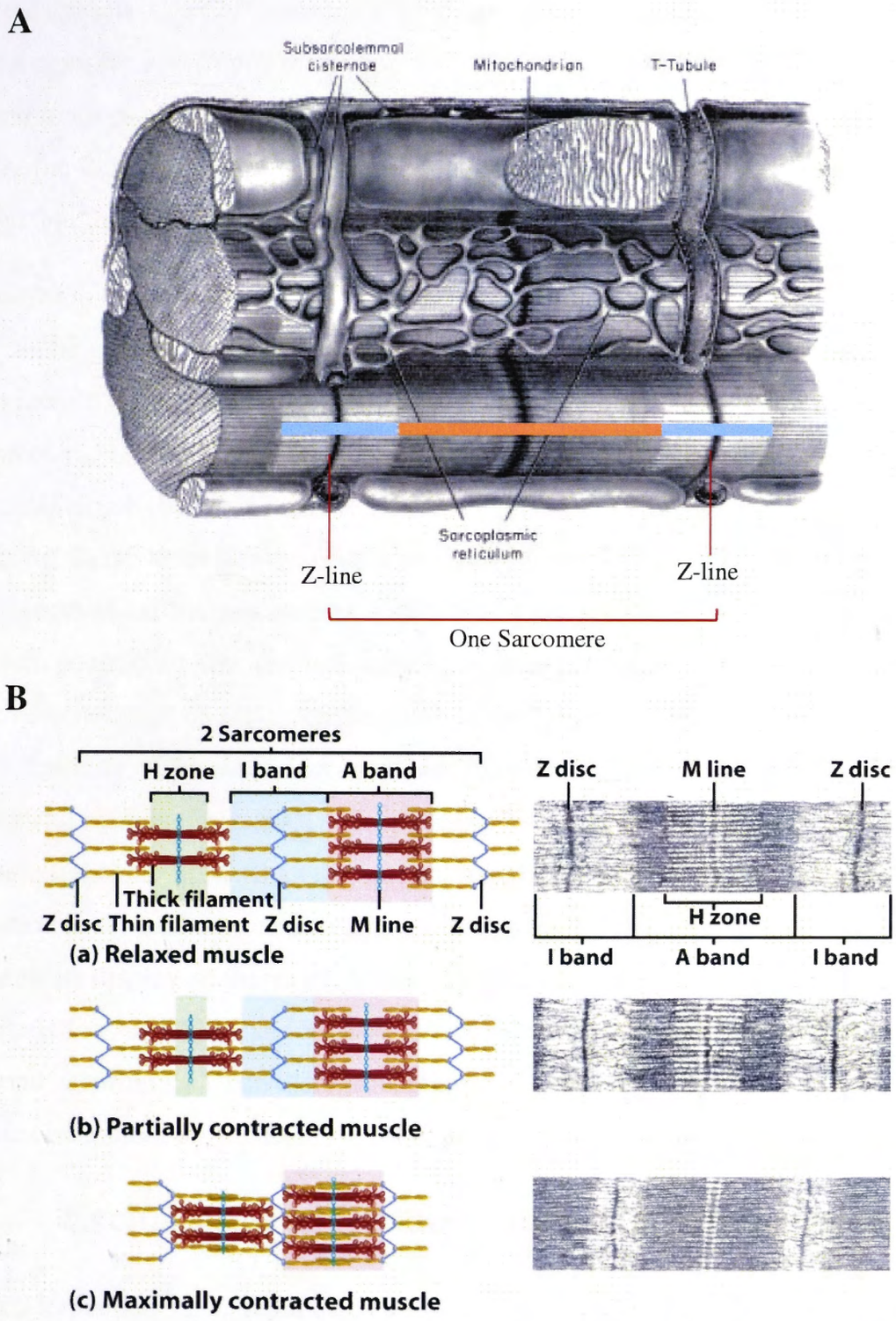

Figure 1.4 – Cardiac muscle contractility (**A**) Ultrastructure of cardiac muscle fibres. One full sarcomere is displayed centrally (bordered by z-lines) with adjacent sarcomeres on each end. Thin filaments (blue shading) and thick filaments (orange shading) are distinct by their lighter and darker shading, respectively. Modified from (Fawcett and McNutt, 1969) (**B**) Sliding filament theory of striated muscle contraction. Increasing overlap between thin and thick filaments is shown as the muscle progressively contracts from (a) total relaxation to (c) maximal contraction (Jenkins et al., 2006)

When the cytoplasmic Ca^{2+} concentration decreases, Ca^{2+} no longer binds to the troponin complex and tropomyosin returns to its site blocking the interaction between actin and myosin. Since the myosin heads can no longer interact with their binding site on actin, the filaments return to their original positions, causing the sarcomere to re-lengthen and the muscle fibre to relax.

A relationship exists between the length of the sarcomere at rest and the maximum force which can be generated. At an optimal sarcomere length, the maximal number of myosin crossbridges can form and maximal force will be generated upon stimulation (Gordon et al., 1966). In skeletal muscle, most resting muscle fibres are maintained at the optimal length (between 2 and 2.2 μm as depicted in Figure 1.5) by their attachment to the bone. In the heart however, such an arrangement does not exist. Rather, the resting length of cardiac sarcomeres is dictated by the amount of blood in the chamber just before contraction (i.e. the end-diastolic volume) (Katz, 2006). Healthy cardiac muscle only operates on the ascending limb of the length-tension curve because the high parallel elasticity of the sarcomeres prevents them from lengthening to the same extent as in skeletal muscle (Bers, 2001; Vinten-Johansen et al., 2004). Because the resting sarcomere length is shorter than the optimal length, the heart can respond dynamically to variation in the end-diastolic volume. Additionally, as sarcomere length increases, the myofilaments display an increased sensitivity to Ca^{2+}, thereby potentiating the length-tension relationship (Allen and Kentish, 1985). These factors and others allow the heart to respond accordingly when there is an increased demand for oxygen delivery to the systemic circulation, during exercise for example.

1.5 Excitation-contraction coupling in cardiac muscle

As stated in Section 1.3.2, rapid electrical signalling via the cardiac conduction system precedes the coordinated contraction of cardiomyocytes, causing the heart to beat. The process linking the electrical signal with the contractile event, is excitation-contraction (EC) coupling and it consists of a complex cascade of events (reviewed in Bers, 2002b). An overview of EC coupling is presented below, but many aspects of the process will be discussed in greater detail later in this chapter.

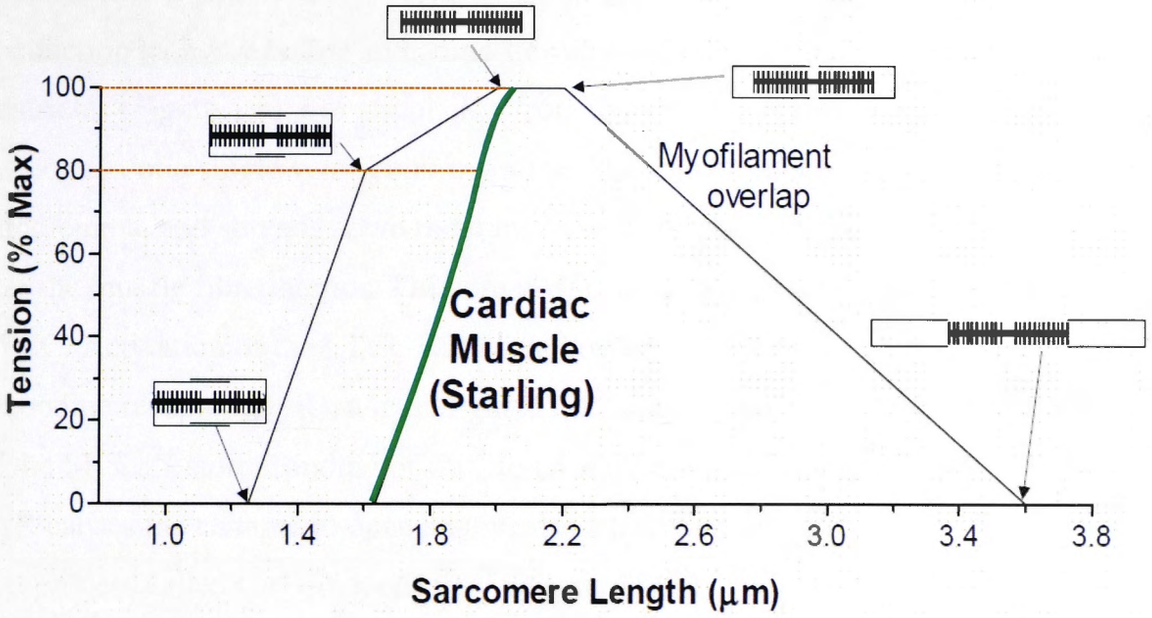

Figure 1.5 – Length-tension relationship in striated muscle. In skeletal muscle (black line), as the sarcomere length increases to ~ 2µm there's an optimal degree of overlap between actin and myosin which will allow maximum crossbridge formation and muscle tension. As the sarcomere is stretched there's less overlap between actin and myosin with subsequent loss of tension. Under physiological conditions cardiac muscle (green line) only operates on the ascending limb of the curve. The steeper curve for cardiac muscle, particularly at between 80 and 100% maximum tension (dashed lines) is thought to be due to increased myofilament Ca^{2+} sensitivity in cardiac muscle. Adapted from (Bers, 2001).

After an action potential is generated in the SA node, it travels along the signal conduction pathway before spreading from the Purkinje fibres into the wall of the ventricles (Figure 1.6). For simplicity, from this point the process will be discussed in the context of a single ventricular myocyte. The action potential depolarises the sarcolemma, and spreads down the transverse (t) tubule invaginations of this membrane, into the muscle fibre interior. The spread of depolarization activates the voltage gated, LTCC. Activation of the LTCC causes an inward Ca^{2+} current (I_{Ca}) which activates the ryanodine receptor (RyR), a ligand-gated Ca^{2+} channel positioned on the junctional face of the SR Ca^{2+} store. Binding of Ca^{2+} to an activation site on the cytoplasmic domain of RyR causes the channel to open and release a large amount of Ca^{2+} into the cytoplasm in a process called Ca^{2+}–induced Ca^{2+} release (CICR).

This raises the cytoplasmic Ca^{2+} concentration ($[Ca^{2+}]$) from nanomolar to micromolar levels which is sufficient to activate the contractile apparatus (Bers, 2002b; Vinten-Johansen et al., 2004). Since cardiomyocytes work as a syncytium, contraction of one cell coincides with contraction of the entire chamber and heart (in the sequence outlined above). When the cytoplasmic $[Ca^{2+}]$ is reduced the muscle can relax. This is primarily achieved by the sarcoplasmic/endoplasmic reticulum Ca^{2+}-ATPase (SERCA) which pumps the majority of the cytoplasmic Ca^{2+} back into the SR. Ca^{2+} extrusion via Na^{+}-Ca^{2+} exchangers (NCX) in the sarcolemma also significantly contributes to relaxation of the cell (Figure 1.6) (Bers, 2002b). The Ca^{2+} cycle is generally divided into two periods known as systole and diastole. The systolic period encompasses the time in which ventricular myocardium contracts and ejects the contents of the ventricle. During the diastolic period, the ventricular muscle relaxes and the chamber refills. In this time the membrane potential remains repolarized and Ca^{2+} is either taken back into the SR to be available for the next release phase, or extruded across the sarcolemma via NCX.

Skeletal EC coupling occurs by a similar process, in that activation of contractile proteins relies on a large efflux of Ca^{2+} from the SR, however this is not initiated by a process of CICR. Rather, when the LTCC senses depolarisation of the t-tubule membrane it undergoes a conformation change and communicates with the RyR via a direct protein-protein interaction. This activates the RyR and allows Ca^{2+} release from the SR to facilitate muscle contraction (Rios and Brum, 1987).

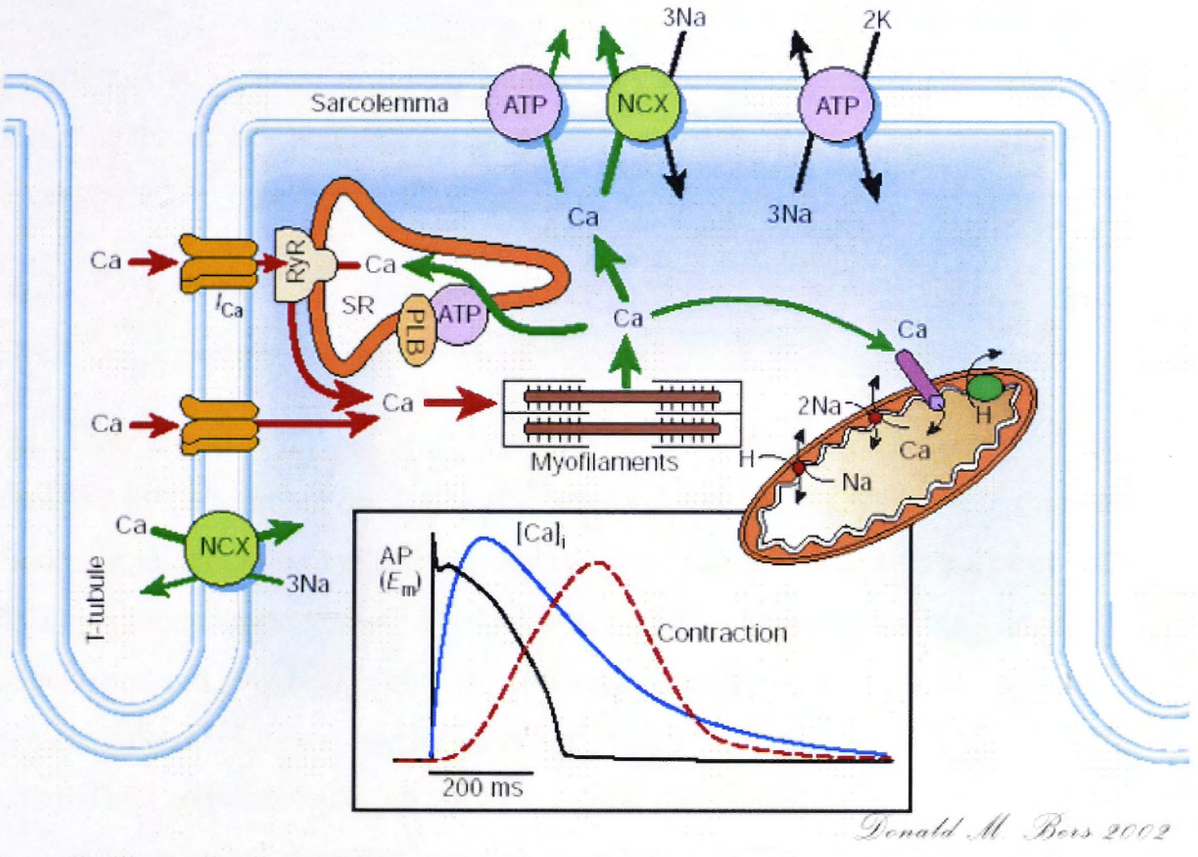

Figure 1.6 – Cardiac Excitation-Contraction Coupling. An illustration of a cardiomyocyte and the movement of Ca^{2+} during EC coupling (Bers, 2001). An action potential (originating in the SA node) spreads along the sarcolemma and down the t-tubules where it depolarises the DHPR. A small influx of extracellular Ca^{2+} (red) activates RyR2 and there is a large efflux of luminal Ca^{2+} (blue) into the cytoplasm where it activates the contractile proteins. For relaxation to occur the cytoplasmic [Ca^{2+}] (green) must be lowered. Most of the Ca^{2+} is pumped into the SR by the SERCA and some is removed from the myocyte by the NCX. Inset compares timescales of the cardiac action potential (AP), the intracellular Ca^{2+} transient ($[Ca]_i$) and contraction of the cell. I_{Ca} = DHPR, dihydropyridine receptor; RyR2, cardiac ryanodine receptor; ATP, Ca^{2+} ATPase (SERCA); NCX, Na^+/Ca^{2+} exchanger

1.6 Sarcolemmal Ca^{2+} fluxes

In cardiomyocytes, there are a large number of ion channels, pumps and transporters located on the surface and t-tubule membrane, including several that contribute to Ca^{2+} movement in and out of the cell.

1.6.1 L-type Ca^{2+} channel

1.6.1.1 Structure and function

While there are several types of voltage gated Ca^{2+} channels, the two predominantly expressed in the heart are the T-type Ca^{2+} channel and LTCC. While the T-type channel is more prominent in pacemaker regions and in the signal conduction pathway, the LTCC predominates in ventricular myocytes. LTCCs are named for their large conductance and long lasting channel openings (Bers, 2001; Hille, 2001). These characteristics permit the large influx of Ca^{2+} that contributes to phase 2 of the action potential and activates RyR2 on the intracellular SR membrane. Other defining characteristics include their activation at more positive resting membrane potentials, and their sensitivity to 1,4-dihydropyridines, hence their alternate name, dihydropyridine receptors.

The cardiac LTCC contains 2171 amino acids with a molecular weight of approximately 240 kDa and has a moderate homology of 66% with the skeletal isoform (Mikami et al., 1989). It is composed of four subunits, with the α_1 subunit being the largest and constituting the pore forming region of the channel. This subunit also contains the voltage-sensing segment of the channel and carries the majority of binding sites for regulatory agents, including second messengers and drugs (Hool and Corry, 2007). The α_1 subunit also contains binding sites for other subunits including the β, α_2-δ and γ subunits. While many details are known about the interactions and specific roles of these auxillary subunits, this will not be discussed any further as they are beyond the scope of this thesis.

The LTCC is activated by depolarization of the sarcolemma, whereas inactivation primarily depends on the presence of cytoplasmic Ca^{2+}, in a Ca^{2+}-induced inactivation mechanism. This is strongly supported by studies in which the rate of inactivation is reduced in the presence of Ca^{2+} chelators, or Ba^{2+}, which has a greater conductance than Ca^{2+} when used as the current carrier, but is unable to initiate the inactivation process

(Hadley and Hume, 1987; Hille, 2001). It has been hypothesised that an inactivation mechanism mediated by Ca^{2+} may also serve as a defence mechanism, preventing pathological Ca^{2+} overload (Bers, 2008). Ca^{2+} dependent inactivation also depends on the presence of calmodulin (CaM) which associates via a binding site on α_1 (Zuhlke et al., 1999; Bers, 2008).

1.6.1.2 L-type Ca^{2+} channel modulation

The LTCC has long been exploited as a target of antihypertensive and antiarrhythmic drugs including dihydropyridines (e.g. nifedipine), phenylalkylamines (e.g. verapamil) and benzothiazipines (e.g. diltiazem) (Mukherjee and Spinale, 1998). The channel is also regulated by several cellular factors. Most notably, it is a principle substrate for β-adrenergic signalling. Activation of β-adrenergic receptors initiates a signalling cascade increasing the level of cyclic AMP, which in turn activates protein kinase A (PKA) (Lohse et al., 2003). PKA phosphorylates residues on the β and α_1 subunits of LTCC which increases I_{Ca} and shifts the voltage dependence of channel activation and inactivation to more negative values which has the effect of increasing I_{Ca} (Mukherjee and Spinale, 1998; Bers, 2001). The functional outcomes of β-adrenergic signalling on whole cell function will be discussed in more detail in Section 1.11.

1.6.2 The Sodium-Calcium Exchanger

The NCX is a major pathway of Ca^{2+} extrusion from the cytoplasm to the extracellular space and hence has an important role in facilitating muscle relaxation. There are three isoforms which have approximately 70% homology, including NCX1 (which is highly expressed in the heart), NCX2 and NCX3 (Linck et al., 1998). NCX1 is the most studied of the three isoforms due to its long recognized role in cardiac function (Nicoll et al., 1990). The full length protein contains 938 amino acids, with nine transmembrane regions and a large loop comprised of nearly 550 amino acids which extends into the cytoplasm (reviewed in Philipson and Nicoll, 2000). In cardiac muscle, NCX1 appears to be located on all surface membranes including the t-tubules (Blaustein and Lederer, 1999).

NCX1 current is reversible, as the exchanger works in a forward mode (Ca^{2+} efflux) and a reverse mode (Ca^{2+} influx). In forward mode there is an influx of three Na^+ in exchange for one Ca^{2+} that is extruded from the cell, resulting in a net inward current ($I_{Na/Ca}$). In reverse mode, there is an efflux of 3 Na^+ in exchange for one Ca^{2+} and hence

a net outward current. Since NCX1 is electrogenic it can influence, and be influenced by, the sarcolemmal membrane potential. According to (Bers, 2001) high intracellular Ca^{2+} and more negative membrane potentials (relative to the reversal potential for $I_{Na/Ca}$) favour Ca^{2+} extrusion (forward mode). Conversely, more positive membrane potentials and high intracellular Na^{+}, conditions that may occur at the peak of the action potential, favour Ca^{2+} influx (Philipson and Nicoll, 2000; Bers, 2002b). Generally NCX1 appears to function in forward mode with its primary role being to extrude Ca^{2+} that had entered via LTCC and in conjunction with Ca^{2+} uptake to the SR, facilitate muscle relaxation (Philipson and Nicoll, 2000; Bers, 2001). The potential role of NCX in pathological situations will be discussed Section 1.11.

1.7 Sarcoplasmic Reticulum Ca^{2+} fluxes

1.7.1 The sarcoplasmic/endoplasmic reticulum Ca^{2+}-ATPase

1.7.1.1 Isoforms

The SERCA pump is a member of the P-type ATPase family of ion transporters, which also includes the Na/K-ATPase, sarcolemmal Ca-ATPase and the H/K-ATPase. The protein has a molecular weight of 110 kDa and the cardiac isoform is made up of 997 amino acids. There are three genes encoding SERCA, including SERCA1, SERCA2 and SERCA3 which produce at least 10 isoforms via alternative splicing (reviewed in Periasamy and Kalyanasundaram, 2007). SERCA1 and SERCA2 products are present in muscle whilst SERCA3 isoforms are only known to be present in non-muscle cells. In adult skeletal muscle, SERCA1A is the predominant form in fast twitch muscle while SERCA2A predominates in slow twitch muscle. SERCA2A is the predominant isoform of cardiac muscle and structurally and functionally similar to SERCA1A, with about 84% homology in their amino acid sequences (Lytton et al., 1992).

1.7.1.2 Structure

The first high resolution crystal structure of a SERCA pump was obtained by Toyoshima and colleagues (2000), illustrating the structure of SERCA1A at a resolution of 2.6 Å. SERCA pumps are composed of 3 cytoplasmic domains which are named for their role in the Ca^{2+} transportation reaction (Figure 1.7A). These domains include the

Figure 1.7 - SERCA structure and function. (**A**) Key features include the 3 cytoplasmic domains including the Phosphorylation (P) and Nucleotide (N) Binding domains, which together form the catalytic site of the pump. The Actuator (A) domain is thought to have a role in protein conformational changes. The Ca^{2+} binding sites are located in the transmembrane (M) domain. Structure of SERCA2B from (MacLennan and Green, 2000), based (Toyoshima et al., 2000) (**B**) SERCA conformational changes during Ca^{2+} translocation (MacLennan and Green, 2000). SERCA transitions between a high energy conformation (E_1) and a low energy conformation (E_2). At the start of cycle (1) SERCA already carries a bound ATP molecule and so is in the E_2 conformation and is non-phosphorylated. (2) Ca^{2+} binds to high affinity binding sites in triggering ATP hydrolysis. SERCA is in the E_1 conformation. (3) ATP hydrolysis and subsequent phosphorylation in the P domain (E_1-P) induces occlusion of the Ca^{2+} binding sites. (4) The pump transitions to the low energy conformation (E_2-P) and there's a reduction in Ca^{2+} affinity (5), allowing Ca^{2+} to be released to the SR lumen. (6) Water enters the catalytic site from the SR lumen and hydrolyses the phosphorylated residue (E_2). (1) ATP once again binds in the cytoplasmic N domain, converting the pump back to the E_1 conformation.

A

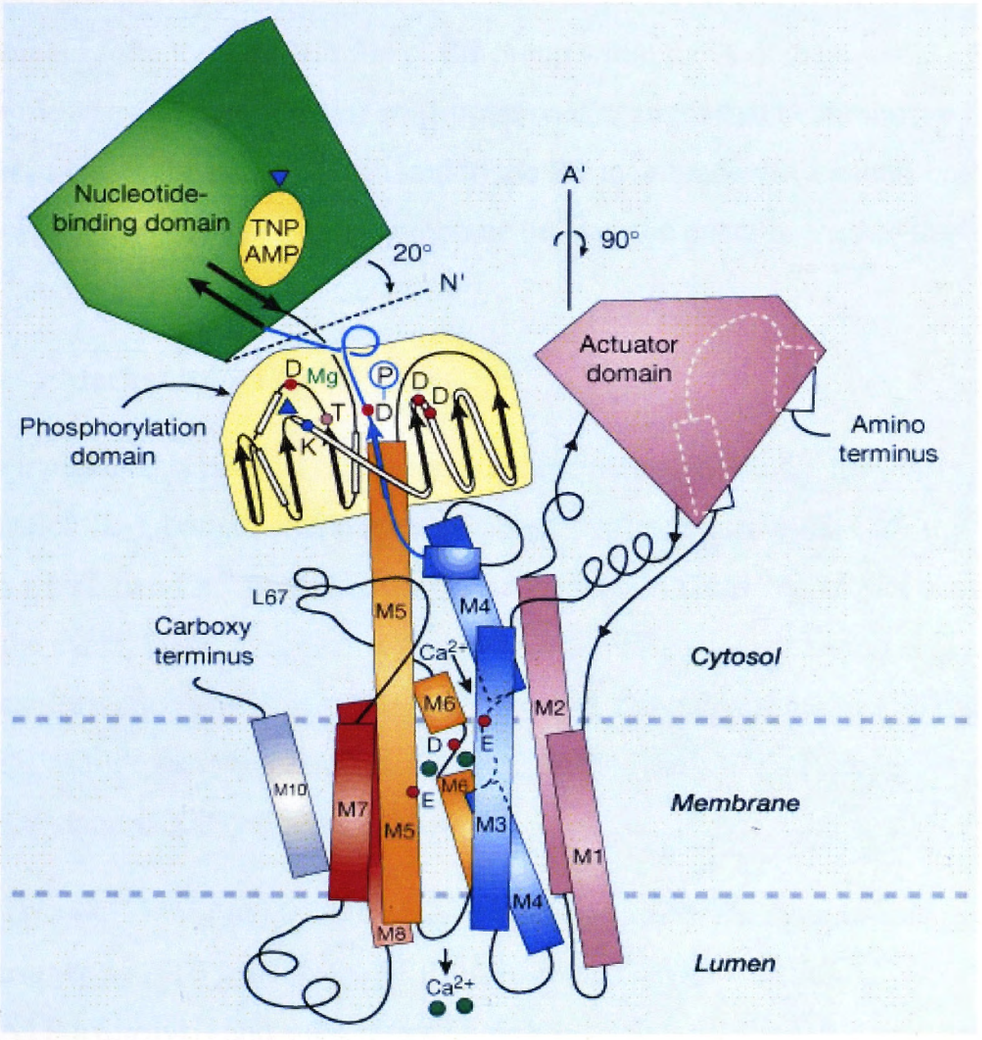
Nucleotide-binding domain
TNP AMP
20°
N'
A'
90°
Actuator domain
Amino terminus
Phosphorylation domain
D
Mg
P
T
K
L67
Carboxy terminus
M5
M4
Ca2+
M6
M2
E
M10
M7
M5
M3
M1
M4
M8
Cytosol
Membrane
Lumen
Ca2+

B

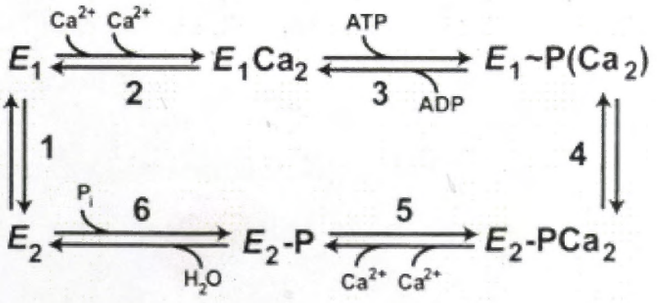
Ca2+ Ca2+
E1
E1Ca2
ATP
E1~P(Ca2)
2
3
ADP
1
4
Pi
6
5
E2
E2-P
E2-PCa2
H2O
Ca2+ Ca2+

phosphorylation (P) domain, the nucleotide binding (N) domain and the actuator or anchor (A) domain (MacLennan and Green, 2000; Kuhlbrandt, 2004). Together the N and P domain form the catalytic site of the pump while the A domain is thought to have a role in the transmission of major conformational changes that occur during the transport of Ca^{2+}. The pump is anchored to the SR membrane via a membrane (M) domain which consists of 10 transmembrane helices and contains the binding sites for two Ca^{2+} ions (Toyoshima et al., 2000).

1.7.1.3 Mechanism of Ca^{2+} Uptake

SERCA transitions between a high energy conformation (E_1) and a low energy conformation (E_2), both of which are also phosphorylated during the Ca^{2+} translocation cycle, in which two Ca^{2+} ions are transported for each ATP molecule that is used. At the start of the cycle, SERCA already carries a bound ATP molecule and so is in the high energy conformation and is non-phosphorylated. A summary of the transportation reaction is as follows (MacLennan and Green, 2000; Katz, 2006; Periasamy and Kalyanasundaram, 2007) (Figure 1.7B):

1. Two Ca^{2+} ions bind to high affinity binding sites in the cytoplasmic region, triggering ATP hydrolysis. SERCA is in the E_1 conformation.
2. ATP hydrolysis and subsequent phosphorylation of an aspartic acid residue in the P domain (E_1-P) induces occlusion of the Ca^{2+} binding sites which are then inaccessible to the cytoplasmic environment.
3. The pump transitions to the low energy conformation (E_2-P) and there's a reduction in Ca^{2+} affinity, allowing Ca^{2+} to be released to the SR lumen.
4. Water enters the catalytic site from the SR lumen and hydrolyses the phosphorylated residue (E_2)
5. ATP once again binds in the cytoplasmic N domain, converting the pump back to the E_1 conformation.

The reduction in Ca^{2+} affinity is essential in allowing Ca^{2+} to be released to the SR lumen where there is still a higher [Ca^{2+}] then in the cytoplasm (Bers, 2002b).

1.7.1.4 SERCA in excitation-contraction coupling

The vast majority of the SR membrane reportedly contains SERCA pumps, including the terminal cisternae (Bers, 2001). Hence, the SERCA pump is believed to be present

at a 170 fold greater concentration than Ca^{2+} release channels (Katz, 2006). While SERCA2A isn't the only method of Ca^{2+} removal from the cytoplasm, it is the predominant form, accounting for 70% of Ca^{2+} removal in rabbit and 92% in rat myocytes. The remainder of the Ca^{2+} is predominantly extruded by the NCX (28% in rabbit, 7% in rat) or the sarcolemmal Ca^{2+} ATPase and mitochondrial uniporter (which together only account for 1-2% of Ca^{2+} extrusion in any species). The situation in humans is thought to be similar to that in rabbit (Bassani et al., 1992, 1995b and reviewed in Bers, 2001). Clearly then, SERCA2A has an essential role in facilitating muscle relaxation. SERCA2A can also function in a backflux mode where Ca^{2+} is transported from the SR to the cytoplasm and ATP is produced (Takenaka et al., 1982). While SERCA backflux is quite high, it usually does not exceed Ca^{2+} uptake by SERCA, rather the two exist in equilibrium in which net Ca^{2+} uptake is favoured (Shannon et al., 2002).

1.7.1.5 SERCA regulation

Ca^{2+} uptake by SERCA2A is under the control of several regulatory proteins including phospholamban, sarcolipin and the histidine rich Ca^{2+} binding protein. In this section, only phospholamban will be discussed as these other proteins are outside the focus of the current research. SERCA2A is also vulnerable to several post-translational modifications, including oxidation which will be discussed in Section 1.10.

1.7.1.5.1 Phospholamban

A key distinction between skeletal and cardiac muscle is the regulation of SERCA2A by phospholamban which is only found in cardiac muscle. Phospholamban is a 6.2 kDa transmembrane protein that colocalizes with SERCA2A in the SR membrane, its principle effect being inhibition of Ca^{2+} uptake by SERCA2A. It is expressed predominantly in cardiac muscle and in slow twitch skeletal muscle, though it has also been found at low levels in smooth muscle (MacLennan and Green, 2000). Each phospholamban monomer is composed of 52 amino acids and includes a cytosolic domain (residues 1 – 30) and a transmembrane domain (residues 31 – 52). The cytosolic domain includes two important phosphorylation sites at Ser-16, which is a phosphorylation site for PKA and at Thr-17, which is a phosphorylation site for CaMKII (Fujii et al., 1986; Wegener et al., 1989). Phospholamban also forms a

homopentamer which is thought to be stabilized by a cysteine residue in the transmembrane domain (Karim et al., 1998).

Phospholamban inhibition of SERCA2A is mediated by direct interactions between the non-phosphorylated, monomeric form of phospholamban and the pump (Figure 1.8). Phospholamban has the greatest affinity for SERCA2A in its low energy (E_2) conformation (James et al., 1989), prolonging the time spent in this conformation. This results in an overall 2 - 3 fold inhibition of Ca^{2+} uptake (MacLennan and Kranias, 2003), due to the E2 conformation promoting the lowest affinity for Ca^{2+}. Phospholamban is dissociated either when it is phosphorylated, or when SERCA2A binds Ca^{2+}, causing a transition from the E_2 to E_1 conformation (James et al., 1989). Thus under basal conditions, phospholamban limits SERCA2A activity and reduces the pool of SR Ca^{2+} available for release. Phosphorylation via β-adrenergic stimulation relieves the inhibitory effect of phospholamban on SERCA2A, enhancing Ca^{2+} uptake which increases the pool of Ca^{2+} available for release for CICR. The increased Ca^{2+} transient causes a subsequent increase in myocyte contractility.

1.7.1.6 SERCA in cardiac pathology

A reduction in SERCA2A function is well documented in several forms of cardiac pathology, including dilated cardiomyopathy (Arai et al., 1993; Hasenfuss et al., 1994; Studer et al., 1994; Meyer et al., 1995; Schwinger et al., 1995; Schmidt et al., 1998), idiopathic cardiomyopathy (Hasenfuss et al., 1994; Schmidt et al., 1998), pulmonary hypertension (Arai et al., 1993) and ischemic heart disease (Arai et al., 1993). In studies that tested samples from two or more of these pathologies there was no difference in the extent of SERCA2A inhibition in different diseases, demonstrating the ubiquitous nature of SERCA2A inhibition in cardiac dysfunction. While a reduction in SERCA2A mRNA levels were found in all of these studies (and in Mercadier et al., 1990), this did not always correspond with a decrease in protein expression. In these studies there was evidence of a reduced basal phosphorylation level of phospholamban, an effect which would enhance the inhibition of Ca^{2+} uptake (Schwinger et al., 1995; Schmidt et al., 1998). If this effect were to occur in combination with an increased ratio of phospholamban to SERCA (as measured in Meyer et al., 1995), the result would be drastically inhibited SERCA uptake function (reviewed in MacLennan and Kranias, 2003). It should be noted that whilst a few studies report reduction in phospholamban

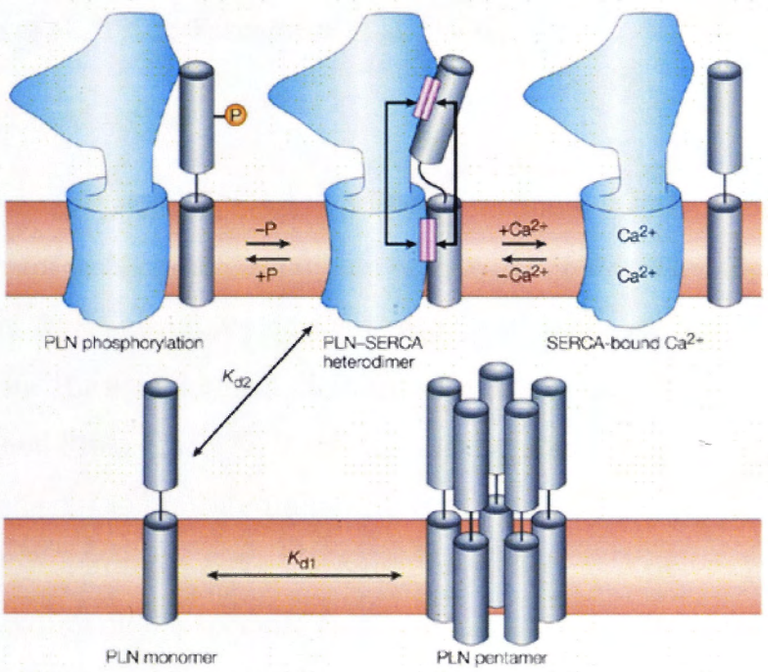

Figure 1.8 - Mechanism of phospholamban inhibition of SERCA2A. Phospholamban (PLN) binds to the E_2 (low energy, low Ca^{2+} affinity) conformation of SERCA2A. Only the monomeric, non-phosphorylated form of phospholamban binds to SERCA2A, prolonging the time the pump spends in the E_2 state, thereby inhibiting Ca^{2+} uptake. Phospholamban is released either when it is phosphorylated or when SERCA2A binds Ca^{2+}. Figure from (MacLennan and Kranias, 2003).

mRNA/protein expression (Arai et al., 1993) other studies report no change (Meyer et al., 1995; Schmidt et al., 1998).

1.7.2 The Ryanodine Receptor

The RyR is a ligand-gated Ca^{2+} release channel whose role is to release Ca^{2+} from the SR during EC coupling. It is named for its ability to bind the plant alkaloid ryanodine with high affinity and high specificity (Inui et al., 1987a, b). RyR is essential for survival, as demonstrated in RyR knockout mice which die *in utero* or soon after birth (Takeshima et al., 1995; Takeshima et al., 1998).

1.7.2.1 Localization

In striated muscle RyRs are clustered in the junctional SR, the area of the SR that comes in close contact with either the t-tubule or sarcolemmal surface membrane. In electron micrographs, RyR appear as electron-dense "feet" that span the gap between the SR membrane and the sarcolemmal membrane (either in the surface or t-tubule) (Franzini-Armstrong and Protasi, 1997). In the surface membrane are clusters of LTCC's which form couplons or Ca^{2+} release units with RyRs in the opposing SR membrane (Flucher et al., 1993). In cardiac muscle, the ratio of RyR:LTCC is between 4-10 RyR for every LTCC, depending on the species. This is in marked contrast to skeletal muscle, where there is thought to be one RyR for every two LTCC (Bers and Stiffel, 1993; Franzini-Armstrong and Protasi, 1997). This difference likely reflects the differential mechanisms of RyR activation in the two muscle types, where in skeletal muscle RyR1 activation requires a mechanical interaction with the LTCC (Dulhunty, 2006), while in cardiac muscle RyR2 is activated by CICR. In some species, a moderate proportion of RyR2 are "uncoupled", located in parts of the cardiac SR that do not form junctions with any component of the surface membrane (Jorgensen et al., 1993). It is currently unclear whether RyR2 localised in this extended or corbular SR has a role in physiological EC coupling.

1.7.2.2 RyR isoforms and tissue distribution

RyR shares several structural and functional characteristics with inositol 1,4,5-triphosphate receptors (IP_3R), the other ligand-gated, intracellular Ca^{2+} channel (Hakamata et al., 1992; Yuchi and Van Petegem, 2011). Although the cardiac isoform (IP_3R1) is also found in the SR of cardiac myocytes, it is not believed to play a major

role in EC coupling, due to a low level of expression and low conductivity compared to RyR2 (reviewed in Marks, 1997). Thus RyR2 is thought to be more functionally relevant to EC coupling and is the primary conduit of SR Ca^{2+} release.

There are three isoforms of RyR; RyR1, RyR2 and RyR3, all encoded by different genes. Although it is evident that all 3 isoforms are expressed to some extent in a variety of tissues, RyR1 is known to be the predominant isoform in skeletal muscle and RyR2 is the predominant form in cardiac muscle (but is also expressed in significant amounts in the brain) (Nakai et al., 1990; Hakamata et al., 1992). RyR3 is expressed at moderate levels in a variety of tissues including smooth muscle and certain regions of the brain (Ledbetter et al., 1994 and reviewed in Franzini-Armstrong and Protasi, 1997; Lanner et al., 2010).

1.7.2.3 Structure

The RyR is the largest known ion channel, consisting of four identical subunits each approximately 560 kDa in size. In humans each RyR2 monomer is 4967 amino acids in length (Tunwell et al., 1996), about 80% of which forms a large, cytoplasmic "foot" domain, while the remainder is located in the SR lumen and as transmembrane segments (Figure 1.9) (Liu et al., 2002). RyR is reported to have high inter-species homology with 88% homology between rabbit, pig and human RyR1 and 98.6% homology between human and rabbit RyR2 (Tunwell et al., 1996). Comparing the homology of the three isoforms, while some regions have up to 90% homology in their amino acid sequence, on average there's a 67 – 70% homology with the greatest similarity being between RyR2 and RyR3 (70%) (Nakai et al., 1990; Hakamata et al., 1992). The reduced overall homology is due to the presence of three regions of higher diversity. In reference to the RyR2 sequence, these regions lie between amino acids 4210 and 4562 (divergent region 1), 1353 – 1397 (divergent region 2), and 1852 – 1890 (divergent region 3) (Figure 1.9A) (Rossi and Sorrentino, 2002). Mutations in these regions have been associated with a form of inherited arrhythmia (Koop et al., 2008) and with changes in the channel's response to ligands such as Ca^{2+} and caffeine in the analogous region of RyR1 (reviewed in Lanner et al., 2010).

While high resolution crystal structures of small segments of RyR have been solved, structural studies of the full-length RyR have been notoriously difficult, due to the proteins large size, instability and transmembrane domain. Studies using cryoelectron

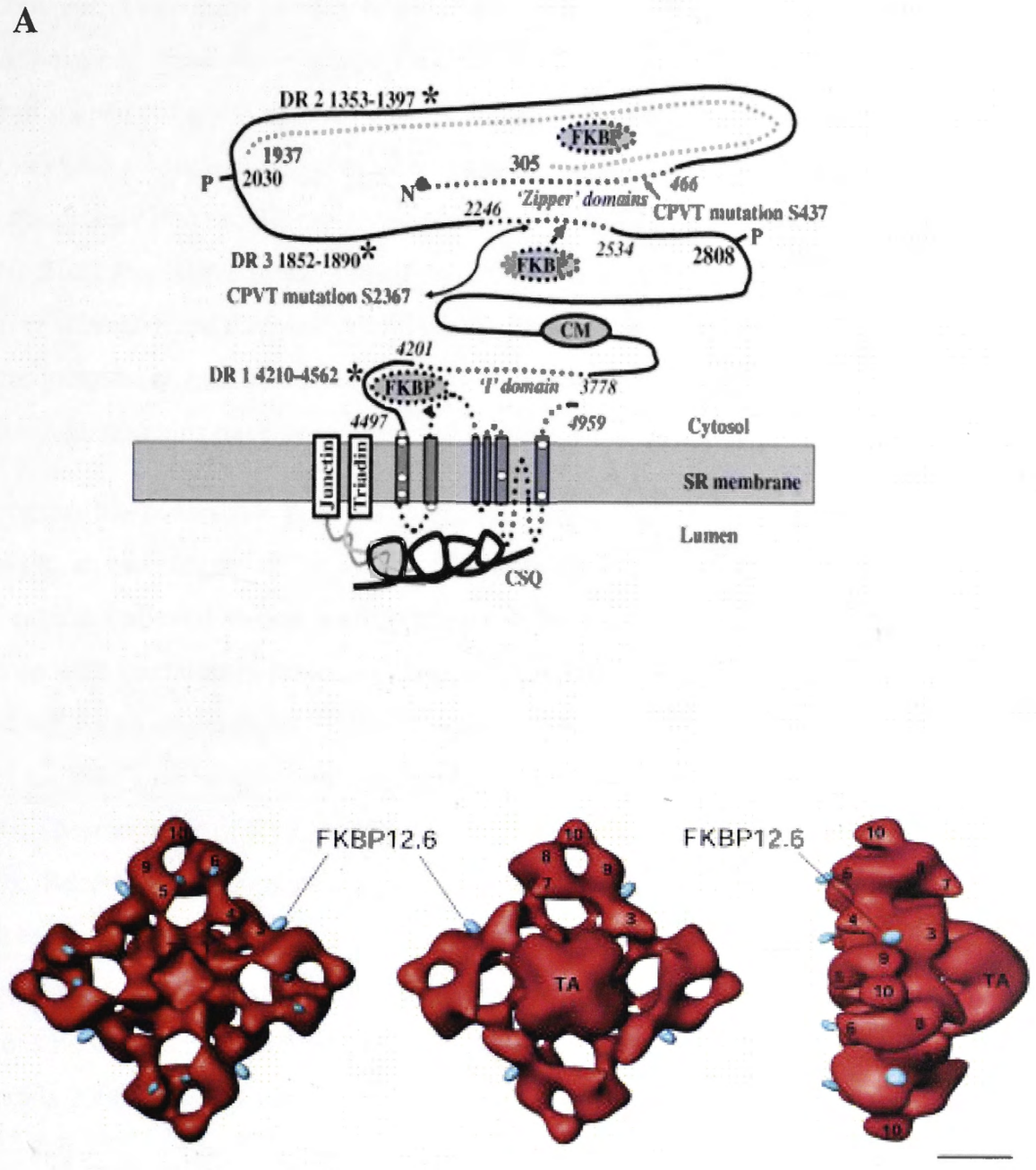

Figure 1.9 – Schematic diagram of RyR2 **(A)** Predicted transmembrane segments and large N-terminal domain are shown, including proposed locations of divergent regions (DR1, DR2 and DR3), binding sites for FK 506 binding proteins (FKBP, dashed grey line) and calmodulin (CM), CPVT mutation clusters (black dashed line) and important phosphorylation sites (P2808 and P2030). Calsequestrin is shown bound in the luminal domain (CSQ). Figure from Blayney and Lai (2009). **(B)** Surface representations of 3D cryo-EM reconstructions of RyR2 with bound FKBP12.6 (blue). The 3D volume is shown in three views: (i), cytoplasmic face; (ii), SR luminal face; (iii), side view. Numbering refers to nomenclature of micordomains. Scale bar ~100 Å. TA, transmembrane assembly (modified from Sharma et al., 2006).

microscopy with three dimensional reconstruction (up to 9.6 Å resolution) (Ludtke et al., 2005) have had some success, reporting that the intact, purified channel forms a mushroom shaped complex, with the large, cytoplasmic "foot" domain (280 x 280 x 120 Å) located in the cytoplasm, and a small transmembrane domain (120 x 120 x 60 Å) that anchors the protein into the SR membrane (Figure 1.9B) (Sharma et al., 1998; Lanner et al., 2010). The cytoplasmic domain itself contains several structural domains with many intervening solvent-filled cavities. Additionally, each of these domains has been divided into microdomains, as numbered in Figure 1.9B. In various models, between 4 -12 transmembrane domains have been proposed though the actual number is unclear.

Some progress has been made in identifying functionally important domains of RyR2. For example, in each corner of the cytoplasmic domain there is an area referred to as the "clamp" region, believed to have an important role in channel gating and in binding interactions with modulatory proteins (Zhang et al., 2003). Additionally, regional "hot spots" of mutations associated with RyR2 pathology have also been mapped to this area (Wang et al., 2007), as have two of the Divergent Regions (Zhang et al., 2003; Liu et al., 2004). These aspects of RyR structure are reviewed more thoroughly in (Lanner et al., 2010). Recently, a phosphorylation domain was also localized to the clamp region (Amador et al., 2013). It has been proposed that in pathologies where RyR2 is excessively active (or "leaky) that there is an "unzipping" of domain-domain interactions between an N-terminal (amino acids 1 - 600) and C-terminal domain (amino acids 2000 – 2500) (Tateishi et al., 2009).

1.8 RyR2 Regulatory ligands

RyR2 forms the hub of a massive macromolecular complex that regulates SR Ca^{2+} release during EC coupling (Figure 1.10) (Zhang et al., 1997; Gyorke et al., 2004). Some of these, including calsequestrin (CSQ), triadin and junctin are localized to the SR lumen, while others like the FK506 binding proteins (FKBPs) and calmodulin are found in the cytoplasm. RyR2 also carries binding sites for various regulatory ligands, including Ca^{2+}, Mg^{2+} and ATP. Several other proteins and ligands are known to bind to RyR2 with varying influences, but are beyond the scope of the thesis.

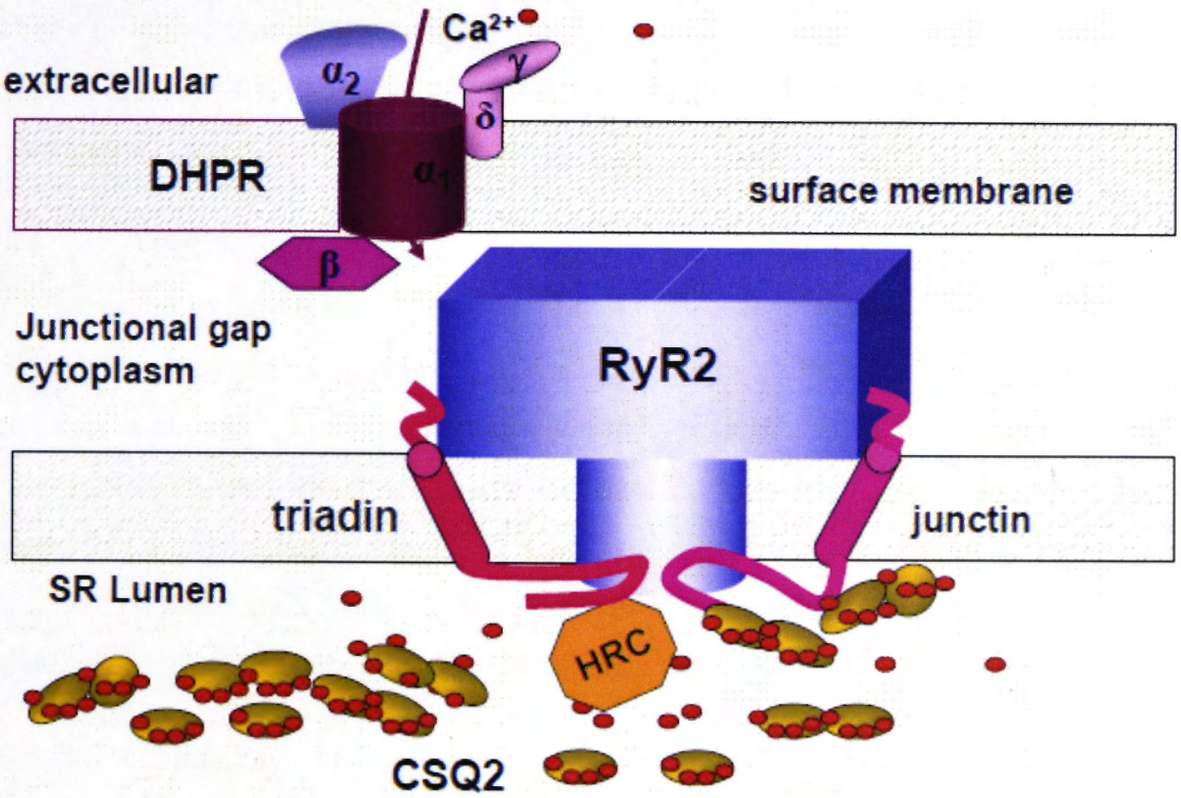

Figure 1.10 – Assembly of key proteins in the dyad. Some key proteins discussed in this chapter are shown in the t-tubule and junctional face SR membrane. The L-type Ca^{2+} channel (DHPR) is shown allowing a small influx of Ca^{2+} into the cell. The bulk of RyR2 (~80 %) is positioned in the cytoplasmic space while the remainder is embedded in the membrane with slight protrusion into the SR lumen. Triadin and junctin both have a short cytoplasmic segment and a longer luminal domain which is thought to bind both calsequestrin (CSQ2) and, for triadin, the histidine-rich Ca^{2+} binding protein (HRC). CSQ2 is portrayed as monomers and dimers bound to Ca^{2+} (red circles). Figure from (Dulhunty et al., 2012).

1.8.1 Adenosine 5'-triphosphate

ATP is a potent activator of RyRs in both skeletal and cardiac muscle (Meissner, 2004). In skeletal muscle RyR1 is activated by ATP in the absence of luminal or cytoplasmic Ca^{2+}, however in cardiac muscle ATP requires Ca^{2+} as a co-agonist to activate RyR2. It has been proposed that ATP activates RyR2 in response to luminal Ca2+-induced activation and also stabilizes the open-state conformation and destabilizes the closed conformation (Laver, 2007).

1.8.2 Magnesium

Mg^{2+} is thought to inhibit RyR2 activity via two independent mechanisms. Type I inhibition involves Mg^{2+} competing with Ca^{2+} for a high-affinity Ca^{2+} binding activation site (Laver et al., 1997; Liu et al., 1998) while in Type II inhibition, Mg^{2+} binds to low affinity inhibition sites which non-selectively bind Ca^{2+} and Mg^{2+}. It has also been reported that at high cytoplasmic [Ca^{2+}] RyR2 is less sensitive to Mg^{2+} inhibition (Laver et al., 1997; Gyorke and Gyorke, 1998). Mg^{2+} inhibition of RyR2 is also reduced in the presence of oxidising agents (Eager and Dulhunty, 1998; Donõso et al., 2000).

1.8.3 Calcium

Ca^{2+} is a hugely influential modulator of RyR activity in skeletal and cardiac muscle. The luminal and cytoplasmic [Ca^{2+}]s are important modulators of SR Ca^{2+} release due to the presence Ca^{2+} binding sites on both the luminal and cytoplasmic domains of RyR (Laver et al., 1995; Gyorke and Gyorke, 1998; Marengo et al., 1998; Gyorke et al., 2004). In the course of the cardiac cycle, the cytoplasmic [Ca^{2+}]'s ranges from 0.1 – 1 μM while the luminal [Ca^{2+}] reportedly cycles between 1- 1.5 mM and ~ 0.3 mM during diastole and systole, respectively (Chen et al., 1994; Bers, 2002b; Shannon et al., 2003a). At a constant luminal [Ca^{2+}] of 1 mM, RyR2 is activated by cytoplasmic [Ca^{2+}]'s up to 1 mM, whilst concentrations > 1 mM inhibit the channel (Laver et al., 1995). It should be noted also that others have measured inhibition with concentrations as low as 100 μM cytoplasmic Ca^{2+} (Gyorke and Gyorke, 1998). Conversely, luminal Ca^{2+} is generally found to activate RyR2 at concentrations >0.1 mM. Some studies find that activation peaks at 1 mM while others find that concentrations as high as 53 mM can further activate the channel (Gyorke et al., 2004; Tencerova et al., 2012; Chen et al., 2013). This biphasic modulation has been attributed to the existence of high-affinity activation sites and low-affinity inactivation sites in the cytoplasmic domain of RyR2

Study	MgATP	Cytoplasmic $[Ca^{2+}]$ (μM)	Luminal Ca^{2+} range and response of RyR2
Sitsapesan & Williams, 1994	-	10	0.01 – 2 mM activated RyR2, required sulmazole Activation due to increase in T_o
Lukyanenko *et al*, 1996	3 mM ATP	0.1 - 1	0.2 – 20 mM activated RyR2, required ATP. EC_{50} = 2.6 mM Activation due to increase in T_o
Gyorke & Gyorke, 1998	3 mM ATP	1	0.2 – 20 mM activated RyR2, required ATP
Gyorke *et al*, 2004	3 mM MgATP Total $[Mg^{2+}]$ = 0.9 mM	2 - 6	0.02 – 5 mM activated native RyR2, no change in purified RyR2 Activation due to increase in F_o and decrease in T_c
Qin *et al*, 2008	-	1	0.01 – 10 mM. Bell shaped dependence, ≥0.05 – 1 mM activate native RyR2,> 1 mM inhibited. CSQ2 stripped channels had no response. CSQ2 mutants caused either enhanced activation (R33Q) or abolished response (L167H)
Laver, 2007	2 mM ATP	0.1	0.01 – 2 mM. Bell shaped dependence, 0.01 – 0.1 mM activated RyR2, 0.1 – 2 mM inhibited. Required ATP for response.
Jiang et al 2007	2.5 mM ATP	0.045	45 nM – 1 mM activated RyR2 RyR2 mutant A4860G mutant had no response between 45 nM – 1 mM, > 1 mM - 30 mM caused minor activation
Chen *et al*, 2013	1 mM Mg^{+} 5 mM ATP	10	0.1 – 1 mM. In presence of MgATP, no response in channels with either WT, CSQ knockout or CSQ R33Q knockin mutants.

Table 1.2 – Summary of studies that have examined RyR2 luminal Ca^{2+} sensitivity and some key experimental conditions.

(Liu et al., 1998; Laver, 2007). The luminal Ca^{2+} dependence is known to vary depending on the cytoplasmic [Ca^{2+}] and the presence of Mg^{2+} and ATP (Table 1.2). SR store load (determining the free luminal [Ca^{2+}]) is an important determinant of cardiac muscle function, having roles in termination of SR Ca^{2+} release, muscle contractility and facilitation of Ca^{2+} uptake by SERCA2A (reviewed in (Bers, 2002b; Gyorke and Terentyev, 2008; Radwanski et al., 2013). Additionally luminal Ca^{2+} actively regulates RyR2, activating the channels up to millimolar concentrations (as discussed above) and sensitizing RyR2 to activation by cytoplasmic Ca^{2+} (Fabiato and Fabiato, 1978; Laver, 2007; Qin et al., 2009). It is generally acknowledged that RyR2 gating is regulated by luminal Ca^{2+}, however the mechanism is unknown and is controversial. One theory is that luminal Ca^{2+} induced activation occurs by a "feed through" mechanism, whereby Ca^{2+} binds to a luminal site on RyR2 causing brief activation. This would allow Ca^{2+} to move through to the cytoplasm and activate high affinity activation sites causing prolonged channel openings (Laver, 2007). Other studies however have indicated that luminal Ca^{2+} acts distinctly at binding sites in the luminal domain of RyR2 to activate the channel (Gyorke and Gyorke, 1998). The mechanism of luminal Ca^{2+} regulation of RyR2 will be discussed more in Section 1.9.3.

1.9 RyR2 Interactions with Cytoplasmic and Luminal Proteins

1.9.1 FK-506 binding proteins

The FKBPs are a family of proteins that bind the immunosuppressive drugs FK506 and rapamycin. There are two isoforms expressed in striated muscle, including the 12 kDa FKBP12 and the 12.6 kDa FKBP12.6. FKBPs are reported to bind to RyR in a 4:1 stoichiometry in both skeletal and cardiac muscle (Timerman et al., 1993; Timerman et al., 1996), although the degree of occupancy of these sites is less certain (Guo et al., 2010; Zissimopoulos et al., 2012).

The role of FKBPs in muscle physiology is controversial. There is substantial evidence that FKBPs stabilise the closed state of the channel by strengthening intersubunit interactions (Ahern et al., 1994a; Mayrleitner et al., 1994; Ahern et al., 1997; Xiao et

al., 1997; Marx et al., 2000). The effects of FKBP dissociation on Ca^{2+} handling have been linked to cardiac disorders (Yano et al., 2000; Xin et al., 2002; Wehrens et al., 2005; Huang et al., 2006), while FKBP12.6 overexpression was cardio protective (Gellen et al., 2008) and normalized cellular Ca^{2+} handling (Prestle et al., 2001). There is some evidence linking FKBP12.6 dissociation with RyR2 phosphorylation (Marx et al., 2000) and more recently, oxidation (Zissimopoulos and Lai, 2005; Shan et al., 2012). This topic is controversial though as other investigators have been unable to find any effect of RyR2 phosphorylation on FKBP12.6 dissociation (Xiao et al., 2004; Guo et al., 2010).

Until recently it was generally considered that RyR2 was only regulated by FKBP12.6 and that RyR1 was regulated FKBP12 (Timerman et al., 1996). However, recent evidence has suggested that the 12kDa isoform may have a more prominent role in cardiac muscle than previously thought (Galfre et al., 2012; Zissimopoulos et al., 2012). While the specific role of each FKBP isoform in cardiac muscle physiology and pathology is still to be elucidated, it is clear that these proteins are important for normal cardiac muscle function.

1.9.2 Calmodulin

Another protein that modulates RyR2 activity is the Ca^{2+} binding protein calmodulin which has an inhibitory effect on RyR2, measured by [^{3}H] ryanodine binding and in single channel experiments (Balshaw et al., 2001; Meissner, 2004). RyR2 binding affinity for calmodulin is decreased under oxidising conditions and this enhances RyR2 sensitivity to cytoplasmic Ca^{2+}. Calmodulin has also been shown to influence LTCC activity in cardiac muscle and thus has an important role in cardiac EC coupling (Hamilton et al., 2000; Balshaw et al., 2001).

1.9.3 Calsequestrin

CSQ is the major SR Ca^{2+} binding protein in skeletal and cardiac muscle. It is localized close to the junctional face membrane, anchored to the RyR by the proteins triadin and possibly junctin (see below) which themselves are bound to RyR2 (Figure 1.10) (Zhang et al., 1997). CSQ binds Ca^{2+} with low affinity (K_d = 1 mM) and in high capacity (35-80 mol/mol) (MacLennan and Wong, 1971; Slupsky et al., 1987; Wang et al., 1998b; Beard et al., 2004; Park et al., 2004). There are two CSQ isoforms which are encoded by

different genes. CSQ1 is found exclusively in skeletal muscle while CSQ2 is found in the heart and in slow twitch skeletal muscle. In humans, the two isoforms have 84% homology. CSQ2 also has high inter-species homology, ranging from 87 – 98% (Beard et al., 2004). CSQ1 and CSQ2 consist of three almost identical domains, which contain thioredoxin-like folds, characterized by four α-helices which border a central β-sheet (Wang et al., 1998a). It is thought that CSQ2 polymerization occurs via Ca^{2+}-dependent dimer and subsequently tetramer formation (Beard et al., 2004).

Several important differences exist between the two CSQ isoforms. At 1 mM luminal Ca^{2+} only relatively small amounts of CSQ2 are associated with the RyR2 complex and at this physiological [Ca^{2+}], CSQ2 exists mainly as monomers (although it can polymerise at higher [Ca^{2+}]) (Wei et al., 2009b; Murphy et al., 2011). In contrast, under the same conditions CSQ1 is mostly polymerized and has greater Ca^{2+} binding capacity than CSQ2 (Beard et al., 2008). The two isoforms also have specific effects on RyR in different muscle types. In skeletal muscle CSQ1 inhibits RyR1 (Beard et al., 2002; Wei et al., 2006), while in the heart the effect of CSQ2 on RyR2 appears to depend on the presence of MgATP. In the presence of both Mg^{+} and ATP CSQ2 inhibits RyR2 (Chen et al., 2013), whilst in the absence of these factors CSQ2 activates RyR2 (Qin et al., 2008; Wei et al., 2009b).

1.9.3.1 Calsequestrin function

CSQ2 is the primary Ca^{2+} buffer in the SR and changes in CSQ2 expression cause corresponding changes in SR Ca^{2+} content (Terentyev et al., 2003; Rizzi et al., 2008). In a CSQ2 knockout mouse, SR Ca^{2+} content, as assessed by caffeine induced transients in intact cardiomyocytes, was preserved but coincided with an approximate 50% increase in SR volume (Knollmann et al., 2006). Even though CSQ2 can polymerize at very high luminal [Ca^{2+}], it was recently proposed that CSQ2 mainly exists in a monomeric form, which binds only <10 Ca^{2+} ions per monomer (Murphy et al., 2011). The authors suggest that the monomeric form of CSQ may permit faster Ca^{2+} binding/unbinding and promote favourable conditions for Ca^{2+} uptake (Murphy et al., 2011). These effects would be important in facilitating Ca^{2+} release and uptake throughout the cardiac cycle.

1.9.3.2 Luminal Ca^{2+} sensing by CSQ2

In addition to its role as a Ca^{2+} buffer, CSQ2 is thought to have an important role communicating store load to RyR2. This is supported by several lines of evidence. In

single channels where CSQ2 was selectively dissociated, RyR2 was unable to respond to changes in luminal Ca^{2+} (unless cytoplasmic Ca^{2+} was increased to 100 μM, a concentration unlikely to be encountered physiologically) (Qin et al., 2008). In another example, purified RyR2 (lacking CSQ2, triadin and junctin) did not respond when *trans* Ca^{2+} was increased from 20 μM to 5 mM, whilst addition of exogenous CSQ2 restored luminal Ca^{2+} sensing, but only if triadin and junctin were also present (Gyorke et al., 2004). These results may imply that CSQ solely confers luminal Ca^{2+} sensitivity to RyR2. However other studies support only a regulatory role for CSQ2. In single channels CSQ2 stripped channels remained reactive to changes in luminal Ca^{2+}, but this response was more sensitive (Dulhunty et al., 2012). In cardiomyocytes from CSQ2 knockout mice, there was a non-linear relationship between SR Ca^{2+} leak and SR Ca^{2+} load (Knollmann et al., 2006). That this relationship was not linear, and was actually steepe in the absence of CSQ2 than it was in myocytes from wildtype mice, implies that RyR2 itself (or another accessory protein) retains an innate ability to respond to luminal Ca^{2+}. CSQ2 has also been shown to influence the cytosolic Ca^{2+} response of RyR2 with CSQ2 dissociation increasing single channel sensitivity to activation by cytoplasmic Ca^{2+} (Qin et al., 2008; Chen et al., 2013).

1.9.3.3 Calsequestrin and arrhythmogenesis

The importance of CSQ in regulating SR Ca^{2+} release is evidenced by studies employing CSQ2 knockdown or knockout. Reduced levels of CSQ2 are associated with decreased SR load, increased amplitude of spontaneous Ca^{2+} waves, enhanced restitution of Ca^{2+} release sites (i.e. reduced refractoriness of Ca^{2+} release) and Ca^{2+} oscillations (Terentyev et al., 2003; Kubalova et al., 2004). Such enhancement of diastolic Ca^{2+} release is likely to be arrhythmogenic, since Ca^{2+} release at this time activates the inward mode NCX (see Section 1.11.2). It is well established that CSQ2 is anti-arrhythmic. Moderate reductions of CSQ2 increased susceptibility to stress induced arrhythmias in mice (Chopra et al., 2007). In humans, a number of mutations in the CSQ2 gene are linked to catecholaminergic polymorphic ventricular tachycardia (CPVT), a hereditary arrhythmogenic disease characterized by exercise or stress-induced syncope and sudden cardiac death (reviewed in Faggioni and Knollmann, 2012; Fernández-Velasco et al., 2012). In murine models of CPVT, animals exhibit arrhythmia upon adrenergic stimulation. At the cellular level, this arrhythmogenesis is associated with severe changes in Ca^{2+} handling including reduced SR load,

spontaneous Ca^{2+} release and Ca^{2+} oscillations, similar to the changes caused by CSQ2 knockdown/knockout (Knollmann et al., 2006; Rizzi et al., 2008; Alcalai et al., 2011). While the mechanisms underlying this disease are not completely understood, CPVT has been linked to a lack of, or alteration in, normal CSQ2-mediated channel modulation by luminal Ca^{2+} (Terentyev et al., 2003; Rizzi et al., 2008; Faggioni and Knollmann, 2012). Additionally, CSQ is a target for some pharmacological agents including trifluoperazine, tricyclic antidepressants and anthracyclines (discussed further in Section 1.12.3). These agents are able to diffuse into the SR (Kim et al., 2005b; Park et al., 2005b) and it is thought that CSQ2 contains a binding site for all three drug classes.

1.9.4 Triadin and Junctin

The RyR2 accessory proteins triadin and junctin were originally thought to have identical roles, which was to anchor CSQ2 to RyR2. It is now known that they have a far more dynamic role in EC coupling and that they independently influence this process. For simplicity, they will be discussed concurrently here.

1.9.4.1 Structure

Triadin and junctin span the SR membrane in skeletal and cardiac muscle and are thought to interact in the SR lumen with each other, with CSQ and with the RyR (Figure 1.10) (Zhang et al., 1997) Three cardiac specific isoforms of triadin have been identified (35, 40 and 75 kDa), with the 40 kDa, triadin-1 isoform the most abundant. A distinguishing feature of triadin-1 is its existence as a disulphide linked oligomer. Junctin is smaller than triadin-1 at 26 kDa, but shares sequence similarity with the N-terminal residues of triadin-1. Both proteins consist of a short cytoplasmic N-terminal segment, a single membrane spanning segment and a long, highly charged C-terminal tail (Zhang et al., 1997; Gyorke and Terentyev, 2008).

1.9.4.2 Function

It has been demonstrated that triadin and junctin bind to both CSQ and RyR and are thought to serve as anchoring proteins, connecting CSQ to the RyR. In addition, triadin-1, and to a smaller extent junctin, play a crucial role in maintaining the ultrastructure of the sarcoplasmic reticulum (Chopra et al., 2009; Boncompagni et al., 2012). It is thought that the combined presence of triadin-1, junctin and CSQ2 are essential in

maintaining proper EC coupling (Zhang et al., 1997; Gyorke et al., 2004; Beard et al., 2009). Identifying the specific roles of triadin-1, junctin and CSQ2 in knockout mouse models is complicated by coexisting changes in expression levels of other SR proteins. Commonly, knockout of one of these proteins also alters the expression of the other two (Chopra et al., 2007), in addition to RyR2, junctophilin, SERCA2A and FKBP12.6 (Chopra et al., 2009; Boncompagni et al., 2012).

Single channel studies have provided some insight into the function of triadin and junctin, although at present much more work has been done in skeletal then in cardiac preparations (reviewed in Beard et al., 2009). Junctin alone was found to mediate the inhibitory effect of CSQ1 on RyR1, suggesting independent roles for triadin and junctin in skeletal muscle EC coupling (Wei et al., 2009a). Earlier work in cardiac muscle suggested that the presence of all three proteins (i.e. triadin, junctin and CSQ2) is essential in conferring RyR2 responsiveness to changes in luminal Ca^{2+} (Gyorke et al., 2004). Recently, it was found that junctin can influence the luminal Ca^{2+} response of RyR2. Single channels from junctin knockout mice revealed a luminal Ca^{2+} dependent role for junctin, where at low luminal Ca^{2+} (<1 mM) junctin activates RyR2, while at higher luminal [Ca^{2+}] junctin inhibits RyR2 (Altschafl et al., 2011). The physiological implications of such regulation are unclear and it is possible that the results of this study were partially attributable to a loss of CSQ regulation of RyR2 (Dulhunty et al., 2012).

1.9.4.3 Roles in cardiac pathology

Studies using transgenic mice overexpressing triadin are also supportive of a more complex function for this protein. Overexpression of triadin in cardiomyocytes stimulated RyR2 activity, enhancing its sensitivity to activation by Ca^{2+} and increasing predisposition to arrhythmias (Terentyev et al., 2005). In another triadin overexpression model, myocytes exhibited cardiac hypertrophy, impaired response to β-adrenergic stimulation and altered Ca^{2+} transients (Kirchhefer et al., 2007). Severe SR restructuring, including a 50% reduction in dyad formation and stress induced arrhythmia, are observed in a triadin knockdown mouse model (Chopra et al., 2009). The clinical relevance of triadin knockdown and overexpression mouse models to humans has been indicated recently by the identification of 3 triadin mutations that cause CPVT (Roux-Buisson et al., 2012).

Changes in junctin expression also cause detrimental changes in cardiac phenotypes. Overexpression of junctin led to depressed myocyte contractility and altered SR Ca^{2+} release (Fan et al., 2007). Junctin knockout (without changes in expression of other SR proteins) also caused aberrant Ca^{2+} handling, increasing the SR load and inducing fatal arrhythmia (Yuan et al., 2007). While the precise roles of CSQ2, junctin and triadin are not fully understood, it is quite clear that the presence of all three proteins in complex with RyR2 and that the optimal functioning of each is vital in maintaining proper EC coupling.

1.10 Redox regulation of excitation-contraction coupling

1.10.1 Cardiomyocyte redox environment

The transfer of electrons in redox (oxidation/reduction) reactions provides the energy needed to build and maintain cellular structures. Electrons are transferred between oxidising agents (electron acceptors) and reducing agents (electron donors), hence in an oxidation reaction there is a loss of electrons as they are transferred from the moiety being oxidized to the oxidizing agent. The cellular redox environment is determined by the balance between oxidizing agents and antioxidant/reducing agents. In cardiomyocytes there are several redox buffer systems which maintain the cellular redox environment. These include the thioredoxin buffer system ($Trx(SH)_2$/TrxSS), the nicotinamide adenine dinucleotide phosphate system (NADPH/NADP+) and the glutathione system (2GSH/GSSG) (reviewed in Schafer and Buettner, 2001; Filomeni et al., 2002). Each couple consists of an oxidised member and a reduced member and these exchange electrons with each other and with other cellular components such as enzymes and proteins. The relative amount of each redox buffer drives the cell toward a more oxidised or a more reduced redox environment. Since GSH is present in concentrations 100 – 1000 fold greater than either the TRX or NADPH system, it is considered to be the principal cellular redox buffer system (Schafer and Buettner, 2001).

Redox state depends on the redox potential (tendency to gain or lose electrons) and the reducing capacity (number of electrons available for transfer) of a substance. In cardiomyocytes, the cytoplasm has a more reducing redox potential of approximately -220 mV, maintained by a large ratio of ≥30:1 of GSH to GSSG, which acts as an important defence against oxidation. In contrast, the reduction potential of the SR lumen

is significantly more oxidised with a redox potential of -180mV, maintained by a ratio of just 3:1 GSH to GSSG. The maintenance of these ratios that favour a more reduced cytoplasm is vital in protecting cellular components, including DNA, lipids and proteins against oxidative damage (Hwang et al., 1992; Feng et al., 2000; Pessah et al., 2002).

Aside from the oxidized members of the redox buffer systems (e.g. GSSG), the principle cellular oxidants are reactive oxygen species (ROS) which include hydrogen peroxide (H_2O_2), superoxide anions (O_2^-) and hydroxyl radicals (OH^-) and peroxynitrite anion ($ONOO^-$) a reactive nitrogen species (RNS). These agents are produced in several sites in cardiomyocytes by enzyme-mediated electron addition to molecular oxygen or nitric oxide. A schematic outlining the main sites and sources of ROS/RNS production is shown in Figure 1.11. The site of action of these molecules depends on the site of production and their stability and diffusion characteristics (Hool and Corry, 2007).

Traditionally, ROS/RNS have been viewed as being detrimental to cardiac health as their accumulation is implicated in the pathogenesis of many diseases including ischaemia-reperfusion injury and cardiac hypertrophy (reviewed in Hool and Corry, 2007; Hidalgo and Donoso, 2008; Santos et al., 2011). However, there is increasing evidence that low-moderate levels of ROS/RNS are important in many cell signalling pathways. Therefore, it is essential that a balance is maintained between ROS/RNS production and elimination. Cardiac muscle possesses several antioxidant defences which work at different stages of ROS/RNS production and elimination pathways, as outlined in Figure 1.11. In cardiomyocytes the most important of these defence systems are superoxide dismutase (SOD), glutathione peroxidase (GPX), catalase and GSH (Singh et al., 1995; Zima and Blatter, 2006; Hidalgo and Donoso, 2008). As a substrate for GPX, GSH acts as an electron donor to neutralize hydrogen peroxide (H_2O_2) and also functions as a scavenger of ROS, thereby protecting cellular targets from oxidation by these agents (Leichtweis and Ji, 2001; Dickinson and Forman, 2002).

1.10.2 Protein thiol modifications

The thiol groups (-SH) of cysteine residues are the most common targets on proteins for redox modification. Under physiological conditions, thiols have a high pKa which promotes their existence in the protonated state and are therefore relatively inert. A small number of thiols are more reactive, having a lower pKa which promotes their existence in the deprotonated state as thiolate anions (RS^-).

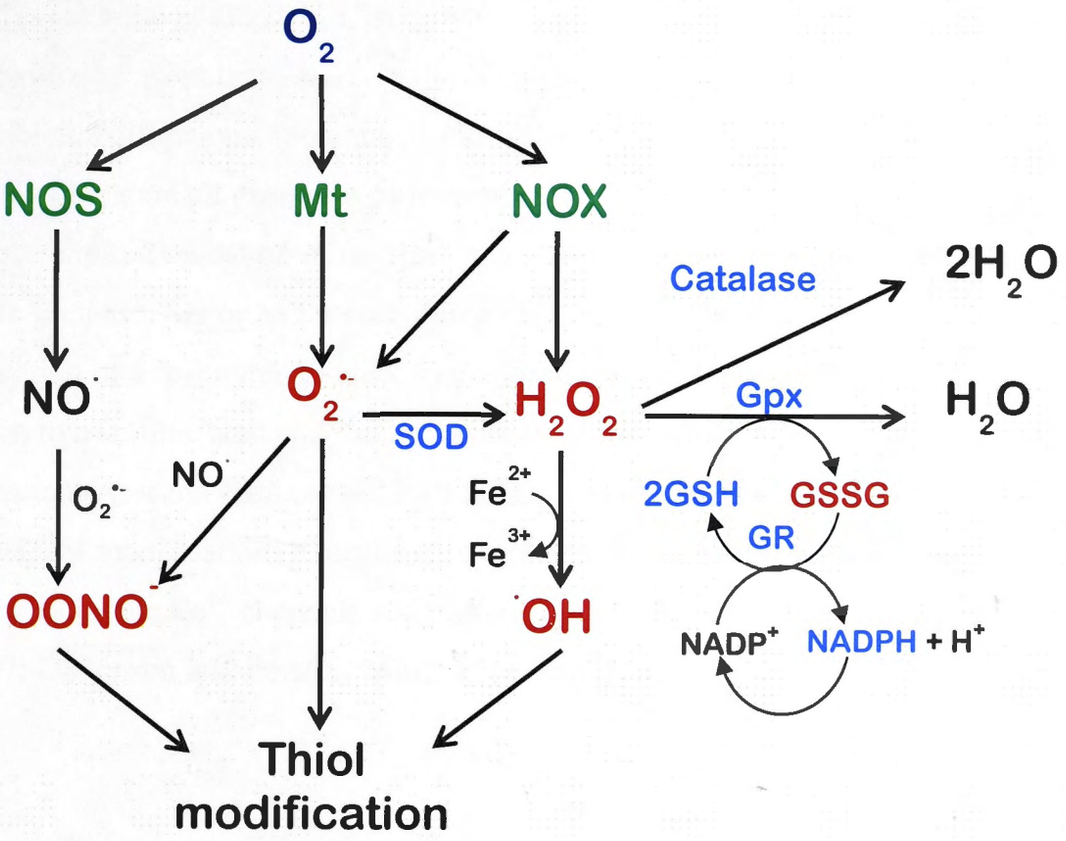

Figure 1.11 – Main pathways of ROS formation and breakdown. Using molecular oxygen (O_2) as a substrate, reactive oxygen species (ROS) including superoxide anion ($O_2^{\cdot-}$) and hydrogen peroxide (H_2O_2), are generated by the mitochondrial respiratory chain and NADPH-oxidases (NOX). Additionally nitric oxide, produced from nitric oxide synthases (NOS) combine with superoxide to produce peroxynitrite ($OONO^{--}$). Superoxide dismutase (SOD) dismutates superoxide to hydrogen peroxide which undergoes the Fenton reaction with ferrous iron (Fe^{2+}) to produce the highly reactive and unstable hydroxyl radical ($^{\cdot}OH$). Hydrogen peroxide is converted to water via either catalase or the glutathione peroxidase (GPX) pathways. Adapted from (Hidalgo and Donoso, 2008; Santos et al., 2011).

This substantially enhances the reactivity of these groups making them vulnerable to oxidative modification by ROS, reactive disulphides, quinones and other redox active molecules (Donoso et al., 2011a; Burgoyne et al., 2012; Wall et al., 2012). Depending on the oxidizing agent these reactive thiols can undergo various reversible or irreversible modifications, including δ-nitrosylation, δ-glutathionylation and disulphide formation which are all examples of reversible thiol modifications (Figure 1.12). These may require initial oxidation of the thiol to a sulfenic acid by ROS. If an appropriate substrate such as GSH or NO (or adjoining neighbouring thiol group) is not available for formation of a reversible modification, the sulfenic group may undergo subsequent oxidation to a sulfinic acid and finally a sulfonic acid, which is an irreversible modification (Aracena-Parks et al., 2006; Hidalgo and Donoso, 2008; Donoso et al., 2011a). Thiol modifications alter the structure and function of the protein and have been shown to modulate Ca^{2+} channels and transporters, NMDA receptors and IP_3R (Zable et al., 1997; Dickinson and Forman, 2002; Zima and Blatter, 2006).

1.10.3 Redox modification of RyR2

It is well recognised that RyRs are sensitive to redox active agents. These include anthracyclines and other quinone-containing compounds (Abramson and Salama, 1989; Ondrias et al., 1990; Pessah et al., 1990), ROS (Hidalgo et al., 2002; Feng et al., 2000; Oba et al., 2002), RNS (Xu et al., 1998; Hart and Dulhunty, 2000; Durham et al., 2008; Cutler et al., 2012) endogenous redox agents (including GSH, GSSG, NAD^+, NADH) (Zable et al., 1997; Cherednichenko et al., 2004; Hidalgo et al., 2005), and thiol-reactive agents (Zaidi et al., 1989; Eager et al., 1997). RyR2 contains 89 cysteine residues including 21 that contain unbound thiols and therefore vulnerable to redox active agents. A relationship is thought to exist between RyR channel activity and the number of available thiol groups (Sun et al., 2001; Zima and Blatter, 2006; Zissimopoulos and Lai, 2006). Generally, oxidising agents have a stimulatory effect on RyR activity, thought to be associated with their oxidation of thiol groups, whilst reducing agents have an inhibitory effect (Zaidi et al., 1989; Zable et al., 1997; Eager and Dulhunty, 1998; Hidalgo et al., 2002). There is however, evidence that RyR1 and RyR2 contain multiple classes of thiol groups which are thought to mediate the time and concentration dependent, biphasic modulation (activation followed by inhibition) of RyR caused by

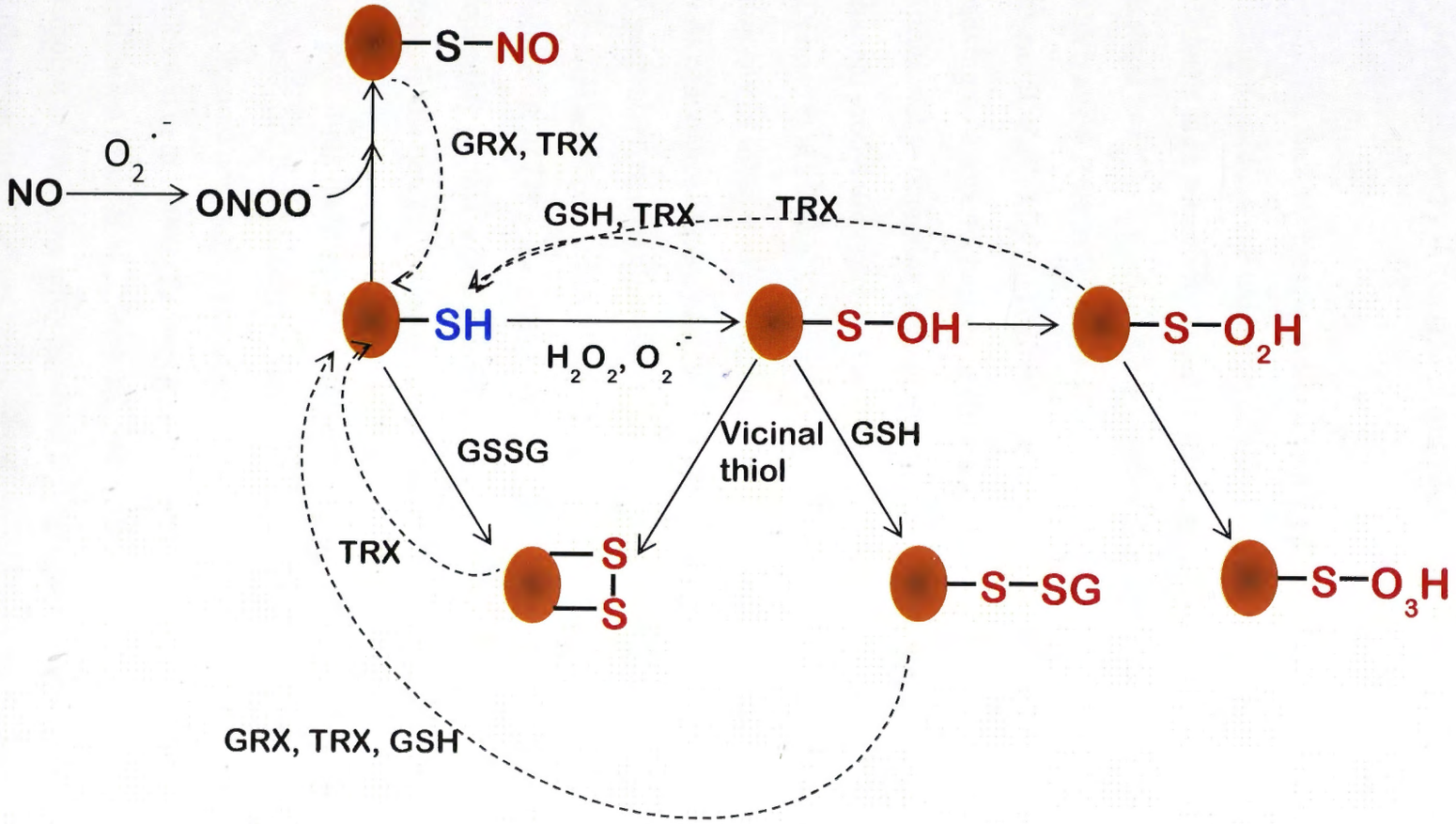

Figure 1.12 – Redox modifications of RyR thiol groups The thiol groups of cysteine residues are common targets of redox modifications including oxidation, S-nitrosylation, S-glutathionylation and intra/intermolecular disulphide formation. Glutathione (GSH), glutaredoxin (GRX) and thioredoxin (TRX) are able to reduce many of these products back to the thiol group (dashed lines) by a thiol-disulphide exchange reaction or by forming mixed disulfide products which are able to be reduced to the thiol by the enzyme glutathione reductase. Adapted from (Hidalgo and Donoso, 2008).

some agents (Liu et al., 1994; Eager et al., 1997; Eager and Dulhunty, 1999). It is thought that the the early activation phase is caused by oxidation of more reactive stimulatory thiols, while the later inhibitory phase is attributed to oxidation of the less reactive inhibitory thiols (Liu et al., 1994; Aghdasi et al., 1997; Eager et al., 1997; Sun et al., 2001).

Studies in skeletal muscle indicate that RyR1 contains a small number of highly reactive cysteine residues, the oxidation of which constitutes a possible mechanism for the channels high sensitivity to redox active agents (Liu et al., 1994). These residues are thought to act as a transmembrane redox sensor and have a defined redox potential, which allow RyR to adjust its activity in response to changes in the local redox potential. Ca^{2+}, Mg^{+} and caffeine are able to alter the redox potential of these thiols, causing subsequent changes in channel activity (Feng et al., 2000; Xia et al., 2000). Additionally, the redox state of these thiols has been found to determine the response to channel modulators such as Ca^{2+}, Mg^{+}, caffeine, adenine nucleotides and CLIC-2 (Donoso et al., 2000; Xia et al., 2000; Oba et al., 2002; Jalilian et al., 2008b). The majority of these studies were done on skeletal SR vesicles and to date, an equivalent class of hyperreactive cysteines in RyR2 has not been defined. Alternatively, it has been hypothesized that modulation of RyR2 gating in response to changes in local redox potential are mediated by electron transfer between redox active agents and the reactive thiols of RyR2 (Pessah et al., 2002; Marinov et al., 2007). Changes in RyR2 gating depending on this redox sensitivity are thought to be potentiated in times of oxidative stress in the heart (Feng et al., 2000; Pessah et al., 2002).

It is becoming increasingly evident that redox modifications could contribute to RyR2 dysfunction. Indeed, several studies have found that RyR2 oxidation is elevated in pathological conditions including various modes of heart failure (Terentyev et al., 2008; Belevych et al., 2009; Belevych et al., 2011), in CPVT (Shan et al., 2012) and atrial fibrillation (Vest et al., 2005). Recently it has been revealed that β-adrenergic stimulation promotes mitochondrial ROS production upon electrical pacing of rabbit cardiomyocytes. The authors were able to attribute the onset of spontaneous Ca^{2+} waves with ROS induced oxidation of RyR2 (Bovo et al., 2012). This finding is important as it suggests that some of the effects of chronic β-adrenergic stimulation previously attributed to phosphorylation may be at least partially due to oxidation. While an association between luminal Ca^{2+} sensitivity and RyR2 oxidation has been observed in

these pathological settings there are only limited studies directly testing the dependence of activation by luminal Ca^{2+} on redox modification of RyR2.

Redox modification of RyR shifts the channel's cytoplasmic Ca^{2+} sensitivity. (Marengo et al., 1998) found that regardless of the RyR isoform, the presence of reducing agents decreased channel activity and allowed the channel to be inhibited with addition of cytoplasmic Ca^{2+}. Conversely, oxidation increased RyR2 activity and enhanced the sensitivity of the channel to activation by cytoplasmic Ca^{2+}. Similar studies utilising GSH:GSSG ratios to set a defined redox potential, conditions promoting thiol oxidation (more positive redox potentials) caused an increase in sensitivity to activation by cytoplasmic Ca^{2+} (Xia et al., 2000; Oba et al., 2002).

1.10.4 Redox modification of SERCA2A

SERCA2A contains 26 cysteine residues, the majority of which reside in the 3 cytoplasmic domains of the protein. It has long been known that SERCA is vulnerable to redox agents including H_2O_2 (Morris and Sulakhe, 1997; Kaplan et al., 2003), NEM (Yoshida and Tonomura, 1976; Yamada and Ikemoto, 1978) peroxynitrite (Sharov et al., 2006), DTNB (Morris and Sulakhe, 1997) and hydroxyl radical (Xu et al., 1997) which cause substantial inhibition of Ca^{2+} uptake (reviewed in Zima and Blatter, 2006; Hidalgo and Donoso, 2008). On the other hand, in the presence of GSH, low concentrations of peroxynitrate promoted *S*-glutathionylation of key cysteine residues which stimulated SERCA2A activity in smooth muscle (Adachi et al., 2004). It is thought that as few as 1 - 3 thiols of the total 26 in SERCA2A (or 24 thiols in SERCA1A) are important for mediating the functional effects of oxidizing agents on SERCA function (Yoshida and Tonomura, 1976; Adachi et al., 2004; Sharov et al., 2006). The mechanisms of oxidation-induced changes in SERCA function are unclear. It has been found that inhibition of Ca^{2+} uptake by DTNB and H_2O_2 is due to a reduction in the maximal velocity of Ca^{2+} uptake, with no effect on Ca^{2+} affinity (Morris and Sulakhe, 1997; Kaplan et al., 2003). Since these key residues (particularly Cys-674) are not localized near the Ca^{2+} binding sites on SERCA2A, it has been suggested that the effects of thiol oxidation are due to general effects on protein structure which uncouple ATP hydrolysis from Ca^{2+} translocation (Sharov et al., 2006).

1.10.5 Redox modification of LTCC

LTCC are also vulnerable to oxidation. The α_1 subunit contains 48 cysteine residues (Hool and Corry, 2007), though as few as 10 may be available for redox modification (Zima and Blatter, 2006). The functional effects of oxidation and reduction of these cysteines is variable and complex. Some investigators have found that oxidation inhibits I_{Ca} (Lacampagne et al., 1995) while others find that oxidizing agents enhanced I_{Ca} (Campbell et al., 1996 and reviewed in Zima and Blatter, 2006; Hool and Corry, 2007). The variation in functional outcomes found by these and other investigators could be due to differences in the type of oxidizing agent and the concentration and duration of exposure. Interestingly, the redox state of LTCC cysteines has been found to mediate hypoxia induced increases in channel sensitivity to β-adrenergic stimulation (Hool, 2000). Hence, while the direct functional effects of oxidative modification of LTCC are unclear, it is evident that redox regulation of this channel could have an important role in EC coupling.

1.11 Ca^{2+} signalling in health and disease

1.11.1 Whole cell Ca^{2+} signalling

It is important to consider Ca^{2+} handling in the context of whole cell Ca^{2+} signalling, given that RyR2 activity is regulated by so many cytoplasmic and luminal factors. The open probability of RyR2 must be high during systole for maximal Ca^{2+} release and very low during diastole for efficient Ca^{2+} accumulation in the SR and to avoid promoting arrhythmogenesis (see Section 1.11.2). The cytoplasmic [Ca^{2+}] ranges from 0.1 – 1 μM while the luminal [Ca^{2+}] cycles between ~ 0.3 mM and 1 - 1.5 mM (Bers, 2002b; Shannon et al., 2003a) during systole and diastole, respectively. It has been shown that there is a steep relationship between SR load and both systolic (Bassani et al., 1995b; Shannon et al., 2000) and diastolic Ca^{2+} release (Shannon et al., 2002). The higher RyR activity at increased SR Ca^{2+} loads is thought to arise from enhanced sensitivity of RyR2 to luminal Ca^{2+} (Shannon et al., 2000; Shannon et al., 2003a). A study by Bode and colleagues (2011) found that reduced SERCA activity caused a drastic decrease in RyR Ca^{2+} release, despite only a minor reduction in SR content. The authors hypothesised that this was due to the steep dependence of RyR Ca^{2+} release on SR load. That is, only a small decrease in SR content is required to reduce SR Ca^{2+}

release so that SR Ca^{2+} release matches the lower SR Ca^{2+} uptake (Bode et al., 2011, reviewed in Eisner et al., 2013).

Elemental Ca^{2+} release occurs as sparks (Cheng et al., 1993). When a Ca^{2+} spark occurs there is a depletion of Ca^{2+} from the release site inside the junctional SR. Measurement of these local depletions, or blinks, have revealed that diffusion of Ca^{2+} through the SR is relatively fast, which limits regions of Ca^{2+} depletion or accumulation under normal conditions. However, with increased spontaneous Ca^{2+} release there can be significant variability in Ca^{2+} diffusion at local release sites, and an arrhythmogenic substrate may develop. That is, there is an increased potential for arrhythmic activity (Picht et al., 2011). It has been found that once SR [Ca^{2+}] falls to 0.3 - 0.5 mM or 40 – 50 % of its diastolic volume, neither Ca^{2+} sparks or stimulated Ca^{2+} release occur (Shannon et al., 2003a; Zima and Blatter, 2006; Guo et al., 2010) indicating RyR Ca^{2+} release terminates well before the SR is depleted. These data illustrate the sensitivity of RyR2 regulation by luminal Ca^{2+}. As discussed (Section 1.9.3 and 1.9.4), several factors in the SR lumen have a substantial effect on RyR2 channel activity, including accessory proteins, redox potential and the SR Ca^{2+} load.

It can be said that there are two Ca^{2+} cycles in cardiomyocytes, one involving Ca^{2+} movement across the sarcolemma and another involving Ca^{2+} movement in and out of the SR (Katz, 2006). Under normal conditions, a balance is maintained so Ca^{2+} that enters via the LTCC upon depolarization is removed via the NCX during diastole. Similarly, the amount of Ca^{2+} that is released from the SR by RyR2 during systole is equivalent to what it taken up via SERCA during diastole (Trafford et al., 2000). Thus in the healthy heart, cellular Ca^{2+} homeostasis is maintained with no net change in [Ca^{2+}] in any of the cellular compartments from one beat to the next.

It should be noted though that the actions of sarcolemmal ion channels influence the activity of SR ion channels (for example in CICR) and vice versa. This is evident in the way the SR [Ca^{2+}] is 'autoregulated', so that if Ca^{2+} flux through one channel or transporter is altered, other Ca^{2+} fluxes will compensate, and overall Ca^{2+} flux balance is maintained (Dibb et al., 2007). The mechanisms contributing to this process were quantified by Trafford & colleagues (2000) who showed that in the presence of the RyR2 agonist caffeine, Ca^{2+} release is only enhanced temporarily before returning to baseline levels. The initial enhanced release via RyR activates NCX, causing an overall

loss of Ca^{2+} from the cell and from the SR. A reduction in store load causes the following Ca^{2+} transients to be decreased in size until the SR load can recover. This is facilitated by Ca^{2+} influx via LTCC, which is increased to balance the increased Ca^{2+} efflux via NCX (Trafford et al., 2000). Thus, Ca^{2+} homeostasis is re-established. Conversely, conditions that alter multiple targets involved in Ca^{2+} signalling are thought to alter the set point at which Ca^{2+} flux balance occurs (reviewed in Eisner et al., 2013). Modifications that increase this set point would be likely to increase contractile function but have an increased risk of arrhythmogenesis and cell death due to Ca^{2+} overload, while modifications that reduce the set point would reduce contractility. Some of the effects of altered Ca^{2+} homeostasis in pathological conditions are discussed below.

1.11.2 Changes in Ca^{2+} handling in cardiac disease

In recent years there has been a huge amount of evidence suggesting altered RyR2 function and changes in SR Ca^{2+} handling in general are important in several pathological conditions including heart failure, sudden cardiac death and several forms of arrhythmia. In the context of the SR autoregulation discussed in the previous section, altered RyR2 activity alone would be unlikely to cause any sustained change in cardiac function. Indeed, there are many examples of human and animal models of the aforementioned conditions, where altered RyR2 function coexists with changes in protein expression, post-translational modifications or altered protein-protein interactions.

Heart failure is an excellent example of such a condition, where there are changes in protein expression, combined with chronic β-adrenergic signalling and altered RyR2 function. Common findings of heart failure include (but are not limited to) impaired contractility, reduced peak systolic Ca^{2+} release, increased diastolic Ca^{2+} release and reduced SR store load. The exact mechanisms underlying these changes are complex and in some cases controversial. It is generally agreed that RyR2 undergoes some form of protein modification causing a reduced threshold for RyR2 activation by luminal Ca^{2+} (Kubalova et al., 2005) and enhanced diastolic leak (Shannon et al., 2003b). Whether this increased sensitivity though is caused by CaMKII (Ai et al., 2005; Fischer et al., 2013) or PKA (Marx et al., 2000; Wehrens et al., 2003) mediated phosphorylation, increased oxidation (Terentyev et al., 2008; Belevych et al., 2011), impaired nitrosylation (Gonzalez et al., 2007), FKBP dissociation (Marx et al., 2000) or

a combination of several of these effects is a contentious area of research. It is possible that differential results may arise from different animal models, aetiologies and experimental protocols. The observation that the SR Ca^{2+} load decreases in heart failure is consistent with the fact that RyR2 leak is increased during diastole. This is compounded by changes in SERCA and NCX expression. As detailed in Section 1.7.1.6, in the failing heart, it is often found that SERCA is downregulated, contributing to the reduced ability of the SR to accumulate Ca^{2+}, and the NCX is upregulated. As a consequence the NCX/SERCA extrusion balance is altered, and as such a greater fraction of cytoplasmic Ca^{2+} is extruded from the cell via NCX (Bers, 2008). As mentioned previously (Section 1.7.1.6) there may also be a reduction in the expression or phosphorylation status of phospholamban both of which would promote SERCA2A inhibition.

As well as contractile failure, many of the aforementioned changes in Ca^{2+} handling are associated with arrhythmia, which is a prevalent cause of sudden death in patients with heart failure. This is believed to occur as a result of enhanced diastolic activity, which greatly increases cytosolic [Ca^{2+}], activating the forward mode NCX (Ca^{2+} efflux) (Pogwizd et al., 2001). The influx of Na^{+} depolarizes the surface membrane and if great enough triggers a delayed afterdepolarization (DAD). These events are associated with aberrant diastolic Ca^{2+} release and cytoplasmic Ca^{2+} overload (Bers, 2001). A similar mechanism has also been proposed for certain types of early afterdepolarizations (EADs). EADs are more likely to occur though with prolonged action potentials. While certain types of EADs are associated with NCX and Ca^{2+} overload mechanisms, other types are associated with reactivation of I_{Ca} (Figure 1.13) (Xie et al., 2013). These afterdepolarizations cause uncoordinated action potentials and arrhythmia. Afterdepolarisations are also implicated in CPVT which is linked to mutations in RyR2, CSQ2 and (most recently discovered) triadin (Jiang et al., 2005; Faggioni and Knollmann, 2012; Roux-Buisson et al., 2012). In CPVT, arrhythmia arises following exercise or stress-induced β-adrenergic stimulation. Mutations in proteins of the Ca^{2+} release complex are thought to lower the threshold for RyR2 activation (Jiang et al., 2004; Lehnart et al., 2004) or cause SR overload (Kashimura et al., 2010), the effects of which, at rest, appears to be asymptomatic. β-adrenergic stimulation induces enhanced Ca^{2+} signalling, resulting in increased store load and excess diastolic Ca^{2+} release which greatly increases cytosolic [Ca^{2+}], activating the forward mode NCX (Pogwizd et al., 2001) and causing DADs.

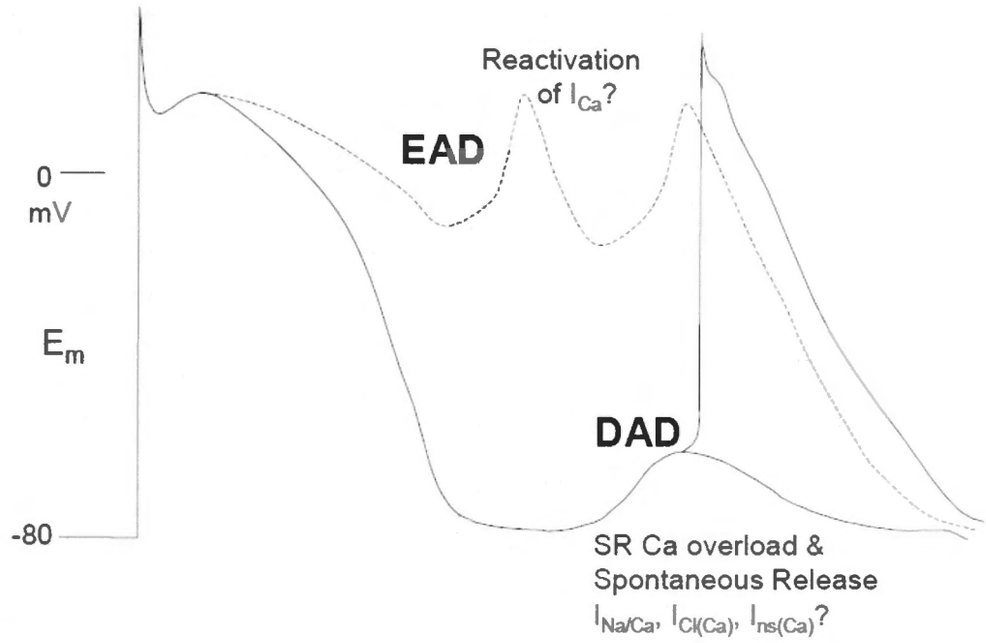

Figure 1.13 – Triggered activity in cardiomyocytes. Afterdepolarizations occur following the ventricular action potential and may occur after the membrane potential has completely repolarized but before the next action potential (delayed afterdepolarization, DAD), or before the completion of repolarization (early afterdepolarization, EAD). The cellular basis of these differs, with DADs more associated with SR Ca^{2+} overload resulting from diastolic Ca^{2+} release or Ca^{2+} alternans, while EADs are linked to reactivation of I_{Ca}. Figure from (Bers, 2001).

In some CSQ2-linked CPVT mutations, the SR buffering capacity is reduced or its ability to regulate RyR2 activity is compromised. It is evident that normal protein-protein interactions within the lumen of the SR are essential for the precise regulation of RyR2 during diastole that maintains and fine tunes the Ca^{2+} release processes essential for normal cardiac function. The central role of RyR2 in arrhythmogenesis makes it a potential target for antiarrhythmic therapy (McCauley and Wehrens, 2011).

1.12 Anthracyclines

1.12.1 History and clinical use

Anthracyclines are a class of cytotoxic agents first isolated from cultures of *Streptomyces* var. *Peucetius* in the 1960s. Since then, anthracyclines, including doxorubicin and daunorubicin, have come to be recognized as some of the most effective chemotherapeutic agents ever developed. According to the National Cancer Institute, doxorubicin is approved either alone or in combination for the treatment of acute lymphoblastic leukaemia, acute myelogenous leukaemia, breast cancer, gastric cancer, hodgkin lymphoma, neuroblastoma, non-hodgkin lymphoma, ovarian cancer, small cell lung cancer, soft tissue and bone sarcomas, thyroid cancer, transitional cell bladder cancer and Wilms tumor. Daunorubicin on the other hand has a much lower spectrum of activity, primarily used for acute nonlymphocytic leukemia or lymphocytic leukaemia in children.

Administration of anthracyclines via bolus intravenous injection results in initial plasma concentrations of approximately 5 μM, which declines rapidly to submicromolar concentrations in in less than 1 hour (Gewirtz, 1999). While the plasma concentration dissipates relatively quickly, anthracyclines have a long half-life in tissues of the body, accumulating in certain organs, including the heart, and attaining concentrations many fold higher than those measured in the plasma (Cusack et al., 1995). This long half-life is promoted by the anthracycline structure. Daunorubicin and doxorubicin are small, flat and amphipathic compounds that are very similar in structure and are known to easily cross cell membranes (Regev and Eytan, 1997). A tetracyclic ring, consisting of adjacent quinone and hydroquinone groups, and a daunosamine sugar moiety constitute the bulk of the structure (Figure 1.14).

Figure 1.14 – Half-life and structural characteristics of anthracyclines and their metabolites. **(A)** Comparison of clearance of doxorubicin and doxOL from a strip of human atrial tissue over time (from Menna et al., 2012) **(B)** Two electron reduction of the carbonyl side chain (solid green box) of daunorubicin yields the secondary alcohol metabolite daunorubicinol and doxorubicinol (dashed green boxes). These metabolites have been shown to be more potent in impairing SR function and are able to accumulate in the heart. The quinone moiety (solid blue box) of daunorubicin and doxorubicin is known to be essential in mediating the cardiotoxic effects of these drugs. The daunorubicin analogue, 5-iminodaunorubicin has an imine (dashed blue box) in place of the quinone and is less potent in reducing cardiac contractility and disrupting SR Ca^{2+} handling than the parent compound. Chemical structures created by (ChemIDplus).

A

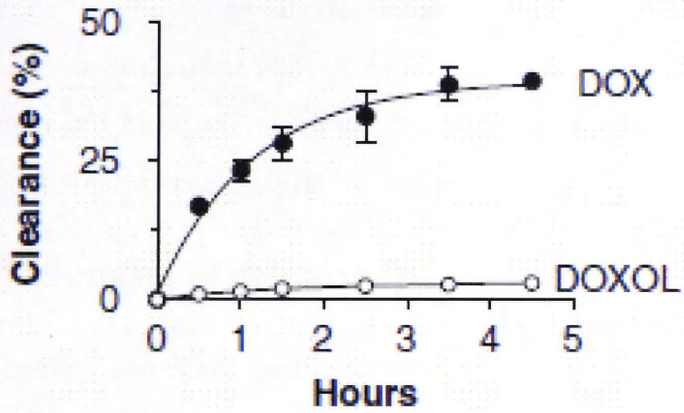

B

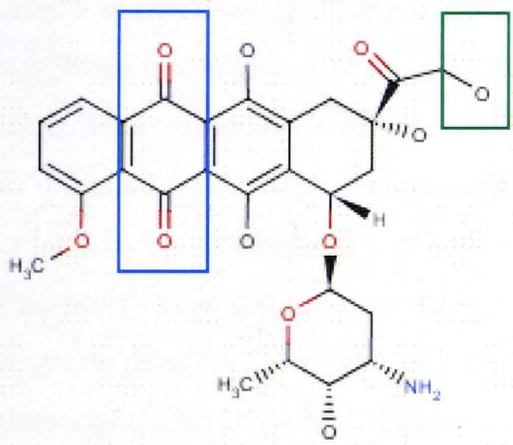

Doxorubicin

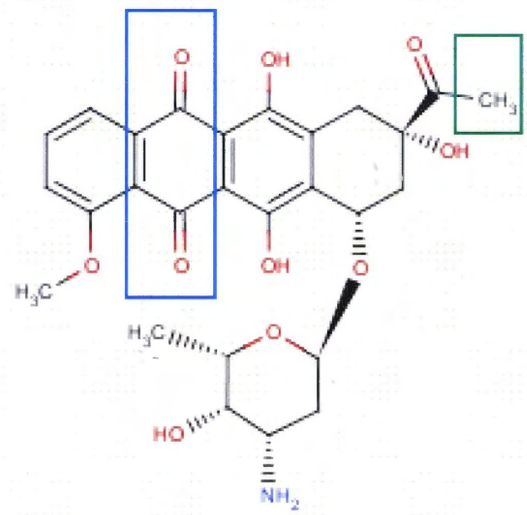

Daunorubicin

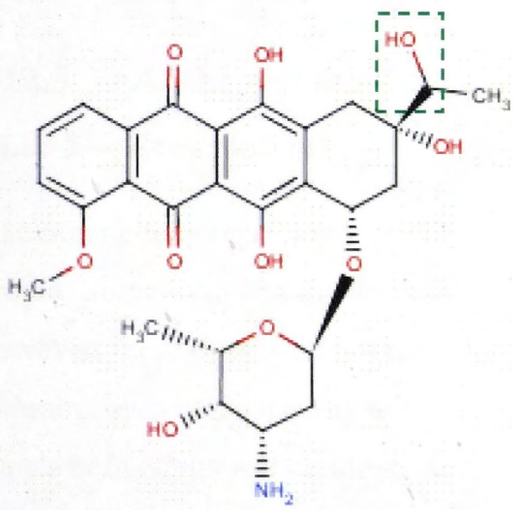

Daunorubicinol

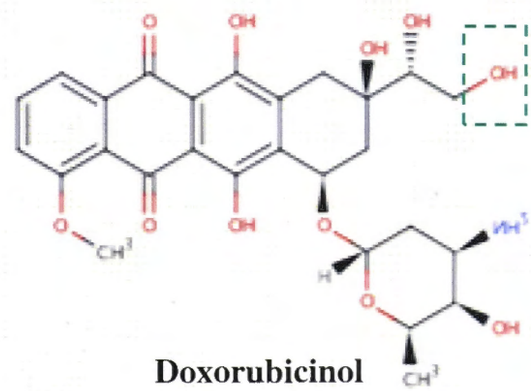

Doxorubicinol

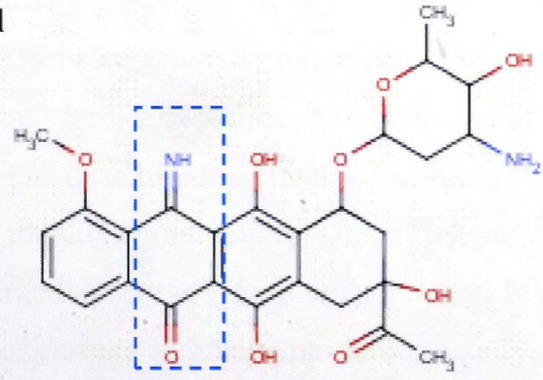

5-iminodaunorubicin

Only a difference in side chains differentiates the two drugs, with the doxorubicin side chain terminating with a primary alcohol and the daunorubicin side chain with a methyl group (Minotti et al., 2004; Menna et al., 2007a). This minor difference is thought to account for the different spectrum of activities of the two drugs (Sacco et al., 2003).

1.12.2 Mechanism of cytotoxicity

Despite their use as chemotherapeutic agents for several decades, the detailed mechanism of their cytotoxicity is uncertain. Much of the research is complicated by the use of high drug concentrations that are not clinically relevant. In a comprehensive review of literature regarding the antitumour mechanism of anthracyclines it was suggested that any studies using anthracycline concentrations $\geq 2 - 4$ μM should be interpreted cautiously (Gewirtz, 1999). These values reflect the maximum concentration of drugs achieved in the plasma after bolus administration. Additional confusion is created by the heterogeneity of cell models used for these types of studies. Therefore, the specific mechanisms of anthracycline cytotoxicity are unclear. Strong evidence supports roles for DNA intercalation, interference with DNA strand separation (via an interaction with DNA helicase), oxidative damage to DNA, and perhaps the best supported pathway, inhibition of topoisomerase II, with subsequent prevention of DNA repair (reviewed in Gewirtz, 1999; Minotti et al., 2004; Barrett-Lee et al., 2009).

1.12.3 Anthracycline-induced cardiotoxicity

1.12.3.1 Presentation

Like other chemotherapeutic agents, anthracyclines have many side effects including nausea, immunological impairment and poor wound healing (Asmis et al., 2005). However, these effects do not limit the use of the drugs. Rather the therapeutic index of anthracyclines is reduced by the existence of a potentially fatal cardiotoxicity that affects both adults and children. Acute cardiotoxicity can occur during the drug administration and usually presents as ECG abnormalities (often asymptomatic) and arrhythmias. These effects are generally minor and resolve themselves without intervention and as such are not cause for ceasing treatment (Horenstein et al., 2000; Pfeffer et al., 2009). The dose limiting effects of anthracyclines include dilated cardiomyopathy and impaired contractility, which first presents as reduced left ventricular ejection fraction. These effects are precursors to congestive heart failure and constitute late onset or chronic anthracycline cardiotoxicity. There is a large variation in

A

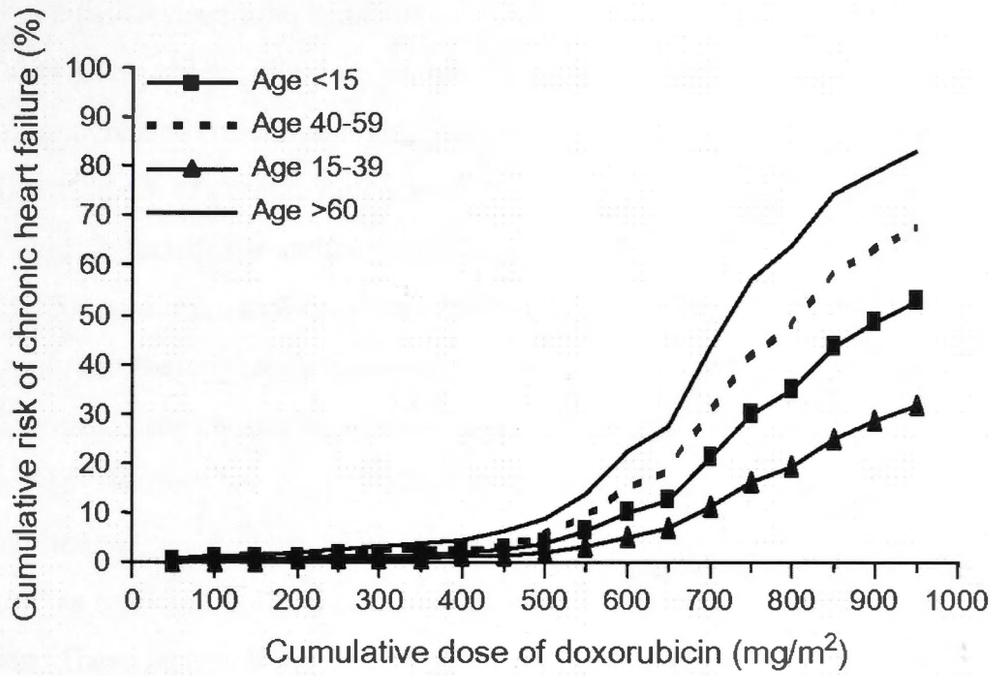

B

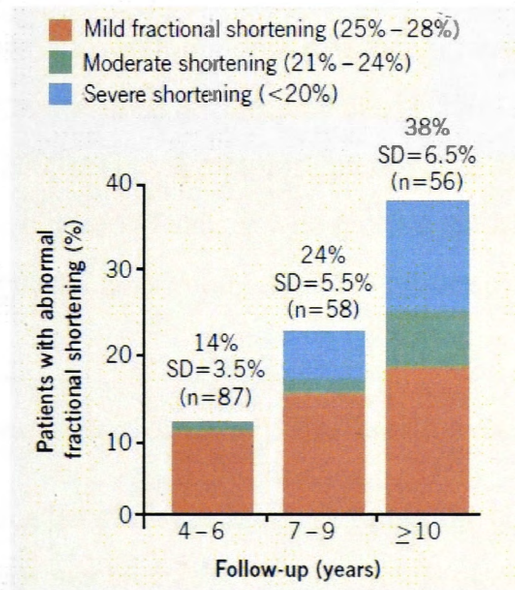

Figure 1.15 - Progression and risk of anthracycline-induced cardiotoxicity **(A)** As the cumulative dose of doxorubicin increases above 500 mg/m^2 there is a drastic increase in the risk of chronic heart failure. The graph also shows that patients < 15 yrs or >60 years of age are at increased risk. Figure from (Barrett-Lee et al., 2009) **(B)** As the duration of patient monitoring after completion of anthracycline treatment increases, there's an increased occurrence of cardiac dysfunction, measured by % fractional shortening i.e. contractile function, with a pronounced increase in patients with severe contractile impairment (blue columns). Figure from (Pfeffer et al., 2009).

the onset and severity of symptoms with cardiac dysfunction appearing anywhere from several months to years after cessation of treatment (Steinherz et al., 1991; Barrett-Lee et al., 2009). The observation in one study that the incidence of reduced fractional shortening increased over time highlights the need for prolonged follow up periods with careful assessment of cardiac function (Figure 1.15B) (Steinherz et al., 1991). Additional risk factors for anthracycline toxicity include age (< 15 and > 60 years) (see Figure 1.15), co-administration with certain drugs (e.g. paclitaxel and trastuzumab), concurrent radiotherapy, the existence of co-morbidities such as hypertension, liver disease, pre-existing cardiac conditions and the total cumulative dose of drug received (Figure 1.15) (Barrett-Lee et al., 2009; Pfeffer et al., 2009). Because of these effects, the use of anthracyclines is restricted and it is current practise to limit cumulative doses to 500mg/m^2 in total and not to administer these to anyone with a pre-existing heart condition. These factors limit the dosage of the drugs and the number of eligible patients (Airoldi et al., 2011; Octavia et al., 2012).

In children, doses as low as 100 mg/m^2 have been associated with cardiac abnormalities (Menna et al., 2008) and there is a striking increase in the incidence of heart failure when the cumulative anthracycline dose is increased above 250 - 300 mg/m^2 (Kremer et al., 2001; Mulrooney et al., 2009). That symptoms can develop decades after the end of treatment means survivors of childhood cancer who receive anthracyclines face a high risk of developing cardiac symptoms as young adults (Mulrooney et al., 2009; Trachtenberg et al., 2011).

1.12.3.2 Proposed mechanisms of anthracycline cardiotoxicity

Although there have been decades of research investigating the underlying cause, there is no consensus on a molecular mechanism for anthracycline cardiotoxicity. The structural characteristics of the drugs enable them to have a long half-life in the body (Cusack et al., 1995). Many cellular components have been hypothesised to have a role in anthracycline cardiotoxicity. Some of these include: calpain-induced dystrophin disruption (Campos et al., 2011) and titin degradation and necrosis (Lim et al., 2004); RyR modulation (Ondrias et al., 1990; Olson et al., 2000; Hanna et al., 2011); SERCA2A inhibition (Boucek et al., 1987; Olson et al., 1988); Na/K ATPase inhibition (Boucek et al., 1987); NCX1 inhibition (Boucek et al., 1987); altered CSQ2 function (Park et al., 2004; Kim et al., 2005b); mitochondrial dysfunction (Boucek et al., 1987; Olson et al., 2000; Kuznetsov et al., 2011); altered β-adrenergic signalling (Calderone et

al., 1991; Nagami et al., 1997; Fajardo et al., 2006) and induction of apoptotic signalling pathways (reviewed in Minotti et al., 2004; Sawyer et al., 2010). Many of these factors can be linked to two central themes: oxidative stress and altered Ca^{2+} handling, which are discussed in more detail below.

1.12.3.2.1 Anthracyclines and oxidation

Oxidative stress-mediated cell damage is the most cited hypothesis of anthracycline induced cardiotoxicity. The quinone moiety of anthracyclines readily undergoes redox cycling (Figure 1.16), which can be catalysed by many enzymes including cytochrome P-450, xanthine dehydrogenase and NADH dehydrogenase (Minotti et al., 2004). One electron addition to the quinone converts the drug to a semiquinone derivative, which regenerates the parent compound by reducing O_2 to O_2^- and H_2O_2 (Davies et al., 1983; Berthiaume and Wallace, 2007; Simunek et al., 2009).

The role of ROS in anthracycline-induced cardiotoxicity is supported by experiments showing that antioxidant treatment in rodents attenuated the cardiotoxic side effects of these drugs (Bast et al., 2007) and by studies using transgenic mice overexpressing cellular antioxidants (Cole et al., 2006). ROS production by anthracyclines has been repeatedly demonstrated *in vivo*, commencing immediately with anthracycline exposure and continuing in a time-dependent manner (Davies and Doroshow, 1986; Kim et al., 2006; Sag et al., 2011). The heart has low levels of antioxidant enzymes, particularly catalase which has been reported to be expressed at levels 50 - 150 times lower in the heart than in other organs. Thus cardiac muscle is particularly susceptible target to anthracycline induced ROS formation (Doroshow et al., 1980; Chen et al., 1994).

In further support of a ROS based mechanism is the finding that cardiotoxic side-effects of anthracyclines depend on the presence of the quinone moiety (Menna et al., 2007b). Studies comparing the effects of daunorubicin to its quinone-deficient analogue 5-iminodaunorubicin (5-ID, Figure 1.13) found that daunorubicin was far more potent in impairing contractility and stimulating Ca^{2+} release from SR vesicles (Shadle et al., 2000a) and modulating RyR2 activity (Pessah et al., 1990; Olson et al., 2000). Anthracyclines also generate ROS through iron-mediated pathways. As shown in Figure 1.11, ferrous iron is a substrate for the Fenton reaction, in which OH^- are produced from H_2O_2. Normally iron is complexed with the storage protein ferritin, however O_2^-, as produced from redox cycling of anthracyclines, can promote the release of iron.

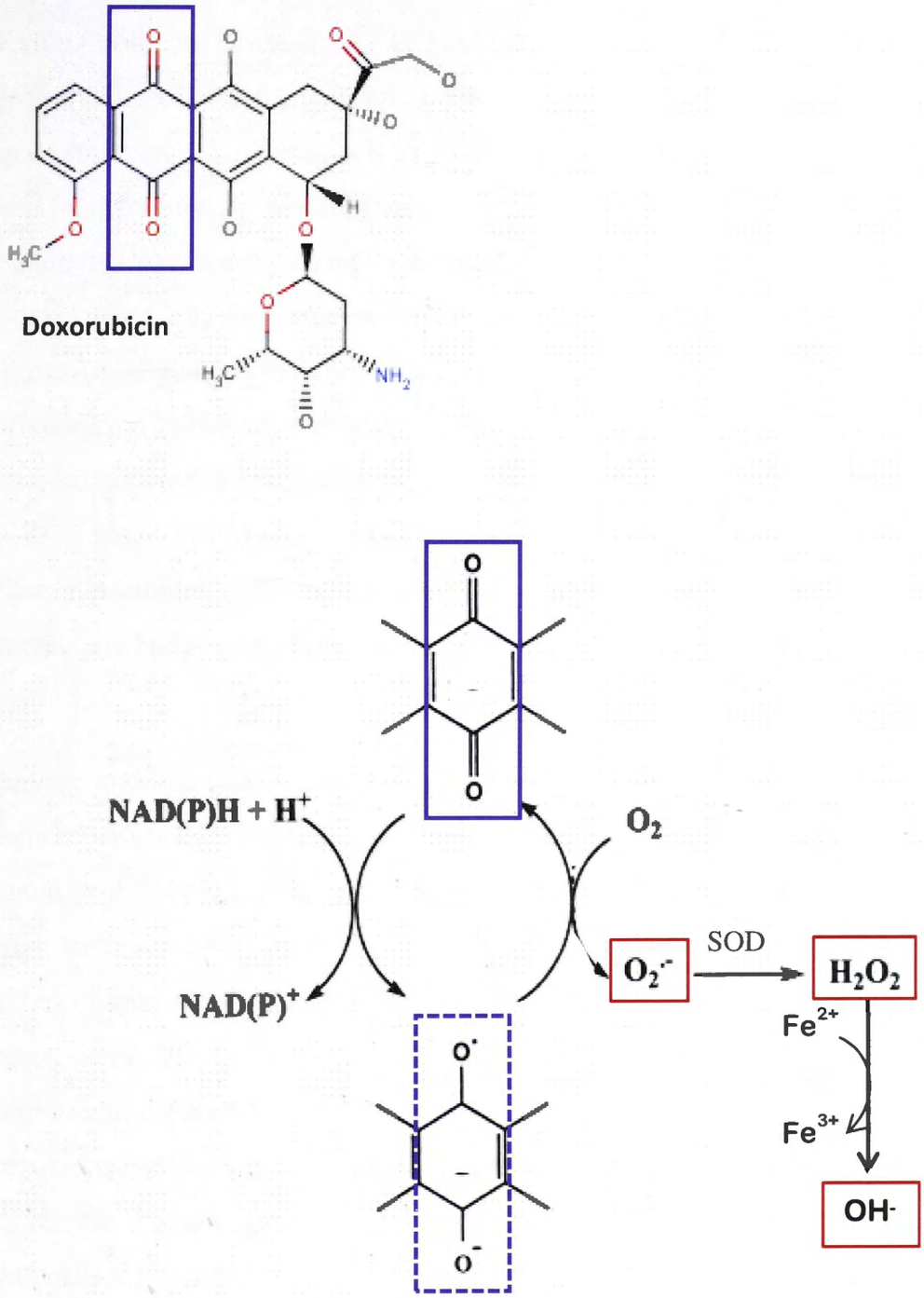

Figure 1.16 – Redox cycling of anthracyclines. One electron reduction of the quinone group in anthracyclines, such as doxorubicin (included for reference) yields a semi-quinone derivative. Oxidation of the semi-quinone with molecular oxygen regenerates the parent compound and produces superoxide anion ($O_2^{\cdot-}$) and hydrogen peroxide (H_2O_2). Formation of the hydroxyl radical ($OH^{\cdot}$) via the Fenton reaction is promoted by the release of iron from its complex with ferritin. Iron complexed with anthracyclines can also act as a substrate in the Fenton reaction. Figure modified from (Minotti et al., 2004)

Additionally, anthracyclines can form complexes with ferric iron, which can be reduced to ferrous iron and, as above, act as a substrate for the Fenton reaction. The importance of iron-mediated ROS formation is supported by the efficacy of the cardioprotective drug dexrazoxane. This drug acts as an iron chelator and is believed to prevent cardiac side-effects by binding free iron and preventing the formation of iron-anthracycline complexes. Dexrazoxane is approved by the United States Food and Drug Administration and the European Medicines Agency as a preventative treatment for cardiomyopathy and is the only officially approved treatment for anthracycline cardiotoxicity. However, a review of clinical trials found that a third of patients who were administered dexrazoxane still developed heart failure, suggesting the existence of non-ROS based mechanisms (van Dalen et al., 2006). Furthermore, it is not approved for use in paediatric patients and is only recommended for use in patients with advanced or metastatic breast cancer who have received a cumulative doxorubicin dose of 300 mg/m^2.

There are important caveats in the oxidative stress hypothesis. The cardioprotective effects of antioxidants in rats and mice were not replicated in large animals or humans (Menna et al., 2007a). This may relate to differences in the models of cardiotoxicity, though are consistent with the disappointing outcomes of clinical trials investigating the efficacy of antioxidant supplements and cardiovascular disease in humans (Kris-Etherton *et al.*, 2004). Furthermore, Shadle and colleagues (2000) found that daunorubicin induced SR Ca^{2+} release and impaired cardiac contractility in a ROS–independent mechanism, while in other studies daunorubicin-induced inhibition of SR Ca^{2+} release was not prevented by pre-treatment with DTT (although this did occur in single channel experiments – see below) (Olson et al., 2000). Furthermore, the time course of cardiac dysfunction does not appear to correlate with a ROS based mechanism, but relate more to increasing concentrations of the primary metabolites (Olson and Mushlin, 1990). While this evidence doesn't exclude a ROS-based mechanism, it points to a need for a better understanding of the mechanisms and targets of anthracycline-induced ROS formation.

Anthracyclines also promote oxidation through non-ROS based pathways. Doxorubicin and other quinone containing compounds have repeatedly been shown to modify RyR thiols, promoting the formation of intra- or inter-molecular disulphides in a ROS independent manner (Abramson et al., 1988; Feng et al., 1999; Marinov et al., 2007),

possibly by promoting deprotonation of the thiol groups (see Section 1.10.1). Abramson and colleagues (1988) suggested that anthracyclines disrupt Ca^{2+} release by directly oxidising a component of the SR Ca^{2+} release complex, since addition of catalase and SOD was unable to prevent the effects of doxorubicin on the RyR. The same theory was proposed by Ondrias and co-workers (1990) and Hanna et al (2011) who prevented anthracycline-induced inhibition of single RyR2s in lipid bilayers by pre-treating with DTT. This has been suggested to occur via an electron exchange mechanism between anthracyclines, which act as electron acceptors, and the reactive thiol groups (Marinov et al., 2007). These findings warrant further investigation of the ROS independent aspect of anthracycline-induced protein oxidation.

1.12.3.2.2 Altered Ca^{2+} handling

Anthracycline treatment causes severe ultrastructural changes to cardiac muscle, with typical effects including progressive disarray and loss of myofibrils, mitochondrial swelling, vacuolization and SR dilation (Lim et al., 2004 reviewed in Singal et al., 2000; Sawyer et al., 2010). These changes are evident in both animal models and in an endomyocardial samples from human patients. Functional studies using skeletal and cardiac preparations have found that anthracyclines disrupt SR function, reducing its storage capacity and modulating the release of Ca^{2+} into the cytoplasm (see below 1.12.3.2.3) (Ondrias et al., 1990; Feng et al., 1999; Olson et al., 2000; Charlier et al., 2005; Kim et al., 2005a). Additional disruptions to cardiac Ca^{2+} handling include decreased SR Ca^{2+} content and increased cytoplasmic [Ca^{2+}] during diastole. It has been suggested that these changes are associated with the increased CaMKII activity that occurs in the presence of anthracyclines (Sag et al., 2011) or as a result of an interaction between anthracyclines and CSQ2 (Kim et al., 2005b). The structural characteristics of the drugs (see above) enable them to easily move across lipid membranes such as the plasmalemma and SR membrane and as mentioned above, several SR and sarcolemmal proteins have been indicated as binding targets, including RyR2, CSQ2, NCX1, SERCA2A and Na/K ATPase (see Section 1.12.3.2), some of which are addressed in more detail below.

1.12.3.2.3 Anthracycline effects on RyR function

RyR2 is the most studied cardiomyocyte binding target of anthracyclines. Its central role in Ca^{2+} handling and cardiac function, and its particular sensitivity to oxidative

modification, make RyR2 an especially likely target of anthracyclines. Similar to other quinone containing compounds, anthracyclines have been found to both stimulate and inhibit RyR Ca^{2+} release in both cardiac and skeletal muscle (Abramson et al., 1988; Pessah et al., 1990; Olson et al., 2000; Kim et al., 2005b). Biphasic modulation of RyR2 has been reported in experiments using single RyR2 channels in lipid bilayers, with an initial activation followed by a later, irreversible inhibition of activity with cytoplasmic exposure to low micromolar (2.5 – 10 μM) doxorubicin (Ondrias et al., 1990) and daunorubicin (Hanna et al., 2011). Olson and co-workers (2000) also reported that daunorubicin in micromolar concentrations inhibited Ca^{2+} release from populations of SR vesicles. The authors found that 5-ID (the quinone-deficient analogue of daunorubicin) had little impact and that inhibition depended upon the extent of SR Ca^{2+} loading.

1.12.3.2.4 Anthracycline effects on CSQ2

Anthracyclines bind to CSQ with micromolar affinity (Kim et al., 2005b). It has been proposed that CSQ2 binding drugs such as anthracyclines and trifluoperazine target a ligand binding site thought to consist of a hydrophobic cleft positioned within each of the thioredoxin-like domains in CSQ2's structure (see Section 1.1.3.2) (Park et al., 2005a). Binding at this site may inhibit the Ca^{2+} binding capacity of CSQ2 and/or alter protein conformation with subsequent reductions in SR Ca^{2+} release and reduced SR Ca^{2+} storage capacity (Charlier et al., 2005; Kim et al., 2005a; Park et al., 2005a). Considering the high concentration of CSQ2 in the SR lumen and the solubility characteristics of anthracycline molecules, it is likely that even low concentrations of anthracyclines may accumulate in the SR and bind to CSQ2, disrupting Ca^{2+} homeostasis (Charlier et al., 2005; Kim et al., 2005a; Park et al., 2005a). Although inhibition of CSQ2 is thought make a substantial contribution to SR dysfunction, interactions between anthracyclines and other SR proteins could not be ruled out by the aforementioned experiments (Charlier et al., 2005).

1.12.3.3 Anthracycline metabolites

Daunorubicin and doxorubicin are metabolized to the hydroxyl derivatives daunorubicinol (daunOL) and doxorubicinol (doxOL) by two electron reduction of the carbonyl side chain (Figure 1.14) (Mordente et al., 2003; Menna et al., 2007b). DaunOL has been found to stimulate and inhibit Ca^{2+} release from SR vesicles and could do so at

≤50% lower concentrations then the parent compound (Olson et al.; Charlier et al., 2005). Cardiac muscle preparations from rabbits treated with a single dose of daunorubicin (15 mg/kg) exhibited a ~30 fold ratio of daunOL to daunorubicin 3-4 days after drug administration and had impaired contractile function. DaunOL, at a similar concentration to what was measured *ex vivo* (approximately 10 μM) could inhibit SERCA2A function whilst daunorubicin, at an equivalent concentration had no effect (Cusack et al., 1993b). DaunOL and daunorubicin do however bind to CSQ2 with similar affinities (Charlier et al., 2005). Similar findings have been made for doxOL which could inhibit SERCA2A, Na/KATPase and the mitochondrial proton pump, while doxorubicin either had no effect or required concentrations 100-fold to cause 50% as much inhibition as the metabolite. DoxOL, but not doxorubicin, also caused a 4-fold increase in myocardial stiffness though this required relatively high concentrations of ~90 μM which could be considered higher than clinically attainable (Boucek et al., 1987; Olson and Mushlin, 1990). A later study found that both doxorubicin and doxOL could impair SR Ca^{2+} release, decrease contractility and increase muscle stiffness. The severity of some of these effects was found to increase in a time dependent manner, which was correlated with increasing levels of doxOL (due to doxorubicin metabolism in cardiac tissue) (Mushlin et al., 1993). The authors suggested then that time-dependent changes in cardiac function are attributable to doxOL, rather than doxorubicin, and that doxOL potentiates the early, acute effects of doxorubicin. The results of these studies should be interpreted carefully however, as very high drug concentrations (up to 175 μM) were used to treat the isolated muscle preparations.

The limited body of published data suggest that anthracycline metabolites have the potential to cause significant cardiac dysfunction and do so with far greater potency then the parent compounds. To date there have been no studies investigating the effects of doxOL on the specific function of the two major binding targets, namely RyR2 and CSQ2. This is an important gap in the literature as the drug metabolites are likely to have an important role in the development of the chronic component of anthracycline-induced cardiotoxicity, possibly as a consequence of their prolonged half-life in the body compared to the parent compounds (Cusack et al., 1995, for a review see Menna et al., 2007a). This difference is illustrated in Figure 1.14A, comparing the clearance of doxorubicin and doxOL from a strip of human atrial tissue (Menna et al., 2012). An important role for the metabolites is also indicated by the findings that 1) over expression of the carbonyl reductase (which catalyses doxorubicin to form doxOL)

accelerates the development of cardiomyopathy (Forrest et al., 2000) and 2) knockdown of the carbonyl reductase gene protected mice against acute cardiotoxicity (Olson et al., 2003, reviewed in Menna et al., 2012). Given that metabolites accumulate in the heart it's difficult to firstly, determine what level of metabolites might be found in human cardiac tissue following anthracycline treatment, particularly months or years after treatment completion, and secondly, predict what concentration of the metabolites actually cause cardiac dysfunction. As Olson & Mushlin (2000) point out, isolated muscle preparations exhibit quite severe dysfunction after as little as one dose of anthracyclines, while in humans, cardiac symptoms may not appear for months or even years after cessation of treatment.

1.12.3.4 Reduced gene expression with chronic anthracycline treatment

Anthracyclines and their metabolites have been shown to reduce the mRNA expression of several SR Ca^{2+} handling proteins. Reduced gene expression of RyR2, PLB, SERCA2A and CSQ2 was measured in rabbits after completion of long-term (8 weeks) anthracycline administration. Although SERCA2A protein expression was reduced, the authors did not check protein levels of any other SR proteins (Arai et al., 1993). In a more recent study utilizing a similar model of anthracycline-induced cardiotoxicity, protein levels of RyR2, SERCA2A, CSQ2 and NCX1 were decreased (Olson et al., 2005). In both studies depressed cardiac function was measured following the completion of anthracycline treatment, suggesting that expression of Ca^{2+} handling proteins may contribute to the chronic component of anthracycline-induced cardiotoxicity. RyR2 mRNA expression has been reduced in other studies, however protein expression was not investigated (Burke et al., 2000; Gambliel et al., 2002). In one case, the decreased mRNA expression could be prevented by dexrazoxane pre-treatment, while in the other it was found that an analogue of doxorubicin that cannot be metabolized by carbonyl reductase (therefore no doxOL production) had no effect on RyR2 expression. These studies suggest that doxOL has an important role in doxorubicin-associated changes in RyR2 gene expression, and that dexrazoxane could ameliorate these changes (Burke et al., 2000; Gambliel et al., 2002).

1.13 Summary and aims of thesis

Optimal cardiac function relies on rapid electrical signalling in the heart, which is facilitated by a specialized signal conduction pathway and the highly interconnected nature of cardiomyocytes. At the cellular level, the translation of the electrical signal to the mechanical contraction of the muscle fibres involves a complex signal conduction pathway in a process known as excitation-contraction coupling. Intrinsic to this process is the movement of Ca^{2+}, which is intricately involved in all aspects of cardiac function including excitation, muscle contraction, relaxation and rhythmicity. Therefore it is essential that Ca^{2+} homeostasis is maintained. Altered function or regulation of ion channels and transporters involved in EC coupling, including LTCC, NCX1, RyR2 and SERCA2A has devastating consequences on cardiac function, including arrhythmia, heart failure and sudden cardiac death.

Severe cardiac dysfunction would likely require concurrent modulation of several of these targets. There is evidence that the anthracycline compounds can cause such effects, with evidence from studies over the last 20 – 30 years suggesting that these drugs may target multiple links in the EC coupling pathway. Considering anthracyclines can promote oxidative stress by both ROS dependent and ROS-independent pathways (see Section 1.12.3.2.1) it seems likely that a redox mechanism is involved in drug-induced cardiotoxicity in some capacity. This is supported by the efficacy of dexrazoxane as a cardioprotective agent. Unfortunately, attempts to attenuate anthracycline cardiotoxicity by targeting ROS pathways, either by treatment or prophylaxis with antioxidants has proven unsuccessful. Also, dexrazoxane has been found to have no benefit in a third of cases. Given the caveats in the oxidative stress theory of anthracycline cardiotoxicity (see Section 1.12.3.2.1), there is a clear need to, firstly, better characterize the effects of anthracycline mediated oxidation on cardiomyocyte function and secondly, identify other potential mechanisms.

There is already significant evidence supporting a role for altered Ca^{2+} homeostasis in anthracycline cardiotoxicity. However there is a need to better describe how clinical concentrations of anthracyclines affect Ca^{2+} handling in the heart. It is also important to address the deficiency in information regarding the anthracycline metabolites. DoxOL and daunOL have a greater half-life in the heart then the parent compounds, and the limited number of studies on the metabolites indicates that they are also more potent than the parent compounds.

Therefore, the primary aims of this thesis were to:

1. **Characterize the effects of anthracyclines and their metabolites on Ca^{2+} handling in the heart**
2. **Determine the mechanisms underlying any functional changes, assessing the role of anthracycline induced oxidation**
3. **Interpret these changes in terms of whole cardiomyocyte function**

Fulfilling these aims will contribute novel information on the molecular mechanism of anthracycline-induced cardiotoxicity. It is considered that the cardiotoxic effects of anthracyclines are distinct from their cytotoxic effects, allowing the possibility that cardiotoxic effects can be attenuated without lessening the efficacy of the drugs as chemotherapeutic agents. This knowledge will significantly enhance efforts to design co-treatments with a view to improving the therapeutic index of these valuable chemotherapeutic agents.

Chapter Two

Materials and Methods

2.1. Materials

Tween-20, Tris, Glycine and MOPS were from Amresco (Solon, USA). Methanol and ethanol were from Merck (Parmstadt, Germany). Readymatic developer and fixer were from Kodak Dental (Stuttgart, Germany). Immobilon-P PVDF membrane and Amicon concentrators were from Millipore (Billerica, USA). Western blot filter paper and ECL reagents were from Thermo Scientific (Rockford, USA). Protein standards for electrophoresis were from Bio-Rad (Gladesville, Australia). The primary antibodies anti-RyR and anti-SERCA2A were from Abcam (Cambridge, UK) and Badrilla (Leeds, UK), respectively. The IgG-HRP conjugated secondary antibodies goat anti-mouse and goat anti-rabbit were from Santa Cruz Biotechnology Inc. (Dallas, United States). Glacial acetic acid and glucose were from VWR (Murrarie, Australia). DaunOL and doxOL were from Toronto Research Chemicals (North York, Canada). Natural mouse laminin was from Life Technologies (Mulgrave, Australia). Potassium phosphate, monobasic was from Mallinckrodt (Paris, USA). Glycerol and hydrochloric acid were from Ajax Chemicals (Sydney, Australia). Sodium pentobarbitone was from Troy Laboratoties (Smithfield, Australia). Lipids were purchased from Avanti Polar Lipids (Alabama, United States). Fluo-4 AM, Alexa Fluor 647 and Pluronic F-127 were from Molecular Probes (Life Technologies, Mulgrave, Australia). Collagenase Type 2 was from Worthington Biochemical Corporation (New Jersey, USA). All other chemicals were purchased from Sigma-Aldrich (Castle Hill, Australia).

2.2. Overview

The methods presented in this chapter are detailed accounts of the general experimental techniques used for the research presented in the results chapters of this thesis. Specific protocols are presented in the methods section of the relevant chapters. Experiments were conducted at room temperature 23±2 °C unless otherwise stated. Unless otherwise stated, all solutions were prepared using high grade, ultra pure water obtained using Milli-Q filtration units (Millipore Corporation, Billerica, USA). The vast majority of experiments conducted for the research presented in this thesis used SR vesicle preparations from sheep cardiac muscle. Functional assays using these vesicles include measurement of single RyR2 channel activity **(Section 2.6),** and Ca^{2+} uptake studies using populations of SR vesicles to assess SERCA2A function **(Section 2.7**). SR

vesicles, either solubilized or native, were also used for affinity chromatography to assess drug-protein interactions (**Section 2.8**) and an assay of thiol oxidation on RyR2 and SERCA2A (**Section 2.9**). To determine the effects of the drugs in a more intact system, cardiomyocytes were isolated from mouse hearts (**Section 2.10**) and the effects of anthracyclines on global Ca^{2+} transients were assessed.

2.3. Cardiac SR vesicle preparation

2.3.1. Crude SR preparation

Preparation of all SR vesicles was carried out by Suzy Pace and Joan Stivala, The John Curtin School of Medical Research, Canberra, Australia.

Cardiac SR vesicles were prepared as described by (Chamberlain and Fleischer, 1988). Hearts were excised from anaesthetized ewes (5% intravenous (I.V.) pentobarbitone followed by oxygen/halothane) and immediately rinsed in ice cold phosphate buffered saline (PBS) with 2 mM EGTA to remove blood. The atria were removed and the ventricles trimmed of fat. Ventricles were cut into small pieces in *homogenizing buffer* which consisted of: (mM) 290 sucrose, 10 imidazole, 0.5 DTT, 3 NaN_3 and the *standard protease inhibitors* leupeptin (1 μM), pepstatin A (1 μM), benzamide (1 mM) and PMSF (0.7 mM) (pH 6.9). Tissue was homogenized in a Waring blender (3 x 10 s on high speed) and the homogenate was centrifuged at 11,000 *g* for 20 min. The resultant supernatant was filtered through four layers of cotton gauze and filtrate was collected and centrifuged at 110,000 *g* for two h. The pellet was resuspended in *homogenizing buffer* plus 0.65 M KCl, pH 6.7, in a Potter homogenizer (Edwards Instrument Company; Narellan, Australia) and placed on ice for 30 min before being centrifuged at 7000 *g* for 10 min to remove insoluble particles. The supernatant was centrifuged at 180,000 *g* for 100 min and the final pellet, containing crude SR vesicles was resuspended in *homogenizing buffer* plus 0.65 M KCl, pH 6.7, snap frozen and stored in liquid nitrogen in 1 mL aliquots or at -80°C in 20 μL aliquots for daily use. All procedures were carried out at 4 °C.

The presence of RyR2 was confirmed by its protein profile on SDS Page and subsequent silver stain, and by Western Blot with anti-RyR antibody. Calcium flux

assays were carried out to test RyR2 and SERCA2A function. The protein concentration was usually between 10 – 20 mg/mL.

2.3.2. Purification of RyR2

Cardiac RyRs were purified from native SR vesicles using the methods of (Lai et al., 1988) as described in (Dulhunty et al., 2005). Vesicles were thawed and homogenized in a Potter homogenizer, on ice for 30 – 60 min in *solubilisation buffer* containing (mM) 25 Na-PIPES (piperazine-N,N′-bis(2-ethanesulfonic acid), 1 000 NaCl, 1 DTT, 0.5% CHAPS/5% PC (phosphatidyl choline), 0.1 EGTA, 0.92 $CaCl_2$, 0.5 AMP, pH 7.4, and *standard protease inhibitors* (see Section 2.3.1). During the incubation, vesicles were homogenized for 1 min every 10 min. After centrifugation for 15 min at 100,000 *g* to remove insoluble membrane fragments, the solubilized SR were loaded onto a continuous 5 – 20% sucrose gradient (5 – 20% sucrose dissolved in *solubilisation buffer*) and centrifuged at 70,000 *g* for 14 – 16 h. Two mL fractions were collected and subjected to SDS-PAGE (see Section 2.4) and immunoblot (see Section 2.5). Fractions enriched in RyR were collected and dialysed against 0.5 mM NaCl, 10 mM Na-PIPES, 1 mM DTT and 1.5 mM PMSF, pH 7.4. Purified RyR was concentrated to 1 mg/mL and stored at -70 °C in single use aliquots. Before use, each batch of purified RyR underwent immunoblot and probe with anti-CSQ2, anti-junctin and anti-triadin to check for contamination.

2.4. Electrophoresis

2.4.1. SDS-PAGE

Polyacrylamide gel electrophoresis was performed under denaturing conditions according to (Laemmli, 1970; Towbin et al., 1992b) using the Invitrogen NuPAGE SDS-PAGE gel system (Life Technologies, Mulgrave, Australia). Proteins were separated on 4 - 12 % NuPage precast bis-tris polyacrylamide gels. Proteins were diluted at a 1:1 (vol/vol) ration in Milli-Q water and sample buffer (mM) 200 Tris-HCl, 40 EDTA, 588 2-Mercaptoethanol, 8% SDS, 40% glycerol and 0.08% bromophenol blue, pH 6.8) so that 5 – 15 µg of crude SR or 1 µg of purified RyR2 was loaded per lane. Standards (5 µL of Bio-rad Dual Colour Protein Standard) and protein samples were loaded and electrophoresis was conducted at a constant voltage of 200 V in

running buffer (mM) 50 MOPS, 50 Tris base, 0.1% SDS and 1 EDTA) until the dye front reached the end of the gel.

2.4.2. Protein stains

Generally to visualize total protein, gels were incubated in a Coomassie stain containing 0.1% Coomassie Brilliant Blue, 40% ethanol and 10% glacial acetic acid, for 30 – 60 min with gentle agitation. Excess stain was removed by washing the gel overnight with a destaining solution, containing 40% ethanol and 10% glacial acetic acid, with 1 – 2 solution changes. The destaining procedure was continued until the gel background was minimized.

2.5. Western blot

2.5.1. Transfer

Western blot procedures were completed according to the method of (Towbin et al., 1992a), using a Bio-Rad transfer system (Gladesville, Australia). Upon completion of electrophoresis (Section 2.4), the gel and transblot components (fibre pads, filter paper and a PVDF membrane), was equilibrated for 15-30 min at 4 °C in *transfer buffer* (pH ~8.2) consisting of 37 mM Tris, 140 mM glycine and 20% methanol before being transferred to a transblot cassette. Due to the hydrophobic nature of the PVDF membrane, it was activated first by exposure to 100% methanol for one minute, before being soaked in *transfer buffer*. The transblot sandwich was assembled under partial submersion in cold transfer buffer as follows: a filter paper was place on top of a fibre pad, followed by the gels and then careful placement of the PVDF membrane so that no bubbles formed between the gel and membrane. The sandwich was completed by placing another filter paper on top of the PVDF, followed by another fibre pad. The cassette was clamped in place in an electrophoresis tank filled with transfer buffer which contained an ice pack and stir bar. Proteins were transferred at 100 V for 60 min and then ~150 V so that the current was 0.5 - 0.6 A for the final 30 min of transfer. Increasing the current assisted in transferring the high molecular weight RyR monomer.

Once transferred, the membrane was blocked in blocking buffer (5% skim milk in PBS) for 1 hour with rotation to prevent non-specific binding. Following a 15 min wash step in TPBS (PBS with 0.05% Tween-20), membranes were incubated overnight at 4 °C in

a primary antibody solution, containing appropriate antibodies in TPBS, to a total volume of 2.5 – 5 mL. After washing in TPBS (5 x 5 min), membranes were incubated with secondary antibody solutions for two hours at room temperature. Secondary antibody solutions contained the horseradish peroxidase (HRP) conjugated, species-relevant antibody, diluted in TPBS. Excess secondary antibody was removed by washing 5 x 5 min in TPBS, followed by one wash in PBS.

2.5.2. Visualization

HRP-conjugated antibodies were visualized using an enhanced chemiluminescence method. After removal of excess wash solution, the membrane was exposed to SuperSignal West Pico Chemiluminescent substrate for 1 – 2 min. Membrane was exposed to autoradiographic medical X-ray Film (Fujifilm, Tokyo, Japan) in a hypercassette (Amersham International, Buckinghamshire, England) for between 5 s – 5 min, before being developed using sequential 1 min washes of Readymatic developer and fixer. Films were allowed to dry and then imaged using the Bio-Rad Geldoc XR system (Gladesville, Australia), and quantified using the associated Quantity One software.

2.6. Single Channel Lipid Bilayers

2.6.1. Overview of lipid bilayer setup

The system for recording single channel activity using lipid bilayer methods was setup as described previously (Ahern et al., 1994b; Laver et al., 1995). Artificial lipid bilayers were formed across the 150 nM aperture of a 1 mL delrin cup. The wall of the cup separated two chambers within a teflon block referred to as *cis* and *trans,* to which stock solutions were added (Figure 2.1). The aperture was visualized under 20x magnification and illuminated by LED lights (Figure 2.1). The entire setup was housed inside a Faraday cage to minimize electrical and vibrational noise.

Current across the bilayer was monitored by silver chloride-coated (AgCl) silver electrodes, connected to the headstage of an Axopatch 200B amplifier (Axon Instruments, Foster City, United States) or a Warner BC-525 Bilayer clamp amplifier (Warner Instruments, Hamden, United States). Contact between the electrodes and solutions was made via agar salt bridges (2% w/v, see Section 2.3.2).

The chamber to which SR vesicles were added was defined as the *cis* chamber and was voltage-clamped for all experiments alternating between +40 mV and -40 mV at 30 s intervals, while the *trans* chamber was held at virtual ground. Current was filtered at 1 kHz with a lowpass 8-pole Bessel filter and sampled at 5 kHz using the in-house analogue/digital conversion program BLM. These parameters give a sampling interval of 200 μs, or one point every 200 μs. Additional digital filtering allowed the channel to be visualized in real time with a computer using BLM.

2.6.2. Silver-chloride coated silver electrodes and agar bridges

New electrodes were made by cutting silver wire to the desired length and cleaning by light rubbing with sandpaper. Cleaned electrodes were immersed in domestic bleach overnight then wiped and connected to the amplifier headstage. Over time, the chloride coating dissolves, requiring used electrodes to be cleaned, sanded and re-chlorided regularly to maintain their sensitivity and avoid baseline drift during experiments.

Agar bridges were positioned on the ends of the electrodes and were the contact point between the electrodes and the solution to minimise liquid junction potentials (Sakmann and Neher, 2009). Bridges were made by dissolving 0.4 g of agar in 20 mL of 250 mM CsCl (2% agar w/v) and heating the solution on a hotplate. The warmed solution was pushed into 20-30 cm sections of tubing (Dow Corning Corporation, Midland, USA) using a warmed pipette. The agar was cooled and allowed to set, and the tubing was cut into 1 cm lengths and stored in 250 mM $CsCl_2$ at 4 °C. A fresh set of agar bridges was used each day.

2.6.3. Bilayer solutions

Pending SR vesicle incorporation, solution compositions were: *cis*: 230 mM $CsCH_3O_3S$ (Caesium Methane Sulfonate, CsMS) 20 mM CsCl, 1 mM $CaCl_2$ and 10 mM TES and *trans:* 30 mM CsMS, 20 mM CsCl, 1 mM $CaCl_2$ and 10 mM TES. The free Ca^{2+} concentration in the solutions was measured with a Ca^{2+} electrode (Radiometer Analytical, Villeurbanne Cedex, France). All solutions were adjusted to pH 7.4 with CsOH using a digital pH meter and stored at 4 °C.

Figure 2.1 – Single Channel Lipid Bilayer Apparatus (**A**) The Teflon bilayer chamber was positioned inside a custom built stage with a built in stirrer, LED lights and perfusion control. The aperture separating the two chambers was visualized with a light microscope and the whole system was housed on an inflated base inside a Faraday cage to minimize electrical, acoustic and vibrational noise. (**B**) A 1 mL delrin cup was positioned inside a Teflon bilayer chamber so that two compartments were formed. Compartments are defined as being either the *cis* chamber or *trans* chamber and platinum electrodes from the amplifier headstage, carrying agar bridges, are positioned in each. Perfusion tubes are inserted or withdrawn as needed. (**C**) SR vesicles are added to the *cis* chamber. The wall of the cup separating the chambers contains a 150 nm aperture, across which lipids are applied to form bilayers. With stirring, SR vesicles incorporate themselves in such a way that the cytoplasmic domain of the RyR2 complex faces the *cis* chamber and the luminal domain faces the *trans* chamber. The *trans* is grounded and voltage (+ or -40 mV) is applied to the *cis* chamber. Current flow alternates with voltage changes, travelling toward the more negatively charged chamber.

A

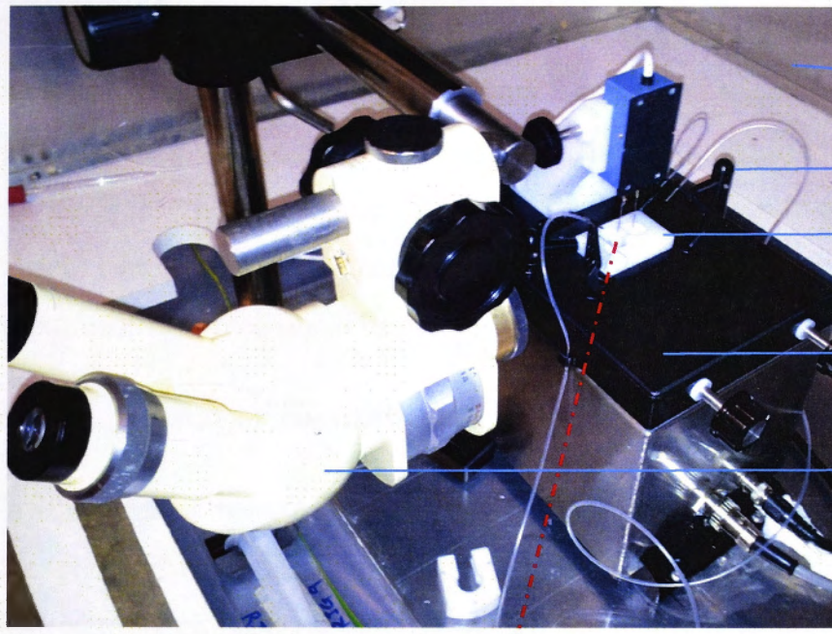
Faraday cage
LED light
Bilayer chamber
Bilayer box
Light microscope

B

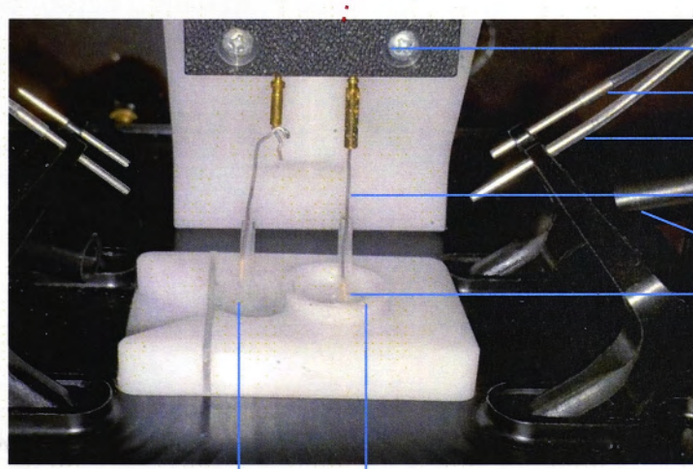
Headstage
Perfusion out
Perfusion in
Platinum electrode
LED light
Agar bridge

C

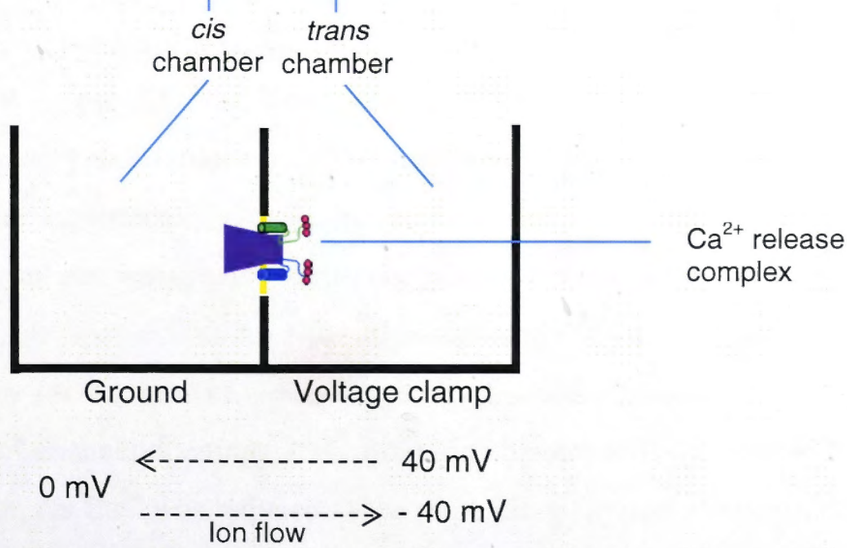
cis chamber
trans chamber
Ca2+ release complex
Ground
Voltage clamp
40 mV
0 mV
- 40 mV
Ion flow

Caesium was used as the current carrying ion, firstly because Cs^+ conductance through RyR2 is higher than that of Ca^{2+}, resulting in a higher signal to noise ratio and secondly, because Cs^+ is a weak modulator of RyR2 compared to Ca^{2+} (Laver et al., 1995). Furthermore Cs^+ blocks K^+ channels which are enriched in muscle SR (Cukierman et al., 1985). Methanesulfonate was used as the major anion to avoid contaminating current from Cl^- channels that are also present in the SR. The Cl^- channels are impermeable to methanesulfonate (Laver et al., 1995).

2.6.4. Bilayer formation and channel incorporation

Artificial bilayers were formed using a mixture of phosphatidylethanolamine, phosphatidylserine, and phosphatidylcholine (5:3:2 w/w). The lipids were mixed in the desired ratio, chloroform was removed under a stream of nitrogen gas and the dried lipid mixture was redissolved in *n*-decane at a final concentration of 50 mg/ml (Ahern et al., 1994a). Lipids were applied to the aperture of the delrin cup using a flame polished glass rod to form a lipid barrier separating the two chambers. Initially the lipid is thick and then it forms a bilayer with two monolayers separated by *n*-decane. Pressure generated from the solutions in each chamber forces drainage of the solvent and the bilayer thins (Miller, 1986; Laver et al., 1995). The bilayer thickness and stability was assessed by monitoring changes in the membrane capacitive current by applying a 1V/s triangular ramp. An increase in capacitance (and therefore an increase in current amplitude since $I = C * (dV/dt)$ indicates a thinning of the bilayer

SR vesicles were added to the *cis* chamber at a final concentration of ~50 μg/mL and stirred until incorporation occurred. Our laboratory has shown that the accessory proteins triadin, junctin and CSQ2 remain associated with RyR2 in the experimental conditions (Wei et al., 2009a). Vesicle fusion is promoted by an osmotic gradient across the bilayer and by millimolar *cis* Ca^{2+} (Miller and Racker, 1976; Laver, 2001). Channels were therefore incorporated into the bilayer in a *cis* solution containing 1 mM Ca^{2+} and an osmotic gradient was created across the bilayer using *cis* 250 mM Cs^+ salt and *trans* 50 mM Cs^+ salt (see Section 2.6.3 for all components of bilayer solutions). Channel incorporation into the bilayer was indicated by a sudden increase in conductance or appearance of channel openings, indicating ion channel activity. Following incorporation, *cis* Ca^{2+} was reduced to the more physiological concentration of 1 μM with addition of 1.32 mM of the fast Ca^{2+} chelator 1,2-bis(2-aminophenoxy)ethane-

N,N,N,N-tetraacetic acid (BAPTA). Concentrations of BAPTA required to adjust the free [Ca^{2+}] were calculated using the program Bound and Determined (Brooks and Storey, 1992) and free [Ca^{2+}] confirmed using a Ca^{2+} electrode. Two hundred mM Cs^+ was added to the *trans* chamber (250:250 mM Cs^+ in *trans*:*cis*) to prevent further vesicle incorporation during the experiment and to provide symmetrical [Cs^+], so that there was no ionic gradient across the bilayer. Therefore when a voltage of +40 mV was applied:

$$V_{applied} = V_{cis} - V_{trans}$$

$$V_{applied} = 40 - 0$$

With this configuration, current would flow from the *cis* to the *trans* chamber, while with -40 mV current would flow from the *trans* to the *cis* chamber.

It has been shown that vesicle incorporation occurs such that in 99% of cases, the channel orients so that the cytoplasmic portion of RyR2 faces the *cis* chamber and the luminal portion faces the *trans* chamber (Figure 2.1C) (Miller and Racker, 1976). In this study, channel orientation was confirmed by testing the response of RyR2 to changes in cytoplasmic [Ca^{2+}] at the beginning of the experiment and by addition of 20 μM ruthenium red, an RyR-specific antagonist which irreversibly blocks RyRs (Ma, 1993).

2.6.5. Solution exchange

Solution exchange of the *trans* chamber was achieved using a back-to-back perfusion set-up. Syringes were positioned with their plungers placed back to back so that fresh solution from one syringe could flow into the chamber at the same rate as original solution was removed by the second syringe. Using this setup, the chamber was perfused with 7 – 10 volumes of fresh solution (resulting in dilutions of ~1000 times) allowing reversibility of a drug's effects on a single RyR2 to be assessed, without any abrupt change in chamber volume that might break the bilayer.

2.6.6. Single channel recording and analysis

Immediately following channel incorporation, reagents were added to the *cis* or *trans* solutions with 15 – 20 s stirring to ensure total dispersion of reagents throughout the solution. Control conditions were maintained and 3 – 4 min of stable control activity was recorded, alternating between +40 mV and – 40 mV every 30 s.

Channel activity was quantified using single channel parameters, measured using the in-house program Channel 2 (developed by P.W. Gage and M. Smith, JCSMR), Canberra, Australia). The measurements of RyR2 activity were from several segments of current recordings (between 60 and 90 s) at each potential. The measurements were: n, the number of openings; open time (OpenT), the total time spent by the channel in the open state (ms); close time (CloseT), the total time spent by the channel in the closed state (ms) and total time (TT) is the total duration of the recording (ms), I' is mean current, the average of all data points of a tracing (pA) and I_{max} is the maximal current of the tracing (pA):

$$\text{Open probability } (P_o) = \frac{OpenT}{TT}$$

$$\text{Mean open time } (T_o) = \frac{OpenT}{n}$$

$$\text{Mean close time } (T_c) = \frac{CloseT}{n}$$

$$\text{Open frequency } (F_o) = \frac{n}{TT}$$

$$\text{Fractional Mean Current } (I'_F) = \frac{I'}{I_{max}}$$

Open probability (P_o) was measured as fractional mean current (I'_F) or as the fraction of time that the channel was open using threshold discriminators. Fractional mean current is approximately equal to the P_o measured by threshold discrimination. Where experiments had only one channel opening, P_o could be measured directly by setting an open threshold discriminator at ~ 30% of the maximum amplitude, while the closed threshold discriminator was set slightly outside the noise level of the baseline (~10% of the maximum amplitude). Currents exceeding the open threshold were detected as channel openings. Accurate measures of P_o and I'_F rely on having a stable baseline over the entire recording period. Therefore, the in-house program Baseline (developed by D.R. Laver, University of Newcastle, Australia) was used to correct significant baseline drift.

Activity is expressed as the average P_o of 60 - 90s of representative activity recording at each potential. Data from +40 mV and -40 mV was pooled if there was no significant difference between each potential. Because of the intrinsic variability in control RyR

channel activity (Wei et al., 2009a), effects of drugs or reagents on RyR2 were evaluated by comparing the P_o of each condition to the P_o of control activity from the same channel. Control P_o was measured from 60 – 90 s of stable control activity prior to drug/reagent addition.

The following reagents were all added from the following stock solutions (stock concentration indicated) to the *cis* or *trans* chambers while stirring for 10 -15 se: doxorubicin (2 mM), doxOL (2 mM), daunorubicin (2 mM), daunOL (10 mM), 4,4'-dithiodipyridine (4'4-DTDP, 4 mM), NEM (200 mM), ruthenium red (1 mM), $CaCl_2$ (100 mM), BAPTA (100 mM), DTT (500 mM), CsMS (2 M). The pH of the CsMS, $CaCl_2$ and ruthenium red was adjusted to 7.4 with CsOH. Addition of the other compounds at the concentrations used did not cause any change in pH. DoxOL and daunOL, were dissolved in ethanol. The ethanol was ≤ 0.1% which has been shown not to affect RyR2 activity (Eager et al., 1997). Ruthenium red, $CaCl_2$ and CsMS were stored at 4 °C, all others compounds were stored at -20 °C. Redox agents (anthracyclines, NEM, 4,4'-DTDP and DTT) were stored in daily use aliquots and thawed as required.

2.7. Ca^{2+} uptake in SR vesicles

2.7.1. Ca^{2+} uptake assays

The method used to assay Ca^{2+} uptake into SR vesicles in shown in Figure 2.2. A Cary 3 spectrophotometer (Varian, Sydney, Australia) was used to monitor extravesicular Ca^{2+} at 710 nm, using the Ca^{2+} indicator antipyrylazo III (Dulhunty et al., 1999; Jalilian et al., 2008a). A calibration curve was generated at the start of each day by measuring changes in absorbance that occurred with 4 consecutive additions of 12.5 μM Ca^{2+} additions of $CaCl_2$ (Eager and Dulhunty, 1999). By measuring the change in absorbance that occurs with addition of known amounts of Ca^{2+}, the extravesicular Ca^{2+} could be calculated:

$$Ca^{2+}\ \text{Calibration} = \frac{25\ \mu M Ca^{2+}}{\Delta adsorbance} \qquad \text{(Chu et al., 1988a)}$$

The calibration curve was repeated at least 3 times to ensure consistent values were obtained. The calibration was not altered by addition of anthracyclines, DTT, nor

ruthenium red. Changes in absorbance as a function of time were observed using the Kinetics program (Varian, Sydney, Australia).

Vesicles were pre-incubated for 20 min with the relevant compounds. Preincubated SR vesicles (200 μg) were added to a solution containing 100 mM KH_2PO_4, 0.2 mM antipyrylazo III, 1 mM Na_2ATP and 1 mM $MgCl_2$. Temperature was maintained at 25 °C and solutions were continually stirred throughout the experiment. The SR was partially loaded with 3 additions of 7.5 μM Ca^{2+}. Uptake of Ca^{2+} from the bathing solution into the SR was evidenced by a decrease in optical density (Figure 2.2). Three min was allowed between each addition of Ca^{2+} so that absorbance could return to baseline. Ruthenium red was then added to block RyR2 before a final addition of Ca^{2+} was made. The uptake of this final, fourth addition of Ca^{2+} was measured, as RyR2 had been blocked and this would be a measure specifically of Ca^{2+} uptake.

2.7.2. Calculation of rate of Ca^{2+} uptake from SR vesicles

Rate of Ca^{2+} uptake was determined by measuring the rate of change in optical density of the 15 s immediately following addition of Ca^{2+}. This initial rate was the most rapid Ca^{2+} uptake per unit time (Olson et al., 2000). The Kinetics program was used to measure the slope of this uptake curve, giving the change in absorbance that occurred with Ca^{2+} release. This was used in the following formula to measure the slope of Ca^{2+} release:

$$\text{Slope of } Ca^{2+} \text{ Release} = \frac{\Delta \, absorbance}{time \text{ (min)}} \qquad \text{(Chu et al., 1988b)}$$

Using this value and the value obtained for the Ca^{2+} calibration (see Section 2.7.1), the rate of Ca^{2+} uptake in nmol Ca^{2+}/mg protein/min was calculated by the following formula:

$$\text{Rate of } Ca^{2+} \text{ Release} = \frac{slope \ of \ Ca^{2+} \ release \ x \ Ca^{2+} \ calibration}{protein \ (mg)} \qquad \text{(Chu et al., 1988b)}$$

An ATP regenerating system was not used. These protocols were strictly adhered to, so that the timing of $CaCl_2$ and drug additions was made at the same timepoints in each experiment to ensure consistency.

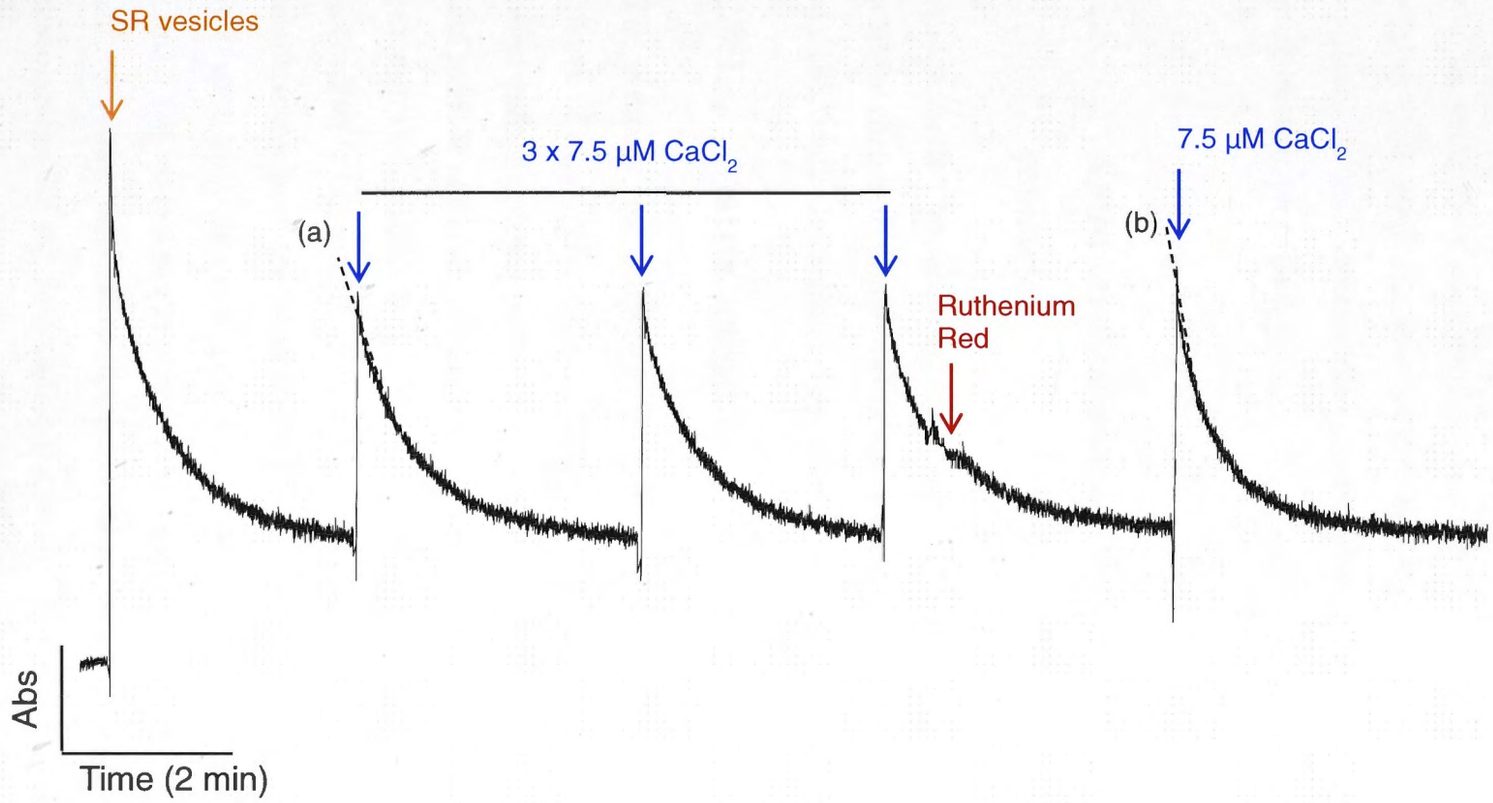

Figure 2.2 – A representative Ca^{2+} uptake experiment. Changes in absorbance as a function of time (total time = 15 min). Changes in extravesicular Ca^{2+} at 710 nm were monitored using antipyrylazo III. Cardiac SR vesicles were added (orange arrow) and the solution was allowed to equilibrate for 3 min, as any extravesicular Ca^{2+} was taken up by SERCA2A. Vesicles were loaded with 22.5 µM Ca^{2+} added in 3 x 7.5 µM aliquots (blue arrows). With 3 min equilibration allowed for each addition. Ruthenium red was added (red arrow) to block RyR2 shortly after the 3rd aliquot of $CaCl_2$. A final addition of Ca^{2+} was made which was used for assessment of Ca^{2+} uptake rate in the presence or absence of anthracyclines. Comparison of uptake before (a) and after (b) ruthenium red showed that the uptake was faster when RyR2 was blocked, as would be expected if Ca^{2+} was being released via RyR2 (which would reduce the gross uptake rate (b).

It is assumed that ATP was used at the same rate in every experiment and that ATP concentration at the time of measurement was the same in each experiment, so difference in ATP availability would be unlikely to be an influential factor in the results (Hewawasam et al., 2010). Experiments were conducted so that the order of controls and experiments at each drug concentration were alternated to minimize any influence of time-dependent changes in Ca^{2+} absorbance, although no such variability were evident. SR vesicles were thawed immediately before use and stored on ice during the drug incubation period.

2.8. Anthracycline-coupled cyanogen-bromide activated sepharose

An interaction between anthracyclines and RyR2 or SERCA2A was confirmed by affinity chromatography, using modifications of the methods described in (Gambetta et al., 1983) and (Jayaraman et al., 1992).

2.8.1. Matrix activation

The anthracycline coupled cyanogen-bromide activated sepharose method utilizes a matrix of cyanogen-bromide (CNBr) activated sepharose which is supplied as a freeze-dried resin stabilized by the presence of additives (e.g. lactose). To activate the resin and remove additives, sepharose was washed in cold, low pH solution to preserve the reactivity of binding sites which hydrolyse at high pH. Sepharose was activated according to the manufacturer's instructions. In brief, 0.075 g of CNBr-activated sepharose was washed and swelled in a total of 50 mL cold, 1 mM HCl. Acid was added in several aliquots and the supernatant was aspirated between additions (total time of 30 mins). The resin was then washed in 5 x 10 mL of distilled water. During this time anthracyclines were dissolved in coupling buffer. Doxorubicin or doxOL (0.2 mg) was dissolved in 0.2 mL of coupling buffer (0.1 M $NaHCO_3$, 0.5 M NaCl pH 8.3) and set aside.

2.8.2. Anthracycline coupling to activated sepharose

After the final wash of distilled water, the activated resin was placed into a 2 mL polypropylene tube. Following removal of the wash solution, 1 mL of coupling buffer

was added to the resin. Anthracyclines were then immediately added to the resin and incubated with rotation for 24 h at 4 °C. Control samples were also prepared, where resin was incubated with coupling buffer containing no anthracyclines.

2.8.3. Pre-clearing protein samples

Protein samples were pre-cleared before addition to the anthracycline-coupled resin to minimise non-specific binding. Proteins were incubated with a second batch of activated resin (which has not been coupled with anthracyclines). Unbound protein was collected and added to the anthracycline coupled resin (prepared on day 1, see Section 2.8.2). Pre-clearing the protein sample helps to ensure that any binding between the anthracycline-coupled resin and the protein reflects an interaction between the protein and the drug itself, not the resin. Proteins were pre-cleared as follows.

Purified RyR vesicles (Section 2.3) were diluted to 0.5 mg/mL in 50 mM Tris-HCl (pH 8), added to activated resin (Section 2.8.1) and incubated for 2 h at 4°C. The supernatant (containing unbound protein) was gently aspirated and set aside until needed (see Section 2.8.4).

2.8.4. Blocking unreacted resin sites and incubation with precleared proteins

Excess anthracycline was removed by extensive washing in coupling buffer. Unreacted binding sites on the resin were blocked by saturating the binding sites. This was achieved by washing the resin with 0.1M Tris HCl, pH 8 at room temperature for 2 h. Blocking solution was removed by washing with 4 - 5 cycles of alternating high pH solution (contained 0.1M Tris HCl and 0.5 M NaCl (pH 8.0)) and low pH solution (0.1 M sodium acetate and 0.5 M NaCl (pH 4.0)). After the final wash, the supernatant was aspirated and pre-cleared protein was added to the resin and incubated with rotation, overnight at 4 °C.

2.8.5. SDS-PAGE of protein samples and immunodetection

To remove unbound protein, the resin was washed 5 times with 10 volumes of 50 mM Tris-HCl. To elute bound proteins, a sample of beads was boiled for 1 min in sample buffer (1:1 ratio, see Section 2.4). Eluted proteins were separated by SDS-PAGE,

subject to western blot and immunodetected with anti-RyR and anti-SERCA2A (Sections 2.4 and 2.5).

2.9. Alexa Fluor thiol assay

To determine the relative degree of thiol modification caused by drug treatment, SR vesicles were exposed to anthracyclines and known redox agents, and the level of thiol modification caused by each of these was compared to untreated vesicles. Thiol modification was assessed using the thiol specific fluorophore, Alexa Fluor 647. Like other maleimides, Alexa Fluor 647 binds to cysteine thiol groups in the following reaction mechanism (Life Technologies Corporation, 2010):

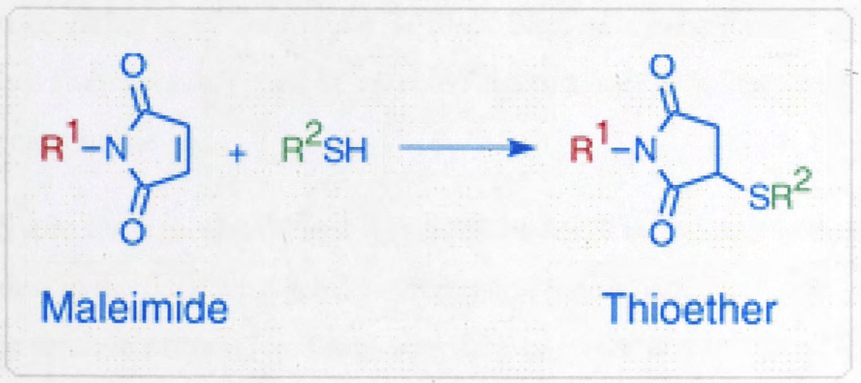

The double bond of the maleimide reacts with the cysteine thiol group to yield a stable thioether product. Excitation of Alexa Fluor 647 at 645 nm emits light at a wavelength of 670 nm which is imaged and quantified. By expressing the detected level of thiol modification to the relative amount of total protein, this method allows a comparison of the ability of different treatments to modify thiol groups.

2.9.1. Alexa thiol assay following anthracycline treatment

SR vesicles were incubated with anthracyclines and known redox agents, including doxOL (0.01 mM), doxorubicin (0.01 mM), tris-(2-carboxyethyl)phosphine (TCEP, a reducing agent, 5 mM) and GSSG (an oxidizing agent, 2 mM). TCEP was used rather than DTT because it does not contain thiol groups that could conjugate with the Alexa Fluor maleimide. The reaction mixture was made in PBS and incubated for 30 min at

room temperature. Untreated samples contained PBS only. Proteins were then incubated with rotation, with a 20 molar excess of the thiol-reactive probe Alexa Fluor 647 maleimide in the dark for 2 h. All subsequent steps were completed in the dark. After washing in 10 x volume of PBS, protein were sedimented by centrifugation at 9500 *g* for 50 - 60 min in a 3 kDa Amicon concentrator (Millipore Corporation, Billerica, USA), until the volume of Alexa-conjugated protein was 20 µls (maximum volume per well is 30 µls). Proteins were heated at 60°C for 10 min in non-reducing sample buffer (187.5 mM Tris-HCl, 15% glycerol and bromophenol blue (pH 6.8)) and separated by SDS PAGE.

2.9.2. Protein stain and visualization

To account for any variation in protein loading between samples, total protein was assessed with Sypro Orange protein stain and the amount of Alexa Fluor maleimide fluorescence per unit of total protein was calculated for each sample. Sypro Orange was used rather than Coomassie Brilliant Blue as it is reportedly more sensitive, and since it is a fluorophore, could be detected concurrently with Alexa Fluor 647 with sequential scans of the gel.

Sypro Orange was diluted to 1:5000 in 7.5 % acetic acid and the gel was stained for 45 min in the dark with gentle rocking and then rinsed for 1 min in fresh 7.5% acetic acid to remove excess dye. Fluorescence imaging was done on a Typhoon FLA 9000 (GE Healthcare, Uppsala, Sweden) fluorometer in the Biomolecular Resource Facility (John Curtin School of Medical Research, Canberra, Australia). Total protein content was measured by Sypro Orange fluorescence at 300 nM and thiol content was measured by Alexa Fluor 647 fluorescence at 645 nM. The order in which Alexa Fluor or Sypro Orange was imaged did not alter results Fluorescence was quantified by densitometry of the protein bands using the ImageQuant TL software (GE Healthcare, Uppsala, Sweden).

2.10. Ca^{2+} transients in adult mouse cardiomyocytes

2.10.1. Overview

Analysis of Ca^{2+} transients in adult mouse cardiomyocytes requires a multi-step protocol including 1) digestion of cardiac connective tissue by Langendorff enzyme

perfusion, 2) isolation and processing of cardiomyocytes, including Ca^{2+} reintroduction and plating of myocytes, 3) imaging of Ca^{2+} transients via confocal microscopy and 4) analysis of Ca^{2+} transients. This was a newly established technique in our laboratory, as such, parameters of the perfusion and cell isolation were optimized from methods reported by literary sources (Liao and Jain, 2007; O'Connell et al., 2007; Guatimosim et al., 2011; Louch et al., 2011) and personal communication with Dr Victoria Benson (University of Sydney, Sydney, Australia) and Dr Michael Watson (University of Queensland, Brisbane, Australia).

Perfusion and experimental solutions were prepared fresh on the day of experiment, the contents of which are listed in Table 2.1. All solutions were equilibrated with Carbogen (95% O_2/5% CO_2) for 20 min prior to experiments. Solutions were adjusted to pH 7.4 with NaOH using a digital pH meter. Mice were obtained from the Australian Phenomics Facility (Australian National University, Canberra, Australia).

2.10.2. Langendorff apparatus

Intact cardiomyocytes were isolated by retrograde perfusion of adult mouse hearts with enzyme solutions. Perfusion solutions were maintained at 37 °C in a circulating water bath and pumped through water jacketed glassware before entering the cannula and perfusing the heart (Figure 2.3). The heart rested on the base of water jacketed chamber (Custom Blown Glassware, Sydney, Australia) and maintained at 37 °C by constant circulation of warm water from the water bath (Figure 2.3). Warm water also circulated through a water jacketed coil through which the perfusate travelled before entering the heart, thus maintaining the perfusate at 37 °C. Minimal distance was maintained between the water jacketed coil and the heart, to minimise cooling of the perfusate before it entered the heart.

2.10.3. Laminin-coated coverslips

Laminin stock (1 mg/mL in 50 mM Tris-HCl and 0.15 M NaCl (pH 7.4)) was stored in daily use aliquots at -20 °C, and thawed at 4 °C on the day of experiment. Immediately before use, laminin was dissolved to a working concentration of 10 μg/mL in PBS (O'Connell et al., 2007). One mL of diluted laminin was applied to each 28 mM coverslip (Sarstedt Australia Pty. Ltd., Technology Park, Australia) and allowed to pool

on the surface of the coverslips for ≥30 min. Solution was removed by aspiration immediately before myocyte plating so that the laminin coating did not dry.

2.10.4. Mouse heart perfusion

All animal procedures were approved by the Australian National University animal ethics committee. Male, 8 week old C57/Bl6Ncrl mice were injected with heparin (100U) via intra peritoneal (i.p.) injection to a lower abdominal quadrant. Animals were weighed, and 60 mg/kg Na-pentobarbitone was administered via i.p. injection. Depth of anaesthesia was determined by corneal and pedal reflexes. Once in the surgical plane of anaesthesia, a transverse incision was made below the rib cage and the thoracic cavity was exposed by making bilateral incisions along the dorsal margin of the ribcage, from the last to first ribs. The heart was gently withdrawn from the thoracic cavity before cutting any vasculature and connective tissue attached to heart. To preserve the maximum length of aorta attached to the heart, the aorta was cut as far from the proximal end as possible. The heart was held briefly in a beaker of ice cold Myocyte Perfusion Buffer (Table 2.1) to remove blood before being placed on a petri dish of frozen buffer covered by a thin layer of liquid buffer to prevent the heart freezing on to the solid buffer. Fat and connective tissue were removed and the aorta was located.

The heart was placed in the heated chamber and the aorta was cannulated. Silk thread (Dynek, Hendon, Australia) was tied to secure the aorta to the cannula (Figure 2.4). For viable cells, the heart had to be cannulated within 4 min of excision, with better isolation (i.e. a higher yield of healthy cells) with faster cannulation times. The heart was perfused at a constant rate of 2 mL/min, first with Myocyte Perfusion Buffer (see Table 2.1) for 5-6 min to remove blood, and then with Myocyte Enzyme Buffer (see Table 2.1) for approximately 15 min to digest connective tissue. Due to batch variation in collagenase quality, the enzyme perfusion time was optimized for the batch of collagenase being used. As digestion proceeded, the heart became pale and pulpy to the touch and at completion of the enzyme perfusion, the heart was cut from the cannula below the atria, so that only ventricular tissue was obtained.

2.10.5. Cardiomyocyte isolation

Ventricles were placed in a petri dish containing 5 – 6 mL of Myocyte Stop Buffer (Myocyte Buffer with 1% BSA and 0.02 mM $CaCl_2$) and cut into small pieces using spring loaded iridectomy scissors. Tissue was placed in a round-bottom tube, and myocytes were dissociated by flicking the tube with intermittent, gentle trituration. Tissue settled and the supernatant was aspirated and collected (wash 1). 2,3-Butanedione monoxime (BDM) has been used in the isolation of adult mouse cardiomyocytes with improvements in the yield of healthy cardiomyocyte (O'Connell et al., 2007; Louch et al., 2011). However, during the optimization process it became evident that BDM was having detrimental effects on myocyte yield and responsiveness to stimuli. Therefore, BDM was only included in the Myocyte Enzyme Buffer and was not included in the Myocyte Stop Buffer Tissue was washed with 5 mL of fresh Myocyte Stop Buffer and the dissociation process was repeated 4 times, so 5 supernatants were collected. A sample of each wash was viewed under 20X magnification to assess the health and yield of myocytes, classified as healthy if they were rod-shaped, had visible striations and were quiescent. With each sequential supernatant (i.e. from washes 1 – 5), there was an increase in myocyte quality, with Wash 1 containing the lowest ratio of healthy-to-unhealthy cells and wash 5 containing the highest ratio of healthy-to-unhealthy cells. As such, wash 4 and wash 5 were generally considered the highest quality and were most often used for experimental procedures. Myocytes were allowed to settle for 10 min before the supernatant was removed and the pellet was resuspended in 1 mL of fresh Myocyte Stop Buffer. If myocytes from both washes were healthy, wash 4 and wash 5 were combined (total suspension volume now was 2 mL).

Myocytes were rendered Ca^{2+} tolerant by stepwise additions of $CaCl_2$ to the cell suspension (initial [Ca^{2+}] of 0.02 mM). The total [Ca^{2+}] was increased to 0.1 mM, 0.2 mM, 0.5 mM and finally 1 mM, by aliquot addition and mixed by gently flicking the tube. Ten – 15 min was allowed between each addition of Ca^{2+}. The pellet was resuspended by gentle trituration and myocytes were plated on laminin-coated coverslips (see Section 2.10.3). After a 10 min attachment period, the health and yield of myocytes was checked under 20X magnification. Cells were usually stable for 4 - 6 hours after isolation.

(A) Myocyte Perfusion Buffer	
Chemical	Molarity (mM)
NaCl	113
KCl	5.4
$MgSO_4$	1.2
NaH_2PO_4	1.2
HEPES	10
Glucose	20
Taurine	20
Na-Pyruvic acid	5
$NaHCO_3$	5
pH 7.4 with NaOH	

(B) Myocyte Enzyme Buffer	
Myocyte Perfusion Buffer (A) +	
Collagenase II	1 mg/mL
Protease from *Streptomyces griseus* Type XIV	0.65 mg/mL
BDM	10 mM
BSA	0.1%

(C) Myocyte Stop Buffer	
Myocyte Perfusion Buffer (A) +	
BSA	1%

(D) Modified Tyrodes Buffer	
Chemical	Molarity (mM)
NaCl	113
KCl	5.4
$MgSO_4$	1.2
HEPES	10
Glucose	20
$CaCl_2$	1.8
BSA	0.1%
pH 7.4 with NaOH	

Table 2.1 – Solutions used for cardiomyocyte isolation and measurement of Ca^{2+} transients. Composition of solutions used for mouse heart digestions (A –B), cardiomyocyte isolation (C) and Ca^{2+} transient stimulation (D). Values in right hand columns are final concentrations/dilutions of chemicals and enzymes. BDM, 2,3-butanedione monoxime, BSA, bovine serum albumin.

Figure 2.3 - Schematic of Langendorff apparatus. Perfusion solutions ((A) and (B) from Table 2.1) were stored in a water bath (**1**) set at 42 °C. Solutions were circulated (blue lines) via a peristaltic pump (**2**) from the waterbath, through the heating coil (**3**) and into the heart which rested against the base of a water jacketed organ chamber (inset, green box) (**4**). After exiting the heart, Myocyte Perfusion Buffer which usually contained blood from the heart was discarded (dashed line). Myocyte Enzyme Buffer could be recirculated if it was free of blood. Warm water from the circulating water bath was pumped (red lines) through the water jacketed heating coil and the water jacketed organ chamber. This ensured that the circulating perfusate and the heart were kept at 37 °C. The water bath was set at 42 °C to allow for cooling of the circulating water as it was pumped through the water jacketed glassware. Arrows show the direction of circulation.

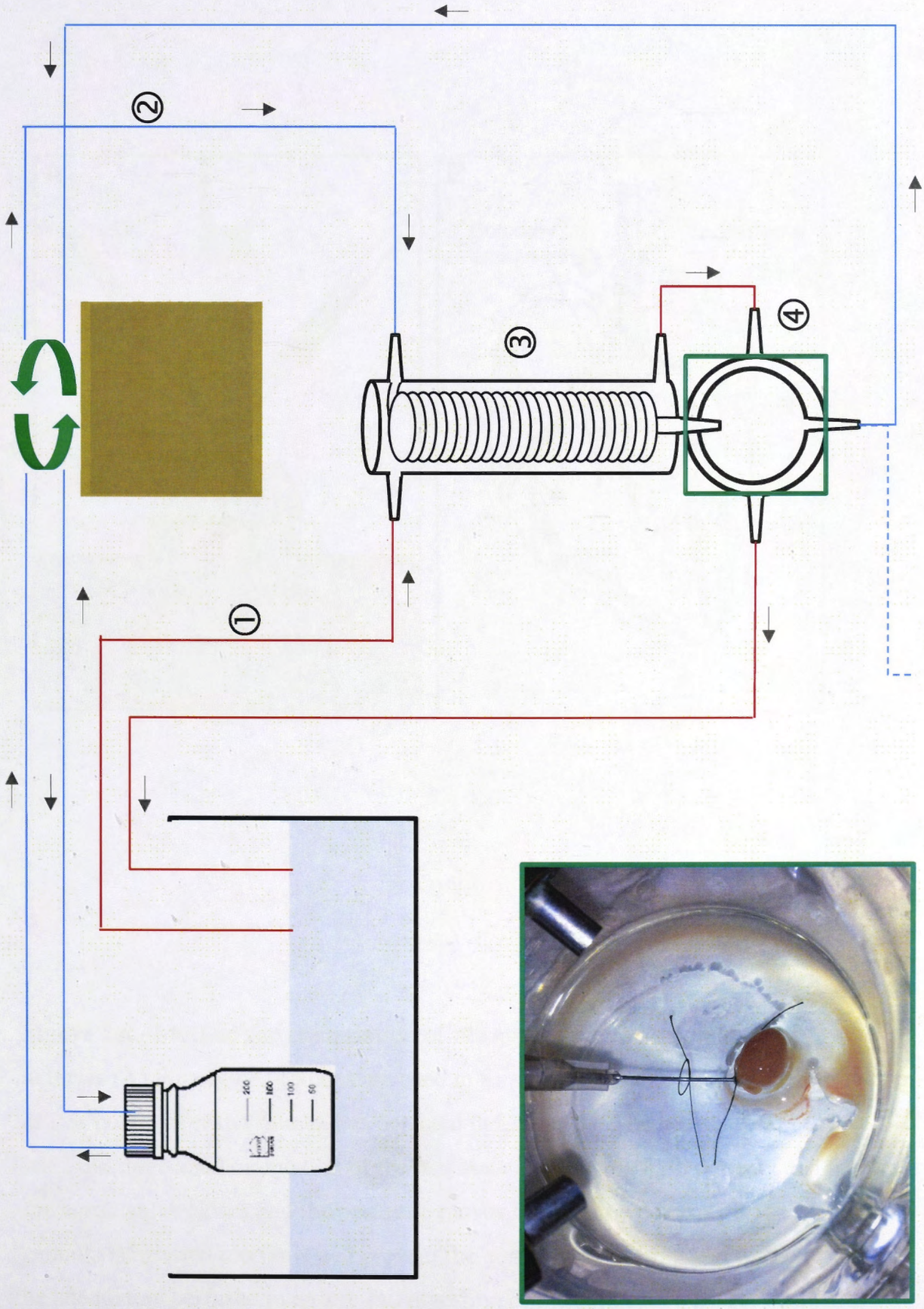
②
③
④
①

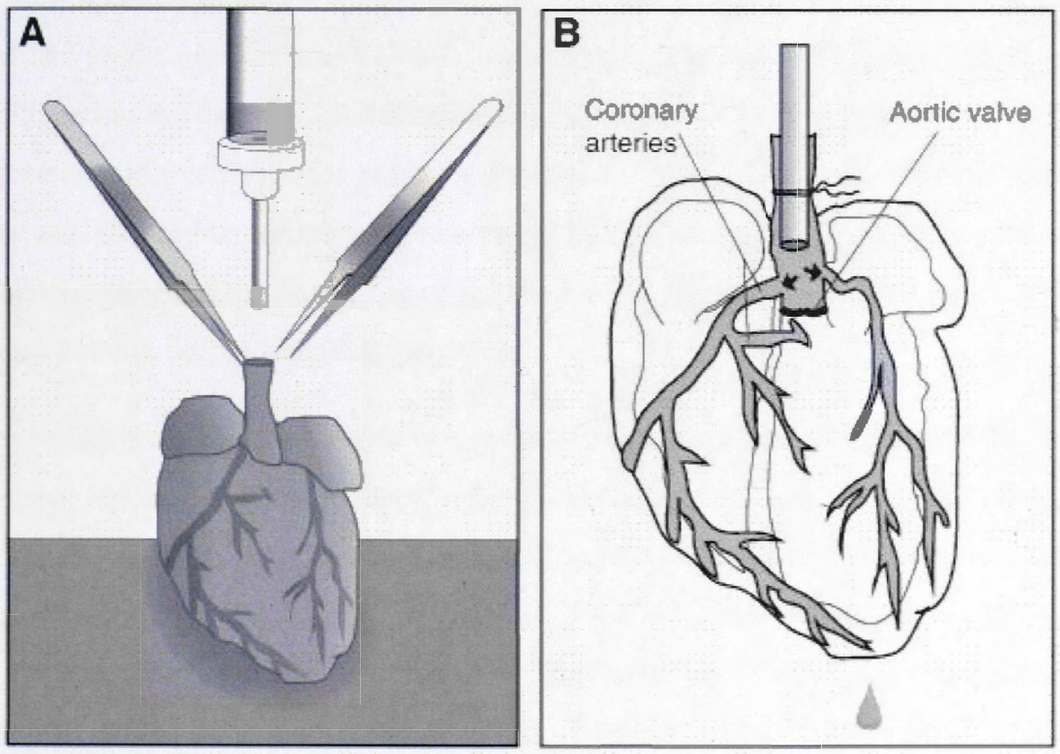

Figure 2.4 - Method for cannulation of the aorta and perfusion of coronary arteries (A) Fine-tipped forceps are used to grip the sides of the aorta and hold it open as it is pulled over the cannula, as depicted in figure **(B)**. The heart is held in place with silk thread and circulation of the perfusate is initiated. With correct cannulation, the aortic valve closes and the perfusate moves through the coronary arteries. If the cannula is inserted too far it will prevent the aortic valve closing and the heart will not be adequately perfused to ensure full digestion of the connective tissue, leading to poor cardiomyocyte yields. Figure modified from (Louch et al., 2011).

2.10.6. Calcium imaging

2.10.6.1. Calcium transient recording

The Ca^{2+} indicator Fluo-4 AM was used for Ca^{2+} transient recording. To aid in dispersion of the dye and prevent intracellular compartmentalization, the surfactant Pluronic F-127 was added to Fluo-4 stocks immediately before use, at a final concentration of 0.02%. Coverslips containing at least 60 – 70 % healthy cells per field of view were chosen for Ca^{2+} imaging. Fluo-4 was diluted to a final concentration of 5 μM in Tyrode's buffer (see Table 2.1) and added to plated myocytes. Cells were incubated in the dark for 20 min at room temperature. The Fluo-4 solution was carefully aspirated and fresh Tyrodes buffer was added to wash away excess dye and a further 20 min was allowed to complete dye de-esterification. In experiments using doxOL, the drug was added at the beginning of the Fluo-4 washout phase, allowing a 20 min preincubation before transient recording.

Coverslips were transferred to a custom built delrin chamber (Research School of Physics and Engineering, Canberra, Australia) containing perfusion ports and platinum electrodes for field stimulation. The two electrodes were placed parallel to each other along the longitudinal axis of the chamber, 3 – 4 mm apart. Electrodes were connected to a constant voltage isolated stimulator (Digitimer, Hertfordshire, United Kingdom) and pacing was set using a pulse generator (Digitimer, Hertfordshire, United Kingdom). Perfusion ports were connected to an external, perfusion system, allowing superfusion of the cells and solution exchange after caffeine perfusion. The chamber was held in an open perfusion micro-incubator (Warner Instruments, Hamden, United States).

Imaging was conducted using a Leica TCS SP5 confocal microscope (Leica, Mannheim, Germany) in line scan (x-t) mode (512 pixels/line, 2.1 ms per line, 0.12 μm per pixel) with a 40X oil-immersion objective. Fluo-4 was excited using the 488 nm line of an argon ion laser. Emission was collected at > 510nm using a HyD detector (Leica, Mannheim, Germany). The line scan was positioned parallel to the longitudinal axis of the cell. Cells were paced at 0.5 Hz using a voltage approximately 30% above the stimulation threshold and steady-state Ca^{2+} transients were recorded for 12 s before an 8 s stimulation free period to detect any spontaneous activity. Separate coverslips were used for control and doxOL–treated cells and were alternated so that recordings done in the presence or absence of doxOL were made at similar time points through the day. In experiments where SR load was measured, 10 mM caffeine was applied by positioning

rigid perfusion tubing in immediate proximity to the cell, and caffeine was added to the bathing solution by a gravity feed system. Caffeine was removed between recordings by superfusion of the chamber solution.

2.10.6.2. Calcium transient analysis

Data was acquired using the Leica Application Suite Advanced Fluorescence software and was analysed using either Axograph X (Axograph, Berkeley, United States) for Ca^{2+} transient analysis or ImageJ (National Institutes of Health, Bethesda, United States) for contractility measurements. Linescans were corrected for background fluorescence. Fluorescence values (F) were normalized to the basal fluorescence (F_o, a region of the recording before electrical stimulation) to obtain the fluorescence ratio:

$$\text{Relative fluorescence} = \frac{F - F_0}{F_0}$$

Ca^{2+} transient kinetics were measured for each cell including, peak amplitude, time to peak, time to 50% decay. For each cell, the average value of each parameter was calculated from 6 stimulated transients.

2.10.7. Contractility measurements

Coverslips were placed in a custom built chamber and positioned in a microincubator, and cells were paced at 0.5 Hz as above (Section 2.10.3.1). Myocyte contractions were recorded using a JVC video camera (KY/F550, Wayne, United States) attached to a TE2000-U microscope (Nikon Australia, Sydney, Australia). Video image sequences were analysed in ImageJ and length measurements were made during systole (most contracted) and diastole (most relaxed). Average % fractional shortening (FS) was calculated for each cell from 5 contractions. Alternate coverslips were preincubated for 20 min with 2.5 μM doxOL and % FS was compared to untreated cardiomyocytes.

2.11. Statistics

Average data are presented as mean ± SEM. The significance of differences between control and treated results was tested using a single factor analysis of variance test (ANOVA) or a student's t-test as appropriate. A p-value < 0.05 was considered significant for all tests.

Chapter Three

Anthracyclines and their Metabolites Modulate RyR2 and SERCA2A

3.1. Introduction

The anthracyclines doxorubicin and daunorubicin are among the most effective chemotherapeutic drugs available. Unfortunately, the full potential of these drugs can't be harnessed, as their use is accompanied by a potentially fatal cardiotoxicity which affects both adults and children. After decades of research, the mechanism of anthracycline-induced cardiotoxicity remains ambiguous. While there is evidence of an oxidative stress mechanism, efforts to treat or prevent cardiotoxicity by targeting this pathway have had limited success. This failure highlights the need for an improved understanding of how these drugs affect the redox environment of cardiomyocytes and has led to the search for coexisting mechanisms.

As detailed in Chapter 1, substantial evidence now exists to suggest changes in Ca^{2+} homeostasis play a prominent role in the effects of these drugs on the heart. Anthracyclines modulate RyR2 activity in single channel studies (Ondrias et al., 1990; Feng et al., 1999), cardiomyocytes (Wang et al., 2001; Sag et al., 2011), Ca^{2+} release assays (Olson et al., 2000; Shadle et al., 2000a) and [^{3}H] ryanodine binding assays (Pessah et al., 1990; Kim et al., 2006). RyR2 is not the only SR protein affected though, with CSQ2 identified as a binding target (Park et al., 2004; Kim et al., 2005b). Anthracyclines reduce the CSQ2 Ca^{2+} binding capacity and as a result, are thought to inhibit SR Ca^{2+} release and reduce SR Ca^{2+} load (Charlier et al., 2005; Kim et al., 2005b; Park et al., 2005b). Anthracycline-induced changes in RyR2 coexist with depressed cardiac function, including decreased ejection fraction and fractional shortening (Cusack et al., 1993a; Shadle et al., 2000a).

The anthracycline metabolites doxOL and daunOL also cause substantial impairment of cardiac function. Effects include depressed contractility and increased the resting tension of cardiac muscle preparations (Olson et al., 1988; Mushlin et al., 1993). Both doxOL and daunOL can inhibit the SERCA2A pump (Boucek et al., 1987; Olson et al., 1988; Mushlin et al., 1993; Olson et al., 2000), although drug concentrations in some of these studies were too high to be clinically relevant. Despite strong evidence demonstrating the efficacy of both metabolites in disrupting cardiac function, there are few studies specifically investigating the effects of these compounds on RyR2. However, Olson and colleagues (2000) found that daunOL could both stimulate and

inhibit Ca^{2+} release from SR vesicles. To date, there are no reports testing the effects of anthracycline metabolites on single RyR2 channels.

In my Honours studies I performed an in depth characterization of the effects of daunorubicin on RyR2 channels. Daunorubicin could both stimulate and inhibit Ca^{2+} release from SR vesicles. Application of 0.01 – 10 μM daunorubicin to single RyR2 channels caused significant activation of RyR2, which was reversed upon washout. With higher daunorubicin concentrations (2.5 – 10 μM) the early RyR2 activation was followed by secondary channel inhibition. While this inhibitory effect was not reversed by washout, it was preventable by preetreatment with dithiothreitol (DTT, 1 mM). Together, these results suggested that the activation of RyR2 by daunorubicin was caused by ligand binding while the inhibitory effect was caused by thiol oxidation (Hanna et al., 2011).

The fact that doxorubicin is the more commonly used of the two drugs, led to the focus of the present experiments on doxorubicin and doxOL. While the current chapter contains some information on daunorubicin and daunOL, the majority of the results concentrate on doxorubicin and doxOL. This direction has allowed more thorough investigation of the functional effects of these drugs, and the mechanisms underlying these functional effects.

Aim:

The primary aim of the experiments detailed in this chapter was to characterize the functional effects of anthracyclines on RyR2 and SERCA2A, focusing on drug concentrations which are known to accumulate in the heart. A secondary aim was to determine whether these functional effects were reversed when the drug was removed. This was the initial step in identifying the mechanism of action of these drugs, the results of which are the basis for all experiments carried out in subsequent chapters.

3.2. Materials and Methods

3.2.1. SR vesicle isolation and RyR2 purification

As detailed in Section 2.3, cardiac SR vesicles were prepared from sheep heart (Laver et al., 1995) and RyRs were solubilised and purified from SR as described by (Dulhunty et al., 2005).

3.2.2. Anthracycline-protein interactions

In brief, doxorubicin or doxOL was coupled to CNBr-activated Sepharose 4B according to the manufacturer's instructions (Section 2.8). Precleared, purified SR vesicles (0.5 mg/ml) were incubated with anthracycline-coupled beads overnight at 4°C with rotation. Unbound RyR2 was removed and proteins bound to the anthracycline-coupled CNBr activated Sepharose 4B were eluted by boiling for 1 min in sample buffer. The resultant supernatant was separated by SDS-PAGE, subject to western blot and immunoprobed with anti-RyR2 or anti-SERCA2A antibodies. Since triadin, junctin and CSQ2 associate with RyR2 it was necessary to use a solubilised SR vesicle preparation. In a crude SR preparation it would not be possible to determine whether the drug had bound to RyR/triadin/junctin or CSQ2 since all three accessory proteins would be eluted along with RyR2. In our solubilised SR protein preparations none of these accessory proteins are present, therefore we can be confident that the presence of RyR immunostaining is indicative of an interaction between the drug and RyR2 itself.

3.2.3. Single channel recording and analysis

The method for single RyR2 channel recordings is described in detail in Section 2.6. Stable control activity was recorded for 3 - 4 min before anthracyclines added to the *trans* chamber. It is unlikely that the drugs only acted at the luminal face of the RyR2 as anthracyclines are lipid soluble, and would cross the bilayer. In washout experiments, drugs were removed by perfusing the *trans* chamber with drug-free solutions. For anthracyclines, P_o in the 60 – 90 s record showing highest activity was defined as Maximal Activation and the 60 - 90 s record with the lowest activity was defined as Maximal Inhibition.

3.2.4. SR Ca^{2+} uptake assay

The method used to measure Ca^{2+} uptake into SR vesicles is shown in Figure 2.2 and 3.10. Vesicles were pre-incubated for 20 min with anthracyclines (or with vehicle buffer alone for control experiments) before they were added to the cuvette. The concentration of anthracycline in the cuvette was adjusted to the incubation concentration. Rate of Ca^{2+} uptake was determined by measuring the rate of change in optical density of the 15 s immediately following addition of Ca^{2+}. To account for day-to-day variability multiple controls and multiple drug experiments were done each day. Drug experiments were compared to the average control value for the same day.

3.3. Results

3.3.1. RyR2 response to pharmacological modulators

The response of RyR2 to modulatory agents such as ATP, Mg^{2+}, Ca^{2+} and ruthenium red has been well characterized and can be used to confirm the identification and orientation of RyR2 channels in lipid bilayers (Meissner, 1994). In this thesis the response to *cis* Ca^{2+} adjustment to physiological levels at the beginning of an experiment, established both the orientation of the channel and identified the channel as a RyR. At completion of an experiment ruthenium red was added for additional confirmation. Channels were also identified as being RyR2 by single channel characteristics, such as conductance.

3.3.1.1. Ruthenium Red

Ruthenium red is an RyR antagonist which is routinely used in single channel experiments using SR vesicle preparations, to identify the ion channel as an RyR (Ma, 1993; Xu et al., 1999). Because ruthenium red irreversibly blocks RyR2 channels, it was added only upon completion of the full experiment. Addition of 20 μM ruthenium red to the *cis* chamber reduced channel open probability (P_o) to levels approaching zero at both +40 and -40 mV (Figure 3.1A). RyR2 block occurred within ~30 s of adding ruthenium red to the *cis* chamber.

3.3.1.2. Cytoplasmic Ca^{2+}

Cytoplasmic Ca^{2+} is a biphasic modulator of RyR2, which between 1 μM and 1 mM activates the channel, while concentrations above 1 mM inhibit (Laver et al., 1995). Following RyR2 incorporation, standard control recording ionic conditions were established by reducing the cytoplasmic [Ca^{2+}] from 1 mM to 1 μM by the addition of the Ca^{2+} chelator BAPTA to the *cis* solution (1.32 mM). A reduction in activity to sub-maximal levels was observed shortly after addition of BAPTA (Figure 3.1B). This change in activity occurred at both +40 mV and -40 mV and in most cases, stabilized within 1 - 2 min, thus confirming the channels identity as RyR2. Additionally, the channel sensitivity to cytoplasmic Ca^{2+} differs to its luminal Ca^{2+} sensitivity (Laver, 2007; Qin et al., 2008). With 1 mM cytoplasmic Ca^{2+} and in the absence of ATP, reducing the luminal [Ca^{2+}] from 1 mM to 1 μM would be expected to cause only a minor change in P_o. Thus, the response of RyR2 to changes in *cis* Ca^{2+} could be used to confirm the orientation of the channel.

3.3.1.3. Channel conductance

In addition to decreasing *cis* [Ca^{2+}] from 1 mM to 1 μM, the establishment of control conditions involved setting symmetrical [Cs^+], which was achieved by increasing the *trans* [Cs^+] from 50 mM to 250 mM. Ion channel conductance (G) is directly influenced by the maximum current flowing through the channel (I) and the voltage (V) being applied:

$$G = \frac{I}{V}$$

Thus, at 0 mV, Cs^+ current was zero, as expected under symmetrical ionic strength (250/250 mM Cs^+). Under these conditions, in a random sample of single channel experiments, the average single channel current was 11.71 ± 0.52 pA at +40 mV (n = 28) and 11.13 ± 0.58 pA at -40 mV (n = 23). These values correspond to average conductances of 292.75 ± 7.2 pS at +40 mV and 278.25 ± 8.52 pS at – 40 mV (Figure 3.1). This yields two important pieces of information. Firstly, that channel conductance was approximately equal at both +40 mV and -40 mV under control conditions and secondly, that under these conditions, Cs^+ conductance is similar to those reported previously under identical experimental conditions (Ahern et al., 1994a; Dulhunty et al., 2001).

As detailed in Section 2.6.3, Cs^+ was used as the current carrier in all single channel experiments. While a RyR2 Cs^+ conductance of 440 ± 8 pS has been reported (Tinker and Williams, 1992), those experiments were done in the absence of divalent cations (such as Ca^{2+}). Since RyR2 favours the passage of divalent cations over monovalent cations (like Cs^+) it is expected that millimolar *trans* Ca^{2+} would competitively displace Cs^+ from the putative binding site in the RyR2 channel pore (Tinker and Williams, 1992; Ahern et al., 1994a; Tu et al., 1994). An example of this effect is shown in Figure 3.1B where the conductance increases when cytoplasmic Ca^{2+} is reduced from 1 mM to 1 μM. Since the *trans* chamber still contained 1 mM Ca^{2+}, the conductance increase was not as great as it would be with a lower *trans* [Ca^{2+}]. None of the experimental compounds used in this study have been reported to influence RyR2 conductance. No changes in RyR2 conductance upon treatment with anthracyclines, redox agents or any other pharmacological agents used during this project were evident.

3.3.2. Anthracycline binding to RyR2 and SERCA2A

Before testing for any functional effect of anthracyclines on RyR2 or SERCA2A it was necessary to first determine whether a ligand binding interaction between the drugs and proteins of interest existed. Binding of doxOL with CSQ2 has been demonstrated (Kim *et al.,* 2005; Park *et al.,* 2005), however the metabolites binding to RyR2 and SERCA2A has not previously been invertigated biochemically. The interaction of doxorubicin and doxOL with RyR2 and SERCA2A was probed using affinity chromatography, with any proteins 'pulled down' by doxorubicin and doxOL eluted and subject to SDS PAGE and western blot. Substantial immunostaining (using primary antibodies anti-RyR and anti-SERCA2A) indicated that doxorubicin and doxOL can bind to both RyR2 and SERCA2A (Figure 3.2). Since triadin, junctin and CSQ2 are not present in our purified RyR2 preparations, we can be confident that the RyR2 immunostaining was indicative of an interaction between anthracyclines and RyR2 itself, not an associated protein. SERCA2A is however present in our purified vesicles but is known not to associate with RyR2. In some experiments, control samples, where beads were not coupled with anthracyclines displayed some non-specific binding but this was only minor. These results demonstrate that in our sheep heart preparations, both RyR2 and SERCA2A are binding targets of anthracyclines.

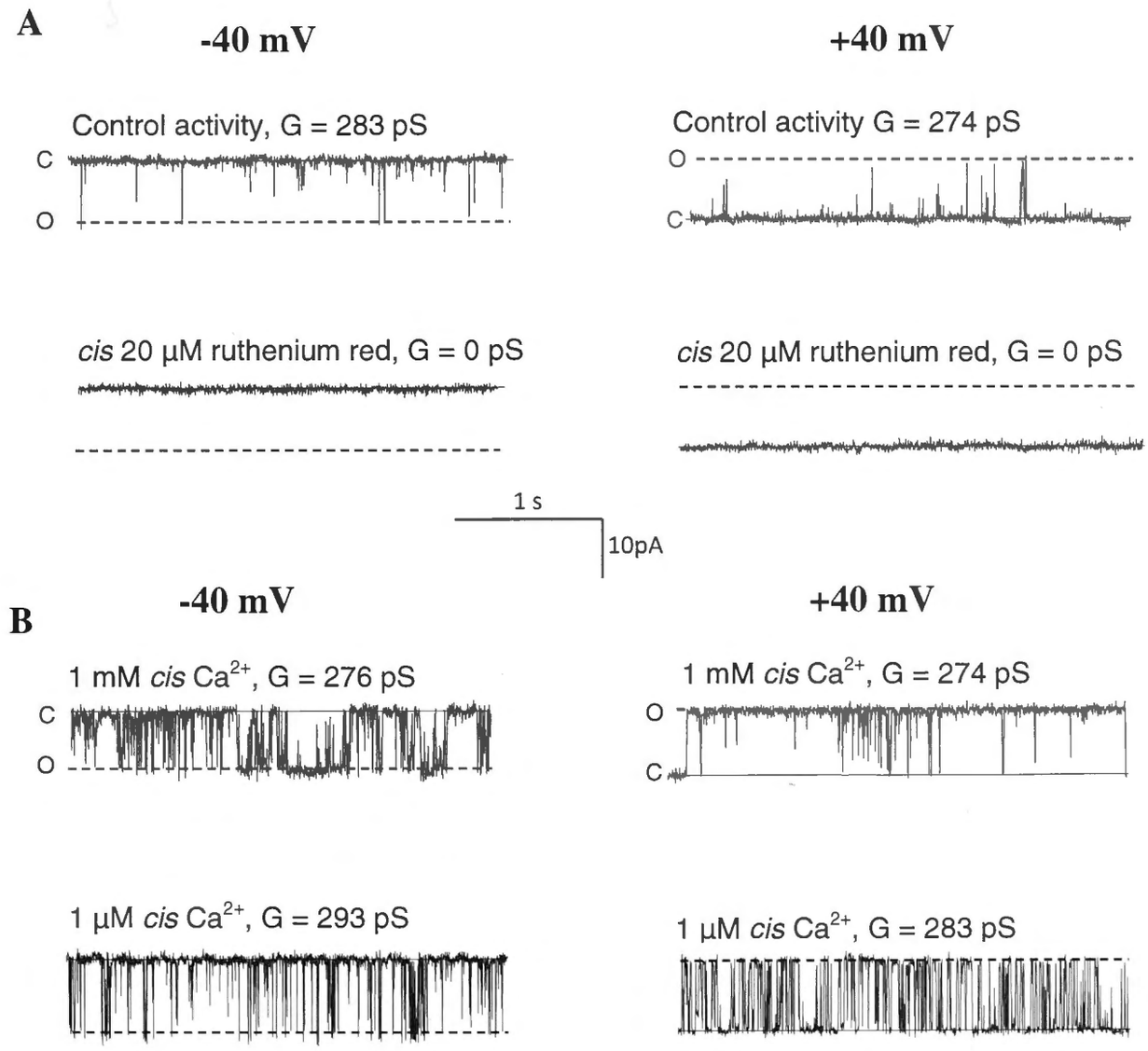

Figure 3.1 – RyR2 regulation by cytoplasmic Ca^{2+} and ruthenium red. **(A) – (B)** Three second recordings of RyR2 activity. *Left panels* Channels are opening downward from zero current (c, solid line) to maximum open conductance (o, dashed line). *Right panels* Channels are opening upward from zero current (c, solid line) to maximum open conductance (o, dashed line) **(A)** Channel activity with symmetrical [Cs^+] of 250 mM. Twenty µM ruthenium red was added to the *cis* chamber (lower recordings), abolishing activity at both +40 mV and -40 mV. **(B)** RyR2 activity at *cis* [Ca^{2+}] from 1 mM (upper traces) and at *cis* 1 µM (lower traces) with the addition of 1.32 mM BAPTA. Traces are representative of changes in RyR2 activity that occur with the known pharmacological agonists ruthenium red (A) and Ca^{2+} (B) in single channel experiments conducted during this project. Maximum conductance values (G) were measured from the recordings displayed.

3.3.3. Anthracyclines cause biphasic modulation of single channel activity

After confirming binding between anthracyclines and RyR2 and SERCA2A, the aim was to determine the functional effect of the drugs on these proteins. Drug effects on SERCA2A will be discussed at length in Section 3.3.5. The isolated environment of the single channel system allows analysis of the specific functional effects of the drug on RyR2. Due to the inherent variability in basal RyR2 activity, data is often expressed in relative terms. This is particularly beneficial when comparing multiple sets of data.

3.3.3.1. Anthracyclines activate RyR2

This project began with my honours investigation of the anthracycline daunorubicin which was completed in June 2009 and therefore not included in this PhD thesis. Those results were also published in 2011, with additional experiments that are presented in Section 4.3.1.1 (Hanna et al., 2011). The results detailed in Chapters Three and Four of this thesis build on that earlier work with daunorubicin and show that daunorubicin, doxorubicin and their primary metabolites can modulate RyR2 channels.

Addition of 0.01 μM doxorubicin caused a significant 3.11±0.78 fold increase in channel open probability (P_o; Figure 3.3). Higher concentrations of doxorubicin also induced RyR2 activation. Addition of 0.5 μM, 1 μM and 2.5 μM doxorubicin induced a 3.91±0.34, 4.35 ±1.08 and 3.28±0.67 fold increase in activity, respectively ($p \leq 0.05$; Figure 3.3). To more easily compare the effects of different drugs, from here in, all P_o changes are expressed relative to control activity unless stated otherwise. Although the increase in P_o was significant across all concentrations, the degree of activation was never significantly higher than that caused by 0.01 μM doxorubicin. This suggests that the activation by doxorubicin is saturated by concentrations as low as 0.01 μM.

The doxorubicin metabolite, doxOL, elicited similar effects on RyR2. There was a 3.70 ± 0.77 fold increase in P_o after addition of 0.01 μM doxOL (Figure 3.4). The greatest effect was caused by 0.5 μM doxOL, with a 6.41 ± 0.92 fold increase in activity, a significantly greater increase than with 0.01 μM doxOL. Higher doxOL concentrations did not evoke any further activity increase, suggesting that 0.5 μM doxOL is a saturating concentration.

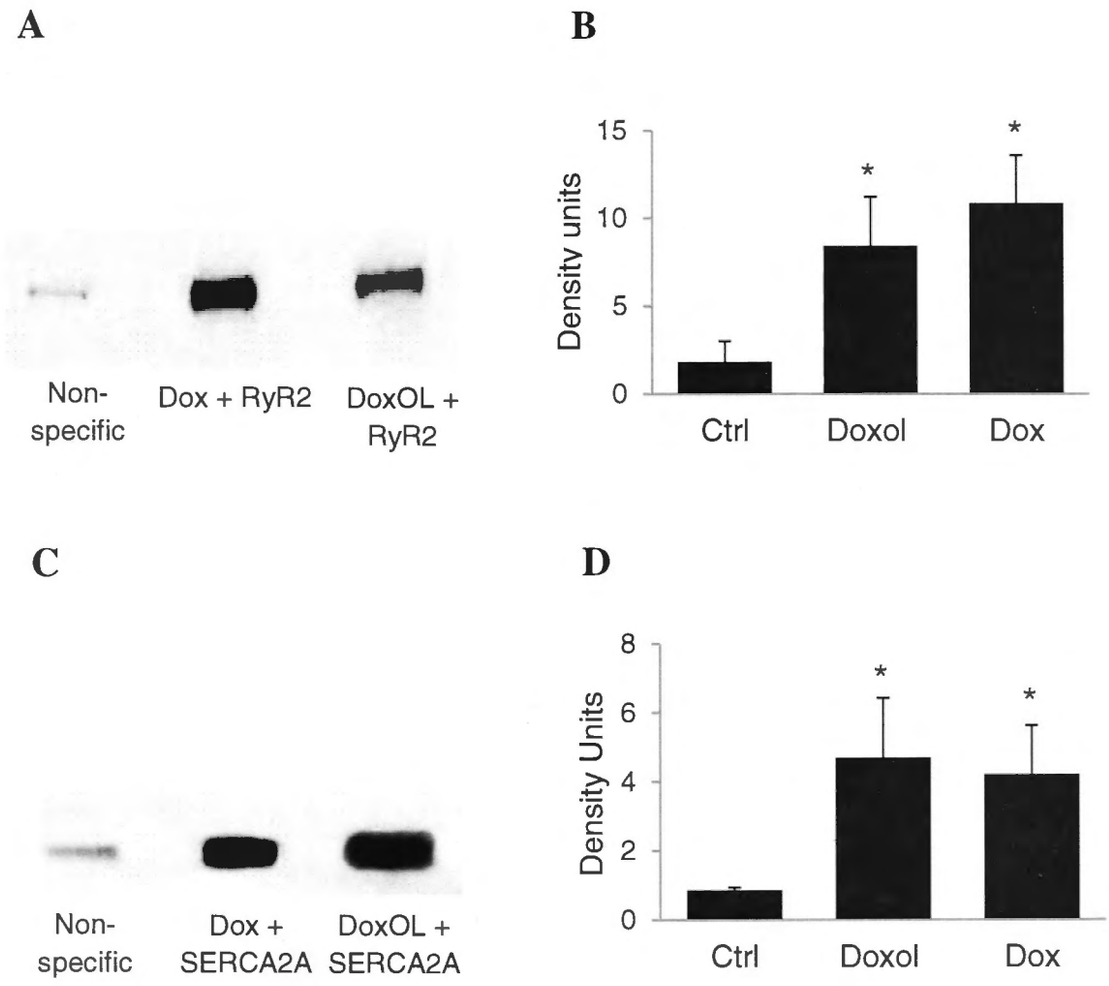

Figure 3.2 - Doxorubicin and doxOL bind to RyR2 and SERCA2A. Western blot showing RyR2 (n = 3 – 5) **(A)** and SERCA2A (n = 3 – 5) **(C)** bound to CNBr-activated Sepharose in the absence of doxorubicin/doxOL (non-specific binding; lane 1), to doxorubicin coupled CNBr-activated Sepharose (lane 2) and doxOL coupled CNBr-activated Sepharose (lane 3). Average density of RyR2 **(B)** and SERCA2A **(D)** from control (bin 1), doxorubicin coupled CNBr-activated Sepharose (bin 2) and doxOL-coupled CNBr-activated Sepharose (bin 3). Asterisk (*) indicates a significant difference in arbitrary densitometry units between the control and anthracycline coupled CNBr-activated Sepharos. The blots presented in **(A)** and **(C)** are taken from the same experiment.

There was a trend for the time to activation to be reduced as higher drug concentrations were used, but this was not significant. Maximal activity was seen after exposure to doxorubicin at: 5.2 ± 0.8 min (with 0.01 μM doxorubicin), 3.2 ± 0.4 (0.5 μM doxorubicin), 5.7 ± 1.2 (1 μM doxorubicin) and 4.1 ± 0.9 min (2.5 μM doxorubicin) (Table 3.1A). Similarly, doxOL activation began within 7.8 ± 1.8 min (with 0.01 μM), 4.9 ± 1.4 (0.5 μM), 4.1 ± 1.2 (1 μM) and 2.3 ± 0.6 min (2.5 μM) of drug addition (Table 3.1B). Comparing doxorubicin and doxOL, there was no significant difference in the time taken to cause maximal activation of RyR2 after addition of either drug to the *trans* chamber.

Whilst the effect of daunorubicin on RyR2 was detailed in my Honours thesis, the effect of daunOL on single channels has not been investigated. However, since the focus of this project was doxorubicin (and its metabolite), daunOL was only tested in the range of 0.5 – 2.5 μM. Addition of 0.5 μM daunOL caused a significant 4.3±1.2 fold increase in P_o. Higher concentrations activated RyR2 to a similar extent with 2.5 μM daunOL causing a maximal 5.35 ± 1.32 fold increase in P_o (Figure 3.5). This was not significantly different from the results with lower daunOL concentrations, illustrating that saturation had been achieved with 0.5 μM. The saturating concentration may have been lower than 0.5 μM (as it was with doxorubicin), but due to time constraints this was not explored. The time to activation by daunOL was comparable to that of the other anthracyclines tested. Following daunOL addition to the *trans* chamber, channel activation began within 3.6 ± 1.7 min (with 0.5 μM daunOL), 4.5 ± 1.6 min (1 μM daunOL) and 1.9 ± 0.4 min with 2.5 μM daunOL (Table 3.1D). For comparison, the time to maximal activation for daunorubicin ranged from 8.5 ± 2.2 min with 0.5 μM to 5.7 ± 2 min with 2.5 μM (Table 3.1C, (Hanna et al., 2011).

3.3.3.2. Anthracyclines inhibit RyR2

Lower concentrations (0.01 – 0.05 μM) of anthracyclines induced channel activation which lasted for the lifetime of the experiment, up to 30 min post drug addition. A secondary inhibitory effect was observed in a minority of channels treated with 0.01 μM doxorubicin (see below). Higher doxorubicin concentrations (1 – 2.5 μM) consistently caused sustained inhibition of channel activity, which occurred immediately following the activation phase (Figure 3.6).

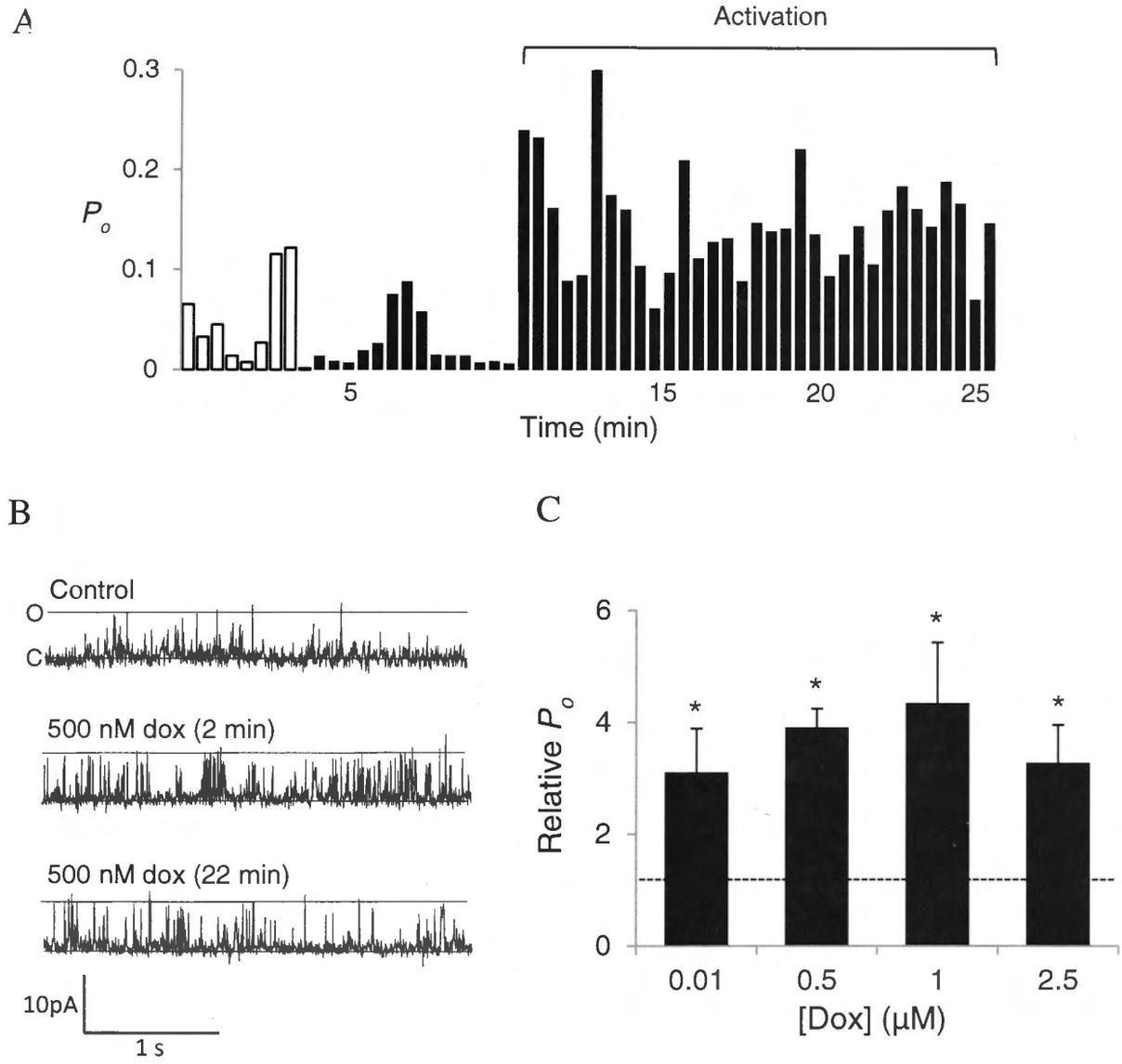

Figure 3.3 Doxorubicin activates native RyR2 channels. (**A**) Running histogram of experimental strategy. RyR2 channel open probability (P_o) was measured every 10 s throughout an experiment before (white bins) and after (black bins) the addition of 0.5 μM doxorubicin at +40 mV. (**B**) Three s recordings of native RyR2 channel activity at +40 mV. Channels open upward from zero current (C, continuous line) to maximum open conductance (O, dashed line). Top panel, control recording of native RyR2 activity in the absence of doxorubicin; middle and bottom panel, after the addition of 0.5 μM doxorubicin to the *trans* chamber. Maximal RyR2 activity was first measured at 2 min in this channel (middle panel), with no further change in activity recorded for 22 min after doxorubicin addition (bottom panel). (**C**) Combined data from measurements of P_o at +40 mV and –40 mV (n = 9 - 16). Data is presented as average P_o during the activation phase (relative to control). Asterisk (*) indicates a significant difference from the control P_o recorded before adding doxorubicin.

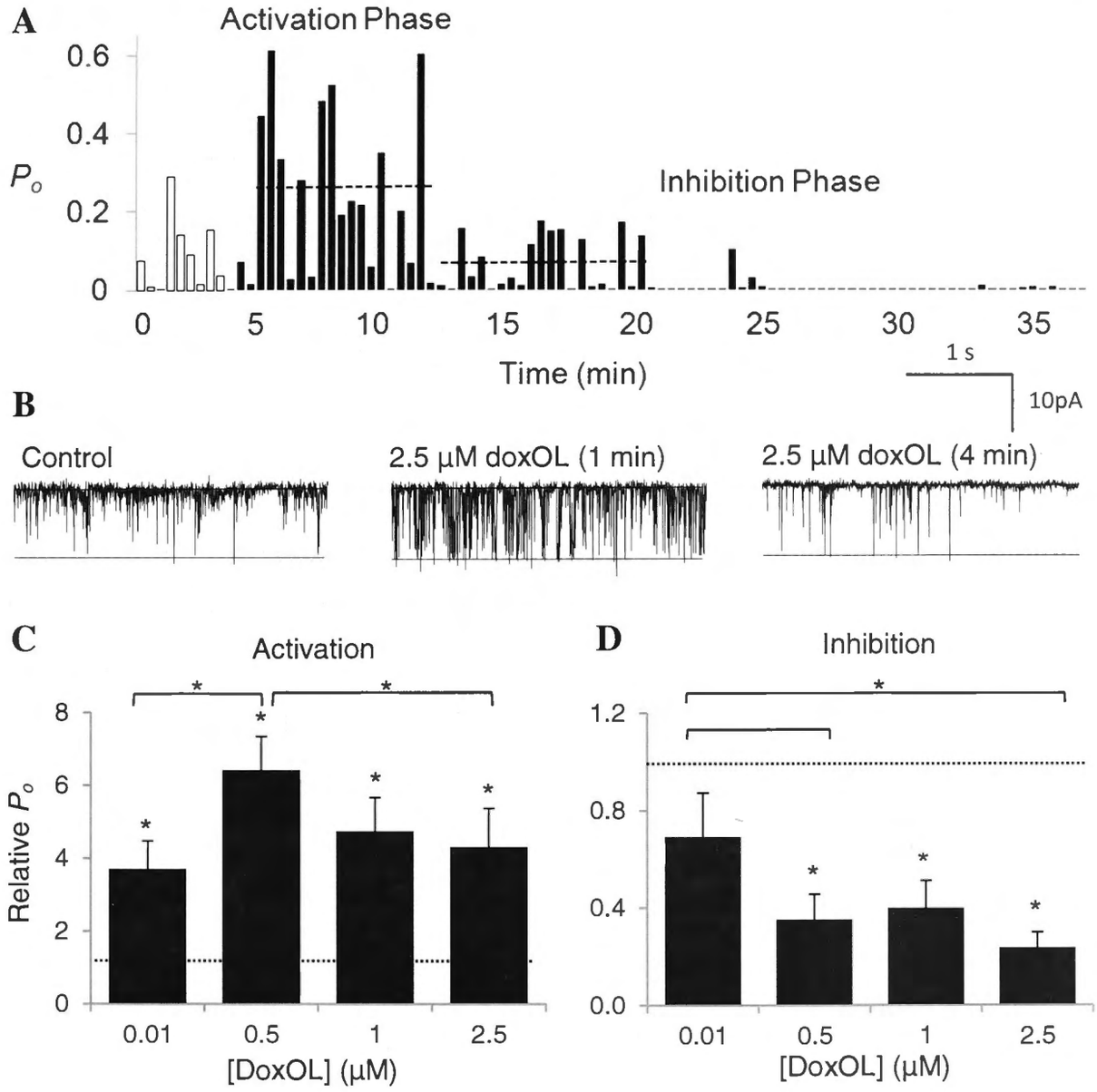

Figure 3.4 - DoxOL causes biphasic modulation of native RyR2 channels. (**A**) Running histogram, where native RyR2 channel P_o was measured every 10 s at +40 mV throughout an experiment before (white bins) and after (black bins) the addition of 2.5 µM doxOL. (**B**). Three s traces of native RyR2 channel activity at -40 mV. Channels open downward from zero current (C, continuous line) to maximum open conductance (O, dashed line). Left panel, control recording of native RyR2 activity in the absence of doxOL; centre and right panel, after the addition of 2.5 µM doxOL to the *trans* chamber. Maximal RyR2 activity was first measured at 1 min after addition of doxOL (centre panel) and maximal RyR2 inhibition measured at 4 min after doxOL addition (right panel). (**C**) – (**D**) Combined data from measurements of P_o at +40 mV and –40 mV (n = 7 -18 at each concentration). Data is presented as average relative P_o. Average relative P_o during the activation phase (relative to control) shown in (**C**) and average relative P_o during the inhibitory phase (relative to activity during control) shown in (**D**). Asterisk (*) indicates a significant difference from the control P_o recorded before adding doxOL.

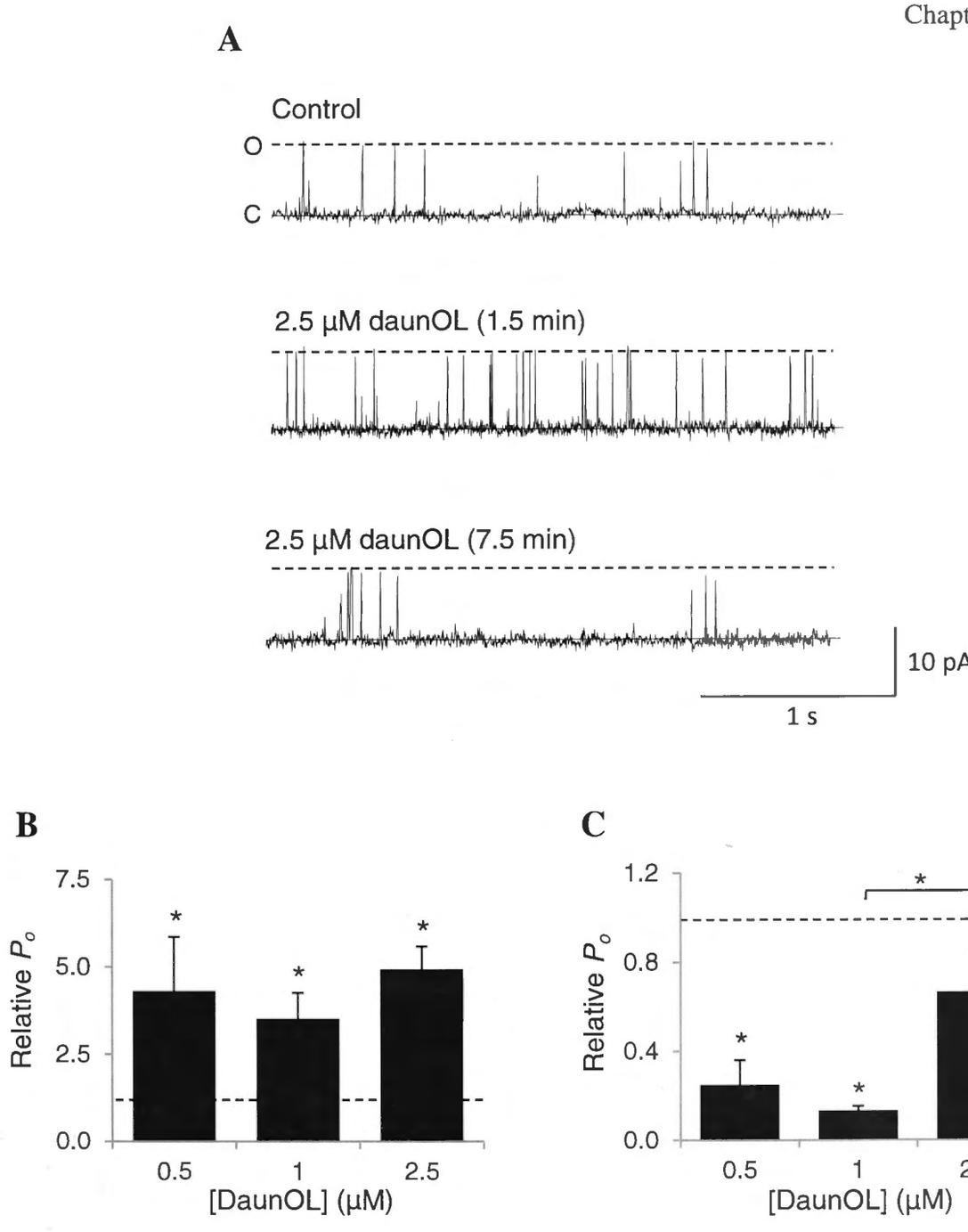

Figure 3.5 - DaunOL causes biphasic modulation of native RyR2 channels. (**A**) Three s recordings of native RyR2 channel activity at +40 mV. Channels open upward from zero current (C, continuous line) to maximum open conductance (O, dashed line). Left panel, control recording of native RyR2 activity in the absence of daunOL; centre and right panel, after the addition of 2.5 µM daunOL to the *trans* chamber. Maximal RyR2 activity was first measured at 1.5 min after addition of daunOL (middle panel) and maximal RyR2 inhibition was measured 7.5 min after daunOL addition (bottom panel). (**B**) – (**C**) Combined data from measurements of P_o at +40 mV and –40 mV (n = 6 - 14). Average data is presented s P_o relative to control activity. Relative P_o during activation shown in (**B**) and relative P_o during inhibition shown in (**C**). Asterisk (*) indicates a significant difference from the control P_o recorded before adding daunOL. Crosshatch (#) indicates a significant difference from activity during the activation phase.

On average, the activity of channels treated with 1 μM and 2.5 μM doxorubicin was reduced to 71% and 48% of control P_o, respectively (Figure 3.6C). This mimicked the effects of daunorubicin (Hanna et al., 2011). On average, inhibition began 11.25 ± 2 min after doxorubicin addition and was sustained for the lifetime of the experiment (Table 3.1A). Given that 10 – 15% of channels treated with 0.01 – 0.5 μM doxorubicin exhibited an inhibitory phase, it is likely that lower concentrations of doxorubicin were capable of inhibiting RyR2, but that it was generally not observed in the time frame of the experiment.

In the first major distinction between the parent compounds and metabolites, doxOL was a more effective inhibitory agent then doxorubicin, as all tested concentrations of doxOL caused significant inhibition of channel activity (Figure 3.4D). P_o fell to 69 % of control with 0.01 μM doxOL and to 24% of control with 2.5 μM doxOL. Even though 1 – 2.5 μM doxorubicin did inhibit RyR2, the equivalent concentrations of doxOL caused more drastic reductions in P_o. As a percentage of control activity, there was a 19% decrease in P_o induced by doxorubicin compared with a 60% decrease with doxOL ($p<0.05$). Similarly, 2.5 μM doxorubicin caused a 52% reduction in P_o, whilst the equivalent dose of doxOL caused a 76% decrease ($p<0.05$). On average, doxOL-induced inhibition began 13.9 ± 2.1 min following drug addition and was fastest with 2.5 μM doxOL, when inhibition occurred within 8 min (Table 3.1B).

All tested concentration of daunOL also inhibited RyR2. This indicates an enhanced efficacy of the metabolite, since daunorubicin required at concentrations ≥2.5 μM to cause significant inhibition. Unexpectedly, the lower concentrations of 0.5 and 1 μM daunOL were significantly more effective at inhibiting RyR2 then the higher concentration of 2.5 μM. P_o was reduced to 34% and 11% of control with 0.5 and 1 μM daunOL (respectively), whereas the average lowest activity measured with 2.5 μM was 67% of control activity (Figure 3.5). Still, this was a significant reduction in P_o compared with activity during the activation phase. The time to maximal inhibition ranged from 12 ± 0.7 min with 2.5 μM to 15.4 ± 0.9 with 0.5 μM daunOL (Table 3.1D). It is curious that lower concentrations of daunOL caused more severe inhibition than the highest daunOL concentrations, as this is inconsistent with results obtained with other anthracyclines where there was a trend for the extent of inhibition to increase with higher drug concentrations.

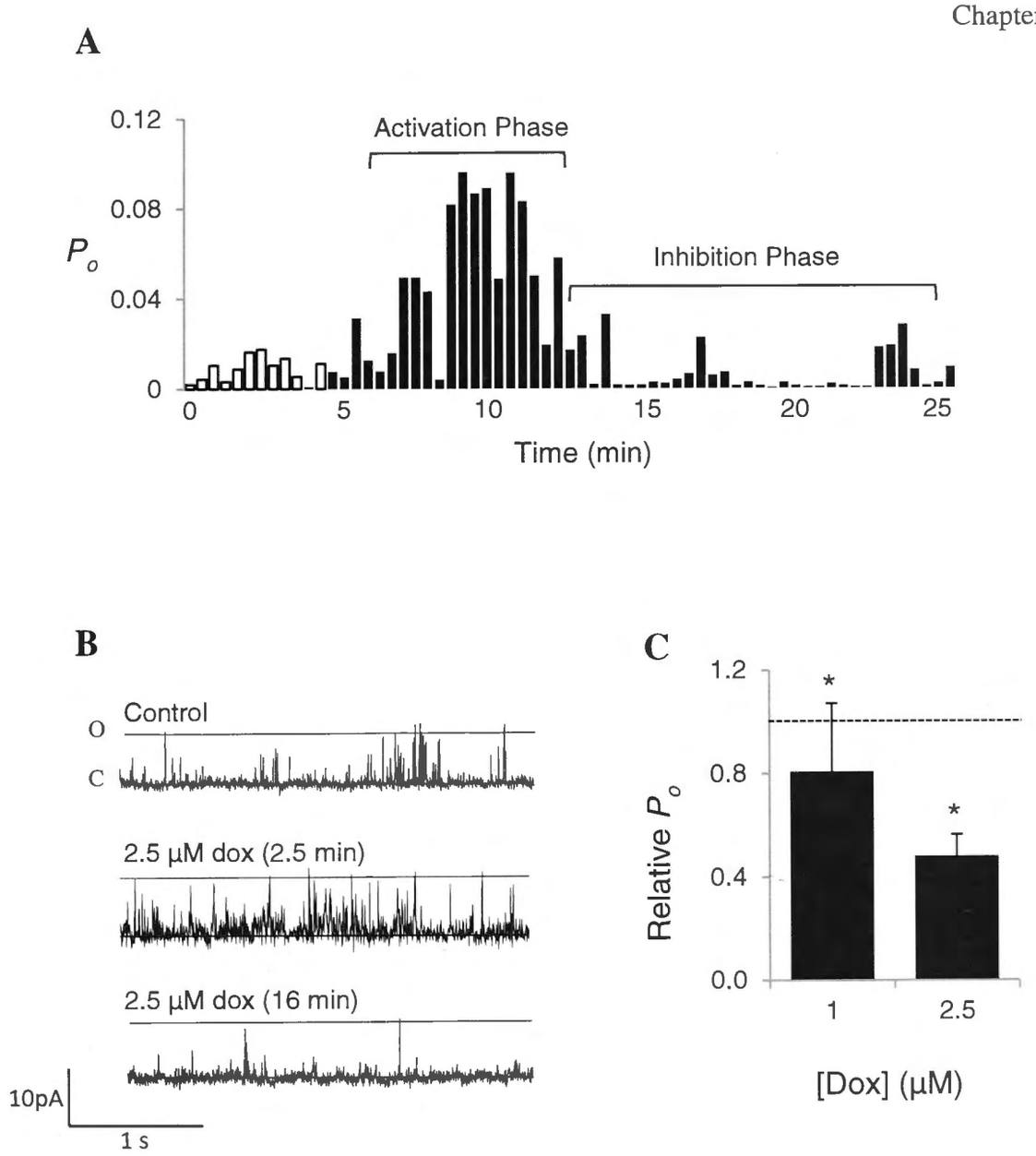

Figure 3.6 - High concentrations of doxorubicin inhibit RyR2 (**A**) Running histogram of experimental strategy. RyR2 channel P_o was measured every 10 s throughout an experiment before (white bins) and after (black bins) the addition of 2.5 μM doxorubicin at +40 mV. (B)Three second traces of native RyR2 channel activity at +40 mV. Channels open upward from zero current (C, continuous line) to maximum open conductance (O, dashed line). Top panel, control recording of native RyR2 activity in the absence of doxorubicin; middle and bottom panel, after the addition of 2.5 μM doxorubicin to the *trans* chamber. Maximal RyR2 activity was first measured at 2.5 min in this channel (middle panel), and maximal RyR2 inhibition was recorded 16 min after doxorubicin addition (bottom panel). (**C**) Combined data from measurements of P_o at +40 mV and –40 mV (n = 8 - 17). Average data is presented as P_o during the inhibitory phase (relative to activity during control). Asterisk (*) indicates a significant difference from the control P_o recorded before adding doxorubicin.

The cause of this anomaly was not pursued but may be due to the unusually low control activity of the channels used for this set of data. The control P_o for channels that were treated with 2.5 μM daunOL was 0.0080 ± 0.003 compared to 0.017 ± 0.01 for 0.5 μM and 0.0254 ± 0.01 for 1 μM.

3.3.3.3. Cytoplasmic addition of anthracyclines cause biphasic modulation of RyR2

In the majority of experiments in this project, drugs were added to the *trans* chamber as one of the original aims of the project was to analyse the effects of the drugs on luminal SR proteins. Since the drug is highly lipid soluble, it is expected that anthracyclines would cross the lipid bilayer within the timeframe of the experiment. Therefore, it was expected that drug addition to the *cis* chamber would induce activation and inhibition of RyR2 activity to a similar degree as *trans* addition of matched concentrations. This was tested using 1 μM doxOL and 1 μM daunOL, since these concentrations should reliably produce both activation and inhibition (as detailed above).

As expected, *cis* addition of both doxOL and daunOL yielded similar results as with *trans* addition, causing activation of RyR2 that was followed by channel inhibition (Figure 3.7). The only statistically significant difference was in the extent of inhibition by daunOL. Compared to control activity, *cis* addition of daunOL caused a 15% reduction in P_o, while *trans* addition induced a more drastic 89% reduction in P_o. DaunOL also activated RyR2 more quickly with *trans* addition (6.5 ± 1.3 min) than with *cis* addition (10.6 ± 2.1 min), though the time to inhibition was approximately equal (14.1±2.2 min with *trans* vs. 13.8±1.3 min with *cis* addition) (Table 3.1D). These results suggest that daunOL may be acting at a luminal or transmembrane domain of RyR2 at a site that is equally accessible to both *cis* and *trans* solutions. Conversely, with 1 μM doxOL the time to maximal effect (activation and inhibition) was always faster with *cis* addition than with *trans* addition. Since *cis* addition would allow doxOL to access the cytoplasmic region faster than it had when added to the *trans* chamber (Table 3.1B) it is possible that doxOL is acting at a cytoplasmic region of RyR2. The possibility that the two drugs are acting at different sites is interesting but no further experiments were done to investigate this possibility.

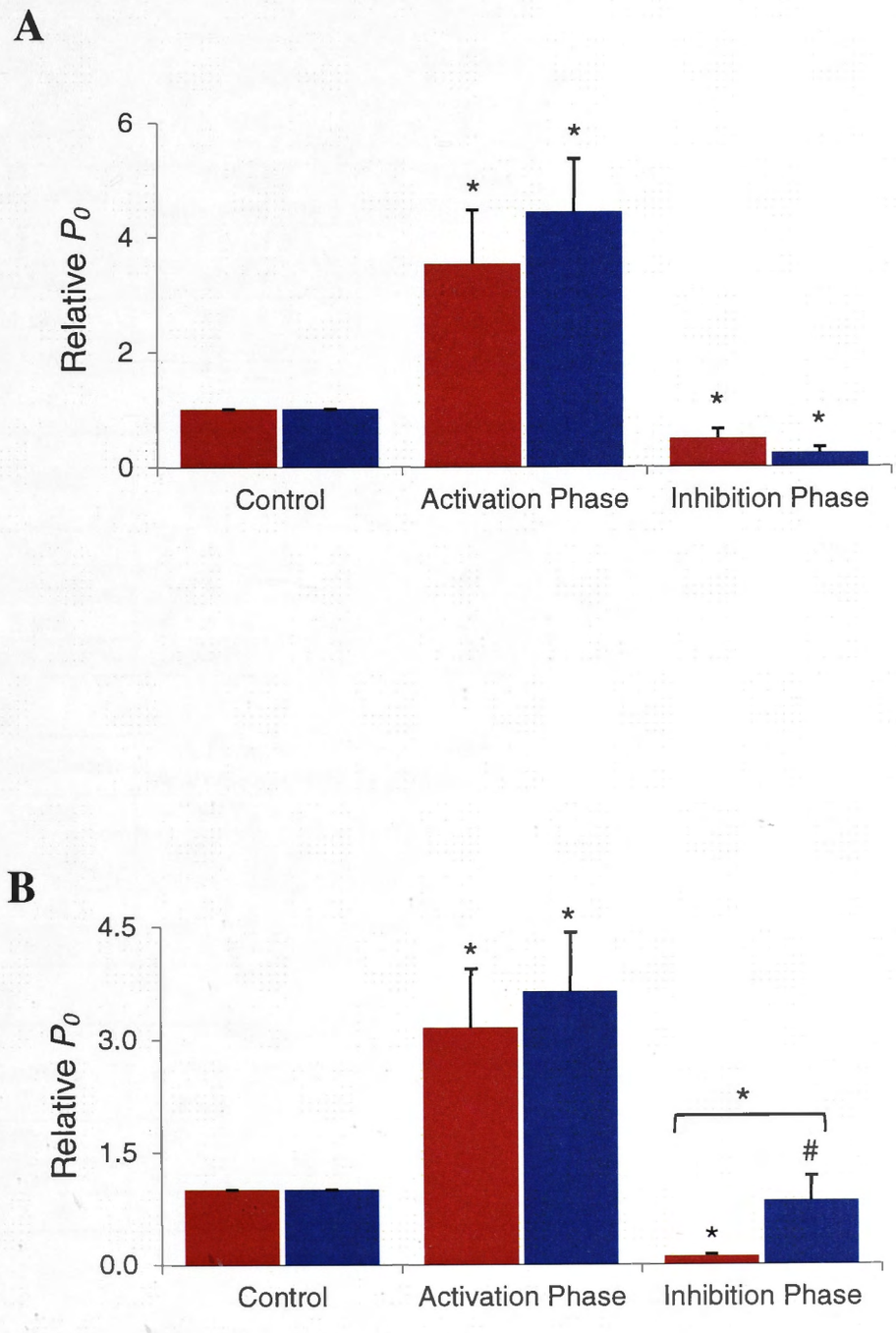

Figure 3.7 - *Cis* and *trans* addition of DoxOL and DaunOL induce similar effects *on* RyR2 channel activity. RyR2 average relative P_o where drugs were added to either *cis* (blue bins) or *trans* (red bins) solutions. After addition of doxOL (n = 6) (**A**) or daunOL (n = 9) (**B**), RyR2 activity was sampled from the phase of maximal activity (Activation) or minimal activity (Inhibition). Asterisk (*) indicates significant difference from control ($p < 0.05$) or between *cis* and *trans* additions as indicated. Crosshatch (#) indicates significant difference to previous phase ($p < 0.05$).

(A)

Doxorubicin	Time to Activation (min)	Time to Inhibition (min)
10 nM	5.2 ± 0.8	
500 nM	3.2 ± 0.4	
1 μM	5.7 ± 1.2	11.3 ± 2.7
2.5 μM	4.1 ± 0.9	11.2 ± 1.3

(B)

DoxOL	Time to Activation (min)		Time to Inhibition (min)	
	trans	*cis*	*trans*	*cis*
10 nM	7.8 ± 1.8		17 ± 2.3	
500 nM	4.9 ± 1.4		14.4 ± 1.1	
1 μM	4.1 ± 1.2	2.3 ± 0.8	16.4 ± 0.8	10.3 ± 1.5
2.5 μM	2.3 ± 0.8		7.7 ± 1.2	

(C)

Daunorubicin	Time to Activation (min)	Time to Inhibition (min)
10 nM	15.7 ± 2.4	
500 nM	5.8 ± 1.8	
1 μM	5.2 ± 0.8	12.6 ± 4.3
2.5 μM	2.4 ± 0.5	11.9 ± 1.7

(D)

DaunOL	Time to Activation (min)		Time to Inhibition (min)	
	trans	*cis*	*trans*	*cis*
500 nM	3.6 ± 1.7		13.6 ± 0.2	
1 μM	4.5 ± 1.6	6.3 ± 1.1	12.6 ± 1.8	12.2 ± 1.91
2.5 μM	1.9 ± 0.4		8.3 ± 0.7	

Table 3.1 – Time to anthracycline-induced RyR2 activation and inhibition. Average time to RyR2 activation and time to RyR2 inhibition are presented for all tested concentrations of (**A**) doxorubicin (n = 8 – 17), (**B**) doxOL (n = 7 – 18) and (**D**) daunOL (n = 6 – 14). Data for daunorubicin (n = 6 – 10) (**C**) are presented for comparison (Hanna et al 2011). The time to effect reflects the time from when the drug was added to the chamber, to the beginning of the activation or inhibition effect. All times are for addition of drug to the *trans* chamber unless otherwise specified.

3.3.4. Reversal of anthracycline induced effects on RyR2

The results from Section 3.3.3 demonstrated anthracyclines could cause significant biphasic modulation of RyR2 activity. To go beyond characterizing the effects of the drugs on RyR2 gating and to gain an understanding of the mechanism of activation and inhibition, two sets of perfusion experiments were done to test the reversibility of these effects. Drug washout from the bathing solutions of single channels is a valuable experimental technique and has not been attempted with anthracyclines previously.

3.3.4.1. Reversal of activation

For these experiments, 0.5 μM doxorubicin was used as it induced sustained activation without causing later inhibition (see Figure 3.3 and 3.6). Doxorubicin was first added to the *trans* chamber and stable activation observed. The chamber was then perfused with drug-free *trans* solution and RyR2 activity was compared before and after drug washout (Figure 3.8A). Almost immediately after washout of doxorubicin, P_o was significantly reduced from 0.226 ± 0.06 to 0.074 ± 0.03 (Figure 3.8A). This low P_o was maintained for the lifetime of the experiment, up to 15 min after perfusion. Similar results were observed for 0.5 μM doxOL, where drug addition caused a 5-fold increase in P_o, which fell to a level comparable with control after drug washout (Figure 3.8B). This decrease in P_o is likely due to washout of the drug and not doxOL induced inhibition (see Section 3.3.3.2) because perfusion was completed within 6 – 8 min of drug addition, whereas RyR2 inhibition by 0.5 μM doxOL took 14.4 ± 1.1 min. Reversal of drug-induced activation is characteristic of low-affinity ligand binding and is also seen with daunorubicin-induced activation (Hanna et al., 2011). As doxorubicin/doxOL CNBr-activated sepharose assays showed that both forms of the drugs bind to RyR2 (Figure 3.2A, B), it is likely that doxorubicin and doxOL activate RyR2 by ligand binding.

3.3.4.2. Reversal of Inhibition

In contrast to the activation effect, the effects of anthracycline-induced RyR2 inhibition were not reversed by washout. RyR2 were first treated with 2.5 μM doxorubicin or 2.5 μM doxOL, concentrations that had the fastest time for induction of RyR2 inhibition. After inhibition was observed, the *trans* chamber was perfused with drug-free solution, and RyR2 activity was compared before and after wash out of the drug.

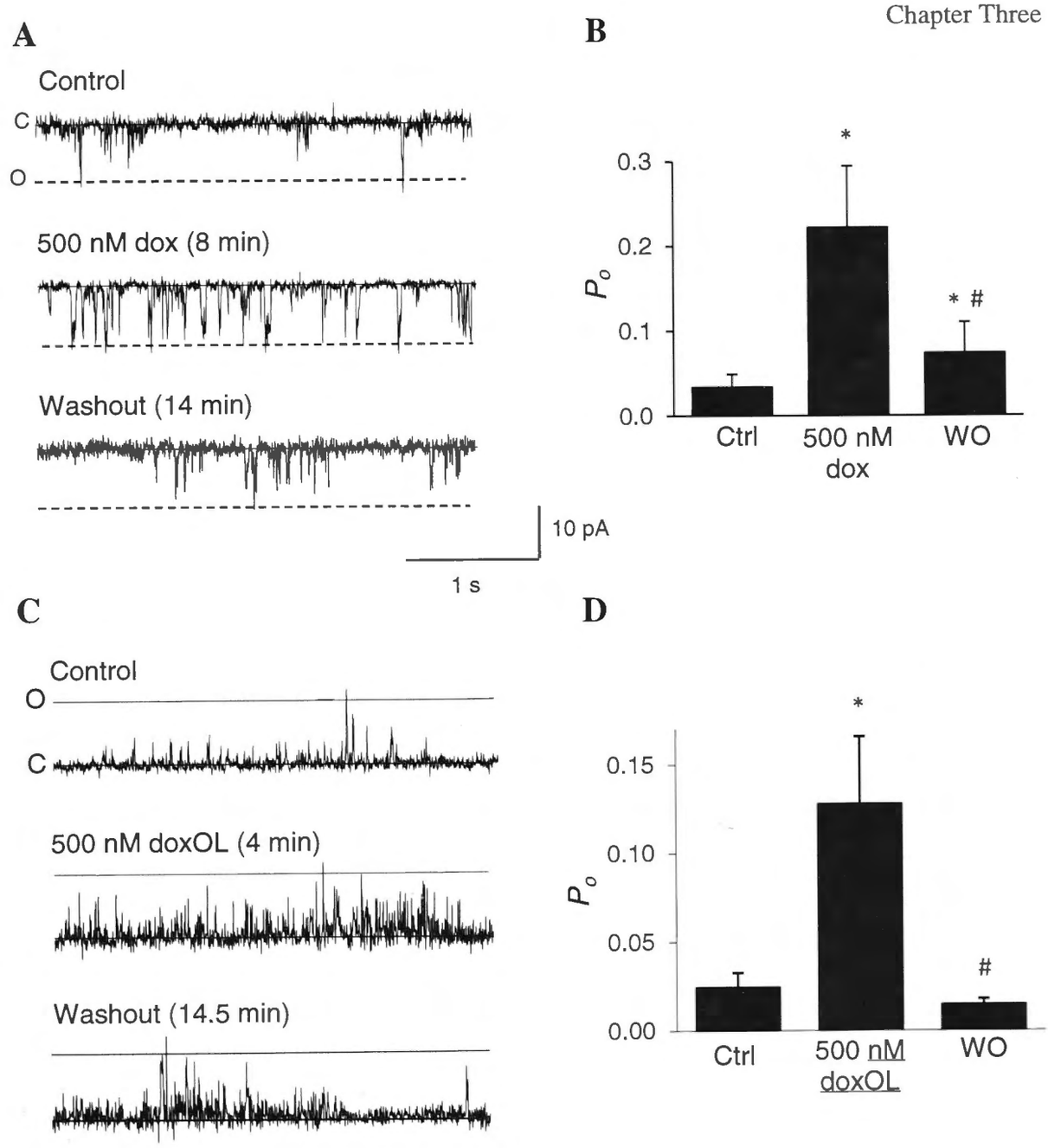

Figure 3.8 - Anthracycline-induced activation is reversible upon removal of the drug. Three s recordings of native RyR2 channel activity at -40 mV (**A**) and +40 mV (**C**). Channels open downward (**A**) or upward (**C**) from zero current (C, continuous line) to maximum open conductance (O, broken line). Top panel, control native RyR2 recording in the absence of doxorubicin (dox) (**A**) and doxOL (**C**); middle panel, after the *trans* chamber addition of 0.5 μM dox (**A**) and doxOL (**C**). Maximal *P*o was measured 8 (**A**) or 4 (**C**) mins after dox addition and 4 min after doxOL addition; bottom panel, after the *trans* chamber was perfused with drug free solution. (**B**) and (**D**) Average combined data from measurements of P_o at +40 mV and -40 mV (n = 6 - 10). Average P_o before 0.5 μM doxOL addition, during the activation phase and after washout of doxorubicin are shown in (**B**). Average P_o before 0.5 μM doxOL addition, during activation and after washout of doxorubicin are shown in (**D**). Asterisk (*) indicates a significant difference from the control P_o recorded before adding dox/doxOL. Crosshatch (#) indicates a significant difference between P_o in the presence of dox/doxOL and after drug washout.

Addition of 2.5 μM doxorubicin caused an initial activation, followed by inhibition, with P_o decreasing from an average of 0.0832±03 during control (i.e. before drug addition), to 0.0043±0.002 (Figure 3.9A - B). Washout of the drug failed to reverse channel inhibition, with P_o remaining at 0.0067 ± 0.003, which was not significantly different to the channel P_o before washout. This low P_o was sustained for the remainder of the experiment, up to 10 min following perfusion. Similarly, perfusion did not reverse doxOL-induced inhibition (Figure 3.9C - D). Indeed P_o actually fell significantly from 0.0119±0.003 before washout to 0.0021±.001 after washout. These results compare well with daunorubicin perfusion experiments, where daunorubicin-induced inhibition was not reversed upon drug washout (Hanna et al., 2011).

The difference in the reversibility of drug induced activation and inhibition indicates the two effects are mediated by different mechanisms. The irreversible nature of the inhibitory effects may be due either to the drug binding to RyR2 with very high affinity, or to a non-ligand binding mechanism such as an amino acid modification. In the isolated environment of the bilayer this modification is most likely to be direct oxidation of reactive thiol groups on cysteines. This effect is reminiscent of the inhibition of RyR2 induced by higher concentrations of daunorubicin which was shown to be due to the oxidation of thiol groups (Hanna et al., 2011).

3.3.5. Anthracyclines inhibit SERCA2A uptake

Anthracyclines have been reported to compromise SERCA2A function (Cusack et al., 1993a). To assess the effects of doxorubicin and doxOL on SERCA2A, SR Ca^{2+} uptake was measured in cardiac SR vesicles. SERCA2A uptake rate was faster in the presence of ruthenium red (compare last transient in Figure 3.10 with preceding transients). This was expected since in the absence of ruthenium red, Ca^{2+} would also be released through the RyR2, reducing the net accumulation rate. This observation indicates that the vesicles contain intact uptake and release pathways.

Vesicles were pre-incubated with varying concentrations of doxorubicin or doxOL for 20 min. In controls for this experiment, vesicles were incubated with buffer. To exclude day-to-day variability, control experiments were done each day and results from drug-treated vesicles were compared to the average of control experiments for that day.

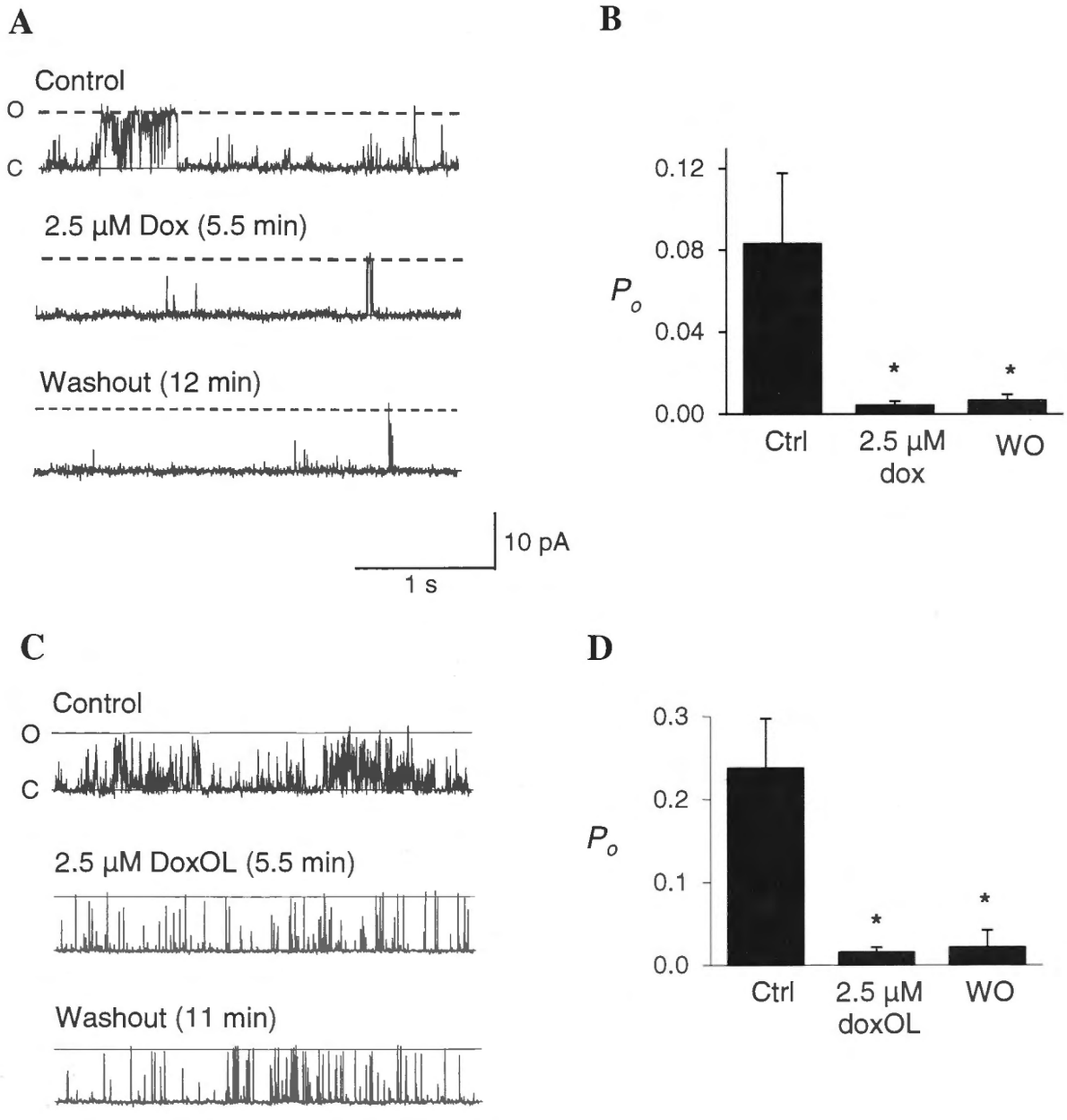

Figure 3.9 - Anthracycline-induced inhibition is not reversible upon removal of the drug. (**A**) and (**C**). Three s recordings of native RyR2 channel activity at +40 mV. Channels open upward from zero current (C, continuous line) to maximum open conductance (O, broken line). Top panel, control native RyR2 recording in the absence of doxorubicin (dox) (**A**) and doxOL (**C**); middle panel, after the addition of 2.5 µM dox (**A**) and doxOL (**C**) to the *trans* chamber minimal activity was measured 5.5 min after dox (**A**) and doxOL (**C**) addition; bottom panel, after the *trans* chamber was perfused with drug free solution, re-establishing control conditions. (**B**) and (**D**), Combined data from measurements of P_o at +40 mV and -40 mV (n = 8 in **B** and **D**). Average P_o before 2.5 µM dox addition, during inhibition and after washout of dox are shown in **B**). Average P_o before 2.5 µM doxOL addition, during inhibition and after washout of doxOL are shown in (**D**). In (**B**) and (**D**), Asterisk (*) indicates a significant difference from the control P_o recorded before adding dox/doxOL.

Pre-incubation of SR vesicles with 0.01 μM or 10 μM doxorubicin did not significantly change the SERCA2A Ca^{2+} uptake rate (Figure 3.10B – C). On the other hand, Ca^{2+} uptake was inhibited by the metabolite doxOL (Figure 3.10 D – E). Pre-incubation with 0.01 μM and 10 μM doxOL significantly reduced Ca^{2+} uptake to 73% - 75% of the rate in SR vesicles that had been exposed to vehicle only. Pre-incubation with the lower concentration of 0.001 μM doxOL did not significantly decrease SERCA2A activity. Taken together, these results indicate that doxOL, but not doxorubicin, causes inhibition of SERCA2A Ca^{2+} uptake.

3.4. Chapter discussion

In this chapter, new evidence of the mechanisms underlying anthracycline cardiotoxicity is presented. The effects of the doxorubicin metabolite, doxOL have been characterized on single RyR2 channels and SERCA2A for the first time and the results provide a novel understanding of the molecular effects of this compound on Ca^{2+} handling in the heart. All the results were consistent with our previous work with daunorubicin (Hanna et al., 2011), providing further evidence that anthracyclines disrupt Ca^{2+} homeostasis in the heart, and have the potential to impair cardiac function by targeting important Ca^{2+} handling proteins.

3.4.1. RyR2 is regulated by anthracyclines

3.4.1.1. Anthracycline effects on RyR2 are likely to be caused by different mechanisms

Anthracyclines caused consistent and effective activation of RyR2, regardless of the drug used and the concentration. Channel activation is completely reversible upon washout, consistent with the effects of anthracyclines reported earlier (Pessah et al., 1990; Hanna et al., 2011). The degree of activation for both doxorubicin and doxOL peaked at the lower end of the tested concentration range (0.01 μM for doxorubicin and 0.5 μM for doxOL). This could be either because all the binding sites on RyR2 are saturated which has prevented further activation, or that the onset of inhibition (see below) masks any further increase in activity.

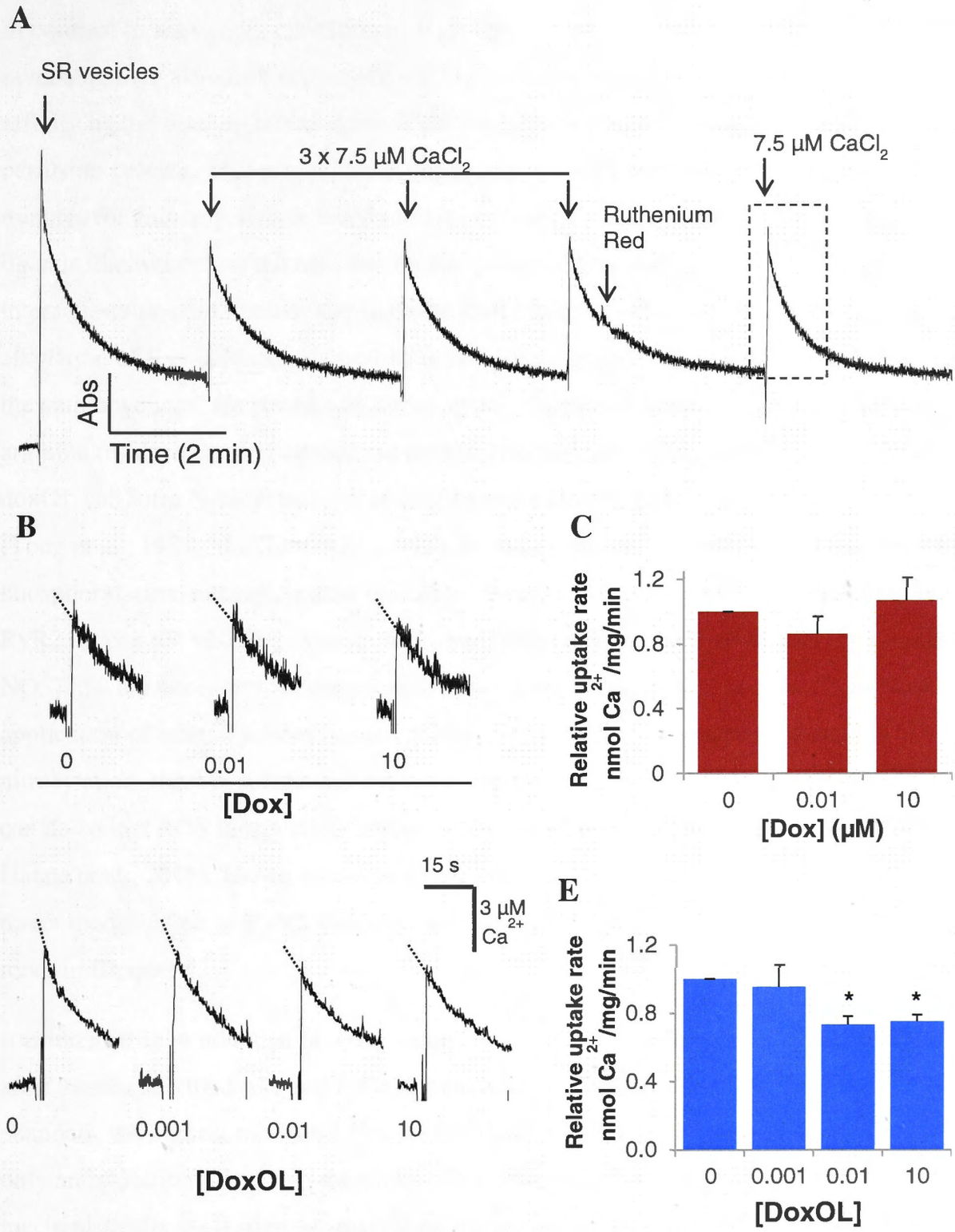

Figure 3.10 - SERCA2A Ca^{2+} uptake is inhibited by doxOL. **(A)** Experimental strategy; Ca^{2+} uptake from SR vesicles was monitored after addition of antipyrylazo III. The initial rate of Ca^{2+} uptake was measured for the final addition of Ca^{2+} (dashed box). Traces show SERCA2A mediated Ca^{2+} uptake from the bathing solution into the SR of vesicles pre-incubated with doxorubicin **(B)** or doxOL **(D)**. The initial slope of the uptake curve was measured (dashed lines) and converted into an uptake rate. Average Ca^{2+} uptake rate of doxorubicin **(C)** and doxOL **(E)** pre-treated vesicles, relative to the uptake rate in the absence of anthracycline preincubation. Asterisk (*) indicates significant difference compared to untreated vesicles, n = 8 – 10.

In contrast to activation, inhibition of RyR2 by doxorubicin and doxOL was not reversible by washout. It is possible that the inhibitory effect is caused by a very high affinity ligand binding interaction and the drug has remained bound during the perfusion process. This possibility is unlikely however, given that it took several minutes for anthracycline-induced inhibition to occur, while known, high affinity ligands like ruthenium red take less than a minute to inhibit RyR2 (Ma, 1993). Another interaction that could potentially underlie RyR2 inhibition by anthracyclines may be alkylation of RyR2. Many chemotherapeutic compounds, including several members of the anthracyclines, are strong alkylating agents which add a methyl group to lysine or arginine residues causing changes in protein function. However, neither doxorubicin nor doxOL can form N-alkyl adducts and thus cannot modify RyR2 via this mechanism (Tong et al., 1979; Marchini et al., 1995). In theory inhibition could also be mediated by phosphorylation, nitrosylation or oxidation, three modifications which are common in RyR2. In our SR vesicle preparations, the enzymes or associated co-factors (eg kinases, NOS) that are necessary for these modifications are absent or inactive. While *in vitro* application of anthracyclines has not been reported to cause phosphorylation or nitrosylation, there is substantial evidence that they can oxidise protein thiol groups, and can do so in a ROS independent manner (Abramson et al., 1988; Ondrias et al., 1990; Hanna et al., 2011). Hence it is most likely that the inhibitory effect is mediated by direct modification of RyR2 thiols by anthracyclines. This possibility will be explored more in Chapter 4.

It is interesting to note that in a small number of channels, activation was not observed after treatment with 1 μM and 2.5 μM doxorubicin, doxOL or daunOL. In these channels, the highest measured P_o with drug was lower than the control activity, i.e. only an inhibition phase was measured. This observation may be important mechanistically, as it suggests that either the secondary inhibitory effect can occur independently of the activation effect, or that the potent RyR2 inhibition of doxorubicin and doxOL at these concentrations masks activation. This may also explain why the extent of activation did not increase in a dose dependent manner, but rather, plateaued or was even reduced with higher concentrations of all tested drugs.

3.4.1.2. Anthracyclines may have different binding sites on RyR2 or an associated protein

Since anthracyclines are lipid soluble, it is impossible to tell from any of these experiments whether the drug is binding in a cytoplasmic, luminal or transmembrane domain. The fact that anthracycline-induced activation is reversed within the timeframe of the chamber perfusion suggests that the ligand-binding interaction is low affinity and not in the transmembrane domain, which would likely be more difficult to reverse. Rather, it has been suggested that doxorubicin shares a binding site with caffeine, in the large cytoplasmic domain of RyR (Pessah et al., 1990). Some insight into the site of action can be gained by comparing the time to activation and inhibition between *cis* and *trans* drug addition. DoxOL both activated and inhibited channels more quickly when added to the *cis* chamber then when it was added to the *trans* chamber, with no difference in the severity of either effect regardless of the chamber it was added to. Conversely, daunOL activated the channel more quickly when added to the *trans* solution than when added to the *cis* chamber (Table 3.1). The magnitude of daunOL inhibition was also significantly greater when it was added to the *trans* chamber, causing a 15% inhibition when added to *cis* compared to an 89 % inhibition when added to the *trans* chamber (Figure 3.5 and Figure 3.7). These results suggest that daunOL could be acting at a luminal or transmembrane domain of RyR2, or possibly in a cytoplasmic microdomain that is more easily accessed from the *trans* chamber. Alternatively the different carbonyl sidechains of the metabolites might alter the ability of the drugs to access certain regions on RyR2. While the present results are not sufficient to draw any firm conclusions, it is not implausible that two drugs so structurally similar would bind to, or access different locations on RyR2. Doxorubicin and daunorubicin have equally similar structures yet have a very different spectrum of clinical use (Section 1.12.1). An experiment with sequential additions of doxOL and daunOL may shed some light on the possibility of separate binding sites, but was not undertaken due to time constraints. Additional mechanistic insight may also be gained by analysis of the mean open time, mean closed time and frequency of channel openings.

Minor modifications to the core anthracycline structure are associated with differences in the drug's affinity for RyR2 (Pessah et al., 1990) . These investigators suggested that doxorubicin shares a binding site on RyR2 with caffeine, a well-characterized channel

agonist which binds in the cytoplasmic domain of the protein. In ^{3}[H] ryanodine binding assays, caffeine was able to reduce the potency of doxorubicin (Pessah et al., 1990), whilst pretreatment with caffeine reduced the extent of doxorubicin binding to RyR2 (Zorzato et al., 1985). DoxOL may be the more pathologically relevant compound, having a longer half-life and causing more severe effects on RyR2 and other cardiomyocyte ion channels (Section 1.12.3.3). Thus it may be beneficial to repeat similar studies with doxOL to gain understanding of the ligand binding interaction with RyR2. With this knowledge, measures to prevent or reduce the cardiotoxicity of anthracyclines by blocking the binding of doxOL to RyR2 may be more effective in the future.

In regard to the putative anthracycline binding site/s, the results presented here cannot exclude a role for other SR proteins that are in complex with RyR2, such as triadin, junctin, CSQ2 or FKBP12/12.6. Previous results demonstrated that daunorubicin could activate and inhibit RyR2 in the absence of CSQ2 (Hanna et al., 2011). Given the similarities so far between the effects of daunorubicin and doxorubicin, doxOL and daunOL, it seems unlikely that CSQ2 would be important in the effects these other drugs have on RyR2 gating. However, this does not exclude a role for CSQ2 in the effects of anthracyclines on other aspects of SR Ca^{2+} handling, nor does this exclude a role for triadin, junctin or any other proteins, such as FKBP that remain bound to RyR2 in our SR vesicle preparations.

3.4.1.3. Anthracycline metabolites have greater efficacy then the parent compounds

There is a tendency for doxOL to be more efficacious than the parent doxorubicin. This is illustrated by doxOL's ability to inhibit RyR2 at lower concentrations, within a faster time frame and to a significantly greater extent than the parent compound. In addition, doxOL but not doxorubicin caused significant SERCA2A dysfunction. Rabbit models of anthracycline cardiotoxicity have shown that metabolite synthesis occurs within 45 min of initial treatment, and that the metabolite has an extended half-life in the heart, compared with the parent compound (Olson et al., 1988). As detailed in Section 1.12.3.3, anthracycline metabolites have been shown to bind to numerous cardiomyocyte ion channels and transporters at substantially lower concentrations then the parent compounds. Furthermore, over expression of the carbonyl reductase that catalyses the conversion of doxorubicin to doxOL accelerates the development of

cardiomyopathy (Forrest et al., 2000), and knockdown of the carbonyl reductase gene protected against acute cardiotoxicity (Olson et al., 2003).These findings, with those presented in this chapter, strongly suggest that the metabolites have an important role in mediating anthracycline induced cardiac dysfunction.

3.4.2. SERCA2A regulation by anthracyclines

The reduced SERCA2A activity observed in these experiments was caused by relatively low concentrations of doxOL and were comparable to levels measured in the hearts of anthracycline treated animals (0.4 ±0.036 μM, (Olson et al., 2003)). The results in this chapter demonstrate that doxOL can bind to SERCA2A. Whether the regulatory protein phospholamban remained bound to SERCA2A in the SR vesicle preparations used for the affinity chromatography assay or if anthracyclines have an effect on phospholamban was not explored. It must also be considered that since SERCA2A contains several accessible thiol residues it is possible that inhibition of SERCA2A function is caused by doxOL induced disulphide formation. This prospect will be explored in the following chapter. In terms of the cellular dynamics of the effect of doxOL on SERCA2A function, a decrease in SR Ca^{2+} uptake would be expected to have severe consequences on SR Ca^{2+} load and subsequent RyR2 Ca^{2+} release (see next section).

3.4.3. Synergistic effects of anthracyclines in the whole heart

While low concentrations of anthracyclines did stimulate RyR2 activity, this influence was transient, with RyR2 inhibition by both the drugs and metabolites being the longer lasting effect. Since these experiments are conducted under conditions likely to be encountered during systole, they can not be used to predict the influence of the drugs on RyR2 during diastole. Such effects will be explored in while cell experiments (see Chapter 6). It is tempting to speculate how alterations in RyR2 and SERCA2A function induced by anthracyclines might lead to arrhythmia. The inhibitory effects on RyR2 may reflect the acute or early phase of anthracycline cardiotoxicity, where two of the earliest symptoms are a reduced left ventricular ejection fraction and arrhythmogenesis (reviewed in Menna et al., 2012). Inhibition in SR Ca^{2+} release and Ca^{2+} uptake reported in the current chapter could have a prominent role in depressed contractile function and impaired relaxation associated with anthracycline use in animal models by 1) reducing the amount of Ca^{2+} available for release during systole and 2) promoting cytoplasmic Ca^{2+} overload (Mushlin et al., 1993; Boucek et al., 1997; Shadle et al., 2000b). This is

supported by studies at the cellular level where cardiomyocytes treated with doxorubicin had reduced Ca^{2+} transient amplitudes, increased diastolic Ca^{2+} leak and depleted SR load (Wang et al., 2001; Sag et al., 2011).

Loss of RyR2 function (resulting from RyR2 mutation or inducible knockdown) has been identified as a factor in certain models of arrhythmia and sudden cardiac death (Thomas et al., 2004; Jiang et al., 2007; Bround et al., 2012). The authors proposed that loss of function mutations or RyR2 knockout promoted arrhythmia via an alternans dependent model, where there is beat to beat variation in Ca^{2+} transient amplitude. This has previously been demonstrated by Diaz and colleagues (2002) who found that in an intact cell, decreasing RyR2 P_o does substantially perturb cardiomyocyte Ca^{2+} handling by desynchronising SR Ca^{2+} release, with subsequent Ca^{2+} alternans. Whether or not anthracycline-induced RyR2 inhibition similarly leads to Ca^{2+} alternans and arrhythmogenesis remains to be elucidated. Sustained RyR2 inhibition by doxorubicin and doxOL could also induce arrhythmogenic early after-depolarizations, a form of triggered activity that occur before cell repolarization is complete (Bers, 2002a). Depressed SERCA2A function is an additional factor common in pathological conditions and contributes to both systolic and diastolic dysfunction in heart failure (Bers et al., 2003). As a consequence of reduced Ca^{2+} uptake, SR load would be lower and contribute to the dysfunction in Ca^{2+} release, further influencing the generation of after-depolarisations and impaired contractility. The use of isolated systems (RyR2 single channels and SR vesicles) provides novel mechanistic insight into such functional effects of anthracyclines. The confirmation of multiple mechanisms and the differential effects of doxorubicin and its metabolite highlight the complexity of anthracycline cardiotoxicity.

3.5. Conclusion

In this chapter the functional effects of anthracyclines and their metabolites on RyR2 and SERCA2A have been characterized. The results demonstrate that these drugs cause functional perturbations of the principle Ca^{2+} release and uptake pathways of the SR of cardiac muscle. Such disruptions of Ca^{2+} handling pathways are likely to have significant effects on Ca^{2+} homeostasis in the whole cell. However, in the interests of future design of less cardiotoxic compounds or protective co-treatments it is imperative that underlying mechanisms of the changes in Ca^{2+}channel/pump function are

identified. Therefore, the results presented in this chapter provide an important basis for the remainder of this thesis where such mechanisms are explored and other aspects of RyR2 function, both at the SR vesicle level and the whole cell level, are probed.

Chapter Four

Anthracycline-induced oxidation of RyR2 and SERCA2A

4.1. Introduction

Redox regulation is an essential aspect of cardiomyocyte homeostasis and is defined as being the specific, usually reversible, oxidation\reduction modifications of cellular signalling pathway components by a reactive species (Forman et al., 2004). A large number of proteins respond to changes in the cellular redox environment via modifications by redox active molecules to amino acid residues, most commonly cysteine thiol groups. In doing so, these proteins are able to act as sensors of the redox environment, responding to alterations in redox state with a change in conformation, stability, molecular interactions and activity (Burgoyne et al., 2012).

RyR in both skeletal and cardiac muscle can be considered such a protein, being highly susceptible to redox modifications which cause changes in RyR activity. Redox based modifications of RyR (and other Ca^{2+} handling proteins) means there is significant interaction between redox pathways and Ca^{2+} signalling, as reviewed in (Hidalgo and Donoso, 2008) . In the heart, oxidative stress and subsequent hyper-oxidation of RyR2 are strongly linked with a number of pathological conditions including heart failure, ischaemia-reperfusion injury and atrial fibrillation (Burgoyne et al., 2012).

There is little doubt that a redox based mechanism has an important role in anthracycline induced cardiotoxicity. As detailed in Section 1.12.3.2.2, several lines of evidence support a role of oxidative stress in the effects of anthracyclines on the heart. These include:

1 The *in vivo* generation of ROS by anthracyclines has been demonstrated repeatedly (Kim et al., 2006; Sag et al., 2011). Cellular ROS production occurs immediately after anthracycline exposure, via redox cycling of the quinone moiety, and increases in a time-dependent manner.
2 Cardiotoxic side effects of these drugs are attenuated with antioxidant treatment in rodents (Bast et al., 2007) and in transgenic mice overexpressing cellular antioxidants (Cole et al., 2006).
3 Anthracyclines can directly oxidize protein thiol residues, and therefore can promote oxidative stress in a ROS independent manner (Abramson et al., 1988; Ondrias et al., 1990).

4 ROS formation and cardiotoxicity are attenuated with the use of 5-iminodaunorubicin - a quinone deficient analogue of daunorubicin (Shadle et al., 2000a).

5 The only proven cardioprotective agent is dexrazoxane. Dexrazoxane is thought to work by binding free iron and preventing the formation of iron-anthracycline complexes which promote ROS production (Simunek et al., 2009).

6 Cardiomyocytes are thought to be more susceptible to oxidative stress because of poor antioxidant defence mechanisms (Doroshow et al., 1980).

Despite the wealth of evidence in support of an oxidation mechanism, attempts to either treat or prevent anthracycline cardiotoxicity with antioxidants in humans have failed. And although dexrazoxane is clinically proved to attenuate cardiotoxicity, at least a third of patients who were administered dexrazoxane still developed heart failure (van Dalen et al., 2006). Further, the protective mechanism of action of dexrazoxane, as summarized above, has been questioned, as stronger iron chelating agents have proved unsuccessful in treating cardiac effects of anthracyclines, raising the possibility that dexrazoxane works in part by a non ROS based mechanism (Simunek et al., 2009).

In Chapter 3 the two actions of anthracyclines were linked to two separate mechanisms, the first being a low affinity activation that and is most likely the consequence of a direct interaction between anthracyclines and the RyR2 complex. The second, inhibitory effect appears to be the result of a posttranslational modification of RyR2, as it is not reversed by drug washout. Given that anthracyclines are known oxidants (Abramson et al., 1988; Ondrias et al., 1990) it was hypothesised that the inhibitory effect of these drugs was caused by thiol oxidation. Since SERCA2A also contains a number of cysteine thiol groups it is possible that the effects of anthracycline metabolites on this protein are also mediated by thiol oxidation.

Aim:

The aim of the experiments presented in this chapter was to confirm whether direct oxidation of cysteine thiol groups by anthracyclines has a role in the drugs effects on RyR2 and SERCA2A, using a combination of functional and biochemical assays.

4.2. Materials and Methods

4.2.1. SR vesicle isolation and RyR2 purification

As detailed in Section 2.3, *c*ardiac SR vesicles were prepared from sheep heart (Laver et al., 1995) and RyRs were solubilised and purified from SR as described by (Lai et al., 1988; Dulhunty et al., 2005).

4.2.2. Single channel recording and analysis

The method for single channel recording and analysis is described in detail in Section 2.6. The redox agents DTT and *N*-ethylmaleimide (NEM) were added to the *cis* chamber as the majority of thiol residues on RyR2 are located in the cytoplasmic domain. Earlier work showed that only *cis* addition of DTT could prevent daunorubicin-induced inhibition, with *trans* DTT having no protective effect. Therefore, redox agents were added only to the *cis* chamber. NEM however is lipid soluble and would be likely to equilibrate across the bilayer. Redox agents were stored at -20 °C in single use aliquots which were thawed daily and then discarded after use.

4.2.3. Protein thiol assay

The thiol content of RyR2 and SERCA2A was assessed using the Alexa Fluor 647 maleimide thiol probe (Section 2.9). Briefly, SR vesicles were incubated with anthracyclines and with the known redox agents TCEP, a reducing agent, and GSSG, an oxidizing agent. Vesicles were then incubated with Alexa Fluor 647. Excess thiol probe was washed out and proteins were subject to SDS PAGE before being stained with the total protein stain Sypro Orange. Gels were scanned on a fluorimager at 300 nm and 645 nm to view total protein and thiol specific fluorescence, respectively. Protein and thiol content was quantified by densitometry allowing calculation of thiol content per unit of total protein.

4.2.4. SR Ca^{2+} uptake assay

The method used to measure Ca^{2+} uptake into SR vesicles is shown in Figure 4.5. Vesicles were pre-incubated for 5 min with DTT, and then for 20 min with anthracyclines before they were added to the cuvette. The final concentration of anthracycline and DTT in the cuvette was adjusted to the incubation concentration. In

control experiments vesicles were preincubated for 5 min with DTT and then with vehicle buffer for 20 min.

4.3. Results

4.3.1. Redox agents prevent anthracycline induced inhibition of RyR2

4.3.1.1. NEM pretreatment prevents daunorubicin-induced inhibition of RyR2

Earlier work showed that pretreatment of RyR2 with *cis* DTT prevented daunorubicin-induced inhibition, suggesting that anthracyclines inhibit the channel by modification of thiol groups. Here it was tested whether an alternate thiol modifying reagent, NEM, could prevent the inhibitory effect of daunorubicin. NEM is a thiol alkylating agent commonly used to irreversibly modify thiol residues, thereby preventing oxidation. NEM is highly lipid soluble. In these experiments, NEM was added to the *cis* chamber, this could presumably block thiol groups on both the luminal and cytoplasmic domains of RyR2, before daunorubicin was added to the *trans* chamber.

NEM has been found to have complex, concentration dependent effects on RyR2 (Aghdasi et al., 1997; Menshikova et al., 2000). Since NEM was to be used as a pre-treatment it was necessary to identify a concentration of NEM that would have consistent effects on P_o over time, so that the independent effect of NEM could be accurately measured and accounted for in the final analysis. Two NEM concentrations, 5 and 10 mM, were tested. NEM was added to the *cis* chamber and the P_o of 30 s segments of activity was measured every 2 – 3 min for the lifetime of the experiment, up to 30 min post NEM addition. Five mM NEM caused activation followed by inhibition. The time to these effects was highly variable between different channels meaning there was no consistent effect in the average data (Figure 4.1A). Conversely, the effects of 10 mM *cis* NEM followed a consistent pattern, with a progressive decline in channel activity over the 30 min recording period (Figure 4.1B). This was consistent and predictable in all channels (n = 12), indicating that 10 mM was an appropriate concentration of NEM to use for pre-treatment experiments.

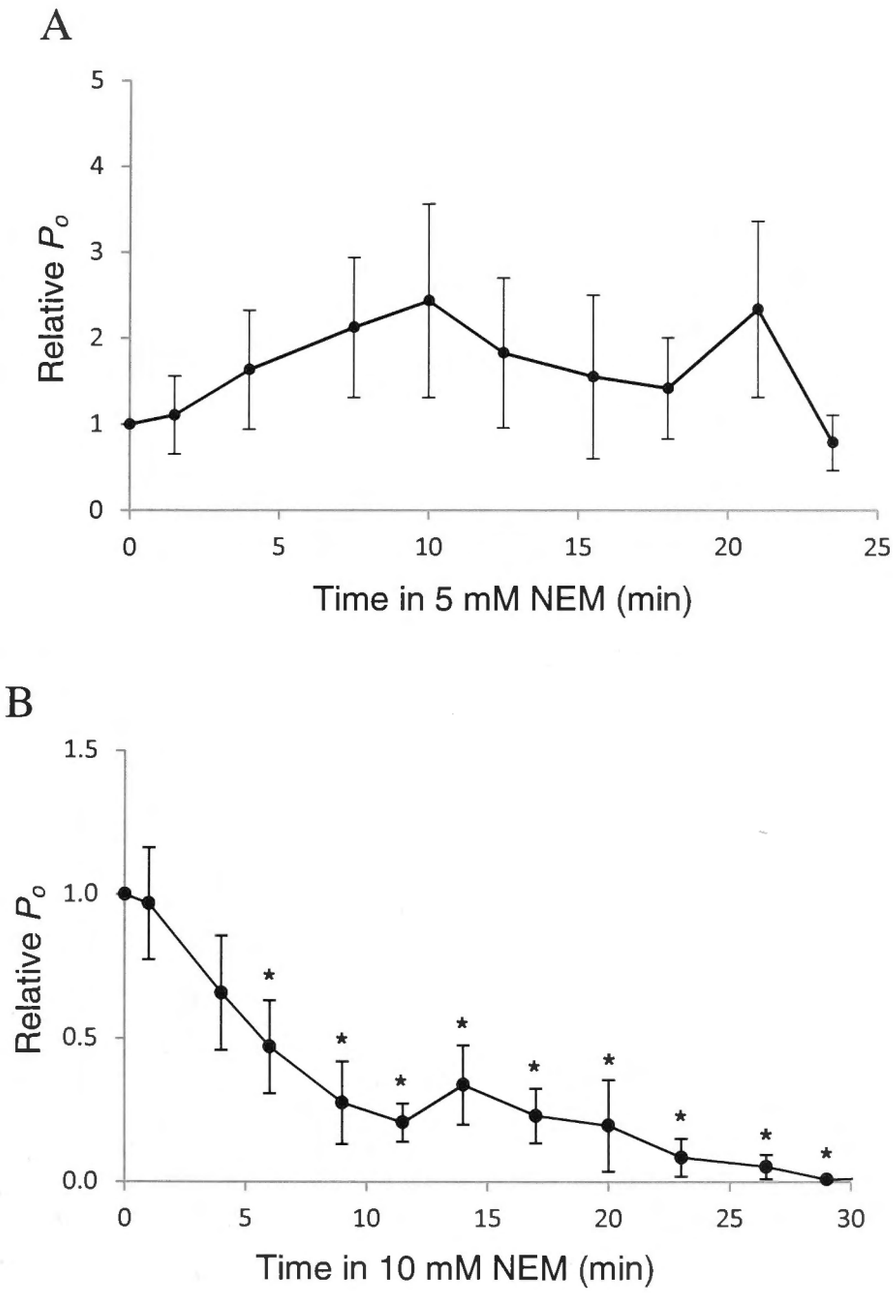

Figure 4.1 – NEM has concentration dependent effects on single channel activity. Combined average data from experiments (40 mV and -40 mV) where 5 mM (**A**, n = 12) or 10 mM (**B**, n = 12) NEM was added to the *cis* chamber. P_o was measured from 30 s segments of single channel activity every 2 -3 min, and was expressed relative to activity before NEM was added. With 5 mM NEM, P_o was initially 0.0686±0.04 and peaked after 20 min at 0.1154±0.07. With 10 mM NEM, P_o was initially 0.1042±0.02 and was maximally inhibited after 30 min at 0.0013±0.0003 Asterisk (*) indicates a significant difference from control activity ($p < 0.05$).

To avoid the complication of the rapid and more variable initial NEM inhibition, daunorubicin was always added 9 mins after NEM, where the decline in channel activity due to NEM reached a more constant rate (Figure 4.1B). To evaluate the specific effect of daunorubicin on RyR2 activity, P_o in the presence of daunorubicin and NEM was normalized to activity in the presence of NEM (alone) immediately prior to daunorubicin addition (Figure 4.2B). Normalized, or relative channel activity increased above the NEM control 10 min after daunorubicin addition and remained greater than NEM control for the life time of the experiment (up to 25 min following daunorubicin addition). The decline in activity due to NEM itself was masked by the addition of 10 μM *cis* daunorubicin. Ten min after daunorubicin addition (~ 20 min after NEM addition), the P_o was 3.45 ± 0.46 fold higher than NEM control activity (pre daunorubicin addition) (Figure 4.2A). Conversely, in the absence of daunorubicin, at the equivalent timepoint there was an 80 % reduction in P_o (Figure 4.1B). The increase in relative P_o was reminiscent of the activation phase of anthracycline treatment, seen in the absence of NEM (Figure 3.3 - 3.4).

Relative P_o during activation and inhibition following 10 μM daunorubicin application in NEM-alkylated channels and in control channels (no NEM) are compared in Figure 4.2B. To aid comparison, the P_o with NEM alone was subtracted from A) maximum activation by daunorubicin (10 min post daunorubicin addition) and B) the lowest measured activity (20 min post daunorubicin addition) following daunorubicin addition. The major findings are as follows:

1. In daunorubicin treated channels, both with and without NEM pre-treatment, there is a significant increase in relative P_o with no significant difference in the extent of activation between channels treated with NEM and those not.
2. The daunorubicin-induced inhibition is not seen in the NEM-modified channels. Rather, with NEM pre-treatment, the relative P_o measured 20 min after daunorubicin addition was still significantly higher than the control activity.
3. These results are in contrast to channels not pre-treated with NEM, where within 13.2 ± 1.2 min of daunorubicin addition, channel activity was inhibited (Table 3.1C and Figure 4.2B).

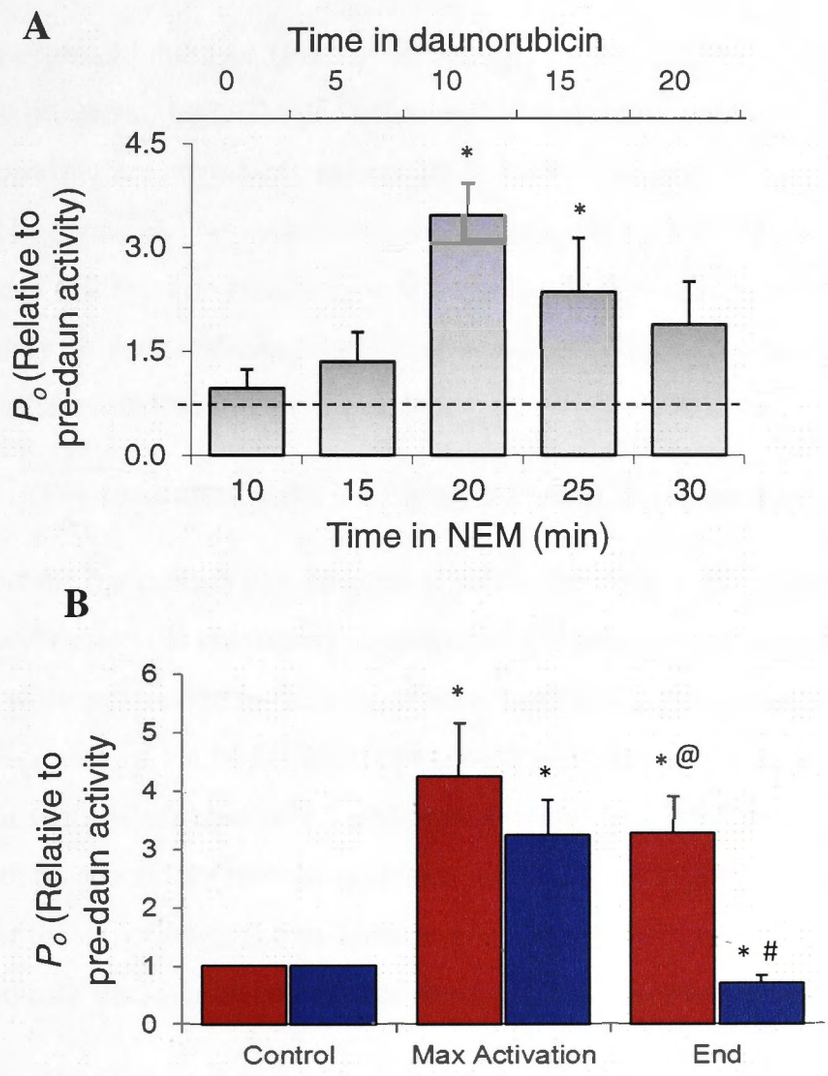

Figure 4.2 - NEM prevents daunorubicin inhibition of RyR2. A) Average data from measurements of P_o at +40 mV and -40 mV. When addition of *trans* daunorubicin P_o was initially 0.0114±0.004 and peaked 10 min later at 0.0474±0.02. The effect of adding 10 μM daunorubicin after 10 min exposure to NEM (following completion of the activation phase) (n = 14). Data is presented as P_o after adding daunorubicin relative, to P_o with NEM immediately prior to adding daunorubicin. Data in **B**) is presented as relative P_o after adding daunorubicin alone (blue bins) (relative to P_o prior to adding daunorubicin), or as P_o after adding daunorubicin in the presence of NEM (red bins) (relative to P_o in NEM prior to adding daunorubicin). In channels that were not pretreated with NEM, P_o was 0.0403±0.01 before daunorubicin was added. P_o was 0.1107±0.02 during maximal activation and 0.0258±0.01 during maximal inhibition. The NEM pretreated data (red bins) is presented as a subtraction of data from (**4.1B**) from the data presented in (**4.2B**) at matched time points, so that the independent effect of NEM alone could be subtracted from the effect of daunorubicin in the presence of NEM. Data obtained for the effect of daunorubicin alone is included for comparison. *, significant difference from control; #, significant difference between activation and inhibition; @, significant difference between daunorubicin alone and NEM plus daunorubicin. Figures modified from (Hanna et al., 2011).

Thus, the channel inhibition (but not activation) due to daunorubicin addition appears to have been prevented by NEM pre-treatment. This is consistent with the possibility that thiol groups that are normally oxidized by daunorubicin to produce inhibition were modified by NEM and no longer available to be oxidized by daunorubicin. These experiments followed on from the work I conducted during my Honours project (which focused only on daunorubicin), and the effects of NEM pre-treatment on doxorubicin or doxOL's effects on RyR2 were not tested.

4.3.1.2. Pre-treatment with DTT prevents doxOL induced inhibition of RyR2

To support the hypothesis that the anthracycline metabolite doxOL inhibits RyR2 via a redox modification (as previously reported for daunorubicin, Hanna et al 2011), channels were pre-treated in the bilayer with 1 mM DTT prior to addition of 2.5 μM doxOL. Addition of 1 mM DTT did not significantly alter channel activity (Figure 4.3A). Subsequent addition of 2.5 μM doxOL caused a 2.7 ± 0.6-fold activation ($p \leq 0.05$), with no secondary inhibition (Figure 4.3). Channel activity remained high for the lifetime of the experiment (up to 35 mins after doxorubicin addition; Figure 4.3). These results indicate that, like daunorubicin, doxOL inhibits RyR2 via thiol oxidation.

4.3.2. DoxOL oxidizes RyR2 thiol groups

The results of the DTT and NEM pre-treatment experiments (Section 4.3.1), provide compelling evidence that anthracyclines can alter RyR2 Ca^{2+} handling through thiol modification. The thiol specific, Alexa Fluor 647 maleimide was used to confirm that doxorubicin and doxOL modified thiol residues on RyR2. The results were quantified using densitometry, as the amount of Alexa 647 fluorescence per unit of total protein (total RyR2 protein quantified post Sypro Orange stain). Compared to untreated RyR2, 10 μM doxorubicin and doxOL caused a ~40% reduction in the relative amount of thiol groups on RyR2, showing the drug can directly modify RyR2 thiols (Figure 4.4). The data also show that the RyR2 preparations from healthy sheep heart are neither maximally reduced or maximally oxidized, verifying their suitability for an assay of modification by redox agents.

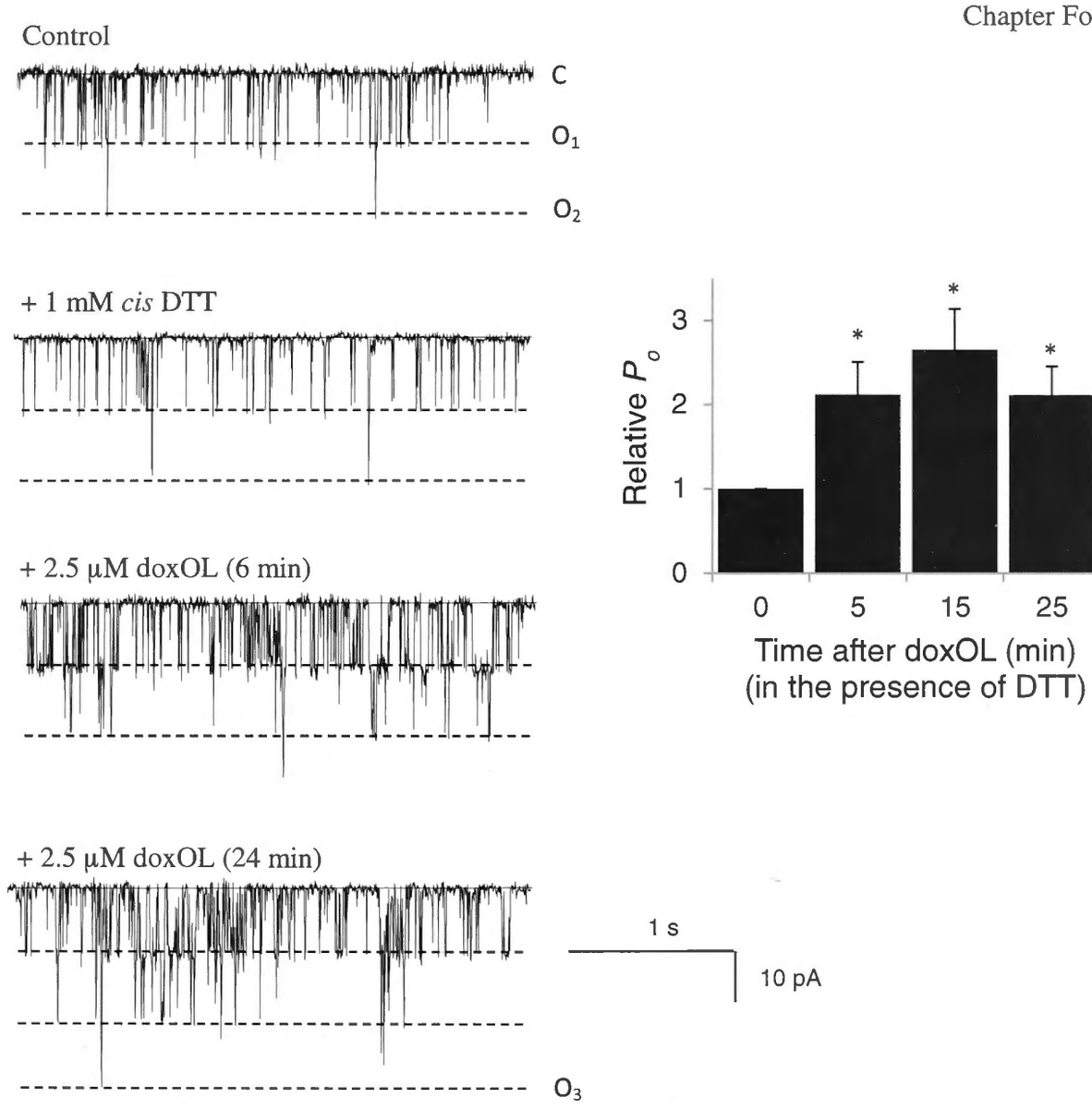

Figure 4.3 – DTT pre-treatment prevents doxOL-induced inhibition of RyR2. (**A**) Three s recordings of multiple RyR2 channel activity. Channels are opening downward from zero current to maximum open conductance (O_1, one channel open; O_2 and O_3, simultaneous opening of two of three channels, respectively). First panel, control recording of RyR2; second panel, RyR2 activity following addition of 1mM DTT to the *cis* chamber; third and fourth panels, after addition of 2.5 µM doxOL to the *trans* chamber. In this channel, activation was first observed ~6 min after addition of doxOL to the *trans* chamber (third panel) and was still evident 24 min after doxOL addition (bottom panel). **(B)** Combined average data from experiments (40 mV and -40 mV (n = 10)), where 1 mM DTT was first added to the *cis* chamber, followed by addition of 2.5 µM doxOL. Where more than one channel was incorporated (as in (**A**)), channel activity was measured as the average mean current and combined with measures of open probability, as detailed in Section 2.6.6. Data is presented as P_o, relative control activity with DTT, before doxOL was added. The average P_o at this time was 0.0706±0.03 Asterisk (*) indicates a significant difference from the P_o recorded after addition of DTT, but prior to doxOL addition.

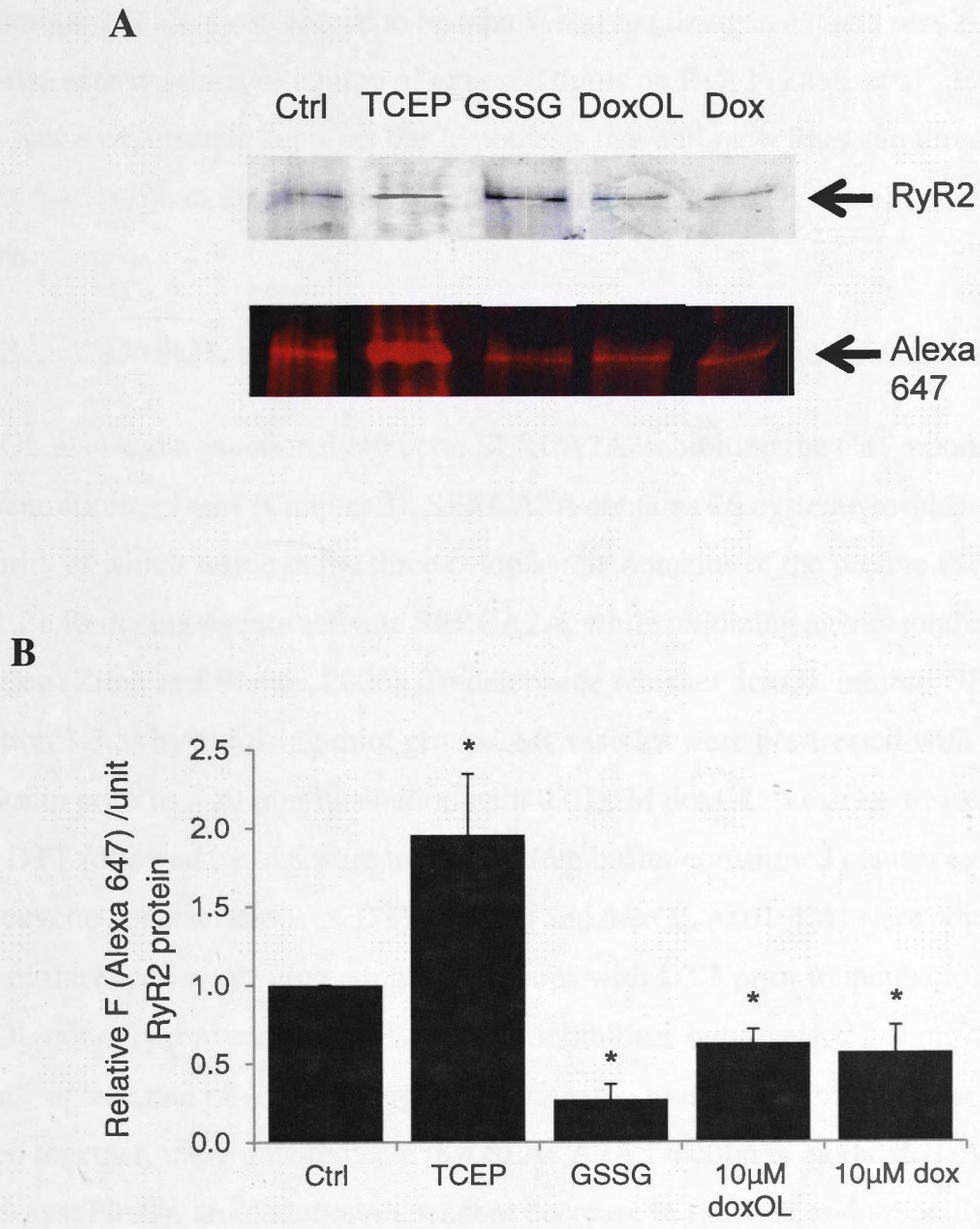

Figure 4.4 – Anthracyclines reduce RyR2 thiol content **(A)** SR vesicles were treated with TCEP, GSSG and anthracyclines and separated by SDS PAGE. *Top panel* - total protein was stained with Sypro Orange. *Bottom panel* - thiol residues were probed with Alexa 647. **(B)** Average density units of Alexa 647 fluorescence (F)/unit total RyR2, illustrating the number of available thiol residues per unit of RyR2 protein. Data is presented as relative to the thiol abundance in untreated samples. Asterisk (*) indicates a significant difference from non-treated (control) samples.

Incubation with the reducing agent TCEP (5 mM) increased thiol abundance, while incubation with the oxidising agent GSSG (2 mM), decreased thiol content (Figure 4.4). Millimolar GSSG is considered to be a powerful oxidizing agent and would be expected to cause near maximal oxidation of exposed thiols on RyR2 (Zable et al., 1997). This thiol probe experiment supports our hypothesis that anthracyclines can directly oxidize RyR2 thiol residues and illustrates that doxorubicin and doxOL are effective oxidizing agents.

4.3.3. DoxOL enhances SERCA2A uptake in the presence of DTT

DoxOL also had a functional effect on SERCA2A, inhibiting the Ca^{2+} uptake rate at concentrations ≥1 μM (Chapter 3). SERCA2A contains 26 cysteine residues, the majority of which reside in the three cytoplasmic domains of the protein (Section 1.7.1.2). Reducing agents activate SERCA2A, while oxidizing agents inhibit pump function (Zima and Blatter, 2006). To determine whether doxOL inhibits SERCA2A (Section 3.3.5) by oxidizing thiol groups, SR vesicles were pre-treated with 1 mM DTT for 5 min prior to a 20 min incubation with 0.01 μM doxOL. Vesicles treated with 1 mM DTT followed by exposure to doxOL-free buffer constituted control experiments. The cuvette concentrations of DTT (1 mM) and doxOL (0.01 μM) were adjusted at the start of the experiment. Protecting thiol groups with DTT prior to incubation with doxOL not only prevented doxOL-induced inhibition, but revealed a significant increase in Ca^{2+} uptake rate of ~30% (Figure 4.5, compared to uptake in the absence of doxOL). Taken together, these data indicate that SERCA2A function is modulated by doxOL in two ways. Firstly, an oxidation-dependent decrease in function and secondly, an increase in Ca^{2+} uptake which is independent of thiol modification.

4.3.4. Anthracyclines oxidize thiol groups on SERCA2A

The results above provide strong evidence that, like RyR2, SERCA2A dysfunction is related to anthracycline-induced oxidation. To confirm this, the ability of anthracyclines to modify SERCA2A thiol groups was compared to known redox agents like TCEP and GSSG. Using the Alexa Fluor 647 thiol probe assay, SERCA2A was shown to have a basal level of thiol modification, demonstrated by the finding that TCEP could increase the abundance of thiols, while GSSG could decrease the number of thiols. The level of thiol modification was significantly increased upon incubation with 10 μM doxorubicin or 10 μM doxOL (Figure 4.6) demonstrating again that these drugs can act directly on

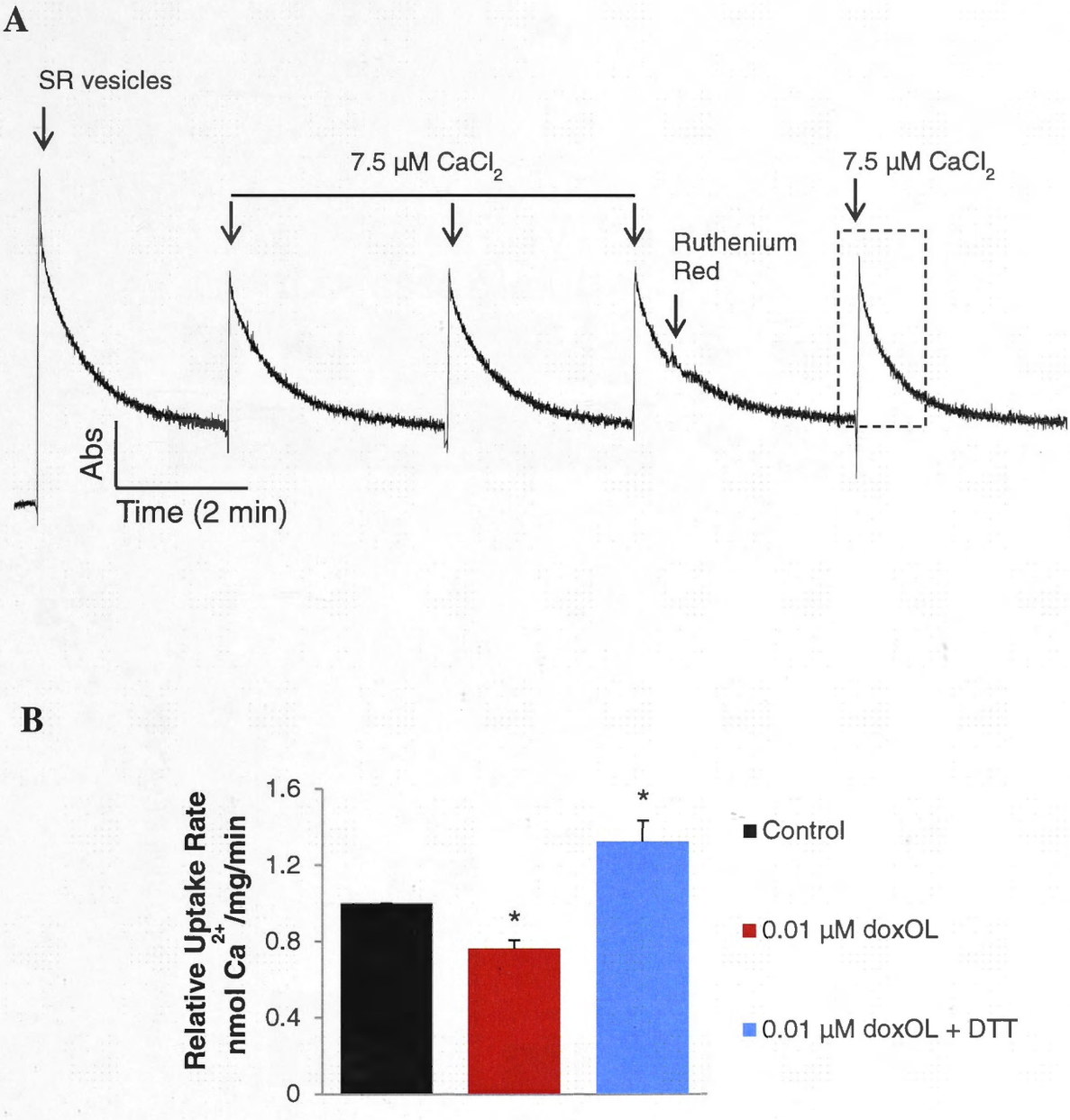

Figure 4.5 - SERCA2A inhibition by doxOL is prevented by DTT. **(A)** Experimental strategy Ca^{2+} uptake from SR vesicles was monitored after using antipyrylazo III. The initial rate of Ca^{2+} uptake was measured for the final addition of Ca^{2+} (dashed box) SR vesicles were exposed to DTT for 5 min before being incubated with 0.01 µM doxOL for 20 min. The uptake rate was expressed relative to the uptake rate measured in vesicles pre-incubated with DTT alone. The average uptake rate in the presence of 0.01 µM doxOL is included for comparison. Asterisk (*) indicates a significant difference to non-treated vesicles ($p<0.05$), n = 8 – 10.

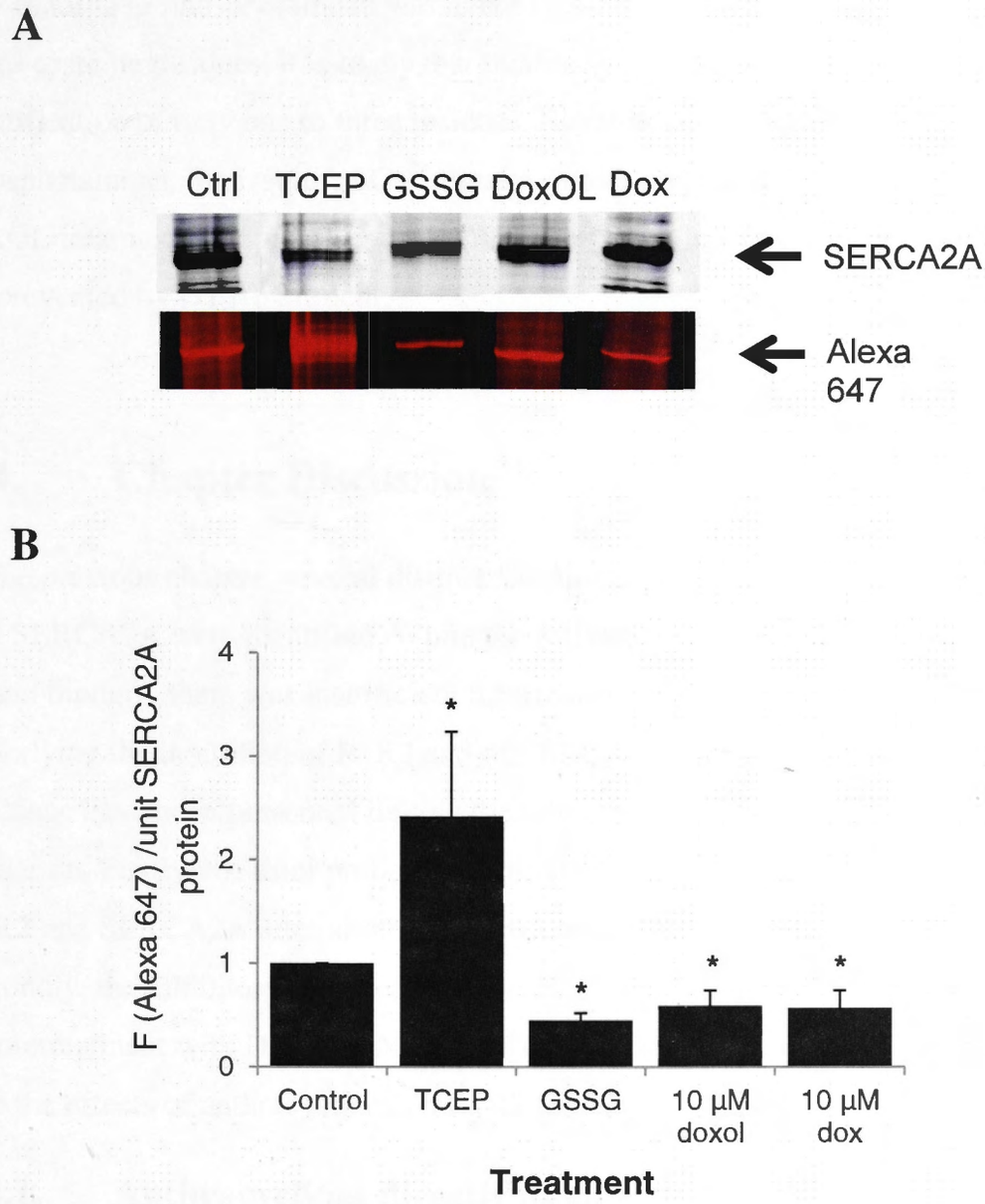

Figure 4.6 – Anthracyclines reduce SERCA2A thiol content. **(A)** SR vesicles were treated with TCEP, GSSG and anthracyclines and separated by SDS PAGE. Top panel - total protein was stained with Sypro Orange. Bottom panel - thiol residues were probed with Alexa Fluor 647. **(B)** Average density units of Alexa 647 fluorescence (F)/unit total SERCA2A, illustrating the number of thiol residues per unit of SERCA2A protein. Data is presented as relative to the fluorescence density units/unit SERCA2A in the absence of drugs. Asterisk (*) indicates a significant difference from non-treated (control) samples.

SERCA2A thiol groups. It is also possible that doxOL modifies free thiols on phospholamban which contains 3 cysteine residues (Karim et al., 1998). No Alexa Fluor 647 binding to phospholamban was able to be measured. As phospholamban has only three cysteine residues, it is likely that this assay may not be sensitive enough to detect modification of only one to three residues. Regardless of whether doxOL also oxidizes phospholamban, the results of Ca^{2+} uptake studies and the thiol assay indicate that doxOL treatment compromises SERCA2A function via a redox mechanism, which can be prevented by DTT treatment.

4.4. Chapter Discussion

In the previous chapter, several distinct functional effects of anthracyclines on RyR2 and SERCA2A were identified. While the activation of RyR2 could be attributed to ligand binding, there was insufficient information to identify the mechanisms underlying the inhibition of RyR2 and of SERCA2A. In the current chapter, two lines of evidence have been presented linking the inhibition of RyR2 and SERCA2A to thiol oxidation. Firstly, the thiol probe assay showed a clear reduction in thiol abundance in RyR2 and SERCA2A after anthracycline treatment, indicative of thiol oxidation. Secondly, the inhibitory effect of these drugs on RyR2 and SERCA2A was prevented by pretreatment with DTT and NEM. Together, Chapters 3 and 4 provide new insight into the effects of anthracyclines on RyR2 function.

4.4.1. Anthracyclines directly modify thiol residues on RyR2 SERCA2A

Both doxorubicin and doxOL reduce the number of thiols on RyR2. Since the enzymes necessary for ROS production are either not present or inactive in our SR vesicles and were not exogenously added, it is highly unlikely that any effects we're seeing on single RyR2 channels are ROS dependent. Direct thiol oxidation by these drugs has been observed before with skeletal RyR (RyR1) (Feng et al., 1999) and has been suggested as a likely mechanism of anthracycline-induced RyR modulation (Abramson et al., 1988; Ondrias et al., 1990; Hanna et al., 2011).

Whilst the thiol probe assay illustrates only the relative change in thiol content induced by the drugs, the data can further be quantified to provide an estimate of the percentage

of thiol groups modified in the presence of both drugs. To do this, the following assumptions were made. 1) An unknown percentage of thiols are buried within the protein structure and thus not accessible to oxidizing or reducing agents. 2) Treatment with the strong reducing agent TCEP reduces all accessible thiol groups. 3) Treatment with GSSG would induce thiol modification/disulphide formation on all exposed thiol groups. Given these assumptions, it can be estimated that doxorubicin and doxOL modify ~60 and 80% of the accessible thiols in RyR2, respectively, and both drugs can be considered relatively strong oxidizing agents.

The ability of anthracyclines to oxidize SERCA2A appears to be even stronger than their ability to oxidize RyR2, with doxorubicin and doxOL inducing a similar degree of disulphide formation as GSSG. All three compounds caused an approximate 40% decrease in thiol abundance compared to untreated samples. Using the same assumptions used for RyR2, it would appear that anthracyclines could oxidize ~100% of accessible thiol groups on the SERCA2A protein. Why anthracyclines appear to have been more effective at oxidizing thiols on SERCA2A than on RyR2 is unclear. Like RyR2, SERCA2A contains several thiol groups and it is likely for both proteins that the accessibility of these thiols is variable, depending on the residue's location. Since anthracyclines are hydrophobic it is likely that doxOL could access most thiol residues on both proteins with relative ease (Kim et al., 2005b). However given the smaller size of the pump (110 kDa) compared to the release channel (2.2 mDa homotetramer/560 kDa monomer), doxOL may access a greater percentage of thiols on SERCA2A then on RyR2. The fact that doxOL induced activation did not have as large an effect on Ca^{2+} uptake (30% decrease) then it did on Ca^{2+} release (76% decrease), may suggest that thiol modification is not as influential in SERCA2A function as in RyR2 function.

While depressed SERCA2A function and/or a decrease in protein expression is a common finding in heart failure models (Arai et al., 1993; Hasenfuss et al., 1994; Studer et al., 1994; Meyer et al., 1995; Schwinger et al., 1995; Schmidt et al., 1998), there is less work investigating the influence of SERCA2A oxidation under pathological conditions. It is known however, that disulphide formation within SERCA2A leads to reduced Ca^{2+} uptake rate (see Section 1.10.4, reviewed in (Zima and Blatter, 2006). That blocking disulphide formation by pre-treatment with DTT induced a large increase in Ca^{2+} uptake rate was an unexpected outcome. Coupled with the novel finding that doxOL can bind to SERCA2A (Section 3.3.2), it appears that like the activation of

RyR2, doxOL enhances SERCA2A function via ligand binding. This outcome of ligand binding interactions between doxOL and SERCA2A is in contrast to the inhibitory effect of some other drugs with ringed structures, such as cyclopiazonic acid (Seidler et al., 1989). In terms of whole cell function, the net effect of doxOL on SERCA2A function would likely be a decrease in SR Ca^{2+} uptake since the inhibitory effect masked the activation. This hypothesis will be discussed more in Chapter 6 when effects of doxOL on whole cell function are explored.

4.4.2. Anthracyclines and the cellular redox environment

That anthracyclines can directly oxidize both RyR2 and SERCA2A and alter function could have important ramifications for cardiomyocyte health. The redox environment is increasingly recognized as a vital determinant of cardiac function. The activity of both the cardiac and skeletal muscle isoforms of RyR responds to changes in either the luminal or cytoplasmic redox potential (Feng et al., 2000; Xia et al., 2000; Oba et al., 2002; Jalilian et al., 2008b). Excess oxidation of RyR2 has been associated with functional changes including excess SR leak and with beat to beat variation in the Ca^{2+} transient amplitude (Ca^{2+} alternans) (Terentyev et al., 2008; Belevych et al., 2011; Shan et al., 2012). These effects lead to loss of contractile function and arrhythmogenesis via generation of spontaneous Ca^{2+} waves and subsequent delayed afterdepolarizations. Exactly how RyR2 oxidation translates to excess leak and Ca^{2+}alternans isn't clear, but has been hypothesized to involve enhanced response to luminal Ca^{2+} during diastole (Belevych et al., 2011).

The majority of this literature has come from intact cardiomyocyte studies where RyR2 oxidation has resulted from oxidative stress as a direct result of ROS generation. This contrasts greatly with the experimental setup used in this thesis to probe the effects of anthracyclines, where oxidation is caused by direct effects of the drugs on protein thiol groups. These experimental differences may explain the dissimilar functional outcomes. In whole cardiomyocytes, ROS induced RyR2 oxidation is associated with enhanced function which manifests as excess SR leak. In contrast, in lipid bilayer experiments, anthracycline oxidation of RyR2 caused significant inhibition of single channel activity. It is plausible that ROS and anthracyclines affect different classes of thiols groups on RyR2, thereby causing different functional effects. It has been shown previously that both RyR1 and RyR2 contain multiple classes of thiols, with modification of some

causing channel activation and modification of others causing inhibition (Liu et al., 1994; Aghdasi et al., 1997; Sun et al., 2001). In terms of the cellular dynamics of the effect of doxOL on SERCA2A function, the overall response would be a potent decrease in SR Ca^{2+} uptake with severe consequences on SR Ca^{2+} load and subsequent RyR2 Ca^{2+} release likely.

4.5. Conclusion

Together chapters 3 and 4 provide novel insight into the complex mechanisms underlying the effects of anthracyclines on cardiac function. While the data in both chapters have shown that the drugs affect both SERCA2A and RyR2 in at least two different ways (i.e. oxidation and ligand binding), it is possible that other aspects of their function are compromised. Further investigation of the effects of anthracyclines on SERCA2A may be valuable, however due to time constraints no further specific testing of SERCA2A function was carried out in this thesis. As detailed in Chapter 1, RyR2 does not act as a simple channel for Ca^{2+} to pass from the SR to cytoplasm during EC coupling. Rather, RyR2 gating is a complex process under dynamic control of a plethora of other cellular factors. As such, to build on the knowledge obtained in the first two chapters, the remaining results in this thesis will focus on 1) whether anthracyclines alter the response of RyR2 to luminal Ca^{2+} and 2) the effects of anthracyclines on Ca^{2+} transients in the intact cell.

Chapter Five

Loss of RyR2 luminal Ca^{2+} sensing with doxOL

5.1. Introduction

The response of RyR2 to changes in cytoplasmic and luminal [Ca^{2+}] is considered a vital aspect of RyR2 function and of cardiac muscle performance in general. Altered RyR2 response to luminal Ca^{2+} has been identified as an important factor in several pathological cardiac conditions including sudden cardiac death (Jiang et al., 2005), ventricular tachycardia (Jiang et al., 2005), CPVT (Fernandez-Velasco et al., 2009; Shan et al., 2012) and heart failure (Kubalova et al., 2005; Belevych et al., 2009). Changes in this response include an enhanced sensitivity to activation by luminal Ca^{2+} (Jiang et al., 2004; Kubalova et al., 2005; Vest et al., 2005; Fernandez-Velasco et al., 2009; Curran et al., 2010), or less commonly, a decreased sensitivity to luminal Ca^{2+} (Thomas et al., 2004; Jiang et al., 2007). In these studies, altered channel sensitivity to luminal Ca^{2+} was associated with enhanced diastolic Ca^{2+} leak, spontaneous Ca^{2+} waves, and Ca^{2+} alternans which create an arrhythmogenic substrate. These studies demonstrate that in changes in RyR2 sensitivity have profound effects on cardiac muscle function and likely to be important in several pathological settings.

It has emerged that redox modifications of RyR2 could contribute to altered luminal Ca^{2+} sensitivity. In a canine model of heart failure, RyR2 was more oxidized then in healthy hearts and channels had higher basal activity but an impaired ability to respond to luminal Ca^{2+} (Terentyev et al., 2008; Belevych et al., 2011). Redox modification also shifts the cytoplasmic Ca^{2+} sensitivity of RyR2. In an environment that promotes thiol reduction, channel activity is depressed allowing the channel to be inhibited with lower levels of cytoplasmic Ca^{2+}. Conversely, oxidation of thiols increased channel activity and increased the sensitivity of the channel to activation by cytoplasmic Ca^{2+} (Marengo et al., 1998; Xia et al., 2000).

Given the increasingly recognized role of luminal Ca^{2+} sensing in pathological conditions (see above), it was hypothesised that anthracyclines alter the luminal Ca^{2+} response of RyR2. It was established in Chapter 4 that anthracyclines readily oxidize thiol groups on RyR2 and SERCA2A and that anthracycline-induced oxidation of RyR2 inhibits the channel, causing substantial, irreversible inhibition of P_o. It is also known that anthracyclines bind to CSQ2, and that CSQ2 is influential in the luminal Ca^{2+} response of RyR2 (Gyorke et al., 2004; Qin et al., 2008; Wei et al., 2009a). Therefore it

was hypothesised that anthracyclines may alter RyR2 luminal Ca^{2+} sensing by a mechanism involving either 1) RyR2 thiol oxidation or 2) CSQ2 dysfunction.

While an association between luminal Ca^{2+} sensitivity and RyR2 oxidation has been observed in several pathological settings, there are no studies directly testing the dependence of the luminal Ca^{2+} response on redox modification of RyR2 under controlled bilayer conditions. Therefore experiments testing RyR2 response to luminal Ca^{2+} under reducing and oxidizing conditions were done by pretreating channels with DTT or 4,4'-DTDP, respectively. These experiments were important for several reasons. Firstly, if the hypothesis that anthracyclines alter luminal Ca^{2+} sensitivity was correct, it would be important to have a positive control for the effects of oxidation. If the effects of 4,4'-DTDP and anthracyclines on luminal Ca^{2+} were similar, it would provide a strong indication that any effect of anthracyclines on the luminal Ca^{2+} response were meditated by thiol oxidation. Secondly, such an oxidation dependent effect would have to be confirmed by pre-treating channels with DTT. It would therefore by necessary to characterize any influence of DTT itself on luminal Ca^{2+} response, so that this independent effect could be accounted for in experiments where DTT was used in combination with anthracyclines.

Aim: The primary aim of the experiments presented in this chapter was to determine if doxOL could alter the luminal Ca^{2+} sensitivity of RyR2. However, as outlined above and detailed in Chapter 1, luminal Ca^{2+} regulation of RyR2 is complex, and is influenced by a number of factors. Therefore, secondary aims were, firstly, to characterize the luminal Ca^{2+} response under reducing and oxidizing conditions, secondly, determine the influence of CSQ2 on the luminal Ca^{2+} response and finally, to confirm the mechanism underlying any anthracycline induced changes in luminal Ca^{2+} sensing.

5.2. Methods

5.2.1. SR vesicle isolation and RyR2 purification

As detailed in Section 2.3, cardiac SR vesicles were prepared from sheep heart (Laver et al., 1995).

5.2.2. Single Channel Recordings

To test the luminal Ca^{2+} response of RyR2, *trans* Ca^{2+} was reduced from 1 mM to 0.1 mM by perfusing the *trans* chamber with *trans* solution containing 0.1 mM Ca^{2+}. The *trans* [Ca^{2+}] was then increased in a stepwise manner to 0.5 mM, 1 mM and 1.5 mM, a range encountered physiologically in the SR lumen. At least 4 min was allowed between each addition of $CaCl_2$ to ensure sufficient stable, consistent activity was available for later analysis (see below). Modifications were made to this protocol so that the luminal Ca^{2+} response was tested under various experimental conditions. In these cases, after control activity was recorded, experimental conditions were established before the *trans* solution was perfused and the luminal Ca^{2+} response was tested. These conditions are outlined in Table 5.1.

All protocols testing the influence of doxOL had the drug included in the perfusion solution, to avoid washout of the activation effect. Due to the challenging nature of these experiments and time constraints, only the doxorubicin metabolite doxOL was used in this series of experiments. DoxOL was chosen as it is likely to be more relevant in anthracycline induced cardiotoxicity and a concentration of 2.5 μM was applied as this caused the most rapid onset of effects with subsequent stabilization of channel activity and is within the range of clinically relevant concentrations (Gewirtz, 1999).

Earlier work showed that DTT could only protect thiols from daunorubicin-induced oxidation when added to the *cis* chamber. While DTT is not membrane permeable at physiological pH (Terentyev et al., 2008; Hanna et al., 2011), 4,4'-DTDP is able to cross the lipid bilayer and would presumably target thiols in both the cytoplasmic and luminal domains of the channel. The effect of 4,4'-DTDP on RyR2 activity varies with 4,4'-DTDP concentration, with concentrations ≥ 0.1 mM causing an initial activation that is followed by inhibition, while lower concentrations simply activate the channels. The relatively low concentration of 20 μM 4,4'-DTDP was used to firstly, avoid later changes in activity that may complicate the response to changes in luminal Ca^{2+} and secondly to avoid the irreversible channel closure that occurs with prolonged excess oxidation. (Eager et al., 1997; Marengo et al., 1998; Eager and Dulhunty, 1999; Terentyev et al., 2008). For simplicity, data obtained with P_o and I'_F are combined in calculations of average P_o or as P_o relative to the activity with 0.1 mM *trans* Ca^{2+}.

(A) Condition tested	(B) Protocol addition before altering *trans* Ca^{2+}	(C) Section
No treatment (control)	None	5.3.1
Anthracycline pretreatment	Add 2.5 μM doxOL, *trans*	5.3.2
Reducing environment	Add 1 mM DTT, *cis*	5.3.3.1.1
Oxidizing environment	Add 20 μM 4,4'-DTDP	5.3.3.1.2
DTT-pretreatment of anthracyclines	Add 1 mM DTT, *cis*, followed by 2.5 μM doxOL, *trans*	5.3.3.2
CSQ2 dissociation	High ionic strength - add 250 mM Cs^+, *trans* to dissociate CSQ2	5.3.4.1
Anthracycline pretreatment with CSQ2 dissociation	High ionic strength - add 250 mM Cs^+, *trans* to dissociate CSQ2, followed by 2.5 μM doxOL, *trans*	5.3.4.2

Table 5.1 – Experimental protocols used in Chapter 5. (**A**) The response of RyR2 to changes in a luminal Ca^{2+} in the range 0.1 – 1.5 mM, was tested under various experimental conditions. After recording control activity, the additions specified in **(B)** were made to the *cis* or *trans* solutions. The *trans* solution was exchanged so that *trans* Ca^{2+} was 0.1 mM, and sequential additions of $CaCl_2$ were made to the *trans* solution so that the total *trans* $[Ca^{2+}]$ were 0.1 mM, 0.5 mM, 1 mM and 1.5 mM. The section of Chapter 5 detailing the results of these protocols is specified in (**C**).

5.3. Results

5.3.1. Untreated RyR2 respond to increases in luminal [Ca^{2+}]

Before testing the effect of doxOL on RyR2 response to luminal Ca^{2+}, it was essential to first characterize the response of untreated RyR2 under our conditions i.e. sheep RyR2 with 1 μM *cis* Ca^{2+} and no added ATP or Mg^{2+}. Following channel incorporation, stable control activity was recorded for 3 – 4 min before the *trans* solution was perfused with a low *trans* Ca^{2+} solution ([Ca^{2+}] = 0.1 mM). Average P_o at this baseline [Ca^{2+}] was 0.0158±0.003 and was increased maximally to 0.061±0.01 with 1.5 mM *trans* Ca^{2+}. With each addition of $CaCl_2$ there was an increase in activity, with the steepest response when *trans* [Ca^{2+}] was increased from 0.5 mM to 1 mM where the effect was saturated between 1 and 1.5 mM.

Further analysis revealed the increase in P_o was due to a significant decrease in the mean closed time (T_c) which was maximally reduced with 1 mM Ca^{2+} to 50% of the baseline value (recorded at 0.1 mM Ca^{2+}) (Figure 5.1D). This was accompanied by a significant increase in the mean open frequency (F_o) (Figure 5.1E). As with T_c this effect was maximal at 1 mM *trans* Ca^{2+} where there was 2.71±0.74 fold increase in F_o compared to baseline activity. There was no significant difference in average mean open time (T_o) over the *trans* [Ca^{2+}] range tested (Figure 5.1C). The changes in P_o are comparable to those measured previously with native RyR2 and comparable cytoplasmic [Ca^{2+}] (Table 1.2) (Gyorke and Gyorke, 1998; Gyorke et al., 2004; Qin et al., 2008; Laver, 2009; Dulhunty et al., 2012).

5.3.2. Anthracyclines abolish the response of RyR2 to changes in luminal [Ca^{2+}]

The impact of anthracyclines on luminal Ca^{2+} sensitivity of RyR2 was examined by pre-treating channels with 2.5 μM doxOL. Addition of *trans* 2.5 μM doxOL caused the expected significant channel activation that was followed by substantial inhibition of RyR2 (Section 3.3.3). On average it took 10 min before sustained inhibition was observed. The *trans* chamber was perfused with *trans* solution containing 2.5 μM doxOL and 0.1 mM Ca^{2+}. Increasing luminal [Ca^{2+}] from 0.1 to 0.5 mM caused only a marginal (and insignificant) change in P_o, from 0.0437±0.01 to 0.0398±0.01 (Figure 5.2).

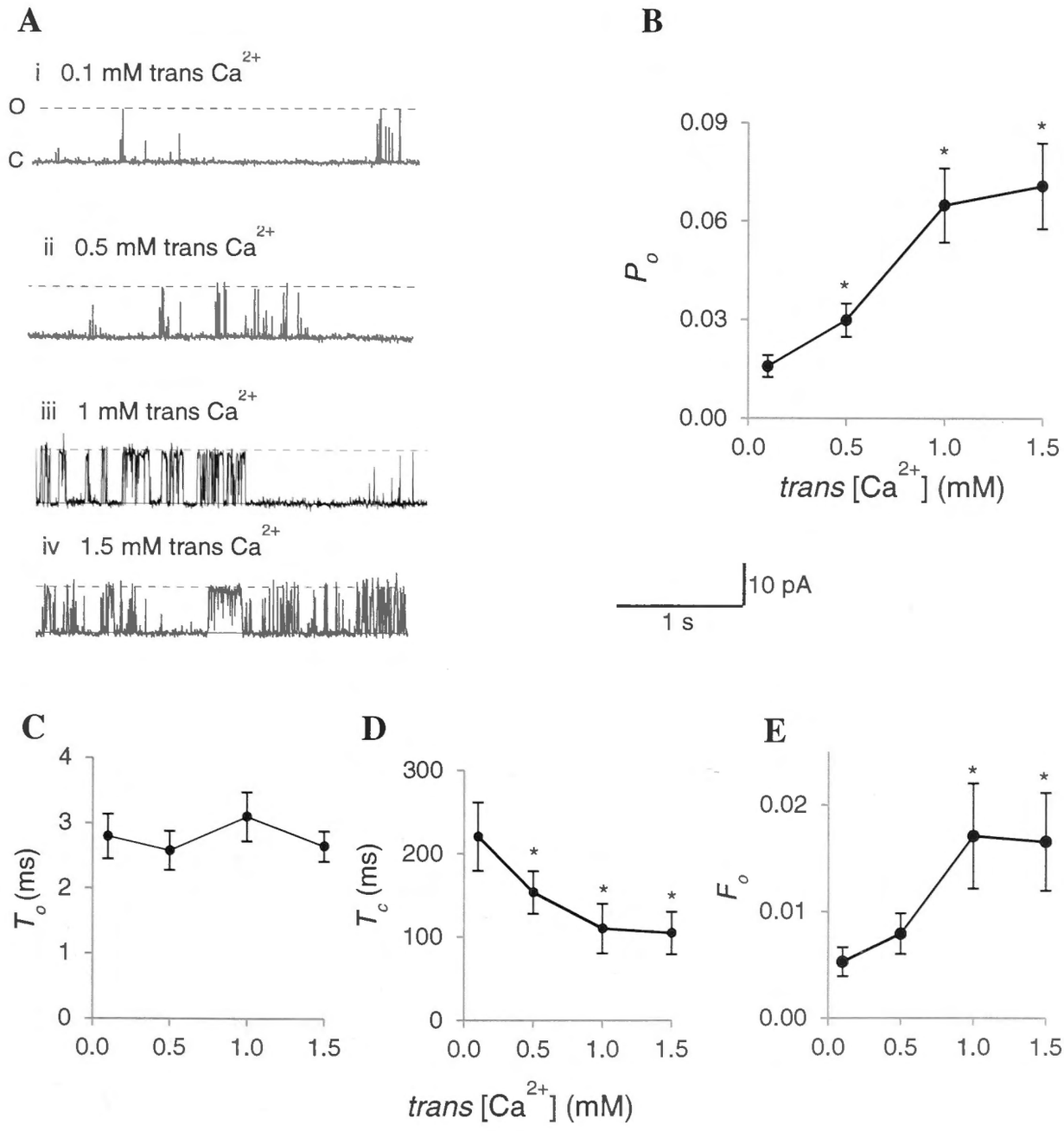

Figure 5.1 – Single channel response of untreated RyR2 to changes in luminal (*trans*) Ca^{2+} (A) i-iv. 3s records of single channel activity, where channel opening is upward from zero current (c, continuous line) to maximum open conductance (o, broken line) at +40mV. (i) Baseline activity following *trans* perfusion. *cis* and *trans* [Ca^{2+}] are 1 μM and 0.1 mM, respectively. (ii) *trans* [Ca^{2+}] increased to 0.5 mM. (iii) *trans* [Ca^{2+}] increased to 1 mM. (iv) *trans* [Ca^{2+}] increased to 1.5 mM. (B - E) Average data for (B) P_o, n = 17 – 24 (C) T_o, n = 12 – 15. (D) T_c, n = 12 – 17 (E) F_o, n = 12 – 17. Error bars are ±SEM. Average data significantly different from baseline activity recorded with 0.1 mM *trans* Ca^{2+} are indicated by (*, $p < 0.05$)

Further increases in luminal Ca^{2+} to 0.5 mM, 1 mM and 1.5 mM Ca^{2+} had no significant effect on P_o, compared either to baseline activity with 0.1 mM Ca^{2+} or with any of the higher Ca^{2+} concentrations. These results suggest that doxOL has abolished the luminal Ca^{2+} response and are in drastic contrast to the increase in activity observed with untreated RyR2 (Section 5.3.1).

In the isolated lipid bilayer system there are only a limited number of interactions that could account for this lack of response to luminal Ca^{2+}. Results presented in Chapters 3 and 4 suggest the hypothesise that the abolition of luminal Ca^{2+} sensing by doxOL could be caused by 1) oxidation of RyR2 thiols, or 2) ligand binding, to either RyR2 or an accessory protein.

5.3.3. Anthracycline oxidation does not mediate the loss of luminal Ca^{2+} response

To determine if doxOL abolishes the luminal Ca^{2+} response by modifying RyR2 thiols, it was necessary to undertake several sets of experiments. The strategy involved protecting thiols with DTT before adding doxOL and testing the luminal Ca^{2+} sensitivity. This necessitated first testing the effect of DTT itself on the luminal Ca^{2+} response so that any DTT-induced alteration of RyR2 luminal Ca^{2+} sensitivity could be taken into account. This would also serve as a positive control for the effect of a reducing agent on RyR2 luminal Ca^{2+} sensitivity. As a positive control for oxidation-induced changes in luminal Ca^{2+} sensing, a second set of experiments were conducted where channels were first treated with 20 μM 4,4'-DTDP before the luminal Ca^{2+} response was tested. Hence this section firstly characterizes the effects of both reducing and oxidizing conditions on RyR2 luminal Ca^{2+} sensitivity, and secondly, determines whether doxOL abolishes luminal Ca^{2+} response via oxidation. Several experiments in this section (Section 5.3.3) were conducted by Mr Alex Lam, a technician with the Muscle Research Group (John Curtin School of Medical Research, Canberra, Australia).

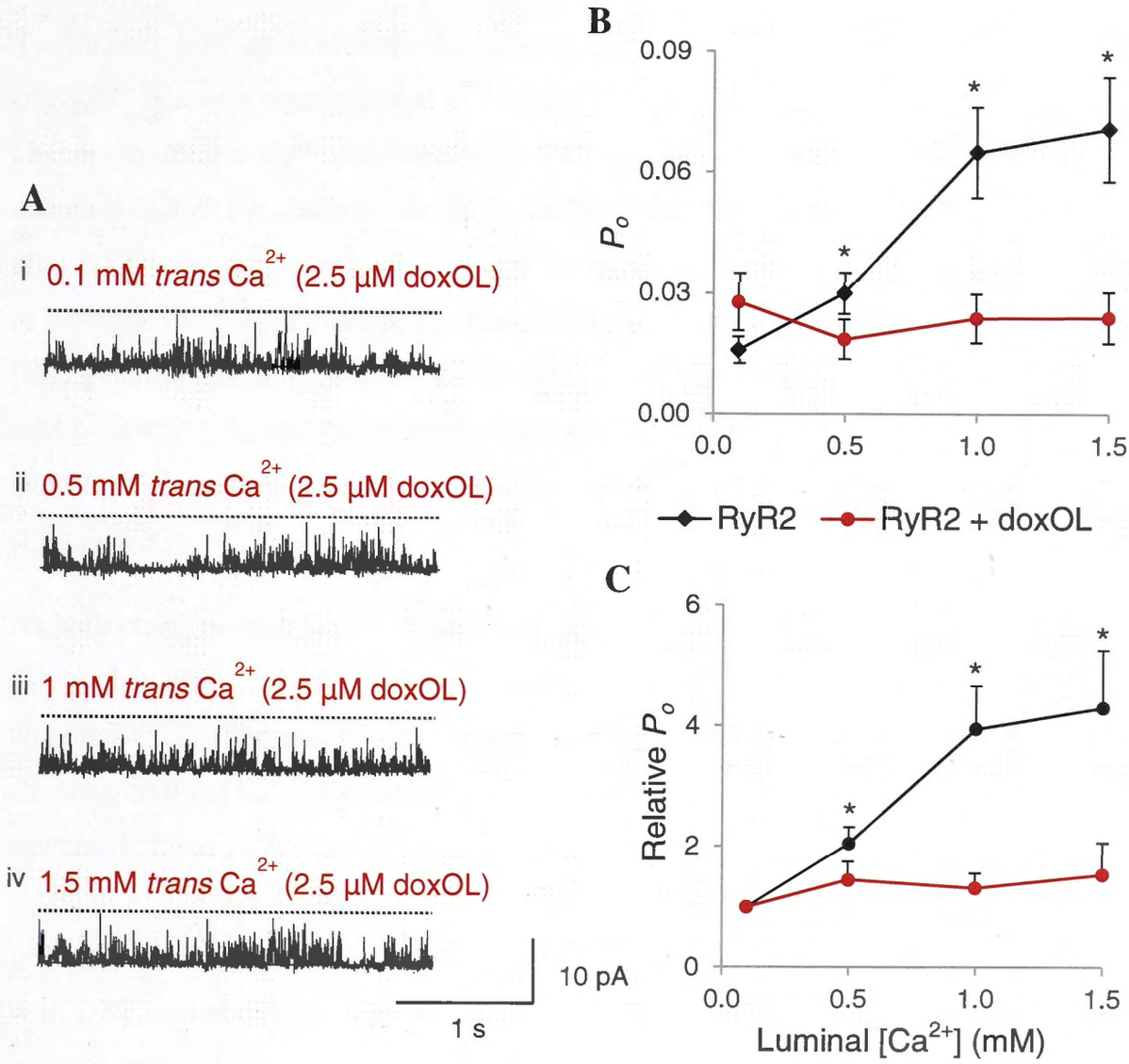

Figure 5.2 – DoxOL abolishes response of RyR2 to changes in *trans* Ca^{2+}. (A) i-iv. Records of 3 s of single channel activity, where channel opening is upward from zero current (c, solid line) to maximum open conductance (o, dashed line) at +40mV. (i) Baseline activity in the presence of 2.5 µM doxOL. Following *trans* perfusion c*is* and *trans* [Ca^{2+}] are 1 µM and 0.1 mM, respectively. (ii) *trans* [Ca^{2+}] increased to 0.5 mM. (iii) *trans* [Ca^{2+}] increased to 1 mM. (iv) *trans* [Ca^{2+}] increased to 1.5 mM. (B) Average data for P_o measured in the presence (red line) or absence (black line) of 2.5 µM doxOL (**C**) Average data for P_o relative to activity measured with 0.1 mM *trans* Ca^{2+} in the presence (red line) or absence (black line) of 2.5uM doxOL pretreatment. n = 17 – 24. Error bars are ±SEM. Average data significantly different from baseline activity recorded with 0.1 mM *trans* Ca^{2+} are indicated by * ($p < 0.05$).

5.3.3.1. Redox agents alter the normal RyR2 response to luminal Ca^{2+}

5.3.3.1.1. Thiol reduction reverses RyR2 response to luminal Ca^{2+}

To establish how an increase in thiol abundance might alter the luminal Ca^{2+} sensitivity of RyR2, channels were exposed to 1 mM DTT before testing the response of the channel to luminal Ca^{2+}. Addition of *cis* DTT caused only a minor and insignificant decrease in RyR2 P_o from 0.0307±0.01 to 0.0270±0.009 (Figure 5.3A-B). Five – 6 min after DTT addition, the *trans* [Ca^{2+}] was lowered to 0.1 mM by perfusing the chamber, as described above. In contrast to untreated RyR2 (Section 5.3.1), increasing the *trans* [Ca^{2+}] caused a significant decrease in RyR2 activity in DTT treated channels. At 0.1 mM *trans* Ca^{2+}, P_o was 0.0390±0.01. This was decreased to 0.0265±0.01 with 0.5 mM *trans* Ca^{2+} and was maximally inhibited to 0.0130±.002 when *trans* Ca^{2+} was 1.5 mM (Figure 5.3C).

As with channels recorded in the absence of DTT (Section 5.3.1), changes in P_o were due to changes in T_c and F_o with no significant changes in T_o. Average P_o, T_c and F_o were maximally decreased with 1.5 mM *trans* Ca^{2+} (Figure 5.3C-F). The response of channels to *trans* Ca^{2+} in a reducing redox environment contrasts greatly with that of untreated channels. Instead of a rise in P_o with increasing *trans* Ca^{2+}, more reduced channels experienced a 30 – 70% inhibition in P_o (Figure 5.5), demonstrating the influence of thiol reduction in RyR2 luminal Ca^{2+} sensitivity. Therefore, pre-treatment with DTT caused a reversal in the luminal Ca^{2+} sensitivity of RyR2.

5.3.3.1.2. 4,4'-DTDP increases RyR2 sensitivity to low luminal Ca^{2+} concentrations and basal RyR2 activity .

To compare how thiol reduction and thiol oxidation each alter the response of RyR2 to luminal Ca^{2+}, another set of experiments was done where channels were exposed to the oxidizing agent 4,4'-DTDP. Addition of 20 μM *cis* 4,4'-DTDP caused a 2 fold increase in P_o from 0.03±0.005 to 0.0601±0.01 (Figure 5.4A-B), and in control experiments this persisted for up to 30 min. Increasing *trans* Ca^{2+} from 0.1 mM to 0.5 mM caused approximate 3-fold increase in P_o from 0.0440±0.01 to 0.1196±0.01 (Figure 5.4C). However, in contrast to untreated channels (Section 5.3.1), additional increases in *trans* Ca^{2+} failed to further activate RyR2 (Figure 5.4C). This is in contrast to untreated channels where increasing the luminal [Ca^{2+}] caused a dose dependent increase in the P_o.

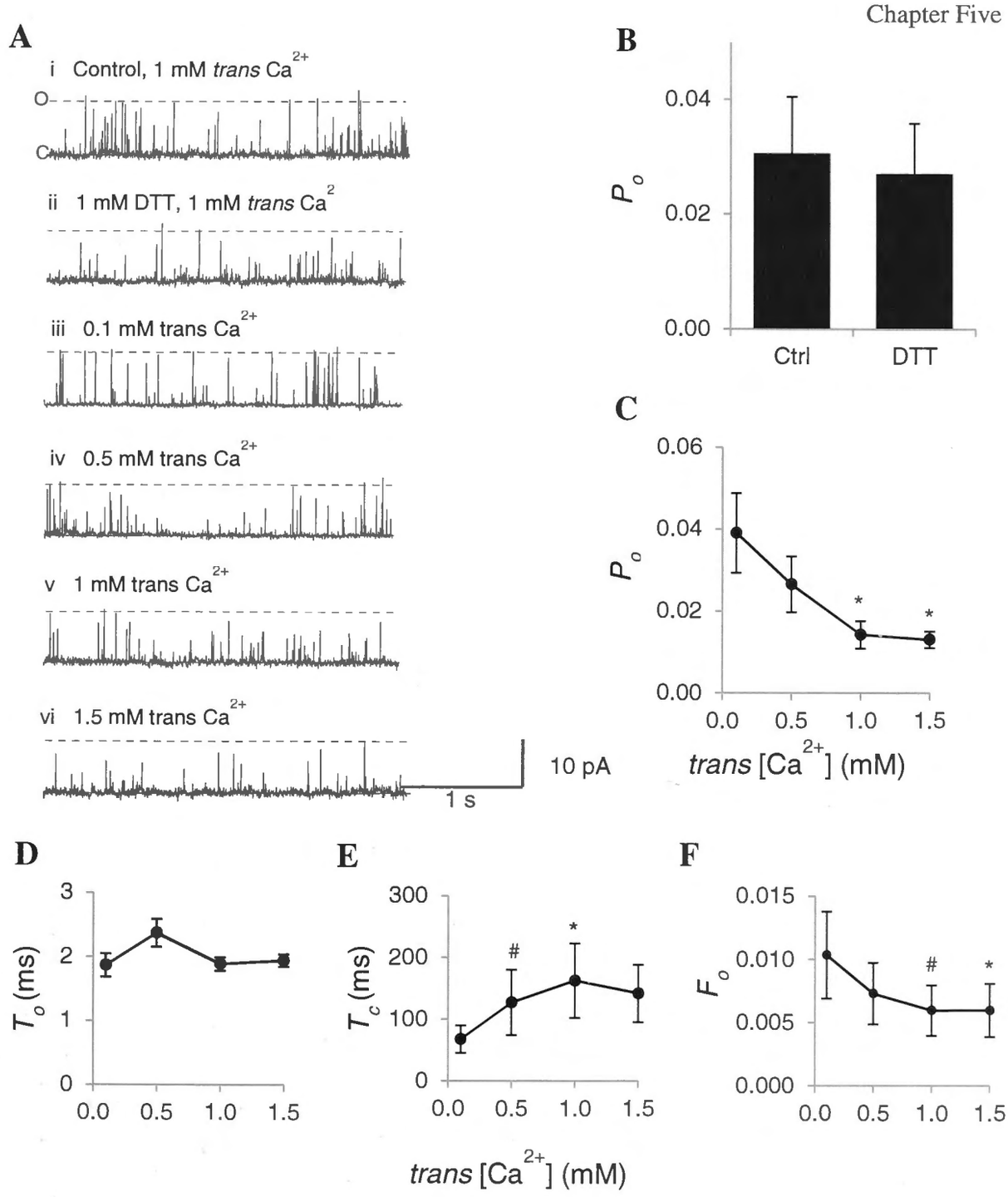

Figure 5.3 – Single channel response of DTT treated RyR2 to changes in *trans* Ca^{2+}. **(A)** i-vi. 3 s records of single channel activity, where channel is opening upward from zero current (c, continuous line) to maximum open conductance (o, broken line) at +40mV. (i) Control activity, *cis* and *trans* [Ca^{2+}] are 1 μM and 1 mM, respectively. (ii) 1 mM DTT added to *cis* chamber, n = 14 (iii) Baseline activity following *trans* perfusion to decrease *trans* [Ca^{2+}] to 0.1 mM. (iv) *trans* [Ca^{2+}] increased to 0.5 mM. (v) *trans* [Ca^{2+}] increased to 1 mM. (vi) *trans* [Ca^{2+}] increased to 1.5 mM. **(B)** Average data for addition of *cis* 1 mM DTT **(C - E)** Average data for **(C)** P_o, n = 13 – 14 **(D)** T_o, n = 10 **(E)** T_c, n = 6 **(F)** F_o, n = 8 – 9. Error bars are ±SEM. Average data significantly different from baseline activity with 0.1 mM *trans* Ca^{2+} are indicated by (*, $p < 0.05$, #, $p < 0.1$).

Although the relative increase in activity with each addition of Ca^{2+} was less robust, the absolute level of activity was significantly higher between 0.1 – 1.5 mM *trans* Ca^{2+} in oxidized channels (Figure 5.5A). Baseline activity was 0.0440±0.01 in oxidized channels compared to 0.0158±0.003 in untreated channels. Furthermore, oxidized channels attained a maximal P_o of 0.1196±0.01 (with 0.5 mM *trans* Ca^{2+}) whereas untreated channels had a maximum P_o of 0.0611±0.01 (with 1.5 mM *trans* Ca^{2+}) implying that oxidized RyR2 are more readily activated by luminal Ca^{2+} than untreated channels (Figure 5.5A). Similar to DTT-treated and untreated channels (Figure 5.2 and 5.3), the effects on P_o were due to changes in T_c and F_o, with no significant alteration in T_o (Figure 5.4D-F) The decrease in T_c and increase in F_o peaked at 0.5 mM Ca^{2+}, with no further change brought on by increasing the luminal Ca^{2+}, similar to the effect on P_o. Hence 4,4'-DTDP treated channels were more active over the entire range of tested [Ca^{2+}] than untreated channels, while the relative response to increasing *trans* Ca^{2+} was dampened compared to untreated channels (Figure 5.5). The effect is more apparent when comparing the relative changes in P_o (Figure 5.5B).

5.3.3.2. Thiol oxidation does not cause loss of luminal Ca^{2+} sensing with doxOL treatment

It was hypothesised that doxOL-induced abolition of luminal Ca^{2+} sensing (Section 5.3.2) may have been due to oxidation of RyR2 thiol residues. Having established the independent effect of DTT on RyR2 activity (Section 5.3.3.1.1) and that 1 mM DTT reliably blocks doxOL induced RyR2 inhibition (Section 4.3.1.2), in the next set of experiments channels were pre-treated with *cis* DTT, prior to doxOL exposure and the response of RyR2 to luminal Ca^{2+} was tested. This was followed by addition of 2.5 μM doxOL which caused channel activation as documented in Section 3.3.3. Due to the already lengthy duration of these experiments, doxOL induced activity was only recorded until sustained activation was observed (usually within 6 – 7 min) before perfusing the *trans* chamber with *trans* solution containing 2.5 μM doxOL and 0.1 mM Ca^{2+}.

In the presence of DTT and doxOL, increasing the *trans* [Ca^{2+}] had little effect on RyR2, with no significant difference in average P_o between any of the luminal Ca^{2+} concentrations tested (Figure 5.6).

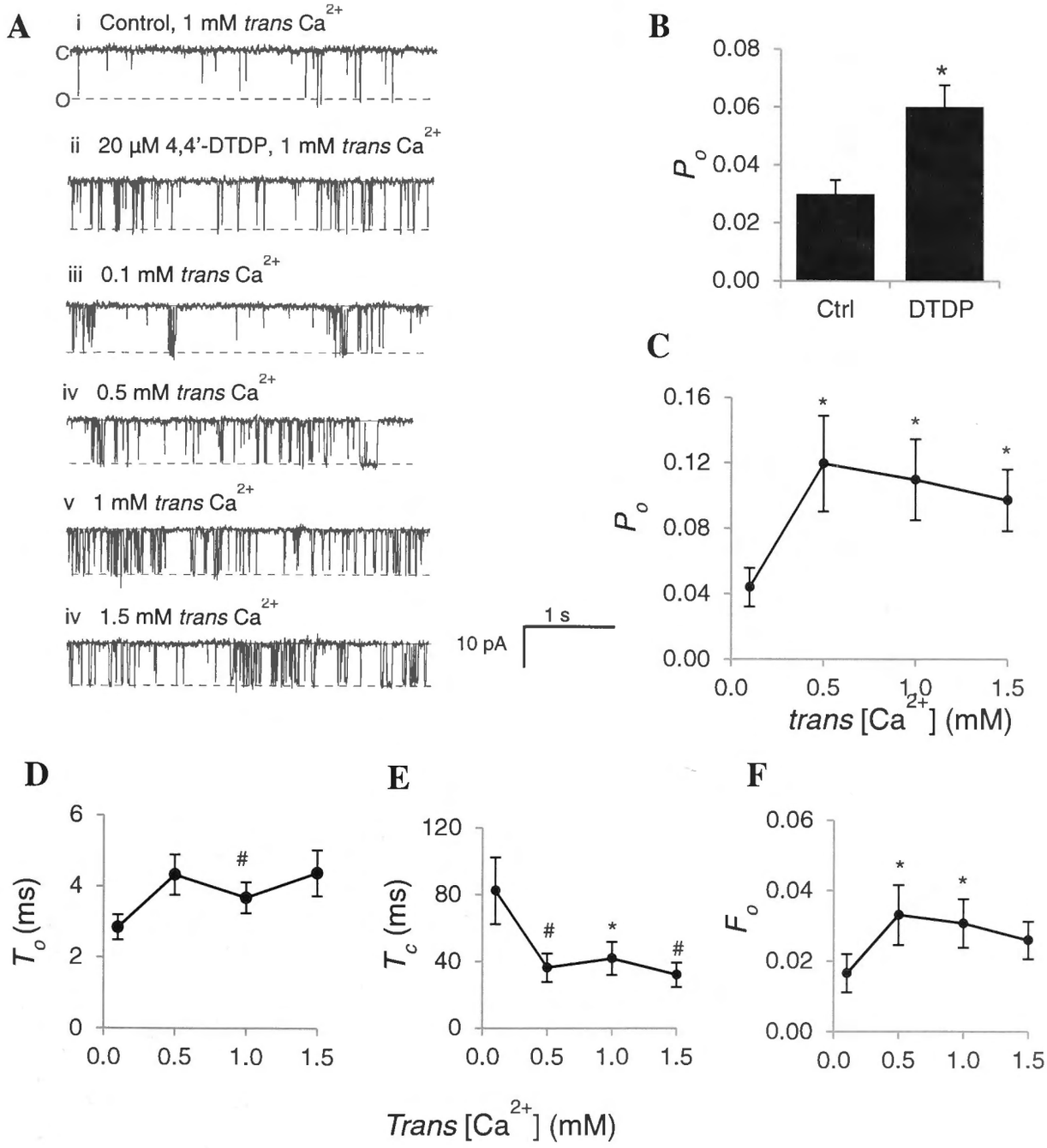

Figure 5.4 – Single channel response of 4,4'-DTDP treated RyR2 to changes in luminal (*trans*) Ca^{2+}. **(A)** i-vi. 3 s records of single channel activity, where channel is opening downward from zero current (c, continuous line) to maximum open conductance (o, broken line) at -40mV. (i) Control activity, *cis* and *trans* [Ca^{2+}] are 1 µM and 1 mM, respectively. (ii) Addition of 20 µM 4,4'-DTDP to the *cis* chamber caused a significant increase in open probability (P_o), (iii) Baseline activity following *trans* perfusion to decrease *trans* [Ca^{2+}] to 0.1 mM. (iv) *trans* [Ca^{2+}] increased to 0.5 mM. (v) *trans* [Ca^{2+}] increased to 1 mM. (vi) t*rans* [Ca^{2+}] increased to 1.5 mM. **(B)** Average data for addition of *cis* 20 µM 4,4'-DTDP, n = 15. **(C - E)** Average data for **(C)** P_o, n = 14 - 16. **(D)** T_o, n = 8- 10. **(E)** T_c, n = 7 – 9. **(F)** F_o , n = 7 – 10. Error bars are ±SEM. Average data significantly different from baseline activity with 0.1 mM *trans* Ca^{2+} are indicated by (*, $p < 0.05$, #, $p < 0.1$)

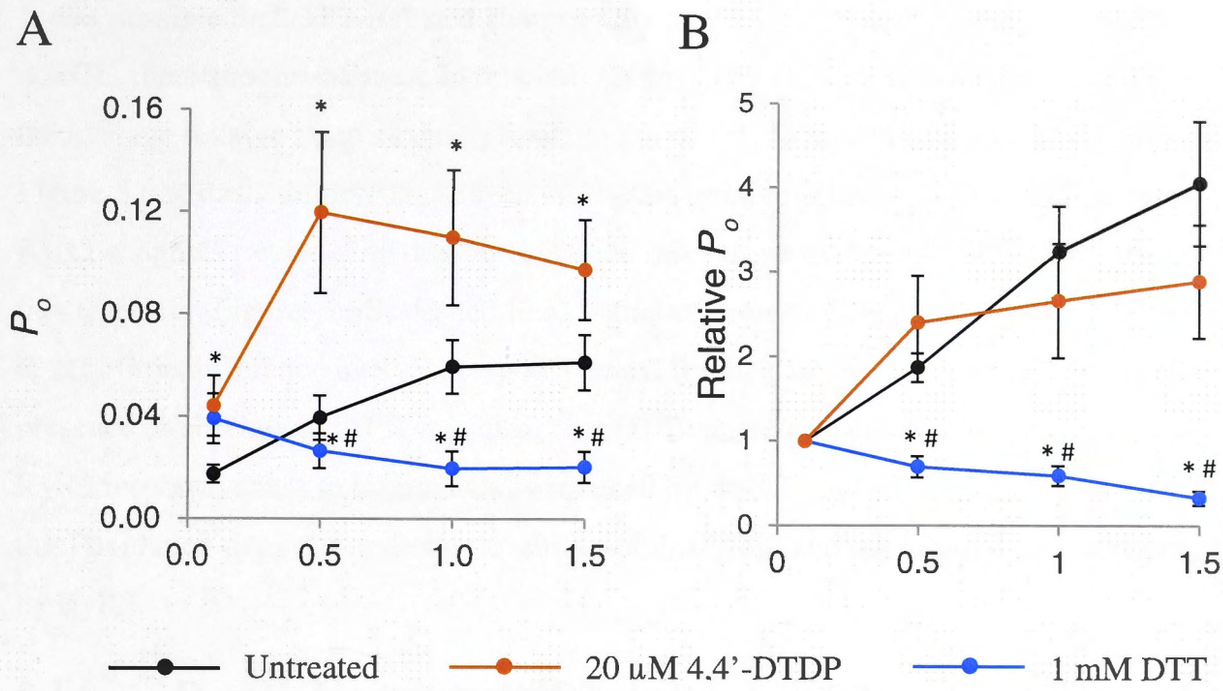

Figure 5.5 – Average response of untreated, DTT treated and 4,4'-DTDP treated single RyR2 channels to changes in luminal Ca^{2+}. Comparison of changes in (**A**) open probability (P_o) and (**B**), relative P_o for untreated (black line), DTT treated (1 mM, blue line) and 4,4'-DTDP treated (20 µM, orange line), as shown individually in Figures 5.1, 5.3 and 5.4) Values in (**B**) are relative to baseline activity measured with 0.1 mM *trans* Ca^{2+}. Asterisk (*) indicates significant difference to untreated channels and crosshatch (#) indicates significant difference between DTT and DTDP treated channels.

It was possible that DTT-induced changes (Section 5.3.3.1.1) masked the effects of doxOL, therefore the decrease in relative P_o caused by DTT alone, was subtracted from the average relative P_o of channels treated with both DTT and doxOL. This is shown in Figure 5.6B (dashed line). Thus, even taking the inhibitory effect of DTT into account, RyR2 channels treated with doxOL remained insensitive to luminal Ca^{2+}. Comparing this response (Figure. 5.6B; dashed line) to that of untreated channels (black line), there is very little difference in RyR2 responsiveness (or lack thereof) to luminal Ca^{2+} in the presence or absence of DTT. It is clear that DTT cannot prevent the disturbances in RyR2 responsiveness to luminal Ca2+ induced by doxOL and strongly indicates that thiol oxidation does not underlie the ability of doxOL to abolish luminal Ca^{2+} sensing by RyR2.

5.3.4. DoxOL binding to CSQ2 abolishes RyR2 sensitivity luminal Ca^{2+}

It was hypothesized that anthracyclines could abolish luminal Ca^{2+} sensing by either an oxidation mechanism or via a ligand binding mechanism, to either RyR2 or an associated protein. The results in Section 5.3.3.2 suggest that thiol oxidation was not responsible for the loss of luminal Ca^{2+} sensitivity, indicating that ligand binding underlies the effect. It was plausible that doxOL binding to CSQ2 was the underlying cause of the drugs abolition of normal RyR2 luminal Ca^{2+} sensitivity as CSQ2 is a known anthracycline binding target and there is significant evidence linking CSQ2 to luminal Ca^{2+} regulation of RyR2 (Gyorke et al., 2004; Qin et al., 2008). Thus the role of CSQ2 was examined.

5.3.4.1. CSQ2 alters the luminal Ca^{2+} response of RyR2

It was necessary to first characterise the effect of CSQ2 dissociation on luminal Ca^{2+} sensing under the current experimental conditions. Following channel incorporation, CSQ2 was dissociated by increasing the *trans* ionic strength with addition of 250 mM Cs^+ (total [Cs^+] is 500 mM *trans* and 250 mM *cis*). Activity was observed until there was an obvious, sustained decrease in activity, which indicated successful dissociation of CSQ2 from the channel (Beard et al., 2008; Wei et al., 2009b). To prevent CSQ2 from reassociating and to restore symmetrical Cs^+ concentrations, the *trans* chamber was perfused with *trans* solution containing 250 mM Cs^+ and 0.1 mM Ca^{2+}.

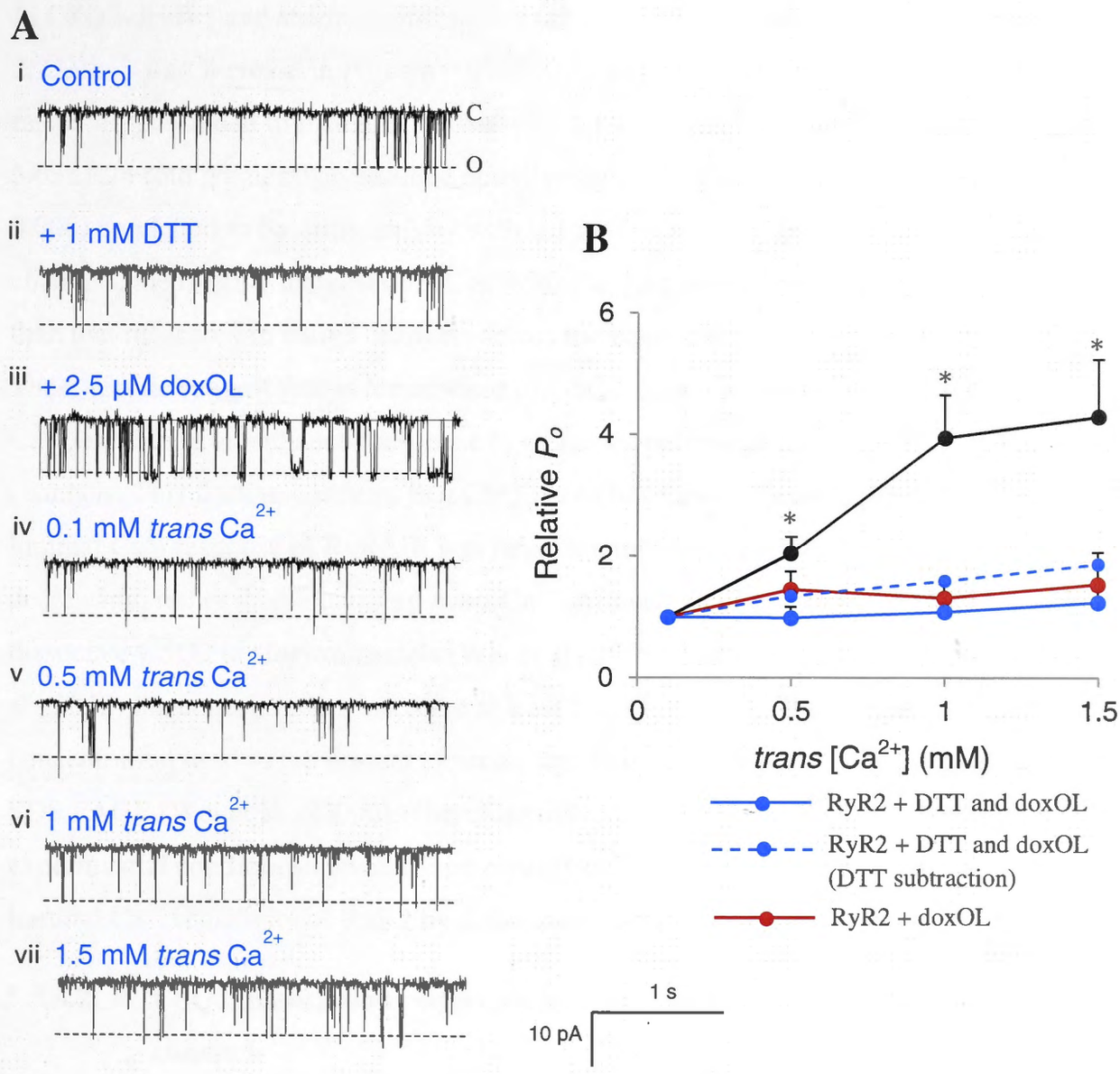

Figure 5.6 – DTT pretreatment does not restore RyR2 Ca^{2+} sensing in the presence of doxOL (A) i-vii. Three s records of single channel activity, where channel is opening downward from zero current (c, solid line) to maximum open conductance (o, dashed line) at -40mV. (i) Control activity, *cis* and *trans* [Ca^{2+}] are 1 µM and 1 mM, respectively. (ii) Addition of 1 mM DTT to the *cis* chamber had little effect on open probability (P_o). (iii) addition of 2.5 µM doxOL to the *trans* chamber caused a significant increase in P_o. (iv) Baseline activity following *trans* perfusion to decrease *trans* [Ca^{2+}] to 0.1 mM. (v) *trans* [Ca^{2+}] increased to 0.5 mM. (vi) *trans* [Ca^{2+}] increased to 1 mM. (vii) *trans* [Ca^{2+}] increased to 1.5 mM. **(B)** Average data for P_o relative to baseline activity with 0.1 mM *trans* Ca^{2+} in the presence of 1 mM DTT and 2.5 µM doxOL (blue solid line, n = 11 - 13) and with the independent effect of DTT on luminal Ca^{2+} subtracted (dashed blue line). Error bars are ±SEM. Average data significantly different from baseline activity with 0.1 mM *trans* Ca^{2+} are indicated by (*, $p < 0.05$). Data for untreated channels (black line) and doxOL treated channels (red line) are included for reference.

In CSQ2-dissociated channels, increasing *trans* Ca^{2+} from 0.1 mM to 0.5 mM caused a 2.75±0.43 fold increase in P_o from 0.0186±0.014 to 0.0443±0.034. As *trans* Ca^{2+} was raised, P_o continued to increase, so that with 1.5 mM *trans* Ca^{2+}, channel activity was 5.63±1.24 fold greater than baseline activity. All of these increases were significant ($p < 0.008$) compared to baseline activity with 0.1 mM *trans* Ca^{2+}. In these CSQ2 dissociated channels, the relative increases in P_o as *trans* Ca^{2+} increased were significantly greater than that measured in native channels across the equivalent [Ca^{2+}] range (Figure 5.7). These results suggest that in the absence of CSQ2, RyR2 is more sensitive to luminal Ca^{2+}, exhibiting an enhanced response to increases in luminal Ca^{2+} compared to native channels. This finding confirms that CSQ2 does have a significant influence on the luminal Ca^{2+} response of RyR2. It was never attempted to test the Ca^{2+} sensitivity by decreasing, rather than increasing *trans* Ca^{2+}. Although a high luminal [Ca^{2+}] can dissociate CSQ2 in single channels (Wei et al., 2009b and reviewed in Gaburjakova et al., 2012) the concentrations used are at least 2 – 3 fold higher than the maximal concentration used in the present experiments. This has also been demonstrated using SDS PAGE (Wei et al., 2009b). Therefore, it would not be expected under the present experimental conditions that an initial *trans* [Ca^{2+}] of 1.5 mM would influence the luminal Ca^{2+} sensitivity of RyR2 by dissociating CSQ2.

5.3.4.2. CSQ2 dissociation restores luminal Ca^{2+} sensing in doxOL treated channels

To determine whether CSQ2 mediates the effect of doxOL on RyR2 luminal Ca^{2+} sensing, channels were treated with 2.5 μM doxOL before CSQ2 was dissociated and the luminal Ca^{2+} response was tested (Figure 5.8). As in Section 3.3.3 addition of *trans* 2.5 μM doxOL increased RyR2 P_o before causing a sustained decrease in activity. In the present experiment, once channel activity had stabilized at a decreased level (approximately 10 – 12 min after drug addition), CSQ2 was dissociated by the high ionic strength protocol (as in Section 5.3.4.1) and the *trans* chamber was perfused with *trans* solution containing 250 mM Cs^+, 0.1 mM Ca^{2+} and 2.5 μM doxOL.

Increasing the *trans* Ca^{2+} from 0.1 mM to 0.5 mM in the CSQ2-dissociated channels in the presence of doxOL caused a 2.84±1.02 fold increase in P_o (Figure 5.8). This was not significantly different ($p = 0.1$) from the 1.21±0.19 fold increase in doxOL treated native channels. Further increasing *trans* Ca^{2+} to 1 mM caused a 4.01±0.69 fold increase in activity. This was the maximal P_o attained with no further increase when *trans* Ca^{2+}

was raised to 1.5 mM. Between 0.5 and 1.5 mM *trans* Ca^{2+}, the response of CSQ2-depeletd RyR2 was significantly greater than the doxOL treated native channels where there was little change in P_o as *trans* Ca^{2+} was increased (Figure 5.7). There is no significant difference between the two Ca^{2+} response curves for CSQ2-stripped channels, with and without doxOL (Figure 5.8, dashed lines). Thus, the results provide compelling evidence in support of a hypothesis that CSQ2 plays the primary role in the loss of RyR2 luminal Ca^{2+} sensing caused by doxOL.

5.4. Chapter Discussion

In this chapter, several important and novel findings regarding SR Ca^{2+} handling have been presented. The response of RyR2 to changes in luminal Ca^{2+} has been examined under a number of conditions which may occur pathologically including oxidative stress and anthracycline induced cardiotoxicity. These results provide valuable knowledge on the normal physiological function of RyR2 and on factors that influence the ability of the channel to respond to luminal Ca^{2+}. The principle findings were firstly and unexpectedly, that doxOL abolishes the luminal Ca^{2+} sensitivity of RyR2. Secondly, this lack of sensitivity is mediated by doxOL binding to CSQ2, and not via doxOL induced thiol oxidation on RyR2. Additionally, it was demonstrated that the redox status of RyR2 thiol residues has an important role in regulating RyR2 sensitivity to luminal Ca^{2+}. Reducing and oxidizing conditions resulted in striking differences in the channel's response to luminal Ca^{2+}. Reduced channels were inhibited by luminal Ca^{2+} in a dose dependent manner, whilst oxidized RyR2 were substantially more active than untreated channels but had an impaired ability to respond to changes in luminal Ca^{2+}.

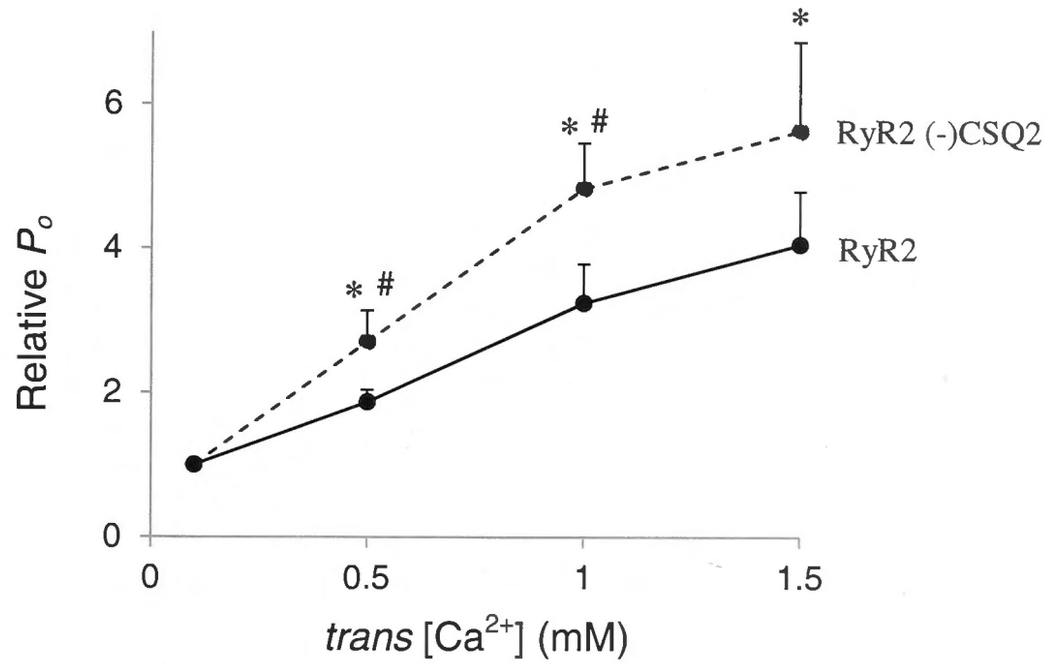

Figure 5.7 – CSQ2 alters the luminal Ca^{2+} sensitivity of RyR2. Average data for P_o (relative to baseline activity in the presence of 0.1 mM *trans* Ca^{2+}) of CSQ2 dissociated channels (dashed line) and native channels (solid line). Relative average data significantly different from baseline activity with 0.1 mM *trans* Ca^{2+} in CSQ2 dissociated channels is indicated with an asterisk (*, $p < 0.05$, n = 8 - 13). Average data of CSQ2 dissociated channels significantly different to the matched concentration in native channels is indicated by crosshatch (#, $p < 0.05$).

5.4.1. Anthracyclines abolish RyR2 luminal Ca^{2+} sensing

The sensitivity of RyR2 to activation by luminal Ca^{2+} is an area of intense study, due to its purported role in heart failure, CPVT and atrial fibrillation (Jiang et al., 2005; Kubalova et al., 2005; Belevych et al., 2009; Fernandez-Velasco et al., 2009; Shan et al., 2012). These conditions are associated with changes in Ca^{2+} handling in cardiomyocytes, including increased diastolic Ca^{2+} leak and generation of spontaneous Ca^{2+} waves. The leak that causes such effects is thought to result from an increased sensitivity of RyR2 to activation by luminal Ca^{2+} during diastole. While the cause of this heightened sensitivity is controversial, enhanced oxidation is now thought to play an important role. Since anthracyclines are powerful oxidizing agents and induce similar phenotypic effects as the aforementioned cardiac conditions, it follows that doxOL pretreatment may enhance the response of RyR2 to luminal Ca^{2+}. That doxOL actually abolished the luminal Ca^{2+} sensing ability of RyR2 was therefore, unexpected.

In subsequent experiments, the failure of DTT pretreatment to restore the normal Ca^{2+} response ruled out a role of doxOL-induced oxidation in mediating the loss of luminal Ca^{2+} sensitivity. DTT blocked the inhibitory effects of doxOL-induced oxidation on channel activity at a constant luminal Ca^{2+} concentration of 1 mM (Section 4.3.3) and would presumably be just as effective in preventing any other functional effect that depended on doxOL modification of these thiols. Even accounting for the independent effect of DTT on the luminal Ca^{2+} response, there was no enhancement in the ability of doxOL treated channels to respond to luminal Ca^{2+} when oxidation was prevented by DTT (Figure 5.6B). We can infer from these results that the oxidative effects of doxOL are separate to its ability to modulate luminal Ca^{2+} sensing.

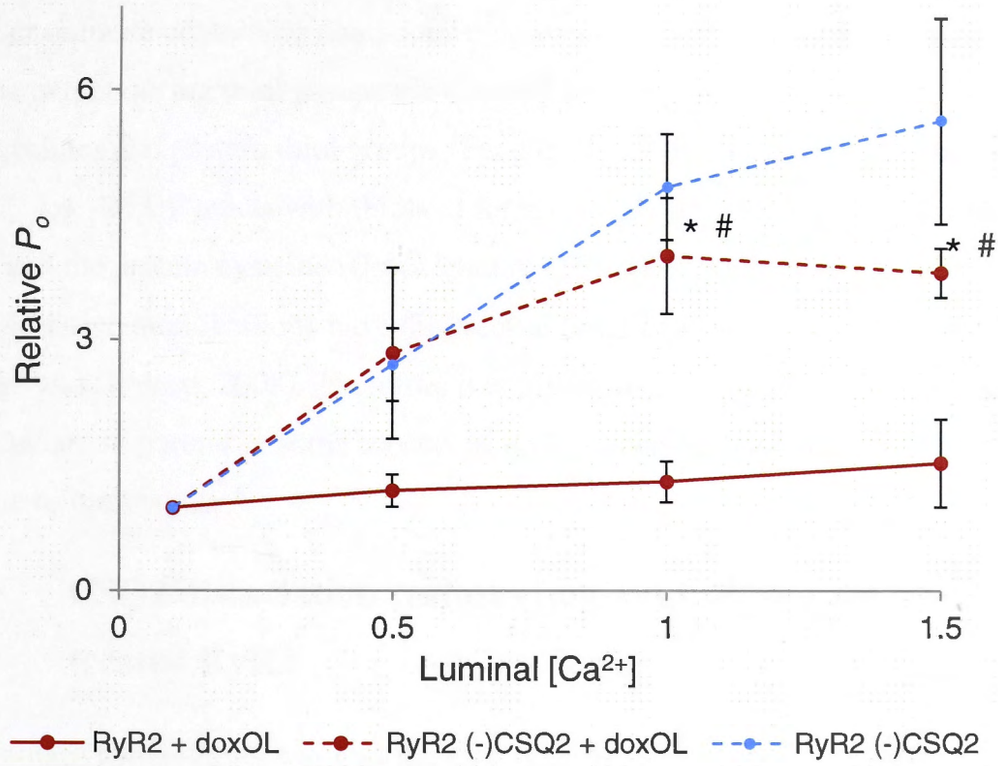

Figure 5.8 - CSQ2 dissociation restores luminal Ca^{2+} sensing in the presence of doxOL
Average data for relative P_o in in CSQ2 dissociated channels ((-)CSQ2, dashed line) in the presence (red dashed line) or absence (blue dashed line) of 2.5 μM. The response of native channels to increasing *trans* Ca^{2+} in the presence of 2.5 μM doxOL (red solid line) is included for comparison. Average data significantly different from baseline activity with 0.1 mM *trans* Ca^{2+} in doxOL treated (-) CSQ2 channels (n = 7 – 10) is indicated with an asterisk (*, $p < 0.05$). Average data of doxOL treated (-)CSQ2 channels significantly different to the matched concentration in doxOL treated native channels is indicated by crosshatch (#, $p < 0.05$).

The difference in effect of doxOL compared to other oxidizing agents that alter luminal Ca^{2+} sensing is likely to be due to differing mechanisms of oxidation. Anthracyclines and other quinone containing compounds reportedly promote disulphide formation between neighbouring thiol groups via electron exchange reactions between anthracyclines and protein thiol groups (Feng et al., 1999; Marinov et al., 2007). In contrast, 4,4'-DTDP reacts with thiols to form a covalent disulphide bond between DTDP and the protein cysteine (Brocklehurst, 1979). It is well recognized that different RyR2 oxidative modifications have differential functional outcomes (reviewed in (Hidalgo and Donoso, 2008). Therefore it is plausible that doxOL targets a group of thiols that are important in some aspects of RyR2 function, but not in mediating the response to luminal Ca^{2+}.

5.4.2. CSQ2 dissociation restores luminal Ca^{2+} sensing of doxOL treated RyR2

The alternative hypothesis was that the effects of doxOL on luminal Ca^{2+} sensing were due to ligand binding to either RyR2 or CSQ2, since both proteins are established binding targets of doxOL. This hypothesis was partly validated when removal of CSQ2 restored luminal Ca^{2+}sensing to similar levels as observed in the absence of doxOL (i.e. CSQ2-stripped RyR2). DoxOL was still present in the solutions after CSQ2 was dissociated, so could still bind to RyR2. The exact role of CSQ2 in luminal Ca^{2+} sensing is controversial. CSQ2 is known to be important in SR Ca^{2+} handling, acting as a SR Ca^{2+} buffer and communicating SR store load to RyR2, possibly via anchoring proteins triadin and/or junctin (Section 1.9.3.2) (Gyorke et al., 2004; Qin et al., 2008; Stevens et al., 2009; Wei et al., 2009b). However, the control CSQ2 dissociation experiments, done in the absence of doxOL (Section 5.3.4.1) suggest that while CSQ2 exerts a regulatory role in the channel's response to luminal Ca^{2+}, RyR2 does possess an innate sensitivity to luminal Ca^{2+}. This is supported by studies in CSQ2 knockout mice where a response to SR load was preserved, despite knockout of the CSQ2 protein (Knollmann et al., 2006). What is most likely is that proper luminal Ca^{2+} sensing requires optimal function of all components of the SR Ca^{2+} release complex. This is highlighted by the fact that knockdown, knockout or induced dysfunction of RyR2, triadin, junctin and CSQ2 have now all been associated with dysregulated Ca^{2+} release (Knollmann et al., 2006; Kashimura et al., 2010; Altschafl et al., 2011; Roux-Buisson et al., 2012). Further delineation of the molecular entities responsible for luminal Ca^{2+} sensing could

be made in experiments using a purified RyR2 and then adding back purified SR proteins such as triadin, junctin and CSQ2, alone or in combination (as in Wei et al., 2009a)

Anthracyclines have been proposed to bind to a site on CSQ2 which lowers the Ca^{2+} storage capacity of the protein, and to inhibit Ca^{2+} dependent polymerization of CSQ2 (Charlier et al., 2005; Kang et al., 2010). While the presence of CSQ2 is not essential for RyR2 to respond to luminal Ca^{2+}, CSQ2 is necessary for normal RyR2 luminal Ca^{2+} sensitivity. That CSQ2 has a vital role in RyR2 sensitivity to luminal Ca^{2+} was shown in studies on the CPVT linked CSQ2 mutant L167H (di Barletta et al., 2006). It was found that this mutant abolished luminal Ca^{2+} sensing by RyR2 (Qin et al., 2008). The authors attributed this loss of response to a change in the Ca^{2+} sensitivity of the interaction between CSQ2 and the unglycosylated form of triadin (Qin et al., 2008). While this mechanism requires validation, it is possible that an altered interaction between CSQ2 and triadin and/or junctin could mediate a loss of luminal Ca^{2+} sensing. Whether anthracyclines alter these protein-protein interactions in a similar manner remains to be elucidated. Alternative explanations for the drastic effect of the doxOL-CSQ2 interaction on luminal Ca^{2+} sensing are implicated by past studies. Daunorubicin has been found to inhibit the Ca^{2+} binding capacity of CSQ2 (Hanna et al., 2011). Additionally, the binding of anthracyclines to CSQ2 has been proposed to alter protein conformation and aggregation (Park et al., 2004; Charlier et al., 2005; Kim et al., 2005b; Kang et al., 2010). In the heart, CSQ2 is thought to exist mainly as monomers or dimers under physiological conditions (Wei et al., 2009b; Murphy et al., 2011) suggesting that inhibition of polymerization by anthracyclines may not necessarily impact physiological function of CSQ2. However this doesn't preclude a role for anthracycline-induced conformational changes, since these changes could still inhibit dimer formation or alter/impede the interaction of CSQ2 with triadin or junctin. Hence, while a precise mechanism for the abolition of luminal Ca^{2+} sensing is unclear, it may involve inhibition or alteration of; 1) Ca^{2+} binding capacity of CSQ2, 2) CSQ2 polymerization or 3) CSQ2 communication with RyR2 via triadin or junctin.

5.4.3. Effects of thiol modification on RyR2 luminal Ca^{2+} sensing

Upon closer analysis of single channel studies (Marengo et al., 1998; Terentyev et al., 2008) where the effect of oxidation has been tested on the luminal Ca^{2+} response, it is

evident that oxidized channels have had a higher basal activity, with an impaired ability to respond to changes in the luminal or cytoplasmic [Ca^{2+}]. This is similar to the observations in the current experiments with 4,4'-DTDP (Figure 5.4). Oxidized channels were far more active than reduced or untreated channels at matched luminal [Ca^{2+}] (Figure 5.5A). This enhanced activity was most significant between 0.1 and 1 mM Ca^{2+}, a range that would be encountered during diastole. Enhanced activity during diastole could be deleterious as it enhances RyR2 leak which could be arrhythmogenic when it causes spontaneous Ca^{2+} waves and subsequent DADs. In some animal models of heart failure, diastolic leak is associated with increased RyR2 oxidation (Terentyev et al., 2008; Belevych et al., 2009; Bovo et al., 2012). If channels were more active following 4,4'-DTDP pre-treatment, then Ca^{2+} addition might cause a greater relative increase in P_o in oxidized channels. This was not the case. There was no significant difference between the response of 4,4'-DTDP treated channels and untreated channels, relative to the channel activity with 0.1 mM *trans* Ca^{2+} (Figure 5.5). For reasons outlined above (see Section 5.2.2), the relatively mild concentration of 20 μM 4,4'-DTDP was used. Higher concentrations of 4,4'-DTDP may have alternate, or additive effects on the Ca^{2+} response properties of RyR2 due to more extensive thiol oxidation.

In DTT-treated channels there was a 30 – 70% reduction in P_o as *trans* [Ca^{2+}] increased from 0.1 – 1.5 mM, respectively. In oxidized channels, this same increase in *trans* [Ca^{2+}] caused a 2 – 4.3 fold increase in P_o. Hence, while RyR2 does remain sensitive to luminal Ca^{2+} under reducing conditions, this sensitivity is opposite to that measured in untreated and oxidized channels. This mimics the effects of reducing agents or promotion of thiol reduction, on the cytoplasmic Ca^{2+} dependence of RyR2 (Marengo et al) and RyR1 (Xia et al., 2000).

Given the detrimental effects of hyperactive RyR2 channels during diastole, the effect of lowering RyR2 activity by thiol reduction could be a protective mechanism, and may explain the existence of the more reducing cytoplasmic redox potential compared to that in the SR lumen (Hwang et al., 1992). Besides oxidation, RyR2 is susceptible to modification by a plethora of cellular factors including phosphorylation, nitrosylation and modulation by several accessory proteins from either the luminal or cytoplasmic domain. In the cell, the activity of both the cardiac and skeletal muscle RyR isoforms depend in part on the combined redox potentials in the luminal and cytoplasmic solutions, which are controlled by several factors, including the GSH:GSSG buffer

system (Feng et al., 2000; Jalilian et al., 2008b). The extreme redox potentials created by adding either 4,4'-DTDP and DTT to the cytoplasmic side of the bilayer are likely to be in excess of that encountered under physiological conditions. However the results suggest that under the more reducing conditions normally encountered in the cytoplasm, the RyR may be less sensitive to activation by luminal Ca^{2+}. It should be considered that a positive relationship between SR load and the Ca^{2+} transient has been well documented (Bassani et al., 1995b; Shannon et al., 2000). This positive relationship likely manifests from the interplay between numerous cellular factors, in addition to the redox state. Nevertheless the finding that in a strong reducing environment the luminal Ca^{2+} sensitivity is reversed is intriguing and worth exploring more in the future. In an oxidative stress environment, RyR2 activity is likely to increase. As detailed above, enhanced RyR activity during diastole could have deleterious effects on the rhythmicity and contractile performance of the heart.

5.4.4. Interplay between Ca^{2+} sensing and RyR2 thiol oxidation

It is evident that redox modifications of RyR2 thiols modify the response of the channel to changes in both luminal and cytoplasmic Ca^{2+} (Section 5.3.3 and Marengo et al., 1998; Xia et al., 2000). Additionally, the activity of both the cardiac and skeletal muscle isoforms of RyR responds to changes in either the luminal or cytoplasmic redox potential (Feng et al., 2000; Jalilian et al., 2008b). While these latter studies did not test the Ca^{2+} dependence of the RyR response to different redox potentials, they provide compelling evidence that the redox state of thiols is linked to RyR gating.

The majority of susceptible thiol residues are on the cytoplasmic domain of the channel. DTT exerted a thiol protective effective against anthracycline induced oxidation, only when added to the *cis* side of RyR2 channels (Hanna et al., 2011). However, 4,4'-DTDP is lipid permeable and therefore can access both cytoplasmic and luminal thiol residues. Previous results have suggested that 4,4'-DTDP may target different classes of thiols located in both the cytoplasmic and luminal domains of RyR2 (Eager and Dulhunty, 1999). The results of the current project cannot exclude a role for luminal (or transmembrane) thiol residues in the effects of 4,4'-DTDP on Ca^{2+} sensitivity.

How modification of thiol residues alters luminal Ca^{2+} sensing of RyR2 is uncertain. RyR2 is susceptible to allosteric modification by a variety of ligands including Ca^{2+}, Mg^{2+} and ATP, whereby binding of one ligand alters the effects of another, either in the

same or opposite domain (Radwanski et al., 2013). It has been suggested that a coupling exists between a Ca^{2+} binding site on RyR1 and the redox potential of reactive thiol groups (Eager et al., 1997; Xia et al., 2000). The present results, and those of others (Marengo et al., 1998) support an analogous mechanism in cardiac muscle. As such, cytoplasmic thiol modification may induce a conformational change which alters either the access to or affinity of Ca^{2+} for either a Ca^{2+} activation of Ca^{2+} inhibition site. A similar mechanism has been proposed to account for oxidation induced changes in cytoplasmic Ca^{2+} sensitivity (Marengo et al., 1998). While it is clear that redox modifications influence both the cytoplasmic and luminal Ca^{2+} responses, it is less clear whether redox agents simultaneously affect the sites in the luminal and cytosolic domains, or whether redox modification of the cytoplasmic domain somehow increases sensitivity to activation by the luminal domain.

5.4.5. Luminal triggered feedthrough

One theory explaining luminal Ca^{2+} control of RyR2 entails direct activation of RyR2 by a luminal Ca^{2+} sensing site, either on RyR2 itself or on an accessory protein such as CSQ2, triadin or junctin. Other theories involve a Ca^{2+} feedthrough mechanism whereby Ca^{2+}, after binding at a luminal activation site, travels through the pore and causes prolonged channel openings by binding to an activation site on the cytoplasmic domain of the channel (Laver, 2009). It is unlikely that the luminal Ca^{2+} regulation documented here involves luminal feed through as this phenomenon is reportedly only detectable in the presence of co-stimulatory agents, such as ATP (Laver, 2007). Additionally the changes in P_o (Figure 5.2) were attributable to changes in the mean closed time and open frequency, rather than to a change in the mean open time, which would be required for significant feed through effect (Gyorke and Terentyev, 2008; Laver, 2009). Because the experiments in this thesis were done with symmetrical ionic strength in the *cis* and *trans* solutions, positive potentials and negative potentials promote current flow in the opposite directions. As has been observed previously (Gyorke and Gyorke, 1998), and in the current study, luminal Ca^{2+} regulation of RyR2 did not exhibit any dependence on the direction of current flow, reducing the likelihood that luminal Ca^{2+} feedthrough is occurring under the present conditions. Therefore, it is likely that in the present study, luminal Ca^{2+} is acting at a luminal site. CSQ2, junctin and triadin have all been proposed to have roles in luminal Ca^{2+} sensing. Since current experiments were done on native RyR2 (i.e. with all associated proteins) the results can

not differentiate between a luminal binding site on RyR2 or on an accessory protein such as CSQ2, although the CSQ2 stripped channels suggest that RyR2 has an innate sensitivity to luminal Ca^{2+} that is modified in the presence of CSQ2.

5.5. Conclusion

Luminal Ca^{2+} sensing is a fascinating aspect of RyR2 function. There is sufficient evidence of altered RyR2 Ca^{2+} response to make it clear that this dynamic process serves a vital physiological function. Many details regarding the molecular mechanisms of luminal Ca^{2+} sensing remain to be elucidated, including firstly, the identity of the luminal Ca^{2+} sensors, secondly the importance of various contributing factors including oxidation and phosphorylation and thirdly, how each of these factors change under pathological conditions such as arrhythmia, heart failure and anthracycline cardiotoxicity. It is apparent from the current experiments that the oxidizing effect of doxOL is separate from its ability to abolish RyR2 luminal Ca^{2+} sensing, with the latter appearing to be mainly due to an interaction between the drug and CSQ2. These findings add to the already complex nature of the effects of these drugs on Ca^{2+} handling in the heart. The fact that anthracyclines interact with multiple protein targets, via more than one mechanism makes it difficult to extrapolate the results of these studies in single channels and SR vesicles to the whole cardiomyocyte. Particularly, as multiple Ca^{2+} cycling proteins in cardiomyocytes are redox sensitive and in an intact cellular environment anthracyclines would also be expected to generate ROS. Therefore, in the final chapter, the effects of doxOL on single cardiomyocytes will be explored to gain an understanding of how the effects observed in these *in vitro* experiments translate to the whole cell environment.

Chapter Six

Ca^{2+} handling in anthracycline–treated cardiomyocytes

6.1. Introduction

Experiments addressing pathways of Ca^{2+} movement in and out of the SR were described in Chapters 3-5. It is clear that many factors in the SR, including luminal proteins, the redox potential and the Ca^{2+} load itself, dynamically influence RyR2 and hence, cardiac function (Gyorke et al., 2004; Hidalgo and Donoso, 2008; Radwanski et al., 2013). The cytoplasmic and luminal Ca^{2+} concentrations are tightly regulated by a combination of Ca^{2+} channels and transporters which ensure there is balance between Ca^{2+} influx and efflux across the sarcolemma and Ca^{2+} movement in and out of the SR (Dibb et al., 2007; Eisner et al., 2013). This balance is essential in maintaining optimal cardiac function, so that the muscle can contract with the necessary force during systole, and can fully relax during diastole. Therefore, it is important to consider the role of RyR2 in the context of the intact cell, not just as an individual pathway for SR Ca^{2+} release.

So far the work in this thesis has established that anthracyclines have functional effects on at least three proteins, including RyR2, SERCA2A and CSQ2. The outcomes of these interactions include:

1. inhibited SR Ca^{2+} release
2. reduced SR Ca^{2+} uptake
3. impaired ability of RyR2 to respond to changes in luminal Ca^{2+}

These findings point to an overall dampening of SR Ca^{2+} handling in the intact cell. One effect of this is likely to be reduced cardiac contractility, since less Ca^{2+} would be released in CICR during EC coupling. Additionally, these alterations in RyR2 and SERCA2A function by anthracyclines may also manifest in the intact cell as erratic Ca^{2+} release events, such as Ca^{2+} alternans or spontaneous Ca^{2+} transients (Diaz et al., 2002; Thomas et al., 2004; Jiang et al., 2007; Xie et al., 2013). The clinical relevance of such effects is indicated by the presentation of anthracycline cardiotoxicity, which is first evident as a decrease in left ventricular ejection fraction and as an increase in arrhythmogenic events (Bristow et al., 1978; Larsen et al., 1992; Barrett-Lee et al., 2009).

The results presented so far in this thesis were all obtained using isolated single channels and SR vesicles. While the use of these preparations was vital to gain an

understanding of the mechanism of anthracycline-induced dysfunction, many cellular factors that also contribute to cardiomyoycte Ca^{2+} handling were absent. Thus, it is difficult to extrapolate the functional outcome of the identified effects of anthracyclines on RyR2 or SERCA2A, to changes in whole cell function. One factor to consider is the cellular redox environment. The number of contributing factors and the unstable nature of many of the ROS (Hool and Corry, 2007), make it impractical to replicate the complex cellular redox environment in single channel studies. It should be considered then that redox active compounds like anthracyclines may have effects in the intact cell that differ or are additive to what is measured on single channels or SR vesicles. Additionally, the functional outcome of interactions between anthracyclines and RyR2 and SERCA2A could be influenced by other Ca^{2+} channels and transporters which can alter their activity to compensate for changes in RyR2 and SERCA2A flux (Dibb et al., 2007). Such compensation may lessen the effect of anthracyclines (at the concentrations and exposure times used in these experiments) on whole cell function. Additionally, anthracyclines may target proteins located on the sarcolemmal membrane, like the NCX or LTCC for example.

Aim:

The aim of the experiments in this chapter was to determine the effects of the anthracycline metabolite, doxOL, on Ca^{2+} handling in an intact cell by assessing global Ca^{2+} transients, SR load and contractile function.

6.2. Methods

6.2.1. Calcium imaging in adult mouse cardiomyocytes

As detailed in Section 2.11, intact cardiomyocytes were isolated by retrograde perfusion of hearts from 8 week old C57/NCrl mice. Myocytes were rendered Ca^{2+} tolerant by sequential additions of $CaCl_2$ and were plated on laminin-coated coverslips.

Ca^{2+} imaging of Fluo-4 AM loaded myocytes was performed using a Leica SP5 confocal microscope in line-scan mode. Fluo-4 was excited with the 488 nm line of an argon laser and fluorescence was measured at > 510 nm. Myocytes were field-stimulated at 0.5 Hz using a voltage ~30% above the stimulation threshold. In experiments where SR load was measured, 10 mM caffeine was rapidly applied by positioning rigid perfusion tubing in immediate proximity to the cell. Measurements

from control and doxOL-treated myocytes were collected each day, and a minimum of three mice were used for each set of data.

6.2.1.1. Calcium transient analysis

Ca^{2+} transient kinetics measured for each cell include peak amplitude, time to peak and time to 50% decay. Due to time constraints and technical limitations, ratiometric analysis was not carried out in the present experiments. Rather, data in this chapter is based on changes in the relative Fluo-4 fluorescence. For each cell, the average value of each parameter was calculated from six electrically evoked transients.

6.2.2. Contractility measurements

Coverslips were placed in a custom built chamber positioned in a microincubator, and myocytes were paced at 0.5 Hz. Videos were analysed in ImageJ and length measurements were made of the myocytes at systole (most contracted) and at diastole (most relaxed). Average % fractional shortening (FS) was calculated for each cell from 5 contractions. Alternate coverslips were pre-incubated for 20 min with 2.5 μM doxOL and % FS was compared to untreated cardiomyocytes.

6.3. Results

Myocytes were usually stable for up to 6 hours after isolation and were only used if they were rod shaped, responsive to stimuli and did not display spontaneous Ca^{2+} waves or contractions before the stimulation protocol.

6.3.1. DoxOL alters cytosolic Ca^{2+} transients

The effect of doxOL on whole cell Ca^{2+} handling was assessed by measuring electrically evoked Ca^{2+} transients in intact cardiomyocytes. The stimulation protocol was 12 s of stimulation at 0.5 Hz followed by a 6 s stimulation free recording period. Representative linescan images and corresponding time-dependent spatial profiles of Ca^{2+} transients from control myocytes and those pre-treated with 10 μM doxOL are shown in Figure 6.1A. Pre-treating myocytes with 2.5 or 10 μM doxOL decreased the amplitude of the peak Ca^{2+} transient by 30 – 35% compared to transients from control myocytes (Figure 6.2A, $p < 0.05$). These concentrations of doxOL also slowed the

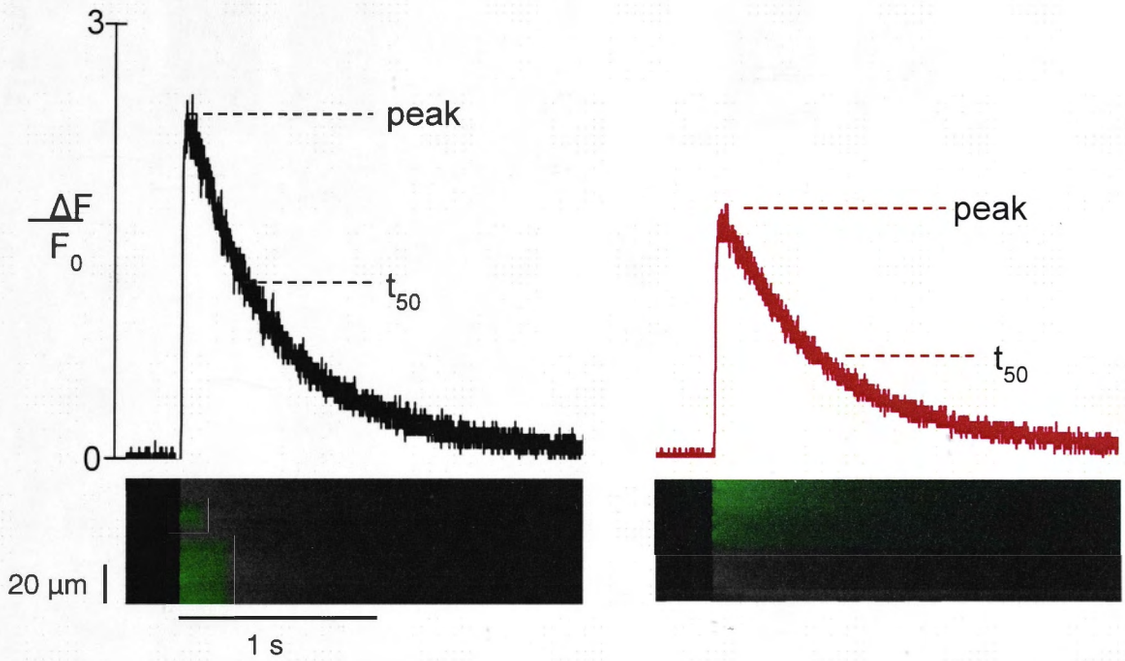

Figure 6.1 – DoxOL reduces peak amplitude and prolongs Ca^{2+} transient kinetics. Representative spatially averaged profiles of Ca^{2+} transients showing changes in relative fluorescence over time. *x-t* line scans (lower panels) were recorded during field stimulation at 0.5 Hz of control myocytes (left panel) and myocytes pre-treated for 20 min with 10 µM doxOL-treated myocytes (right panel).

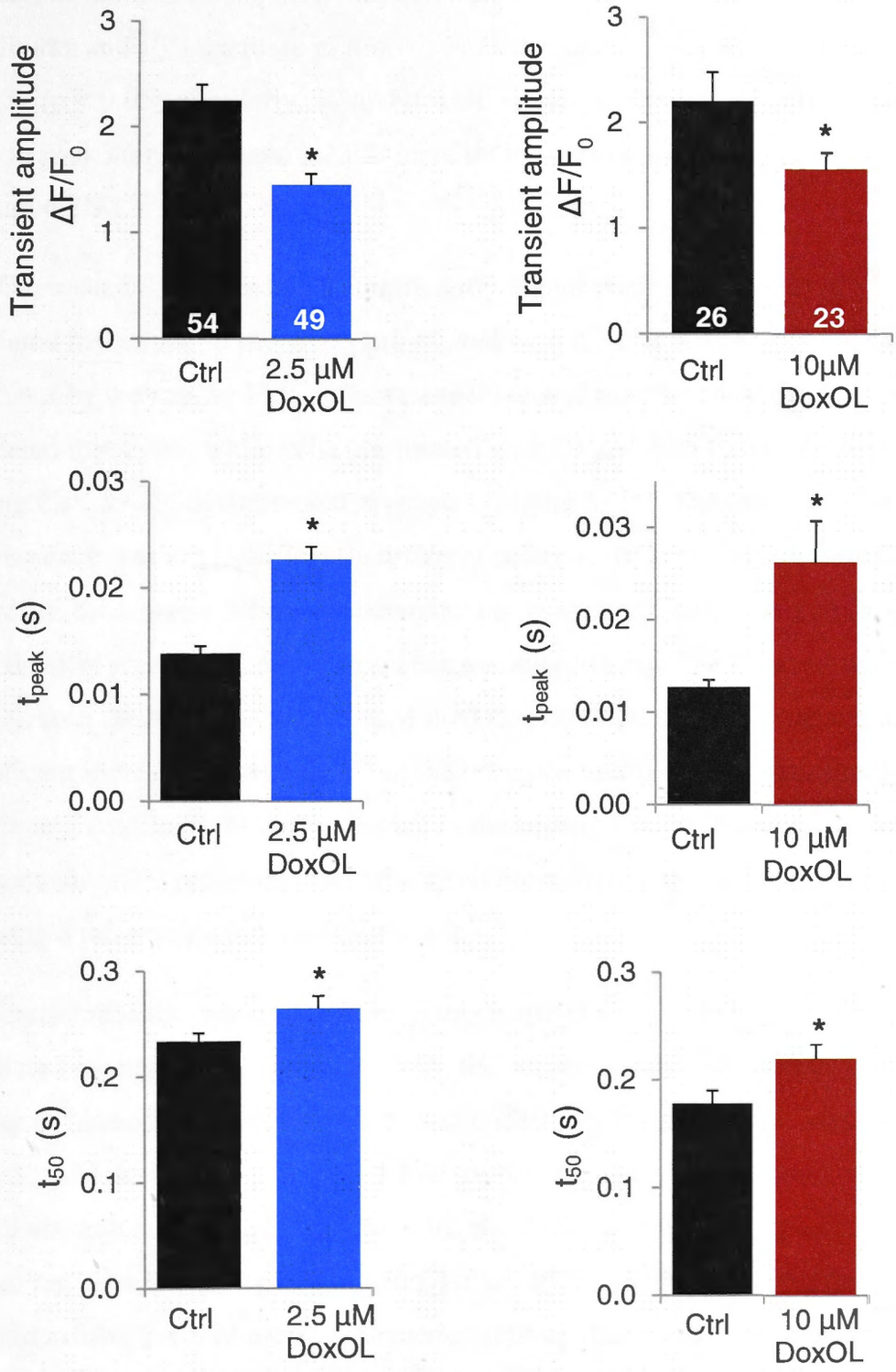

Figure 6.2 – DoxOL reduces peak Ca^{2+} transient and prolongs transient kinetics.
Average data for **(A)** peak amplitude **(B)** time to peak (s) and **(C)** time to 50 % decay of Ca^{2+} transients recorded during 0.5 Hz stimulation of control myocytes and myocytes treated with 2.5 μM and 10 μM doxOL. Numbers in bars are n numbers for each set of data. Asterisk (*) indicates a significant difference between control and doxOL treated myocytes.

kinetics of the transient. There was a significant, 64% increase in the time to peak amplitude, and 13% increase in time to 50 % decay in myocytes treated with 2.5 μM doxOL ($p < 0.05$). Similarly, 10 μM doxOL caused a significant ~2 fold increase in the time to peak amplitude, and a 23 % increase in the time to 50 % decay ($p < 0.05$) (Figure 6.2B-C).

DoxOL treated myocytes had a significantly higher resting (diastolic) [Ca^{2+}] than untreated myocytes. In myocytes pre-treated with 2.5 μM doxOL, resting Ca^{2+}, as indicated by the resting Fluo-4 fluorescence, was almost two-fold that measured untreated myocytes, while cells pre-treated with 10 μM doxOL had a 52% higher resting Ca^{2+} level than untreated myocytes (Figure 6.3A). The initial resting fluorescence was not significantly different between the two sets of control cells. However, there was a difference between the two sets of doxOL treated cells, with a significantly greater resting fluorescence measured in myocytes treated with 2.5 μM doxOL than those treated with 10 μM doxOL. Although there is a statistically significant increase in resting Ca^{2+} in the presence of doxOL, the data should be interpreted cautiously as only a change in the resting Fluo-4 fluorescence is measured. More quantitative analysis could arise from normalizing the data to the baseline F_o and by using a ratiometric dye such as Fura-2.

To determine if the relatively higher cytoplasmic [Ca^{2+}] in doxOL treated cells translated to aberrant functional activity, the occurrence of spontaneous Ca^{2+} transients during or immediately after a period of stimulation was determined. Myocytes treated with 2.5 μM doxOL exhibited a 3.5 fold higher frequency of spontaneous Ca^{2+} transients than control cells (Figure 6.3C, $p < 0.05$), as might be expected from the higher resting Ca^{2+} (Lukyanenko and Gyorke, 1999). While myocytes treated with 10 μM did exhibit 2.4 fold more spontaneous activity than control cells, this was not a significant increase ($p = 0.1$). It was surprising that 10 μM doxOL treated myocytes had lower resting Ca^{2+} and less frequent spontaneous Ca^{2+} release then myocytes treated with 2.5 μM doxOL. It is possible that the higher drug concentration was having an inhibitory effect on the diastolic Ca^{2+} release process that was not evident with the lower concentration, though this hypothesis requires validation. These results suggest that doxOL pretreatment promotes diastolic Ca^{2+} release in cardiomyocytes and that the mechanisms to extrude Ca^{2+} are impaired in doxOL treated myocytes.

Figure 6.3 – DoxOL increases resting Ca^{2+} and spontaneous transients. (**A**) Average resting fluorescence of untreated (ctrl) and doxOL treated myocytes measured under steady state conditions. (**B**) Fluorescence profiles and corresponding line scan images from a control and doxOL (2.5 μM) treated cell displaying spontaneous Ca^{2+} transients during voltage pulse stimulation at 0.5 Hz. (**C**) The number of cells displaying spontaneous Ca^{2+} transients was compared between control and doxOL treated cells. Data is presented as the average percentage of control and doxOL treated cells that displayed spontaneous transients. Data is averaged across 4 days for 2.5 μM doxOL and 3 days for 10 μM doxOL. Asterisk (*) indicates a significant difference between control and doxOL treated myocytes.

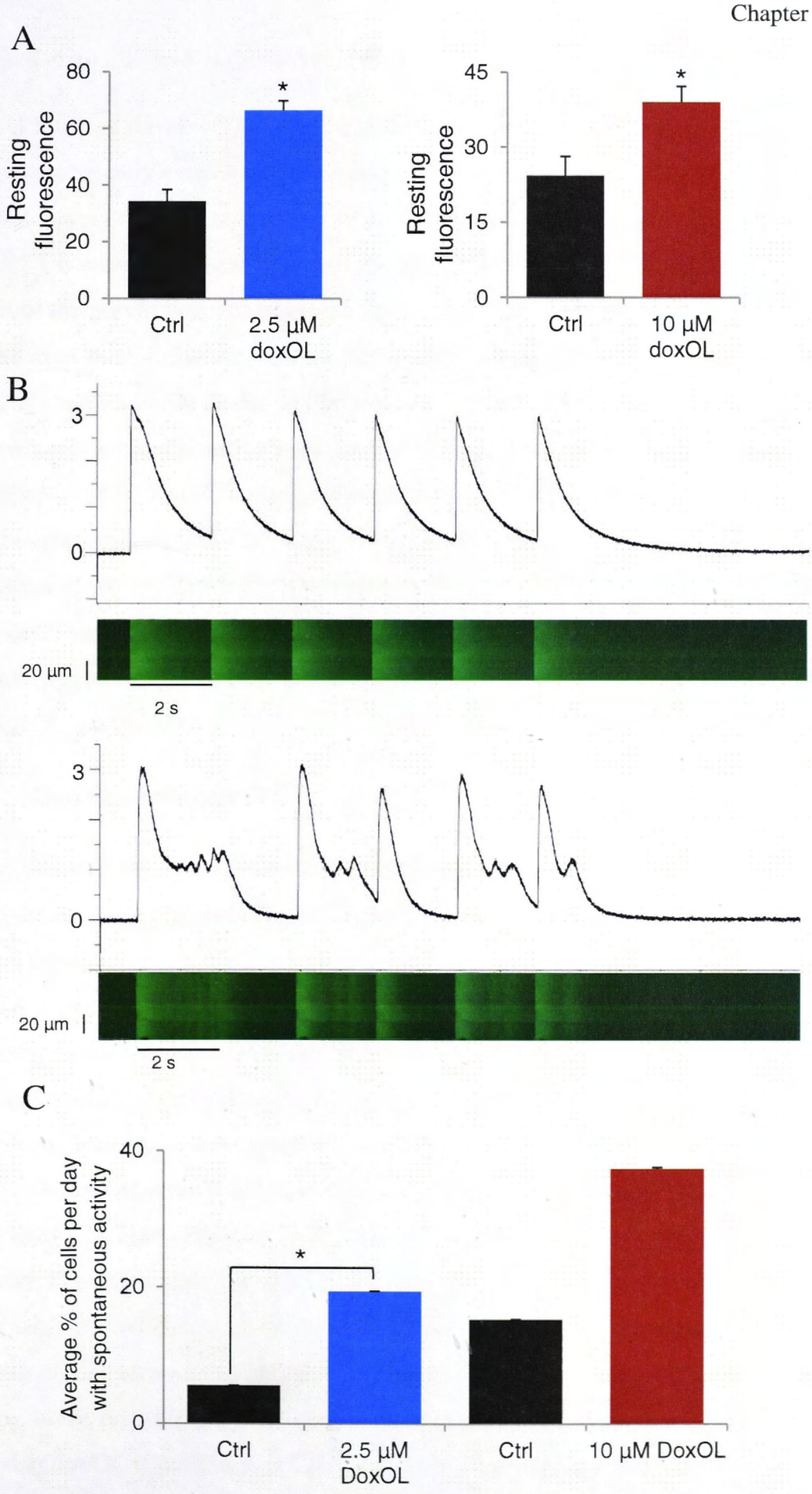
A
Resting fluorescence
80
60
40
20
0
*
Ctrl
2.5 µM doxOL
Resting fluorescence
45
30
15
0
*
Ctrl
10 µM doxOL
B
3
0
20 µm
2 s
3
0
20 µm
2 s
C
Average % of cells per day with spontaneous activity
40
20
0
*
Ctrl
2.5 µM DoxOL
Ctrl
10 µM DoxOL

6.3.2. Doxorubicinol reduces SR store load

A potential cause of the reduction in peak transient amplitude is a decrease in SR load. In a normal electrically evoked action potential, RyR2 are activated and Ca^{2+} release will depend largely on the amount of Ca^{2+} stored in the SR. Hence, the amplitude of the global $[Ca^{2+}]_i$ transient depends highly on the SR Ca^{2+} load (Gomez et al., 2004). Results from the previous three chapters confirm that RyR2 is inhibited by the concentration of doxOL that also reduces the peak transient amplitude. Therefore, to determine if changes in SR load could be a factor, another series of experiments was done where cells were exposed to a maximally activating concentration of 10 mM caffeine (Bers, 1987). The Ca^{2+} transient evoked by rapid application of caffeine is attributed to the release of SR Ca^{2+} and thus provides a measure of the total SR Ca^{2+} content (Shannon et al., 2000). DoxOL caused a 30 % reduction in the caffeine-induced Ca^{2+} transient, indicating that doxOL treatment does indeed cause a significant decrease in SR load (Figure 6.4A - B). Due to time constraints, only the lower concentration of 2.5 μM doxOL was tested.

6.3.3. DoxOL inhibits NCX

The decay phase of the voltage-activated (twitch) transient is primarily due to Ca^{2+} reuptake into the SR by SERCA2A. In contrast, the decay of the caffeine-induced transient is primarily due to Ca^{2+} extrusion from the cell by the NCX (Callewaert et al., 1989). This is because during the Ca^{2+} transient evoked in the constant presence of caffeine (Figure 6.4), RyR2 P_o remains high and Ca^{2+} reuptake via SERCA2A is constant and doesn't contribute to the net decay of the Ca^{2+} signal. That is, in the presence of caffeine there is no net re-accumulation of Ca^{2+} by the SR. Therefore, a decrease in the cytoplasmic $[Ca^{2+}]$ can be attributed to NCX mediated extrusion, which is unaffected by caffeine (Bassani et al., 1992; Bers, 2000). To assess if doxOL had an effect on NCX activity, the time to 50 % decay of the caffeine-induced Ca^{2+} transient was measured. In doxOL treated (2.5 μM) cells, there was a 40 % increase in the time to 50 % decay of the caffeine-induced Ca^{2+} transient compared to control cells indicating an increase in the time taken to extrude Ca^{2+} across the sarcolemma membrane. This suggests that doxOL is inhibiting NCX function, confirming the exchanger as an anthracycline target (Boucek et al., 1987). Although there are other pathways of Ca^{2+} efflux from the cytoplasm (e.g. mitochondria and PMCA), these constitute only 1 % of

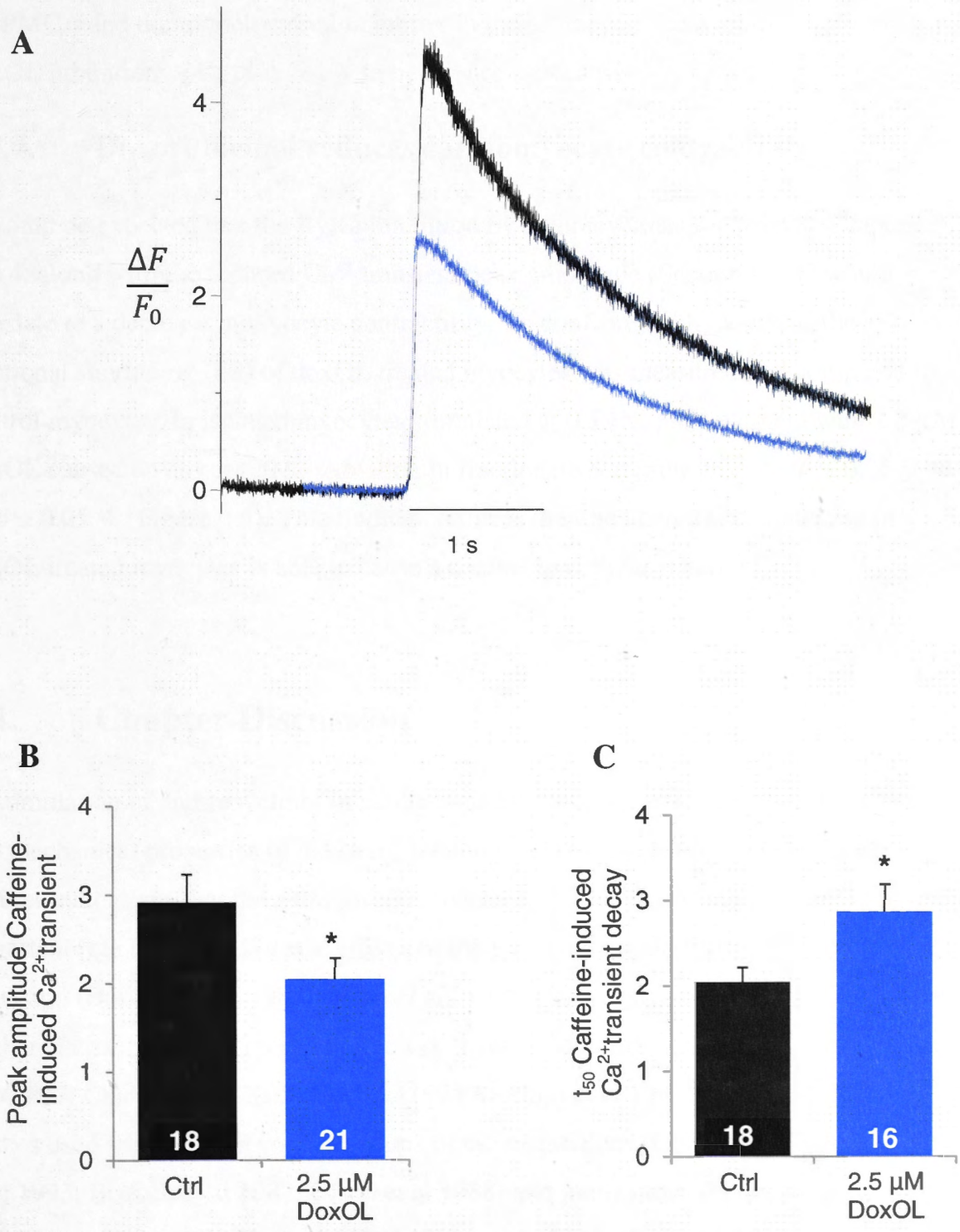

Figure 6.4 – DoxOL reduces store load and inhibits NCX activity. **(A)** Representative caffeine-induced Ca^{2+} transients from control and doxOL treated myocytes, **(B)** Average peak amplitude and **(C)** average time to 50 % decay of caffeine induced Ca^{2+} transients. Numbers in bars are n numbers for each set of data, which used myocytes from at least three mice. Asterisk (*) indicates a significant difference between control and 2.5 µM doxOL treated myocytes.

the total Ca^{2+} efflux pathway, compared to (in rodents) 10 % by the NCX and 89 % by SERCA2A (Bers, 2001). Therefore, although the present results cannot exclude roles for PMCA and the mitochondrial uniporter in the prolonged decay of the Ca^{2+} transient, doxOL inhibition of NCX is likely to be the primary cause.

6.3.4. Doxorubicinol reduces cardiomyocyte contractility

It would be expected that the RyR2 inhibition by anthracyclines reported in Chapters 3 and 4, along with the reduced Ca^{2+} transient peak amplitude (Section 6.3.1) would translate to a decrease in myocyte contractility. To confirm this hypothesis, the fractional shortening (FS) of doxOL treated myocytes was measured and compared to control myocytes. In isolated myocytes stimulated at 0.5 Hz, pre-treatment with 2.5 μM doxOL caused an almost 20 % reduction in fractional shortening from 5.46 ± 0.06 % to 4.45 ± 0.05 % (Figure 6.5). This finding confirms that the altered Ca^{2+} handling in doxOL treated myocytes is able to cause a decline in cellular function.

6.4. Chapter Discussion

Accumulation of anthracyclines in cardiac muscle causes drastic effects on the electrical and mechanical properties of the heart, inducing arrhythmogenesis and contractile failure. Indications that the anthracycline metabolites doxOL and daunOL could have an important role in the cardiotoxic effects of the parent compounds first appeared over 25 years ago (Boucek et al., 1987; Olson et al., 1988). However, only limited studies have further characterised the specific effects of these metabolites at the cellular level (Olson, 2000 #87; Charlier et al 2005; Cusack, 1993 Mushlin et al 1993). Several of these studies used supraclinical concentrations of the metabolites (Olson et al 1988; Mushlin et al 1993; Boucek et al 1987; Olson et al 1988) and many more studies focus on redox based mechanisms (Davies et al., 1983; Cole et al., 2006; Kim et al 2006; Bast et al., 2007; Berthiaume and Wallace, 2007 and reviewed in Minotti et al., 2004 and Simunek et al., 2009). The results presented in this chapter show for the first time that even short-term exposure of cardiomyocytes to doxOL has a significant impact on Ca^{2+} handling and contractility.

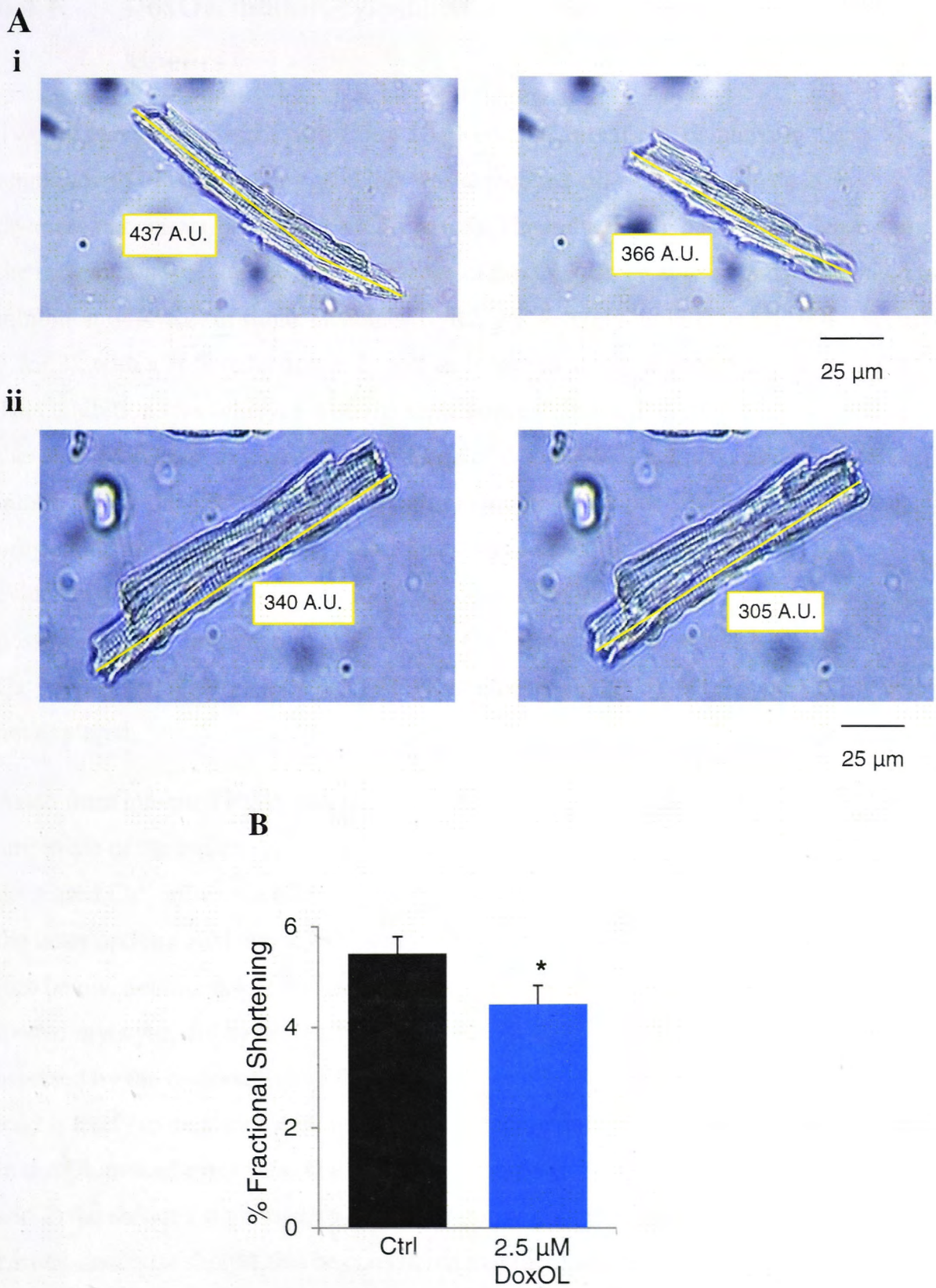

Figure 6.5 – DoxOL reduces myocyte contractility. (**A**) Representative images showing **(i)** untreated and **(ii)** doxOL treated myocytes in their most contracted (systole) and most dilated (diastole) states. Measurements are in arbitrary units (A.U.). (**B**) Average data for % fractional shortening of control myocytes and myocytes treated with 2.5 µM doxOL. Numbers in bars are n numbers for each set of data. Asterisk (*) indicates a significant difference between control and 2.5 µM doxOL treated myocytes.

6.4.1. DoxOL inhibits cytosolic Ca^{2+} transient amplitude and kinetics

Twenty min pre-treatment with 2.5 or 10 μM doxOL significantly inhibited the amplitude of SR Ca^{2+} release, and this was associated with an approximate 20% decrease in contractility (Figures 6.2A & 6.5). The reduction in peak Ca^{2+} release and the increase in time to peak in the presence of doxOL, can be at least partly attributed to inhibition of RyR2. In single channels, RyR2 was severely inhibited by doxOL (Section 3.3.3.2), with a 76% reduction in P_o and an impaired ability to respond to luminal Ca^{2+}. This inhibition was achieved with the same concentrations of doxOL to those used in this chapter. Although lower concentrations of doxOL (0.01 – 1 μM) can effectively inhibit RyR2, the effects of these on cardiomyocytes were not explored in the current project due to time constraints. Nevertheless, these experiments provide the first evidence that doxOL can impact RyR2 function in an intact cardiomyocyte system. It is possible that the prolongation of the twitch Ca^{2+} transient decline was due to diminished Ca^{2+} dependent inactivation via LTCC (Kubalova et al., 2005), but this possibility was not explored.

Aside from inhibited RyR2 function, other factors could account for the reduced amplitude of the twitch Ca^{2+} transient, including a depleted SR Ca^{2+} load and a decreased Ca^{2+} influx via LTCC (Bassani et al., 1995a; Shannon et al., 2000). Although the latter option could not be explored in the current project due to technical limitations (see below, Section 6.4.4) this aspect could be worth exploring in future work. DoxOL treated myocytes did have significantly lower SR Ca^{2+} loads then control myocytes, as assessed by the response to rapid application of caffeine. Therefore, the reduction in SR load is likely to be a contributing factor to the decreased amplitude of the Ca^{2+} transient in doxOL treated myocytes. The relative contributions of 1) inhibition of RyR2 gating and 2) the reduced store load, to decreased transients cannot be evaluated from the current results. It should also be considered that there is temporal overlap between SR Ca^{2+} release and Ca^{2+} uptake, which may truncate the Ca^{2+} transient amplitude (Bassani et al., 1993). The extent of the truncation may differ between doxOL-treated and untreated cells since Ca^{2+} uptake by both NCX and SERCA2A was inhibited in the presence of doxOL. This effect of doxOL on SERCA2A and NCX would likely cause an underestimation of the inhibitory effect of the drugs on RyR2, since in untreated myocytes SERCA2A and NCX would be able to reduce the Ca^{2+} transient amplitude

more than they do in doxOL treated cells. This could mean that there is actually a greater difference in the amplitude of control and doxOL treated cells than what is reflected by the present data. The ambiguity of these results could be resolved by measuring the initial rate of Ca^{2+} uptake into the SR rather than time to 50% decline from the peak of the Ca^{2+} transient.

6.4.2. Mechanisms of SR load reduction

Despite a reduction in twitch transient Ca^{2+} release and in NCX activity, which both could be expected to increase Ca^{2+} load, the SR load in cardiomyocytes was decreased by ~30% in doxOL pre-treated cells. There are several potential explanations for this finding, including inhibition of SERCA2A mediated Ca^{2+} uptake and increased RyR2 release during diastole. These possibilities are discussed below.

DoxOL, but not doxorubicin, was shown to inhibit SERCA2A mediated Ca^{2+} uptake in SR vesicles at concentrations as low as 0.01 μM (see Section 3.3.5/4.2.4). This was attributed to doxOL induced oxidation of SERCA2A thiol residues. Results in the current chapter show that that the time to 50% decay of the Ca^{2+} transient was prolonged in doxOL treated myocytes (Section 6.3.1). In an action potential-induced transient, the decay phase is primarily due to Ca^{2+} reuptake via SERCA2A (Bassani et al., 1995b), illustrating that doxOL inhibits SERCA2A function in whole cells. The extent to which this 13% increase in the decay time of the Ca^{2+} transient, contributes to the almost 30% decrease in SR load is unclear.

Another potential mechanism of SR load depletion is increased diastolic Ca^{2+} release. It has been shown that spark and non-spark mediated Ca^{2+} release is a prominent form of Ca^{2+} release via RyR2 and, along with SERCA2A activity, is a primary determinant of the SR Ca^{2+} concentration (Santiago et al., 2010; Zima et al., 2010). Single channel experiments indicated that aside from an initial, transient activation phase, anthracyclines caused severe inhibition of RyR2 P_o (Section 3.3.3 and Hanna et al., 2011). However, those experiments were done under what would be considered early systolic conditions, with 1 μM *cis* (cytoplasmic) Ca^{2+} and 1 mM *trans* (luminal) Ca^{2+}. Single channel experiments conducted with diastolic *cis* and *trans* [Ca^{2+}] would be useful in determining if doxOL can actually increase RyR P_o during diastole. However these will be difficult to perform as previous work in our laboratory and by others has

shown that channel activity is very low under such conditions (Chen et al., 2013), personal communication Prof. Esther Gallant, Muscle Research Group).

It was hypothesised in Section 3.4.3 that inhibition of RyR2 by anthracyclines may lead to Ca^{2+} alternans in whole-cell experiments. Such peak-to-peak variation was only observed in a minority of cells, possibly due the relatively brief and slow pacing protocols used in these experiments compared to other studies where alternans have been prevalent (Diaz *et al.,* 2002; Belevych *et al.,* 2009). Myocytes pre-treated with 2.5 μM or 10 μM doxOL had 60 – 90% higher levels of resting Ca^{2+}, respectively then untreated myocytes (Figure 6.3A) and this was associated with an increase in the percentage of myocytes that exhibited spontaneous Ca^{2+} transients (Figure 6.3B). It is possible that both the spontaneous activity and the increased levels of resting Ca^{2} were due to doxOL induced inhibition of NCX activity, rather than enhanced diastolic Ca^{2+} release (Figure 6.4C). More quantitative assessments of SR Ca^{2+} leak and I_{NCX} in the presence of doxOL would provide valuable insight into these prospective mechanisms. DoxOL has been reported to inhibit the Na/K ATPase, though the effect has not been well characterized (Boucek *et al.,* 1989). Inhibiting the Na/KATPase would increase the intracellular [Na^{+}] and potentially slow the rate of Na^{+}:Ca^{2+} exchange by NCX (Pogwizd *et al.,* 2001). However, this mechanism would also be predicted to increase the SR Ca^{2+} load and is therefore unlikely to be significant in the present experiments, since the SR load was decreased in doxOL treated myocytes (Section 6.3.2). Any doxOL-induced change in the backflux of Ca^{2+} via SERCA2A (which could also deplete store load (Shannon et al., 2002)) was not investigated. From the data obtained in this chapter, it can be hypothesised that the decrease in store load with doxOL pretreatment is caused by a combination of increased diastolic Ca^{2+} release and impaired Ca^{2+} uptake by SERCA2A.

6.4.3. Limitations

Due to time and technical constraints certain aspects of doxOL's effect on intact myocytes could not be tested, leaving several questions to be answered. One limitation was that myocytes were not voltage clamped, hence LTCC current was not examined. Reduced Ca^{2+} influx via LTCC could contribute to the decreased amplitude of the Ca^{2+} transient, as there would be less Ca^{2+} to activate RyR2. This may also result in a prolonged time to peak Ca^{2+} release. Although no direct effects of anthracyclines on the

LTCC have been reported previously, investigating this interaction may be beneficial in the future.

The results presented in this chapter also show that doxOL can promote diastolic Ca^{2+} release and increase the cytoplasmic [Ca^{2+}], an effect that would be expected to promote arrhythmogenesis. Therefore, another benefit of voltage clamping the myocytes would be the ability to detect DADs and EADs. At present there are no studies investigating doxOL-induced arrhythmogenesis at the cellular level. Thus, further experiments testing anthracyclines on voltage clamped myocytes would provide valuable information on the mechanism of anthracycline cardiotoxicity.

Experiments detailed in this chapter were conducted on myocytes that were pretreated for 20 min with either 2.5 or 10 μM doxOL and paced at a frequency of 0.5 Hz. These drug concentrations were chosen as they were used in single channel experiments. Given the reported hydrophobicity of anthracyclines (Park *et al.,* 2005) and the timeframe of drug-induced effects in chapters 3 – 5, it is likely that a 20 min preincubation period is sufficient to allow the drug to equilibrate across the sarcolemmal membrane. However, it is possible that the 20 min incubation did not allow doxOL to equilibrate in certain subcellular compartments. Experimentation using a greater range of drug concentrations and preincubation times would provide a more thorough characterization of the concentration dependent effects of anthracyclines. Potential arrhythmogenic mechanisms may also be revealed by exploring different pacing frequencies.

It has repeatedly been shown that doxorubicin and doxOL increase cellular ROS formation (Kim et al., 2006; Sawyer et al., 2010; Sag et al., 2011). Therefore it is highly likely that the effects of doxOL reported in this chapter result from both ROS-dependent and ROS-independent mechanisms. Some insight can be gained with the use of modification specific reducing agents. It is possible to distinguish between disulphide formation, *S*-nitrosylation and *S*-glutathionylation (Aracena-Parks et al., 2006; Terentyev et al., 2008), all of which may be induced by doxOL treatment in cardiomyocytes. However, the results in Chapter 4 of this thesis demonstrate that doxOL can directly modify the thiol residues of RyR2 and SERCA2A independent of ROS, most likely by promoting disulphide formation. Therefore, distinguishing between disulphide formation that is promoted by (A) doxOL induced ROS formation and (B) a direct interaction between doxOL and RyR2 and SERCA2A thiols may not be possible.

Nevertheless valuable mechanistic insight could be gained by defining ROS-dependent and ROS-independent effects of anthracycline in cardiomyocytes.

6.5. Conclusion

The results presented in this chapter provide novel information on the cellular mechanisms of anthracycline-induced cardiotoxicity. For the first time, it has been demonstrated that clinically relevant concentrations of the doxorubicin metabolite, doxOL, can induce Ca^{2+} handling abnormalities at the whole cell level. These changes affected cardiomyocyte contractility and, although membrane potential wasn't measured, it is likely that the aberrant Ca^{2+} release induced by doxOL would be arrhythmogenic. While more quantitative measures of some aspects of doxOL-induced dysfunction are necessary, the current findings confirm that doxOL can perturb Ca^{2+} homeostasis in intact cardiomyocytes. Further exploration of doxOL induced impairment of the contractile and electrical components of cardiomyocyte function may provide valuable insight into the clinical manifestation of anthracycline induced cardiac dysfunction.

Chapter Seven

General Discussion

7.1. Summary

The work presented in this thesis represents the first in-depth characterization of the anthracycline doxorubicin and it metabolite, doxOL on Ca^{2+} handling in cardiomyocytes. The principle findings were as follows:

1. Anthracyclines modulate RyR2 channel activity.
   Doxorubicin, daunorubicin and their primary metabolites were found to cause a pronounced increase in RyR2 P_o. With higher concentrations of the parent compounds and with all concentrations of the metabolites, channel activation was followed by sustained inhibition.

2. Anthracycline-induced activation and inhibition are mediated by different mechanisms.
   Anthracycline-induced activation is reversible by washout, suggestive of a ligand binding mechanism. In contrast, RyR2 inhibition was not reversed by washout but was preventable with DTT and NEM, suggesting an oxidative mechanism. These thiol modifying reagents had no effect on anthracycline-induced activation of RyR2

3. CSQ2 has a role in the RyR2 response to changes in luminal Ca^{2+}.
   Selective dissociation of CSQ2 caused RyR2 single channels to become more sensitive to activation by luminal Ca^{2+} compared to native channels.

4. Redox active agents modulate RyR2 luminal Ca^{2+} sensitivity,
   Pre-treatment with reducing agents and pre-treatment with oxidizing agents had different effects on the RyR2 response to luminal Ca^{2+}. DTT exposure, and therefore promotion of unmodified thiols, caused RyR2 activity to decrease as the luminal $[Ca^{2+}]$ increased. Conversely, oxidation of RyR2 thiols by 4,4'-DTDP caused channels to have a higher P_o but a dampened response to activation by luminal Ca^{2+}.

5. DoxOL abolishes the luminal Ca^{2+} response of RyR2 via an interaction with CSQ2

   DoxOL treatment abolished normal response of RyR2 to changes in the luminal [Ca^{2+}]. This response was restored when CSQ2 was dissociated from doxOL-treated RyR2.

6. DoxOL inhibits SERCA2A function by thiol oxidation

   Incubation of SR vesicles with doxOL, but not doxorubicin, decreased the Ca^{2+} uptake rate. With DTT pre-treatment, doxOL actually enhanced Ca^{2+} uptake. Thus, doxOL inhibits SERCA2A via thiol oxidation but can also activate SERCA2A, most likely by a ligand binding interaction. Inhibition of SERCA2A is also evident in intact cardiomyocytes, where there was an increase in the decline of the cytoplasmic Ca^{2+} transient.

7. DoxOL alters whole cell Ca^{2+} signalling and reduces cardiomyocyte contractility.

   In adult mouse cardiomyocytes, doxOL pre-treatment reduced the amplitude of Ca^{2+} transients and prolonged the time to peak and decay time compared to untreated myocytes. DoxOL treated myocytes also had a reduced SR Ca^{2+} load, impaired NCX function, and a higher cytoplasmic [Ca^{2+}] then control myocytes. These effects were likely to cause the aberrant diastolic Ca^{2+} release and reduced contractile function exhibited by doxOL treated myocytes.

DoxOL was found to interact with multiple proteins that are important for SR Ca^{2+} handling, including RyR2, SERCA2A and CSQ2.

7.2. Consideration of whole cell Ca^{2+} handling

Intact cardiomyocytes treated with doxOL showed reduced Ca^{2+} transients, a decrease in store load and prolonged decay time of both the twitch transient and caffeine-induced transient, suggesting impaired SERCA2A and NCX function, respectively. These alterations in myocyte Ca^{2+} handling were consistent with the effects of doxOL identified in the isolated single channels and in SR vesicles. These functional effects in the isolated preparations included changes in RyR2 channel gating, SERCA function

and response of the channel to luminal Ca^{2+}. The long-term, sustained effect of doxOL in each of these cases was inhibitory and therefore consistent with the effect of doxOL in the whole cell in dampening Ca^{2+} signalling and impairing contractile function.

The changes in Ca^{2+} transient kinetics coexisted with an increase in spontaneous Ca^{2+} release and an increase in resting Ca^{2+}. The findings suggest that doxOL causes RyR2 to be more active during diastole than untreated channels. This is in contrast to the results of the single channel experiments, as the same concentration and incubation time with doxOL caused pronounced inhibition of RyR2. It must be remembered though that the majority of single channel studies were done under conditions more likely to be encountered during systole (i.e. with 1 μM *cis* Ca^{2+} and 1 mM *trans* Ca^{2+}). Although the measurements of RyR2 luminal Ca^{2+} response did temporarily use 0.1 mM *trans* Ca^{2+}, these were still done in the presence of 1 μM *cis* Ca^{2+} and so are not a true representation of diastolic conditions where cytoplasmic Ca^{2+} drops to ~100nM (Bers, 2008). Future experiments using 1 μM *cis* Ca^{2+} and 0.1 mM *trans* Ca^{2+} would be a more accurate way of characterizing the effects of anthracyclines on RyR2 under diastolic conditions. As discussed in Chapter 6 however, experiments conducted at these [Ca^{2+}] are likely to have low levels of activity making it difficult to accurately measure P_o.

Based on the finding that doxOL a) inhibited RyR2 and b) abolished luminal Ca^{2+} sensing it would be expected that the effects of anthracyclines in whole cell systems would be arrhythmogenic. There are studies identifying RyR2 inhibition (Diaz et al., 2002; Bround et al., 2012) or a loss of luminal Ca^{2+} sensing (Thomas et al., 2004; Jiang et al., 2007; Qin et al., 2008) as a factor in arrhythmogenic Ca^{2+} release. This phenomenon was most quantitatively explored in intact cardiomyocytes by Diaz and colleagues (2002). Inhibition of RyR2 by tetracaine caused spatial and temporal desynchronisation of SR Ca^{2+} release and prolonged the rise and decay of the Ca^{2+} transients (Diaz et al., 2002). In the current study, spontaneous Ca^{2+} release occurred more frequently in doxOL treated cells (2.5 μM) then in control cells. These spontaneous Ca^{2+} transients would be expected to cause afterdepolarisations (Pogwizd and Bers, 2004), however, due to technical limitations it was not possible to monitor changes in membrane potential. It was observed however, that doxOL inhibited NCX function, as indicated by the prolonged decay of the caffeine transient. Therefore it is more likely that anthracyclines would induce EADs rather than DADs, since the latter are more often associated with enhanced NCX function (Pogwizd et al., 2001).

However, the present results do not exclude either mechanism. Further explorations of these processes may give valuable insight into the mechanisms of anthracycline induced arrhythmogenesis.

The spontaneous Ca^{2+} transients and decreased amplitude and kinetics of the twitch transient could be due to altered RyR2 gating or the abolition of luminal Ca^{2+} sensing. Therefore it is difficult to ascertain whether the loss of luminal Ca^{2+} sensing caused by doxOL in single channels was translated to the whole cell environment. This would best be explored by simultaneous quantitative measurement of the SR Ca^{2+} load and cytoplasmic Ca^{2+} release in intact myocytes to determine if there was a relationship between RyR2 function (e.g. fractional release or propensity for spontaneous Ca^{2+} release) and the SR load, as measured in (Shannon et al., 2000, 2002; Jiang et al., 2005; Guo et al., 2007). The absence of such a relationship may indicate that doxOL could effectively block RyR2 luminal Ca^{2+} sensitivity in a cellular environment. While such measurements have been used to confirm an increase in luminal Ca^{2+} sensitivity (Guo et al., 2007), there are few studies that have quantified such changes in a loss-of-function situation (Jiang et al., 2007). This can be attributed to the prevalence of gain-of-function mutations associated with arrhythmia, sudden cardiac death and heart failure, compared to loss-of-function mutations (reviewed in (Gomez and Richard, 2004).

Hence, the mechanisms responsible for loss of luminal Ca^{2+} sensing remain ambiguous. In one example, RyR2 channels carrying a mutation associated with catecholaminergic idiopathic ventricular fibrillation had lost the ability to respond to activation by luminal, but not cytoplasmic Ca^{2+} (Jiang et al., 2007). The mutated residue (A4860G) was located in the pore inner helix, a region associated with activation and gating of RyR2. In this case, the loss of luminal Ca^{2+} sensing was attributed to the location of the mutated residue. The effects of anthracyclines on luminal Ca^{2+} sensing, on the other hand, could be attributed to an interaction between doxOL and CSQ2. This result underlines the importance of CSQ2 in determining the characteristics of the RyR2 response to changes in luminal Ca^{2+}. How the CSQ2 interaction abolished the ability of RyR2 to be activated by luminal Ca^{2+} is unclear from the present experiments. It is possible that doxOL modifies the interaction between CSQ2 and another protein like triadin and junctin, preventing the communication of the luminal $[Ca^{2+}]$ to RyR2. Disruption to this communication pathway was suggested by Qin and colleagues (2008) to account for the loss of luminal Ca^{2+} sensitivity in RyR2 associated with a CPVT-

linked CSQ2 mutant. That CSQ2 null myocytes (Knollmann et al., 2006) and CSQ2 stripped channels (this study, and (Qin et al., 2008) show evidence of luminal Ca^{2+} sensitivity but that an interaction between doxOL and CSQ2, and a CSQ2 mutant (Qin et al., 2008) can abolish luminal Ca^{2+} sensitivity demonstrates the necessity of optimal protein function and emphasizes the complexity of the luminal Ca^{2+} sensing process.

7.3. Anthracyclines and protein modifications

7.3.1. Thiol modification

It is evident from the results of Chapters 4 and 5 that anthracycline-induced oxidation causes substantial modification of SR Ca^{2+} handling, inhibiting both RyR2 and SERCA2A function. It should be considered what the consequences of anthracycline induced ROS and RNS formation might be in the intact cell. The effects characterized in this thesis as a result of thiol modification by anthracyclines are likely to (a) be additive with additional ROS and RNS-induced effects and (b) could constitute the cardiotoxicity pathway in patients treated with dexrazoxane to suppress oxidative dysfunction. ROS induced thiol modifications including *S*-glutathionylation and *S*-nitrosylation promote arrhythmogenesis and heart failure via RyR2 dysregulation (Yano et al., 2005b; Belevych et al., 2009; Donoso et al., 2011b). Further work is needed to elucidate the precise effects of anthracycline-induced ROS/RNS formation on cardiomyocyte Ca^{2+} handling. This includes determining what reactive species are produced in response to anthracycline exposure, the site of production, the specific targets of these reactive species and the functional outcome of these interactions. The compounded dysregulation induced by production of ROS and RNS may be a significant cause of the cardiotoxic side effects observed in patients treated with anthracyclines and warrants better characterization.

Although doxOL could enhance SERCA2A Ca^{2+} uptake, this effect was only evident when DTT pre-treatment blocked doxOL-induced oxidation of SERCA2A. Therefore, physiologically it would be expected that doxOL's inhibitory effect would mask any activation. This is supported by the finding that in cardiomyocytes, doxOL pretreatment prolonged the decay of the twitch Ca^{2+} transient, a measure of SERCA2A function (Bassani et al., 1995b).

7.3.2. Anthracyclines and phosphorylation

RyR2 is also susceptible to phosphorylation by PKA and CaMKII. Evidence from the Cardiac and Skeletal Muscle Proteomics Group shows that doxorubicin treated mice exhibit a significantly higher level of phosphorylation at serine residues 2808 and 2814 (personal communication, Dr Nicole Beard) than untreated mice. While the functional role of anthracycline-induced RyR2 phosphorylation is unknown, the detrimental effects of hyperphosphorylation in other cardiac pathologies is well documented. In several models of heart failure, sudden cardiac death and arrhythmia, RyR2 is hyperphosphorylated, usually due to enhanced or chronic β-adrenergic stimulation. Under such conditions RyR2 exhibits a heightened response to Ca^{2+}, increased diastolic leak and spontaneous Ca^{2+} waves (Yano et al., 2005a; Belevych et al., 2009; Donoso et al., 2011a). The molecular mechanism underlying phosphorylation-induced RyR2 dysfunction is controversial, hypothesized to involve either a dissociation of FKBP (Marx et al., 2000), or a decrease in the threshold for diastolic Ca^{2+} release (Jiang et al., 2005; Venetucci et al., 2007; Curran et al., 2010). Recently it has been suggested that RyR2 oxidation and phosphorylation co-exist, together promoting RyR2 dysfunction. Shan and colleagues (2010) found that the oxidation state influenced the extent to which PKA phosphorylation was able to dissociate FKBP and cause subsequent spontaneous Ca^{2+} release. In another study it was found that phosphorylation and oxidation were involved at successive stages of heart failure (Belevych et al., 2011). Interestingly, CaMKII is itself activated via oxidation in heart failure (Erickson *et al.,* 2008) and in cardiomyocytes exposed to doxorubicin (Sag *et al.,* 2011).

Observations of concurrent or successive RyR2 phosphorylation and/or oxidation are consistent with the suggestion that alteration of RyR2 P_o alone, by either oxidation or phosphorylation for example, may not necessarily induce arrhythmogenic Ca^{2+} release (Venetucci et al., 2007; Chelu et al., 2009). In a normal, healthy cardiomyocyte, the increase in P_o should lead to a decrease in SR Ca^{2+} content and thus, reduce P_o to lower levels (Venetucci et al., 2007). The existence of this autoregulation implies that changes in RyR2 P_o may not have a drastic effect on cardiac function under physiological conditions. However, it has been suggested that altered RyR2 activity may provide an arrhythmogenic background, which in the presence of an additional insult, could lead to spontaneous Ca^{2+} waves and arrhythmia (Jiang et al., 2007; Venetucci et al., 2007; Chelu et al., 2009; Curran et al., 2010). Additional contributors could include (but are

not limited to) changes in protein expression, thiol oxidation and phosphorylation of RyR2 or SERCA2A, many of which are seen in heart failure (Shannon et al., 2003a; Vest et al., 2005; Curran et al., 2010; Belevych et al., 2011; Shan et al., 2012). An analogous situation may occur in people carrying RyR2 mutations associated with CPVT, who are asymptomatic without the additional trigger of β-adrenergic stimulation. Such an inter-dependence has been named the "double hit concept" (Chelu et al., 2009).

7.3.3. Nitroso-redox balance

There is limited evidence indicating that anthracyclines also perturb NO signalling in the heart via several pathways (Fogli et al., 2004). Doxorubicin-induced cardiac dysfunction has been associated with increased cellular levels of $ONOO^-$, which resulted from doxorubicin-induced upregulation of iNOS (Weinstein et al., 2000; Pacher et al., 2003). It was also found that doxorubicin can interact with eNOS, which promotes redox cycling of the anthracycline quinone moiety with subsequent O_2^- production (Vasquez-Vivar et al., 1997). In the heart a balance exists between nitrosative and oxidative signalling, both of which play important roles in physiological Ca^{2+} signalling. As shown in Figure 1.11, there is crosstalk between these two systems. Superoxide can interact with NO to produce the highly reactive $ONOO^-$ which acts as a potent oxidant. Additionally, excess oxidation may reduce the number of thiols available for *S*-nitrosylation with subsequent changes in protein function (Fogli et al., 2004; Hare, 2004). Thus it is likely that anthracyclines severely disrupt the nitroso-redox balance in the heart by effects either on oxidative or nitrosative signalling, or both.

7.4. Anthracyclines and skeletal muscle

Muscle fatigue is a common occurrence in patients undergoing treatment with chemotherapeutic drugs, including anthracyclines. Fatigue that is induced by chemotherapy differs from general muscle fatigue, in that it is not alleviated by a period of rest and is described as a whole body affliction that is unrelated to physical activity or exertion (Morrow et al., 2002; Gilliam and St Clair, 2011). A review of studies investigating the incidence of fatigue in anthracycline-treated patients found that 47% of

patients described disabling fatigue that prevented normal physical activity (Gilliam and St Clair, 2011). Animal models have consistently found an impairment of skeletal muscle function following doxorubicin administration. These effects include a decrease in maximum specific force, prolonged relaxation time, impaired fractional shortening and severe ultrastructural changes (Doroshow et al., 1985; Gilliam et al., 2009; van Norren et al., 2009; Gilliam and St Clair, 2011; Hydock et al., 2011).

Skeletal muscle fatigue is thought to have many contributing factors. One of the more prominent mechanisms is oxidative stress (Allen et al., 2008; Reid, 2008), and this has been identified as a potential mechanism in anthracycline-induced skeletal muscle fatigue. In animal models, doxorubicin administration increased ROS generation and oxidative protein modifications in skeletal muscle, which were associated with decreased contractile function (Gilliam et al., 2011; Smuder et al., 2011). However, in these studies the increase in oxidative stress coexisted with an increase in the levels of calpain activity (Smuder et al., 2011) and depended on the route of administration, occurring with i.p. but not i.v. dosage (Gilliam et al., 2011). Conversely, overnight incubation of skeletal myotubes with doxorubicin found that the effects of the drug on Ca^{2+} handling were not influenced by oxidative stress (van Norren et al., 2009). These studies highlight a need for an improved understanding of the role of oxidative stress in skeletal muscle dysfunction caused by anthracyclines.

It should be remembered that RyR1 is similarly susceptible to oxidative modifications as RyR2, containing 100 cysteines in total, of which 12 are vulnerable to redox modification (Aracena-Parks et al., 2006). Anthracyclines have indeed been shown to stimulate RyR1 activity (Abramson et al., 1988; Feng et al., 1999; Marinov et al., 2007). In two of these studies, modulation of RyR1 was associated with thiol modification (Feng et al., 1999; Marinov et al., 2007). Thus, it would be surprising if oxidative stress had no influence since, like cardiac muscle, skeletal muscle function can be negatively affected by excess oxidation. Examples of this dysfunction include fatigue and Duchenne Muscular Dystrophy, both of which are thought to be at least partially influenced by pronounced ROS formation (Reid, 2008).

7.5. Future directions

While the work presented in this thesis has made a great contribution to the present knowledge of anthracycline cardiotoxicity, there are still many avenues of research worth exploring. Some of these lead on directly from the results presented here, while others are aspects that were outside the scope of the current project but are related to cardiomyocyte Ca^{2+} handling.

- It is likely that the oxidative modifications observed in single channel studies are ROS/RNS independent, while the results in cardiac myocytes are a combination of ROS/RNS -dependent and ROS/RNS-independent effects. Mechanistic insight could be gained by determining the relative importance of each in the whole cell environment, as well as the sites of ROS (and RNS) production and the specific targets of these reactive species.
- In Chapter 5 it was demonstrated that redox agents significantly influence RyR2 activation by luminal Ca^{2+}. However, these results were obtained with high concentrations of either oxidizing or reducing agents. Experiments in the Muscle Research Group laboratory are currently underway to determine the luminal Ca^{2+} sensitivity in the presence of physiological and pathological redox potentials set by relevant amounts of the glutathione redox buffer system. These experiments will yield important information on RyR2 Ca^{2+} handling and will aid in our understanding of changes in Ca^{2+} signalling that occur in cardiac disease.
- DoxOL increased the percentage of myocytes displaying spontaneous Ca^{2+} transients and increased the resting cytoplasmic [Ca^{2+}]. These findings suggest that doxOL may have stimulatory effect on RyR2 at a diastolic cytoplasmic [Ca^{2+}]. As detailed in Section 7.1, assessing the impact of doxOL on single channel activity using diastolic [Ca^{2+}] in the *cis* and *trans* solutions will clarify the effect of anthracyclines on diastolic Ca^{2+} handling, if such experiments are possible (see previous comments).
- The arrhythmogenic effects of anthracyclines could be better understood using voltage clamped cardiomyocytes. In the current project, technical limitations prevented measurement of changes in sarcolemmal membrane potential upon myocyte stimulation. Thus, while it can be predicted that the spontaneous Ca^{2+} transients would be arrhythmogenic, such events were not recorded. It would also

be beneficial to experiment with different pacing frequencies as the propensity for arrhythmogenic activity can increase as pacing frequency in accelerated (Liu et al., 2011).

- Anthracyclines have been shown to activate calpains, Ca^{2+} dependent proteases which degrade multiple targets in striated muscle. Two proteins that have been shown to be affected following doxorubicin-induced calpain activation include titin (Lim et al., 2004) and dystrophin (Campos et al., 2011). Calpain induced proteolysis of titin was associated with severe disruption of myofilament ultrastructure and cellular necrosis, (Lim et al., 2004) whilst delocalization of dystrophin occurred with left ventricular contractile impairment (Campos et al., 2011). In skeletal muscle, calpain activation is implicated in exercise–induced muscle injury (Belcastro et al., 1998), muscle atrophy (Bartoli and Richard, 2005) and in muscular dystrophies (Richard et al., 1995; Tidball and Spencer, 2000). Furthermore, it has recently been shown that calpain activation degrades junctophilin, a protein thought to be important for triad formation in both skeletal and cardiac muscle (Murphy et al., 2013). These studies suggest that anthracycline-induced calpain activation (in either skeletal or cardiac muscle) could have as yet unrecognized detrimental effects on muscle function.
- Finally, preliminary evidence from the Cardiac and Skeletal Muscle Proteomics Group indicates that anthracyclines can increase RyR2 phosphorylation at S2808 and S2814 and reduce FKBP association with RyR2 (personal communication, Dr Nicole Beard). Either individually or in combination, these effects have been implicated in various forms of cardiac pathology (Marx et al., 2000; Wehrens et al., 2003; Shan et al., 2012), however neither phosphorylation nor FKBP dissociation has been implicated in the effects of anthracyclines on the heart. Further investigation of these modifications in anthracycline-induced cardiotoxicity will give valuable new mechanistic insight.

7.6. Conclusion

This project has provided novel information on the cellular mechanisms underlying anthracycline-induced cardiotoxicity. Over the course of this thesis, the focus progressed from the effects of the drugs on single RyR2 channels and on the SERCA2A pump, to the sensitivity of the channel to luminal Ca^{2+}. Finally, intact cardiomyocytes

were used to assess the effect of doxOL in a whole cell environment. Hence the drugs were tested in systems of increasing complexity, from the single channel, to the SR, to the intact cardiomyocyte. In each case the drugs dampened proper Ca^{2+} movement which promoted aberrant, spontaneous Ca^{2+} release and reduced myocyte contractile function. The results, while representing acute effects of the drugs, are consistent with the clinical manifestation of anthracycline-induced cardiotoxicity, which include reduced contractility and arrhythmogenesis (Barrett-Lee et al., 2009; Menna et al., 2012).

In the course of the project important new information regarding mechanisms of physiological SR Ca^{2+} handling has been revealed. Of particular interest is the role of CSQ2 and redox modifications on the luminal Ca^{2+} response of RyR2. These findings shed important light on factors affecting RyR2 regulation by luminal Ca^{2+}, building on the information already gathered in recent years by others in the field. Knowledge of this aspect of cardiac muscle physiology may prove to be important in understanding mechanisms of heart failure, sudden cardiac death and arrhythmia and in the subsequent design of treatments for these and other cardiac pathologies.

While there are many aspects of the cellular and whole organ effects of the drugs to be elucidated, the present project is the most in-depth characterization of the effects of anthracyclines on RyR2 and SR Ca^{2+} handling to date. Of particular importance are the new details regarding the effects of the metabolite, doxOL. This information may be used for future drug design and the testing of better targeted co-treatments which are more beneficial in preventing the devastating effects of anthracyclines on the heart while allowing their continued use as some of the most efficacious chemotherapeutic drugs yet discovered.

References

Abramson, J.J., E. Buck, G. Salama, J.E. Casida, and I.N. Pessah. 1988. Mechanism of anthraquinone-induced calcium release from skeletal muscle sarcoplasmic reticulum. *J Biol Chem.* 263:18750-18758.

Abramson, J.J., and G. Salama. 1989. Critical sulfhydryls regulate calcium release from sarcoplasmic reticulum. *J Bioenerg Biomembr.* 21:283-294.

Adachi, T., R.M. Weisbrod, D.R. Pimentel, J. Ying, V.S. Sharov, C. Schoneich, and R.A. Cohen. 2004. S-Glutathiolation by peroxynitrite activates SERCA during arterial relaxation by nitric oxide. *Nat Med.* 10:1200-1207.

Aghdasi, B., M.B. Reid, and S.L. Hamilton. 1997. Nitric oxide protects the skeletal muscle Ca2+ release channel from oxidation induced activation. *J Biol Chem.* 272:25462-25467.

Ahern, G.P., P.R. Junankar, and A.F. Dulhunty. 1994a. Single channel activity of the ryanodine receptor calcium release channel is modulated by FK-506. *FEBS Lett.* 352:369-374.

Ahern, G.P., P.R. Junankar, and A.F. Dulhunty. 1994b. Single channel activity of the ryanodine receptor calcium release channel is modulated by FK-506. *FEBS letters.* 352:369-374.

Ahern, G.P., P.R. Junankar, and A.F. Dulhunty. 1997. Subconductance states in single-channel activity of skeletal muscle ryanodine receptors after removal of FKBP12. *Biophys J.* 72:146-162.

Ai, X., J.W. Curran, T.R. Shannon, D.M. Bers, and S.M. Pogwizd. 2005. Ca2+/calmodulin-dependent protein kinase modulates cardiac ryanodine receptor phosphorylation and sarcoplasmic reticulum Ca2+ leak in heart failure. *Circ Res.* 97:1314-1322.

Airoldi, M., D. Amadori, S. Barni, S. Cinieri, S. De Placido, A. Di Leo, A. Gennari, S. Iacobelli, M.T. Ionta, V. Lorusso, M. Lotrionte, P. Marchetti, R. Mattioli, G. Minotti, P. Pronzato, G. Rosti, C.A. Tondini, and A. Veronesi. 2011. Clinical activity and cardiac tolerability of non-pegylated liposomal doxorubicin in breast cancer: a synthetic review. *Tumori.* 97:690-692.

Alcalai, R., H. Wakimoto, M. Arad, D. Planer, T. Konno, L. Wang, J.G. Seidman, C.E. Seidman, and C.I. Berul. 2011. Prevention of ventricular arrhythmia and calcium dysregulation in a catecholaminergic polymorphic ventricular tachycardia mouse model carrying calsequestrin-2 mutation. *J Cardiovasc Electrophysiol.* 22:316-324.

Allen, D.G., and J.C. Kentish. 1985. The cellular basis of the length-tension relation in cardiac muscle. *J Mol Cell Cardiol.* 17:821-840.

Allen, D.G., G.D. Lamb, and H. Westerblad. 2008. Skeletal muscle fatigue: cellular mechanisms. *Physiol Rev.* 88:287-332.

Altschafl, B.A., D.A. Arvanitis, O. Fuentes, Q. Yuan, E.G. Kranias, and H.H. Valdivia. 2011. Dual role of junctin in the regulation of ryanodine receptors and calcium release in cardiac ventricular myocytes. *J Physiol.* 589:6063-6080.

Amador, F.J., P.B. Stathopulos, M. Enomoto, and M. Ikura. 2013. Ryanodine receptor calcium release channels: lessons from structure-function studies. *Febs J.*

Aracena-Parks, P., S.A. Goonasekera, C.P. Gilman, R.T. Dirksen, C. Hidalgo, and S.L. Hamilton. 2006. Identification of cysteines involved in S-nitrosylation, S-glutathionylation, and oxidation to disulfides in ryanodine receptor type 1. *J Biol Chem.* 281:40354-40368.

Arai, M., N.R. Alpert, D.H. MacLennan, P. Barton, and M. Periasamy. 1993. Alterations in sarcoplasmic reticulum gene expression in human heart failure. A possible mechanism for alterations in systolic and diastolic properties of the failing myocardium. *Circ Res.* 72:463-469.

Asmis, R., Y. Wang, L. Xu, M. Kisgati, J.G. Begley, and J.J. Mieyal. 2005. A novel thiol oxidation-based mechanism for adriamycin-induced cell injury in human macrophages. *Faseb J.* 19:1866-1868.

Balshaw, D.M., L. Xu, N. Yamaguchi, D.A. Pasek, and G. Meissner. 2001. Calmodulin binding and inhibition of cardiac muscle calcium release channel (ryanodine receptor). *J Biol Chem.* 276:20144-20153.

Barrett-Lee, P.J., J.M. Dixon, C. Farrell, A. Jones, R. Leonard, N. Murray, C. Palmieri, C.J. Plummer, A. Stanley, and M.W. Verrill. 2009. Expert opinion on the use of anthracyclines in patients with advanced breast cancer at cardiac risk. *Ann Oncol.* 20:816-827.

Bartoli, M., and I. Richard. 2005. Calpains in muscle wasting. *Int J Biochem Cell B.* 37:2115-2133.

Baruscotti, M., G. Bottelli, R. Milanesi, J.C. DiFrancesco, and D. DiFrancesco. 2010. HCN-related channelopathies. *Pflugers Arch.* 460:405-415.

Bassani, J.W., R.A. Bassani, and D.M. Bers. 1993. Twitch-dependent SR Ca accumulation and release in rabbit ventricular myocytes. *Am J Physiol.* 265:C533-540.

Bassani, J.W., W. Yuan, and D.M. Bers. 1995a. Fractional SR Ca release is regulated by trigger Ca and SR Ca content in cardiac myocytes. *Am J Physiol.* 268:C1313-1319.

Bassani, R.A., J.W. Bassani, and D.M. Bers. 1992. Mitochondrial and sarcolemmal Ca2+ transport reduce [Ca2+]i during caffeine contractures in rabbit cardiac myocytes. *J Physiol.* 453:591-608.

Bassani, R.A., J.W. Bassani, and D.M. Bers. 1995b. Relaxation in ferret ventricular myocytes: role of the sarcolemmal Ca ATPase. *Pflugers Arch.* 430:573-578.

Bast, A., H. Kaiserova, G.J. den Hartog, G.R. Haenen, and W.J. van der Vijgh. 2007. Protectors against doxorubicin-induced cardiotoxicity: flavonoids. *Cell biology and toxicology.* 23:39-47.

Beard, N.A., D.R. Laver, and A.F. Dulhunty. 2004. Calsequestrin and the calcium release channel of skeletal and cardiac muscle. *Prog Biophys Mol Biol.* 85:33-69.

Beard, N.A., M.M. Sakowska, A.F. Dulhunty, and D.R. Laver. 2002. Calsequestrin is an inhibitor of skeletal muscle ryanodine receptor calcium release channels. *Biophys J.* 82:310-320.

Beard, N.A., L. Wei, S.N. Cheung, T. Kimura, M. Varsanyi, and A.F. Dulhunty. 2008. Phosphorylation of skeletal muscle calsequestrin enhances its Ca2+ binding capacity and promotes its association with junctin. *Cell Calcium.* 44:363-373.

Beard, N.A., L. Wei, and A.F. Dulhunty. 2009. Ca(2+) signaling in striated muscle: the elusive roles of triadin, junctin, and calsequestrin. *Eur Biophys J.* 39:27-36.

Belcastro, A.N., L.D. Shewchuk, and D.A. Raj. 1998. Exercise-induced muscle injury: a calpain hypothesis. *Mol Cell Biochem.* 179:135-145.

Belevych, A.E., D. Terentyev, R. Terentyeva, Y. Nishijima, A. Sridhar, R.L. Hamlin, C.A. Carnes, and S. Gyorke. 2011. The relationship between arrhythmogenesis and impaired contractility in heart failure: role of altered ryanodine receptor function. *Cardiovasc Res.* 90:493-502.

Belevych, A.E., D. Terentyev, S. Viatchenko-Karpinski, R. Terentyeva, A. Sridhar, Y. Nishijima, L.D. Wilson, A.J. Cardounel, K.R. Laurita, C.A. Carnes, G.E. Billman, and S. Gyorke. 2009. Redox modification of ryanodine receptors underlies calcium alternans in a canine model of sudden cardiac death. *Cardiovasc Res.* 84:387-395.

Bers, D. 2001. Excitation-Contraction Coupling and Cardiac Contractile Force. Springer.

Bers, D.M. 1987. Ryanodine and the calcium content of cardiac SR assessed by caffeine and rapid cooling contractures. *Am J Physiol.* 253:C408-415.

Bers, D.M. 2000. Calcium fluxes involved in control of cardiac myocyte contraction. *Circ Res.* 87:275-281.

Bers, D.M. 2002a. Calcium and cardiac rhythms: physiological and pathophysiological. *Circ Res.* 90:14-17.

Bers, D.M. 2002b. Cardiac excitation-contraction coupling. *Nature.* 415:198-205.

Bers, D.M. 2008. Calcium cycling and signaling in cardiac myocytes. *Annu Rev Physiol.* 70:23-49.

Bers, D.M., D.A. Eisner, and H.H. Valdivia. 2003. Sarcoplasmic reticulum Ca2+ and heart failure: roles of diastolic leak and Ca2+ transport. *Circ Res.* 93:487-490.

Bers, D.M., and V.M. Stiffel. 1993. Ratio of ryanodine to dihydropyridine receptors in cardiac and skeletal muscle and implications for E-C coupling. *Am J Physiol.* 264:C1587-1593.

Berthiaume, J.M., and K.B. Wallace. 2007. Adriamycin-induced oxidative mitochondrial cardiotoxicity. *Cell biology and toxicology.* 23:15-25.

Blaustein, M.P., and W.J. Lederer. 1999. Sodium/calcium exchange: its physiological implications. *Physiol Rev.* 79:763-854.

Bode, E.F., S.J. Briston, C.L. Overend, S.C. O'Neill, A.W. Trafford, and D.A. Eisner. 2011. Changes of SERCA activity have only modest effects on sarcoplasmic reticulum Ca2+ content in rat ventricular myocytes. *J Physiol.* 589:4723-4729.

Boncompagni, S., M. Thomas, J.R. Lopez, P.D. Allen, Q. Yuan, E.G. Kranias, C. Franzini-Armstrong, and C.F. Perez. 2012. Triadin/Junctin double null mouse reveals a differential role for Triadin and Junctin in anchoring CASQ to the jSR and regulating Ca(2+) homeostasis. *PLoS One.* 7:e39962.

Boucek, R.J., Jr., D.A. Dodd, J.B. Atkinson, N. Oquist, and R.D. Olson. 1997. Contractile failure in chronic doxorubicin-induced cardiomyopathy. *J Mol Cell Cardiol.* 29:2631-2640.

Boucek, R.J., Jr., R.D. Olson, D.E. Brenner, E.M. Ogunbunmi, M. Inui, and S. Fleischer. 1987. The major metabolite of doxorubicin is a potent inhibitor of membrane-associated ion pumps. A correlative study of cardiac muscle with isolated membrane fractions. *J Biol Chem.* 262:15851-15856.

Bovo, E., S.L. Lipsius, and A.V. Zima. 2012. Reactive oxygen species contribute to the development of arrhythmogenic Ca(2)(+) waves during beta-adrenergic receptor stimulation in rabbit cardiomyocytes. *J Physiol.* 590:3291-3304.

Bristow, M.R., M.E. Billingham, J.W. Mason, and J.R. Daniels. 1978. Clinical Spectrum of Anthracycline Antibiotic Cardiotoxicity. *Cancer Treat Rep.* 62:873-879.

Brocklehurst, K. 1979. Specific covalent modification of thiols: applications in the study of enzymes and other biomolecules. *International Journal of Biochemistry.* 10:259-274.

Brooks, S.P., and K.B. Storey. 1992. Bound and determined: a computer program for making buffers of defined ion concentrations. *Anal Biochem.* 201:119-126.

Bround, M.J., P. Asghari, R.B. Wambolt, L. Bohunek, C. Smits, M. Philit, T.J. Kieffer, E.G. Lakatta, K.R. Boheler, E.D. Moore, M.F. Allard, and J.D. Johnson. 2012. Cardiac ryanodine receptors control heart rate and rhythmicity in adult mice. *Cardiovasc Res.* 96:372-380.

Burgoyne, J.R., H. Mongue-Din, P. Eaton, and A.M. Shah. 2012. Redox signaling in cardiac physiology and pathology. *Circ Res.* 111:1091-1106.

Burke, B.E., H. Gambliel, R.D. Olson, F.K. Baur, and B.J. Cusack. 2000. Prevention by dexrazoxane of down-regulation of ryanodine receptor gene expression in anthracycline cardiomyopathy in the rat. *Br J Pharmacol.* 131:1-4.

Calderone, A., J. de Champlain, and J.L. Rouleau. 1991. Adriamycin-induced changes to the myocardial beta-adrenergic system in the rabbit. *J Mol Cell Cardiol.* 23:333-342.

Callewaert, G., L. Cleemann, and M. Morad. 1989. Caffeine-induced Ca2+ release activates Ca2+ extrusion via Na+-Ca2+ exchanger in cardiac myocytes. *Am J Physiol.* 257:C147-152.

Campbell, D.L., J.S. Stamler, and H.C. Strauss. 1996. Redox modulation of L-type calcium channels in ferret ventricular myocytes. Dual mechanism regulation by nitric oxide and S-nitrosothiols. *The Journal of general physiology.* 108:277-293.

Campos, E.C., J.L. O'Connell, L.M. Malvestio, M.M. Romano, S.G. Ramos, M.R. Celes, C.M. Prado, M.V. Simoes, and M.A. Rossi. 2011. Calpain-mediated dystrophin disruption may be a potential structural culprit behind chronic doxorubicin-induced cardiomyopathy. *Eur J Pharmacol.* 670:541-553.

Chamberlain, B.K., and S. Fleischer. 1988. Isolation of canine cardiac sarcoplasmic reticulum. *Methods Enzymol.* 157:91-99.

Charlier, H.A., Jr., R.D. Olson, C.M. Thornock, W.K. Mercer, D.R. Olson, T.S. Broyles, D.J. Muhlestein, C.L. Larson, B.J. Cusack, and S.E. Shadle. 2005. Investigations of calsequestrin as a target for anthracyclines: comparison of functional effects of daunorubicin, daunorubicinol, and trifluoperazine. *Molecular pharmacology*. 67:1505-1512.

Chelu, M.G., S. Sarma, S. Sood, S. Wang, R.J. van Oort, D.G. Skapura, N. Li, M. Santonastasi, F.U. Muller, W. Schmitz, U. Schotten, M.E. Anderson, M. Valderrabano, D. Dobrev, and X.H. Wehrens. 2009. Calmodulin kinase II-mediated sarcoplasmic reticulum Ca2+ leak promotes atrial fibrillation in mice. *J Clin Invest*. 119:1940-1951.

ChemIDplus. Daunorubicinol. *In*. U.S. National Library of Medicine, Bethesda.

Chen, H., G. Valle, S. Furlan, A. Nani, S. Gyorke, M. Fill, and P. Volpe. 2013. Mechanism of calsequestrin regulation of single cardiac ryanodine receptor in normal and pathological conditions. *The Journal of general physiology*. 142:127-136.

Chen, Y., J.T. Saari, and Y.J. Kang. 1994. Weak antioxidant defenses make the heart a target for damage in copper-deficient rats. *Free Radic Biol Med*. 17:529-536.

Cheng, H., W.J. Lederer, and M.B. Cannell. 1993. Calcium sparks: elementary events underlying excitation-contraction coupling in heart muscle. *Science*. 262:740-744.

Cherednichenko, G., A.V. Zima, W. Feng, S. Schaefer, L.A. Blatter, and I.N. Pessah. 2004. NADH oxidase activity of rat cardiac sarcoplasmic reticulum regulates calcium-induced calcium release. *Circ Res*. 94:478-486.

Chopra, N., P.J. Kannankeril, T. Yang, T. Hlaing, I. Holinstat, K. Ettensohn, K. Pfeifer, B. Akin, L.R. Jones, C. Franzini-Armstrong, and B.C. Knollmann. 2007. Modest reductions of cardiac calsequestrin increase sarcoplasmic reticulum Ca2+ leak independent of luminal Ca2+ and trigger ventricular arrhythmias in mice. *Circ Res*. 101:617-626.

Chopra, N., T. Yang, P. Asghari, E.D. Moore, S. Huke, B. Akin, R.A. Cattolica, C.F. Perez, T. Hlaing, B.E. Knollmann-Ritschel, L.R. Jones, I.N. Pessah, P.D. Allen, C. Franzini-Armstrong, and B.C. Knollmann. 2009. Ablation of triadin causes loss of cardiac Ca2+ release units, impaired excitation-contraction coupling, and cardiac arrhythmias. *Proc Natl Acad Sci U S A*. 106:7636-7641.

Chu, A., M.C. Dixon, A. Saito, S. Seiler, and S. Fleischer. 1988a. Isolation of sarcoplasmic reticulum fractions referable to longitudinal tubules and junctional terminal cisternae from rabbit skeletal muscle. *Methods Enzymol*. 157:36-46.

Chu, A., M.C. Dixon, A. Saito, S. Seiler, and S. Fleischer. 1988b. Isolation of sarcoplasmic reticulum fractions referable to longitudinal tubules and junctional terminal cisternae from rabbit skeletal muscle. *Methods Enzymol.* 157:36-46.

Cole, M.P., L. Chaiswing, T.D. Oberley, S.E. Edelmann, M.T. Piascik, S.M. Lin, K.K. Kiningham, and D.K. St Clair. 2006. The protective roles of nitric oxide and superoxide dismutase in adriamycin-induced cardiotoxicity. *Cardiovasc Res.* 69:186-197.

Cukierman, S., G. Yellen, and C. Miller. 1985. The K+ channel of sarcoplasmic reticulum. A new look at Cs+ block. *Biophys J.* 48:477-484.

Curran, J., K.H. Brown, D.J. Santiago, S. Pogwizd, D.M. Bers, and T.R. Shannon. 2010. Spontaneous Ca waves in ventricular myocytes from failing hearts depend on Ca2+-calmodulin-dependent protein kinase II. *J Mol Cell Cardiol.* 49:25-32.

Cusack, B.J., P.S. Mushlin, L.D. Voulelis, X. Li, R.J. Boucek, Jr., and R.D. Olson. 1993a. Daunorubicin-induced cardiac injury in the rabbit: a role for daunorubicinol? *Toxicology and applied pharmacology.* 118:177-185.

Cusack, B.J., P.S. Mushlin, L.D. Voulelis, X. Li, R.J. Boucek, Jr., and R.D. Olson. 1993b. Daunorubicin-induced cardiac injury in the rabbit: a role for daunorubicinol? *Toxicol Appl Pharmacol.* 118:177-185.

Cusack, B.J., S.P. Young, and R.D. Olson. 1995. Daunorubicin and daunorubicinol pharmacokinetics in plasma and tissues in the rat. *Cancer Chemother Pharmacol.* 35:213-218.

Cutler, M.J., B.N. Plummer, X. Wan, Q.A. Sun, D. Hess, H. Liu, I. Deschenes, D.S. Rosenbaum, J.S. Stamler, and K.R. Laurita. 2012. Aberrant S-nitrosylation mediates calcium-triggered ventricular arrhythmia in the intact heart. *Proc Natl Acad Sci U S A.* 109:18186-18191.

Davies, K.J., J.H. Doroshow, and P. Hochstein. 1983. Mitochondrial NADH dehydrogenase-catalyzed oxygen radical production by adriamycin, and the relative inactivity of 5-iminodaunorubicin. *FEBS Lett.* 153:227-230.

Davies, K.J.A., and J.H. Doroshow. 1986. Redox Cycling of Anthracyclines by Cardiac Mitochondria .1. Anthracycline Radical Formation by Nadh Dehydrogenase. *Journal of Biological Chemistry.* 261:3060-3067.

di Barletta, M.R., S. Viatchenko-Karpinski, A. Nori, M. Memmi, D. Terentyev, F. Turcato, G. Valle, N. Rizzi, C. Napolitano, and S. Gyorke. 2006. Clinical phenotype and functional characterization of CASQ2 mutations associated with catecholaminergic polymorphic ventricular tachycardia. *Circulation.* 114:1012-1019.

Diaz, M.E., D.A. Eisner, and S.C. O'Neill. 2002. Depressed ryanodine receptor activity increases variability and duration of the systolic Ca2+ transient in rat ventricular myocytes. *Circ Res.* 91:585-593.

Dibb, K.M., H.K. Graham, L.A. Venetucci, D.A. Eisner, and A.W. Trafford. 2007. Analysis of cellular calcium fluxes in cardiac muscle to understand calcium homeostasis in the heart. *Cell Calcium.* 42:503-512.

Dickinson, D.A., and H.J. Forman. 2002. Cellular glutathione and thiols metabolism. *Biochem Pharmacol.* 64:1019-1026.

DiFrancesco, D. 2010. The role of the funny current in pacemaker activity. *Circ Res.* 106:434-446.

Donoso, P., P. Aracena, and C. Hidalgo. 2000. Sulfhydryl oxidation overrides Mg(2+) inhibition of calcium-induced calcium release in skeletal muscle triads. *Biophys J.* 79:279-286.

Donoso, P., G. Sanchez, R. Bull, and C. Hidalgo. 2011a. Modulation of cardiac ryanodine receptor activity by ROS and RNS. *Front Biosci (Landmark Ed).* 16:553-567.

Donoso, P., G. Sanchez, R. Bull, and C. Hidalgo. 2011b. Modulation of cardiac ryanodine receptor activity by ROS and RNS. *Front Biosci.* 16:553-567.

Doroshow, J.H., G.Y. Locker, and C.E. Myers. 1980. Enzymatic defenses of the mouse heart against reactive oxygen metabolites: alterations produced by doxorubicin. *J Clin Invest.* 65:128-135.

Doroshow, J.H., C. Tallent, and J.E. Schechter. 1985. Ultrastructural features of Adriamycin-induced skeletal and cardiac muscle toxicity. *Am J Pathol.* 118:288-297.

Dulhunty, A., P. Gage, S. Curtis, G. Chelvanayagam, and P. Board. 2001. The glutathione transferase structural family includes a nuclear chloride channel and a ryanodine receptor calcium release channel modulator. *J Biol Chem.* 276:3319-3323.

Dulhunty, A.F. 2006. Excitation-contraction coupling from the 1950s into the new millennium. *Clinical and experimental pharmacology & physiology.* 33:763-772.

Dulhunty, A.F., D.R. Laver, E.M. Gallant, M.G. Casarotto, S.M. Pace, and S. Curtis. 1999. Activation and inhibition of skeletal RyR channels by a part of the skeletal DHPR II-III loop: effects of DHPR Ser687 and FKBP12. *Biophys J.* 77:189-203.

Dulhunty, A.F., P. Pouliquin, M. Coggan, P.W. Gage, and P.G. Board. 2005. A recently identified member of the glutathione transferase structural family modifies cardiac RyR2 substate activity, coupled gating and activation by Ca2+ and ATP. *Biochem J.* 390:333-343.

Dulhunty, A.F., E. Wium, L. Li, A.D. Hanna, S. Mirza, S. Talukder, N.A. Ghazali, and N.A. Beard. 2012. Proteins within the intracellular calcium store determine cardiac RyR channel activity and cardiac output. *Clinical and experimental pharmacology & physiology.* 39:477-484.

Durham, W.J., P. Aracena-Parks, C. Long, A.E. Rossi, S.A. Goonasekera, S. Boncompagni, D.L. Galvan, C.P. Gilman, M.R. Baker, N. Shirokova, F. Protasi, R. Dirksen, and S.L. Hamilton. 2008. RyR1 S-nitrosylation underlies environmental heat stroke and sudden death in Y522S RyR1 knockin mice. *Cell.* 133:53-65.

Eager, K.R., and A.F. Dulhunty. 1998. Activation of the cardiac ryanodine receptor by sulfhydryl oxidation is modified by Mg2+ and ATP. *The Journal of membrane biology.* 163:9-18.

Eager, K.R., and A.F. Dulhunty. 1999. Cardiac ryanodine receptor activity is altered by oxidizing reagents in either the luminal or cytoplasmic solution. *The Journal of membrane biology.* 167:205-214.

Eager, K.R., L.D. Roden, and A.F. Dulhunty. 1997. Actions of sulfhydryl reagents on single ryanodine receptor Ca(2+)-release channels from sheep myocardium. *Am J Physiol.* 272:C1908-1918.

Eisner, D., E. Bode, L. Venetucci, and A. Trafford. 2013. Calcium flux balance in the heart. *J Mol Cell Cardiol.* 58:110-117.

Fabiato, A., and F. Fabiato. 1978. Calcium-induced release of calcium from the sarcoplasmic reticulum of skinned cells from adult human, dog, cat, rabbit, rat, and frog hearts and from fetal and new-born rat ventricles. *Ann N Y Acad Sci.* 307:491-522.

Faggioni, M., and B.C. Knollmann. 2012. Calsequestrin 2 and arrhythmias. *Am J Physiol Heart Circ Physiol.* 302:H1250-1260.

Fajardo, G., M. Zhao, J. Powers, and D. Bernstein. 2006. Differential cardiotoxic/cardioprotective effects of beta-adrenergic receptor subtypes in myocytes and fibroblasts in doxorubicin cardiomyopathy. *J Mol Cell Cardiol.* 40:375-383.

Fan, G.C., Q. Yuan, W. Zhao, G. Chu, and E.G. Kranias. 2007. Junctin is a prominent regulator of contractility in cardiomyocytes. *Biochem Biophys Res Commun.* 352:617-622.

Fawcett, D.W., and N.S. McNutt. 1969. The ultrastructure of the cat myocardium. I. Ventricular papillary muscle. *J Cell Biol.* 42:1-45.

Feng, W., G. Liu, P.D. Allen, and I.N. Pessah. 2000. Transmembrane redox sensor of ryanodine receptor complex. *J Biol Chem.* 275:35902-35907.

Feng, W., G. Liu, R. Xia, J.J. Abramson, and I.N. Pessah. 1999. Site-selective modification of hyperreactive cysteines of ryanodine receptor complex by quinones. *Molecular pharmacology.* 55:821-831.

Fernández-Velasco, M., A.M. Gómez, J.-P. Benitah, and P. Neco. 2012. Ryanodine Receptor Channelopathies: The New Kid in the Arrhythmia Neighborhood.

Fernandez-Velasco, M., A. Rueda, N. Rizzi, J.P. Benitah, B. Colombi, C. Napolitano, S.G. Priori, S. Richard, and A.M. Gomez. 2009. Increased Ca2+ sensitivity of the ryanodine receptor mutant RyR2R4496C underlies catecholaminergic polymorphic ventricular tachycardia. *Circ Res.* 104:201-209, 212p following 209.

Filomeni, G., G. Rotilio, and M.R. Ciriolo. 2002. Cell signalling and the glutathione redox system. *Biochem Pharmacol.* 64:1057-1064.

Fischer, T., J. Herting, T. Tirilomis, A. Renner, S. Neef, K. Toischer, D. Ellenberger, A. Forster, J. Schmitto, J. Gummert, F. Schondube, G. Hasenfuss, L. Maier, and S. Sossalla. 2013. CaMKII and PKA Differentially Regulate SR Ca2+-Leak in Human Cardiac Pathology. *Circulation.*

Flucher, B.E., H. Takekura, and C. Franzini-Armstrong. 1993. Development of the excitation-contraction coupling apparatus in skeletal muscle: association of sarcoplasmic reticulum and transverse tubules with myofibrils. *Dev Biol.* 160:135-147.

Fogli, S., P. Nieri, and M.C. Breschi. 2004. The role of nitric oxide in anthracycline toxicity and prospects for pharmacologic prevention of cardiac damage. *FASEB journal : official publication of the Federation of American Societies for Experimental Biology.* 18:664-675.

Forman, H.J., J.M. Fukuto, and M. Torres. 2004. Redox signaling: thiol chemistry defines which reactive oxygen and nitrogen species can act as second messengers. *American journal of physiology. Cell physiology.* 287:C246-256.

Forrest, G.L., B. Gonzalez, W. Tseng, X. Li, and J. Mann. 2000. Human carbonyl reductase overexpression in the heart advances the development of doxorubicin-induced cardiotoxicity in transgenic mice. *Cancer Res.* 60:5158-5164.

Franzini-Armstrong, C., and F. Protasi. 1997. Ryanodine receptors of striated muscles: a complex channel capable of multiple interactions. *Physiol Rev.* 77:699-729.

Fujii, J., M. Kadoma, M. Tada, H. Toda, and F. Sakiyama. 1986. Characterization of structural unit of phospholamban by amino acid sequencing and electrophoretic analysis. *Biochem Biophys Res Commun.* 138:1044-1050.

Galfre, E., S.J. Pitt, E. Venturi, M. Sitsapesan, N.R. Zaccai, K. Tsaneva-Atanasova, S. O'Neill, and R. Sitsapesan. 2012. FKBP12 activates the cardiac ryanodine receptor Ca2+-release channel and is antagonised by FKBP12.6. *PLoS One.* 7:e31956.

Gambetta, R.A., A. Colombo, C. Lanzi, and F. Zunino. 1983. Purification and partial characterization of a daunorubicin-binding protein from rat liver. *Mol Pharmacol.* 24:336-340.

Gambliel, H.A., B.E. Burke, B.J. Cusack, G.M. Walsh, Y.L. Zhang, P.S. Mushlin, and R.D. Olson. 2002. Doxorubicin and C-13 deoxydoxorubicin effects on ryanodine receptor gene expression. *Biochem Biophys Res Commun.* 291:433-438.

Gellen, B., M. Fernandez-Velasco, F. Briec, L. Vinet, K. LeQuang, P. Rouet-Benzineb, J.P. Benitah, M. Pezet, G. Palais, N. Pellegrin, A. Zhang, R. Perrier, B. Escoubet, X. Marniquet, S. Richard, F. Jaisser, A.M. Gomez, F. Charpentier, and J.J. Mercadier. 2008. Conditional FKBP12.6 overexpression in mouse cardiac myocytes prevents triggered ventricular tachycardia through specific alterations in excitation-contraction coupling. *Circulation.* 117:1778-1786.

Germann, W.J., and C.L. Stanfield. 2004. Principles of Human Physiology. Pearson Education, Limited.

Gewirtz, D.A. 1999. A critical evaluation of the mechanisms of action proposed for the antitumor effects of the anthracycline antibiotics adriamycin and daunorubicin. *Biochem Pharmacol.* 57:727-741.

Gilliam, L.A., L.F. Ferreira, J.D. Bruton, J.S. Moylan, H. Westerblad, D.K. St Clair, and M.B. Reid. 2009. Doxorubicin acts through tumor necrosis factor receptor subtype 1 to cause dysfunction of murine skeletal muscle. *J Appl Physiol.* 107:1935-1942.

Gilliam, L.A.A., J.S. Moylan, L.A. Callahan, M.P. Sumandea, and M.B. Reid. 2011. Doxorubicin Causes Diaphragm Weakness in Murine Models of Cancer Chemotherapy. *Muscle Nerve.* 43:94-102.

Gilliam, L.A.A., and D.K. St Clair. 2011. Chemotherapy-Induced Weakness and Fatigue in Skeletal Muscle: The Role of Oxidative Stress. *Antioxid Redox Signal.* 15:2543-2563.

Gomez, A.M., and S. Richard. 2004. Mutant cardiac ryanodine receptors and ventricular arrhythmias: is 'gain-of-function' obligatory? *Cardiovasc Res.* 64:3-5.

Gomez, A.M., I. Schuster, J. Fauconnier, J. Prestle, G. Hasenfuss, and S. Richard. 2004. FKBP12.6 overexpression decreases Ca2+ spark amplitude but enhances [Ca2+](i) transient in rat cardiac myocytes. *Am J Physiol-Heart C.* 287:H1987-H1993.

Gonzalez, D.R., F. Beigi, A.V. Treuer, and J.M. Hare. 2007. Deficient ryanodine receptor S-nitrosylation increases sarcoplasmic reticulum calcium leak and arrhythmogenesis in cardiomyocytes. *Proc Natl Acad Sci U S A.* 104:20612-20617.

Gordon, A.M., A.F. Huxley, and F.J. Julian. 1966. The variation in isometric tension with sarcomere length in vertebrate muscle fibres. *J Physiol.* 184:170-192.

Guatimosim, S., C. Guatimosim, and L.S. Song. 2011. Imaging calcium sparks in cardiac myocytes. *Methods Mol Biol.* 689:205-214.

Guo, T., X. Ai, T.R. Shannon, S.M. Pogwizd, and D.M. Bers. 2007. Intra-sarcoplasmic reticulum free [Ca2+] and buffering in arrhythmogenic failing rabbit heart. *Circ Res.* 101:802-810.

Guo, T., R.L. Cornea, S. Huke, E. Camors, Y. Yang, E. Picht, B.R. Fruen, and D.M. Bers. 2010. Kinetics of FKBP12.6 binding to ryanodine receptors in permeabilized cardiac myocytes and effects on Ca sparks. *Circ Res.* 106:1743-1752.

Gyorke, I., and S. Gyorke. 1998. Regulation of the cardiac ryanodine receptor channel by luminal Ca2+ involves luminal Ca2+ sensing sites. *Biophys J.* 75:2801-2810.

Gyorke, I., N. Hester, L.R. Jones, and S. Gyorke. 2004. The role of calsequestrin, triadin, and junctin in conferring cardiac ryanodine receptor responsiveness to luminal calcium. *Biophys J.* 86:2121-2128.

Gyorke, S., and D. Terentyev. 2008. Modulation of ryanodine receptor by luminal calcium and accessory proteins in health and cardiac disease. *Cardiovasc Res.* 77:245-255.

Hadley, R.W., and J.R. Hume. 1987. An intrinsic potential-dependent inactivation mechanism associated with calcium channels in guinea-pig myocytes. *J Physiol.* 389:205-222.

Hakamata, Y., J. Nakai, H. Takeshima, and K. Imoto. 1992. Primary structure and distribution of a novel ryanodine receptor/calcium release channel from rabbit brain. *FEBS Lett.* 312:229-235.

Hall, J.E. 2010. Guyton and Hall Textbook of Medical Physiology: Enhanced E-book. Elsevier Health Sciences.

Hamilton, S.L., I. Serysheva, and G.M. Strasburg. 2000. Calmodulin and Excitation-Contraction Coupling. *News Physiol Sci.* 15:281-284.

Hanna, A.D., M. Janczura, E. Cho, A.F. Dulhunty, and N.A. Beard. 2011. Multiple actions of the anthracycline daunorubicin on cardiac ryanodine receptors. *Mol Pharmacol.* 80:538-549.

Hare, J.M. 2004. Nitroso-redox balance in the cardiovascular system. *N Engl J Med.* 351:2112-2114.

Hart, J.D.E., and A.F. Dulhunty. 2000. Nitric oxide activates or inhibits skeletal muscle ryanodine receptors depending on its concentration, membrane potential and ligand binding. *J Membrane Biol.* 173:227-236.

Hasenfuss, G., M. Meyer, W. Schillinger, B. Pieske, A. Scheffler, C. Holubarsch, and H. Reinecke. 1994. Expression of Sarcoplasmic-Reticulum Proteins in Failing and Nonfailing Human Myocardium. *Circulation.* 90:216-216.

Hewawasam, R., D. Liu, M.G. Casarotto, A.F. Dulhunty, and P.G. Board. 2010. The structure of the C-terminal helical bundle in glutathione transferase M2-2 determines its ability to inhibit the cardiac ryanodine receptor. *Biochem Pharmacol.* 80:381-388.

Hidalgo, C., P. Aracena, G. Sanchez, and P. Donoso. 2002. Redox regulation of calcium release in skeletal and cardiac muscle. *Biological research.* 35:183-193.

Hidalgo, C., and P. Donoso. 2008. Crosstalk between calcium and redox signaling: from molecular mechanisms to health implications. *Antioxid Redox Signal.* 10:1275-1312.

Hidalgo, C., P. Donoso, and M.A. Carrasco. 2005. The ryanodine receptors Ca2+ release channels: cellular redox sensors? *IUBMB Life.* 57:315-322.

Hille, B. 2001. Ionic Channels of Excitable Membranes. Sinauer Associates, Incorporated.

Hool, L.C. 2000. Hypoxia increases the sensitivity of the L-type Ca(2+) current to beta-adrenergic receptor stimulation via a C2 region-containing protein kinase C isoform. *Circ Res.* 87:1164-1171.

Hool, L.C., and B. Corry. 2007. Redox control of calcium channels: from mechanisms to therapeutic opportunities. *Antioxid Redox Signal.* 9:409-435.

Horenstein, M.S., R.S. Vander Heide, and T.J. L'Ecuyer. 2000. Molecular basis of anthracycline-induced cardiotoxicity and its prevention. *Mol Genet Metab.* 71:436-444.

Huang, F., J. Shan, S. Reiken, X.H. Wehrens, and A.R. Marks. 2006. Analysis of calstabin2 (FKBP12.6)-ryanodine receptor interactions: rescue of heart failure by calstabin2 in mice. *Proc Natl Acad Sci U S A*. 103:3456-3461.

Huxley, A.F., and R. Niedergerke. 1954. Structural changes in muscle during contraction; interference microscopy of living muscle fibres. *Nature*. 173:971-973.

Huxley, H., and J. Hanson. 1954. Changes in the cross-striations of muscle during contraction and stretch and their structural interpretation. *Nature*. 173:973-976.

Huxley, H.E. 2004. Fifty years of muscle and the sliding filament hypothesis. *Eur J Biochem*. 271:1403-1415.

Hwang, C., A.J. Sinskey, and H.F. Lodish. 1992. Oxidized redox state of glutathione in the endoplasmic reticulum. *Science*. 257:1496-1502.

Hydock, D.S., C.Y. Lien, B.T. Jensen, C.M. Schneider, and R. Hayward. 2011. Characterization of the effect of in vivo doxorubicin treatment on skeletal muscle function in the rat. *Anticancer Res*. 31:2023-2028.

Inui, M., A. Saito, and S. Fleischer. 1987a. Isolation of the ryanodine receptor from cardiac sarcoplasmic reticulum and identity with the feet structures. *J Biol Chem*. 262:15637-15642.

Inui, M., A. Saito, and S. Fleischer. 1987b. Purification of the ryanodine receptor and identity with feet structures of junctional terminal cisternae of sarcoplasmic reticulum from fast skeletal muscle. *J Biol Chem*. 262:1740-1747.

Jalilian, C., E.M. Gallant, P.G. Board, and A.F. Dulhunty. 2008a. Redox potential and the response of cardiac ryanodine receptors to CLIC-2, a member of the glutathione S-transferase structural family. *Antioxid Redox Signal*. 10:1675-1686.

Jalilian, C., E.M. Gallant, P.G. Board, and A.F. Dulhunty. 2008b. Redox potential and the response of cardiac ryanodine receptors to CLIC-2, a member of the glutathione S-transferase structural family. *Antioxid Redox Signal*. 10:1675-1685.

James, P., M. Inui, M. Tada, M. Chiesi, and E. Carafoli. 1989. Nature and Site of Phospholamban Regulation of the Ca-2+ Pump of Sarcoplasmic-Reticulum. *Nature*. 342:90-92.

Jayaraman, T., A.M. Brillantes, A.P. Timerman, S. Fleischer, H. Erdjument-Bromage, P. Tempst, and A.R. Marks. 1992. FK506 binding protein associated with the calcium release channel (ryanodine receptor). *J Biol Chem*. 267:9474-9477.

Jenkins, G., C. Kemnitz, and G.J. Tortora. 2006. Anatomy and Physiology, Illustrated Notebook: From Science to Life. Wiley.

Jiang, D., W. Chen, R. Wang, L. Zhang, and S.R. Chen. 2007. Loss of luminal Ca2+ activation in the cardiac ryanodine receptor is associated with ventricular fibrillation and sudden death. *Proc Natl Acad Sci U S A.* 104:18309-18314.

Jiang, D., R. Wang, B. Xiao, H. Kong, D.J. Hunt, P. Choi, L. Zhang, and S.R. Chen. 2005. Enhanced store overload-induced Ca2+ release and channel sensitivity to luminal Ca2+ activation are common defects of RyR2 mutations linked to ventricular tachycardia and sudden death. *Circ Res.* 97:1173-1181.

Jiang, D., B. Xiao, D. Yang, R. Wang, P. Choi, L. Zhang, H. Cheng, and S.R. Chen. 2004. RyR2 mutations linked to ventricular tachycardia and sudden death reduce the threshold for store-overload-induced Ca2+ release (SOICR). *Proc Natl Acad Sci U S A.* 101:13062-13067.

Jorgensen, A.O., A.C. Shen, W. Arnold, P.S. McPherson, and K.P. Campbell. 1993. The Ca2+-release channel/ryanodine receptor is localized in junctional and corbular sarcoplasmic reticulum in cardiac muscle. *J Cell Biol.* 120:969-980.

Kang, C., M.S. Nissen, E.J. Sanchez, K.S. Lam, and H. Milting. 2010. Potential adverse interaction of human cardiac calsequestrin. *Eur J Pharmacol.* 646:12-21.

Kaplan, P., E. Babusikova, J. Lehotsky, and D. Dobrota. 2003. Free radical-induced protein modification and inhibition of Ca2+-ATPase of cardiac sarcoplasmic reticulum. *Mol Cell Biochem.* 248:41-47.

Karim, C.B., H.A. Remmer, C.G. Marquardt, G.B. Fields, and D.D. Thomas. 1998. Evaluation of cysteine residues in the stability of the transmembrane domain of phospholamban pentamer. *Biophys J.* 74:A357-A357.

Kashimura, T., S.J. Briston, A.W. Trafford, C. Napolitano, S.G. Priori, D.A. Eisner, and L.A. Venetucci. 2010. In the RyR2(R4496C) Mouse Model of CPVT, beta-Adrenergic Stimulation Induces Ca Waves by Increasing SR Ca Content and Not by Decreasing the Threshold for Ca Waves. *Circ Res.* 107:1483-+.

Katz, A.M. 2006. Physiology of the Heart. Lippincott Williams & Wilkins.

Kim, E., M. Tam, W.F. Siems, and C. Kang. 2005a. Effects of drugs with muscle-related side effects and affinity for calsequestrin on the calcium regulatory function of sarcoplasmic reticulum microsomes. *Molecular pharmacology.* 68:1708-1715.

Kim, E., M. Tam, W.F. Siems, and C. Kang. 2005b. Effects of drugs with muscle-related side effects and affinity for calsequestrin on the calcium regulatory function of sarcoplasmic reticulum microsomes. *Mol Pharmacol.* 68:1708-1715.

Kim, S.Y., S.J. Kim, B.J. Kim, S.Y. Rah, S.M. Chung, M.J. Im, and U.H. Kim. 2006. Doxorubicin-induced reactive oxygen species generation and intracellular Ca2+ increase are reciprocally modulated in rat cardiomyocytes. *Exp Mol Med.* 38:535-545.

Kirchhefer, U., J. Klimas, H.A. Baba, I.B. Buchwalow, L. Fabritz, M. Huls, M. Matus, F.U. Muller, W. Schmitz, and J. Neumann. 2007. Triadin is a critical determinant of cellular Ca cycling and contractility in the heart. *American journal of physiology.* 293:H3165-3174.

Klabunde, R. 2011. Cardiovascular Physiology Concepts. Wolters Kluwer Health.

Knollmann, B.C., N. Chopra, T. Hlaing, B. Akin, T. Yang, K. Ettensohn, B.E. Knollmann, K.D. Horton, N.J. Weissman, I. Holinstat, W. Zhang, D.M. Roden, L.R. Jones, C. Franzini-Armstrong, and K. Pfeifer. 2006. Casq2 deletion causes sarcoplasmic reticulum volume increase, premature Ca2+ release, and catecholaminergic polymorphic ventricular tachycardia. *J Clin Invest.* 116:2510-2520.

Koop, A., P. Goldmann, S.R. Chen, R. Thieleczek, and M. Varsanyi. 2008. ARVC-related mutations in divergent region 3 alter functional properties of the cardiac ryanodine receptor. *Biophys J.* 94:4668-4677.

Kremer, L.C., E.C. van Dalen, M. Offringa, J. Ottenkamp, and P.A. Voute. 2001. Anthracycline-induced clinical heart failure in a cohort of 607 children: long-term follow-up study. *J Clin Oncol.* 19:191-196.

Kubalova, Z., I. Gyorke, R. Terentyeva, S. Viatchenko-Karpinski, D. Terentyev, S.C. Williams, and S. Gyorke. 2004. Modulation of cytosolic and intra-sarcoplasmic reticulum calcium waves by calsequestrin in rat cardiac myocytes. *J Physiol.* 561:515-524.

Kubalova, Z., D. Terentyev, S. Viatchenko-Karpinski, Y. Nishijima, I. Gyorke, R. Terentyeva, D.N. da Cunha, A. Sridhar, D.S. Feldman, R.L. Hamlin, C.A. Carnes, and S. Gyorke. 2005. Abnormal intrastore calcium signaling in chronic heart failure. *Proc Natl Acad Sci U S A.* 102:14104-14109.

Kuhlbrandt, W. 2004. Biology, structure and mechanism of P-type ATPases. *Nat Rev Mol Cell Biol.* 5:282-295.

Kuznetsov, A.V., R. Margreiter, A. Amberger, V. Saks, and M. Grimm. 2011. Changes in mitochondrial redox state, membrane potential and calcium precede mitochondrial dysfunction in doxorubicin-induced cell death. *Biochim Biophys Acta.* 1813:1144-1152.

Lacampagne, A., A. Duittoz, P. Bolanos, N. Peineau, and J.A. Argibay. 1995. Effect of sulfhydryl oxidation on ionic and gating currents associated with L-type calcium

channels in isolated guinea-pig ventricular myocytes. *Cardiovasc Res.* 30:799-806.

Laemmli, U.K. 1970. Cleavage of structural proteins during the assembly of the head of bacteriophage T4. *Nature.* 227:680-685.

Lai, F.A., H.P. Erickson, E. Rousseau, Q.Y. Liu, and G. Meissner. 1988. Purification and reconstitution of the calcium release channel from skeletal muscle. *Nature.* 331:315-319.

Lanner, J.T., D.K. Georgiou, A.D. Joshi, and S.L. Hamilton. 2010. Ryanodine receptors: structure, expression, molecular details, and function in calcium release. *Cold Spring Harb Perspect Biol.* 2:a003996.

Larsen, R.L., R.I. Jakacki, V.L. Vetter, A.T. Meadows, J.H. Silber, and G. Barber. 1992. Electrocardiographic changes and arrhythmias after cancer therapy in children and young adults. *Am J Cardiol.* 70:73-77.

Laver, D. 2001. The power of single channel recording and analysis: its application to ryanodine receptors in lipid bilayers. *Clinical and experimental pharmacology & physiology.* 28:675-686.

Laver, D.R. 2007. Ca2+ stores regulate ryanodine receptor Ca2+ release channels via luminal and cytosolic Ca2+ sites. *Biophys J.* 92:3541-3555.

Laver, D.R. 2009. Luminal Ca(2+) activation of cardiac ryanodine receptors by luminal and cytoplasmic domains. *Eur Biophys J.* 39:19-26.

Laver, D.R., T.M. Baynes, and A.F. Dulhunty. 1997. Magnesium inhibition of ryanodine-receptor calcium channels: evidence for two independent mechanisms. *The Journal of membrane biology.* 156:213-229.

Laver, D.R., L.D. Roden, G.P. Ahern, K.R. Eager, P.R. Junankar, and A.F. Dulhunty. 1995. Cytoplasmic Ca2+ inhibits the ryanodine receptor from cardiac muscle. *The Journal of membrane biology.* 147:7-22.

Ledbetter, M.W., J.K. Preiner, C.F. Louis, and J.R. Mickelson. 1994. Tissue distribution of ryanodine receptor isoforms and alleles determined by reverse transcription polymerase chain reaction. *J Biol Chem.* 269:31544-31551.

Lehnart, S.E., X.H. Wehrens, P.J. Laitinen, S.R. Reiken, S.X. Deng, Z. Cheng, D.W. Landry, K. Kontula, H. Swan, and A.R. Marks. 2004. Sudden death in familial polymorphic ventricular tachycardia associated with calcium release channel (ryanodine receptor) leak. *Circulation.* 109:3208-3214.

Leichtweis, S., and L.L. Ji. 2001. Glutathione deficiency intensifies ischaemia-reperfusion induced cardiac dysfunction and oxidative stress. *Acta Physiol Scand.* 172:1-10.

Liao, R., and M. Jain. 2007. Isolation, culture, and functional analysis of adult mouse cardiomyocytes. *Methods Mol Med.* 139:251-262.

Lim, C.C., C. Zuppinger, X. Guo, G.M. Kuster, M. Helmes, H.M. Eppenberger, T.M. Suter, R. Liao, and D.B. Sawyer. 2004. Anthracyclines induce calpain-dependent titin proteolysis and necrosis in cardiomyocytes. *J Biol Chem.* 279:8290-8299.

Linck, B., Z.Y. Qiu, Z.P. He, Q.S. Tong, D.W. Hilgemann, and K.D. Philipson. 1998. Functional comparison of the three isoforms of the Na+/Ca2+ exchanger (NCX1, NCX2, NCX3). *Am J Physiol-Cell Ph.* 274:C415-C423.

Liu, G., J.J. Abramson, A.C. Zable, and I.N. Pessah. 1994. Direct evidence for the existence and functional role of hyperreactive sulfhydryls on the ryanodine receptor-triadin complex selectively labeled by the coumarin maleimide 7-diethylamino-3-(4'-maleimidylphenyl)-4-methylcoumarin. *Mol Pharmacol.* 45:189-200.

Liu, N., Y. Ruan, M. Denegri, T. Bachetti, Y. Li, B. Colombi, C. Napolitano, W.A. Coetzee, and S.G. Priori. 2011. Calmodulin kinase II inhibition prevents arrhythmias in RyR2(R4496C+/-) mice with catecholaminergic polymorphic ventricular tachycardia. *J Mol Cell Cardiol.* 50:214-222.

Liu, W., D.A. Pasek, and G. Meissner. 1998. Modulation of Ca(2+)-gated cardiac muscle Ca(2+)-release channel (ryanodine receptor) by mono- and divalent ions. *Am J Physiol.* 274:C120-128.

Liu, Z., J. Zhang, P. Li, S.R. Chen, and T. Wagenknecht. 2002. Three-dimensional reconstruction of the recombinant type 2 ryanodine receptor and localization of its divergent region 1. *J Biol Chem.* 277:46712-46719.

Liu, Z., J. Zhang, R. Wang, S.R. Wayne Chen, and T. Wagenknecht. 2004. Location of divergent region 2 on the three-dimensional structure of cardiac muscle ryanodine receptor/calcium release channel. *J Mol Biol.* 338:533-545.

Lohse, M.J., J.P. Vilardaga, and M. Bunemann. 2003. Direct optical recording of intrinsic efficacy at a G protein-coupled receptor. *Life Sci.* 74:397-404.

Louch, W.E., K.A. Sheehan, and B.M. Wolska. 2011. Methods in cardiomyocyte isolation, culture, and gene transfer. *J Mol Cell Cardiol.* 51:288-298.

Ludtke, S.J., Serysheva, II, S.L. Hamilton, and W. Chiu. 2005. The pore structure of the closed RyR1 channel. *Structure.* 13:1203-1211.

Lukyanenko, V., and S. Gyorke. 1999. Ca2+ sparks and Ca2+ waves in saponin-permeabilized rat ventricular myocytes. *J Physiol-London.* 521:575-585.

Lynch, P.J., and C.C. Jaffe. 2006. Introduction to Cardiothoracic Imaging. *In.* Yale University School of Medicine, New Haven.

Lytton, J., M. Westlin, S.E. Burk, G.E. Shull, and D.H. MacLennan. 1992. Functional comparisons between isoforms of the sarcoplasmic or endoplasmic reticulum family of calcium pumps. *J Biol Chem.* 267:14483-14489.

Ma, J. 1993. Block by ruthenium red of the ryanodine-activated calcium release channel of skeletal muscle. *J Gen Physiol.* 102:1031-1056.

MacLennan, D.H., and N.M. Green. 2000. Structural biology. Pumping ions. *Nature.* 405:633-634.

MacLennan, D.H., and E.G. Kranias. 2003. Phospholamban: a crucial regulator of cardiac contractility. *Nat Rev Mol Cell Biol.* 4:566-577.

MacLennan, D.H., and P.T. Wong. 1971. Isolation of a calcium-sequestering protein from sarcoplasmic reticulum. *Proc Natl Acad Sci U S A.* 68:1231-1235.

Marchini, S., O. Gonzalez Paz, M. Ripamonti, C. Geroni, A. Bargiotti, M. Caruso, S. Todeschi, M. D'Incalci, and M. Broggini. 1995. Sequence-specific DNA interactions by novel alkylating anthracycline derivatives. *Anticancer Drug Des.* 10:641-653.

Marengo, J.J., C. Hidalgo, and R. Bull. 1998. Sulfhydryl oxidation modifies the calcium dependence of ryanodine-sensitive calcium channels of excitable cells. *Biophys J.* 74:1263-1277.

Marinov, B.S., R.O. Olojo, R. Xia, and J.J. Abramson. 2007. Non-thiol reagents regulate ryanodine receptor function by redox interactions that modify reactive thiols. *Antioxid Redox Signal.* 9:609-621.

Marks, A.R. 1997. Intracellular calcium-release channels: regulators of cell life and death. *Am J Physiol.* 272:H597-605.

Marx, S.O., S. Reiken, Y. Hisamatsu, T. Jayaraman, D. Burkhoff, N. Rosemblit, and A.R. Marks. 2000. PKA phosphorylation dissociates FKBP12.6 from the calcium release channel (ryanodine receptor): defective regulation in failing hearts. *Cell.* 101:365-376.

Mayrleitner, M., A.P. Timerman, G. Wiederrecht, and S. Fleischer. 1994. The calcium release channel of sarcoplasmic reticulum is modulated by FK-506 binding protein: effect of FKBP-12 on single channel activity of the skeletal muscle ryanodine receptor. *Cell Calcium.* 15:99-108.

McCauley, M.D., and X.H. Wehrens. 2011. Targeting ryanodine receptors for anti-arrhythmic therapy. *Acta Pharmacol Sin.* 32:749-757.

Meissner, G. 1994. Ryanodine receptor/Ca2+ release channels and their regulation by endogenous effectors. *Annu Rev Physiol.* 56:485-508.

Meissner, G. 2004. Molecular regulation of cardiac ryanodine receptor ion channel. *Cell Calcium.* 35:621-628.

Menna, P., G. Minotti, and E. Salvatorelli. 2007a. In vitro modeling of the structure-activity determinants of anthracycline cardiotoxicity. *Cell biology and toxicology.* 23:49-62.

Menna, P., O.G. Paz, M. Chello, E. Covino, E. Salvatorelli, and G. Minotti. 2012. Anthracycline cardiotoxicity. *Expert Opin Drug Saf.* 11 Suppl 1:S21-36.

Menna, P., S. Recalcati, G. Cairo, and G. Minotti. 2007b. An introduction to the metabolic determinants of anthracycline cardiotoxicity. *Cardiovascular toxicology.* 7:80-85.

Menna, P., E. Salvatorelli, and G. Minotti. 2008. Cardiotoxicity of antitumor drugs. *Chemical research in toxicology.* 21:978-989.

Menshikova, E.V., E. Cheong, and G. Salama. 2000. Low N-ethylmaleimide concentrations activate ryanodine receptors by a reversible interaction, not an alkylation of critical thiols. *J Biol Chem.* 275:36775-36780.

Mercadier, J.J., A.M. Lompre, P. Duc, K.R. Boheler, J.B. Fraysse, C. Wisnewsky, P.D. Allen, M. Komajda, and K. Schwartz. 1990. Altered sarcoplasmic reticulum Ca2(+)-ATPase gene expression in the human ventricle during end-stage heart failure. *J Clin Invest.* 85:305-309.

Meyer, M., W. Schillinger, B. Pieske, C. Holubarsch, C. Heilmann, H. Posival, G. Kuwajima, K. Mikoshiba, H. Just, G. Hasenfuss, and et al. 1995. Alterations of sarcoplasmic reticulum proteins in failing human dilated cardiomyopathy. *Circulation.* 92:778-784.

Mikami, A., K. Imoto, T. Tanabe, T. Niidome, Y. Mori, H. Takeshima, S. Narumiya, and S. Numa. 1989. Primary structure and functional expression of the cardiac dihydropyridine-sensitive calcium channel. *Nature.* 340:230-233.

Miller, C. 1986. Ion Channel Reconstitution. Plenum Press.

Miller, C., and E. Racker. 1976. Ca++-induced fusion of fragmented sarcoplasmic reticulum with artificial planar bilayers. *The Journal of membrane biology.* 30:283-300.

Minotti, G., P. Menna, E. Salvatorelli, G. Cairo, and L. Gianni. 2004. Anthracyclines: molecular advances and pharmacologic developments in antitumor activity and cardiotoxicity. *Pharmacological reviews*. 56:185-229.

Mordente, A., G. Minotti, G.E. Martorana, A. Silvestrini, B. Giardina, and E. Meucci. 2003. Anthracycline secondary alcohol metabolite formation in human or rabbit heart: biochemical aspects and pharmacologic implications. *Biochemical pharmacology*. 66:989-998.

Morris, T.E., and P.V. Sulakhe. 1997. Sarcoplasmic reticulum Ca(2+)-pump dysfunction in rat cardiomyocytes briefly exposed to hydroxyl radicals. *Free Radic Biol Med*. 22:37-47.

Morrow, G.R., P.L.R. Andrews, J.T. Hickok, J.A. Roscoe, and S. Matteson. 2002. Fatigue associated with cancer and its treatment. *Support Care Cancer*. 10:389-398.

Mukherjee, R., and F.G. Spinale. 1998. L-type calcium channel abundance and function with cardiac hypertrophy and failure: a review. *J Mol Cell Cardiol*. 30:1899-1916.

Mulrooney, D.A., M.W. Yeazel, T. Kawashima, A.C. Mertens, P. Mitby, M. Stovall, S.S. Donaldson, D.M. Green, C.A. Sklar, L.L. Robison, and W.M. Leisenring. 2009. Cardiac outcomes in a cohort of adult survivors of childhood and adolescent cancer: retrospective analysis of the Childhood Cancer Survivor Study cohort. *Bmj*. 339:b4606.

Murphy, R.M., T.L. Dutka, D. Horvath, J.R. Bell, L.M. Delbridge, and G.D. Lamb. 2013. Ca2+-dependent proteolysis of junctophilin-1 and junctophilin-2 in skeletal and cardiac muscle. *J Physiol*. 591:719-729.

Murphy, R.M., J.P. Mollica, N.A. Beard, B.C. Knollmann, and G.D. Lamb. 2011. Quantification of calsequestrin 2 (CSQ2) in sheep cardiac muscle and Ca2+-binding protein changes in CSQ2 knockout mice. *Am J Physiol Heart Circ Physiol*. 300:H595-604.

Mushlin, P.S., B.J. Cusack, R.J. Boucek, Jr., T. Andrejuk, X. Li, and R.D. Olson. 1993. Time-related increases in cardiac concentrations of doxorubicinol could interact with doxorubicin to depress myocardial contractile function. *Br J Pharmacol*. 110:975-982.

Nagami, K., T. Yoshikawa, M. Suzuki, Y. Wainai, T. Anzai, and S. Handa. 1997. Abnormal beta-adrenergic transmembrane signaling in rabbits with adriamycin-induced cardiomyopathy. *Jpn Circ J*. 61:249-255.

Nakai, J., T. Imagawa, Y. Hakamat, M. Shigekawa, H. Takeshima, and S. Numa. 1990. Primary structure and functional expression from cDNA of the cardiac ryanodine receptor/calcium release channel. *FEBS Lett*. 271:169-177.

Nicoll, D.A., S. Longoni, and K.D. Philipson. 1990. Molecular-Cloning and Functional Expression of the Cardiac Sarcolemmal Na+-Ca-2+ Exchanger. *Science*. 250:562-565.

O'Connell, T.D., M.C. Rodrigo, and P.C. Simpson. 2007. Isolation and culture of adult mouse cardiac myocytes. *Methods Mol Biol*. 357:271-296.

Oba, T., T. Murayama, and Y. Ogawa. 2002. Redox states of type 1 ryanodine receptor alter Ca(2+) release channel response to modulators. *American journal of physiology*. 282:C684-692.

Octavia, Y., C.G. Tocchetti, K.L. Gabrielson, S. Janssens, H.J. Crijns, and A.L. Moens. 2012. Doxorubicin-induced cardiomyopathy: From molecular mechanisms to therapeutic strategies. *J Mol Cell Cardiol*. 52:1213-1225.

Olson, L.E., D. Bedja, S.J. Alvey, A.J. Cardounel, K.L. Gabrielson, and R.H. Reeves. 2003. Protection from doxorubicin-induced cardiac toxicity in mice with a null allele of carbonyl reductase 1. *Cancer Res*. 63:6602-6606.

Olson, R.D., H.A. Gambliel, R.E. Vestal, S.E. Shadle, H.A. Charlier, Jr., and B.J. Cusack. 2005. Doxorubicin cardiac dysfunction: effects on calcium regulatory proteins, sarcoplasmic reticulum, and triiodothyronine. *Cardiovascular toxicology*. 5:269-283.

Olson, R.D., X. Li, P. Palade, S.E. Shadle, P.S. Mushlin, H.A. Gambliel, M. Fill, R.J. Boucek, Jr., and B.J. Cusack. 2000. Sarcoplasmic reticulum calcium release is stimulated and inhibited by daunorubicin and daunorubicinol. *Toxicology and applied pharmacology*. 169:168-176.

Olson, R.D., and P.S. Mushlin. 1990. Doxorubicin cardiotoxicity: analysis of prevailing hypotheses. *FASEB journal : official publication of the Federation of American Societies for Experimental Biology*. 4:3076-3086.

Olson, R.D., P.S. Mushlin, D.E. Brenner, S. Fleischer, B.J. Cusack, B.K. Chang, and R.J. Boucek, Jr. 1988. Doxorubicin cardiotoxicity may be caused by its metabolite, doxorubicinol. *Proc Natl Acad Sci U S A*. 85:3585-3589.

Ondrias, K., L. Borgatta, D.H. Kim, and B.E. Ehrlich. 1990. Biphasic effects of doxorubicin on the calcium release channel from sarcoplasmic reticulum of cardiac muscle. *Circ Res*. 67:1167-1174.

OpenStax College. 2013. Mammalian Heart and Blood Vessels. *In*. Connexions

Pacher, P., L. Liaudet, P. Bai, J.G. Mabley, P.M. Kaminski, L. Virag, A. Deb, E. Szabo, Z. Ungvari, M.S. Wolin, J.T. Groves, and C. Szabo. 2003. Potent metalloporphyrin peroxynitrite decomposition catalyst protects against the development of doxorubicin-induced cardiac dysfunction. *Circulation*. 107:896-904.

Park, H., I.Y. Park, E. Kim, B. Youn, K. Fields, A.K. Dunker, and C. Kang. 2004. Comparing skeletal and cardiac calsequestrin structures and their calcium binding: a proposed mechanism for coupled calcium binding and protein polymerization. *J Biol Chem.* 279:18026-18033.

Park, I.Y., E.J. Kim, H. Park, K. Fields, A.K. Dunker, and C. Kang. 2005a. Interaction between cardiac calsequestrin and drugs with known cardiotoxicity. *Molecular pharmacology.* 67:97-104.

Park, I.Y., E.J. Kim, H. Park, K. Fields, A.K. Dunker, and C. Kang. 2005b. Interaction between cardiac calsequestrin and drugs with known cardiotoxicity. *Mol Pharmacol.* 67:97-104.

Periasamy, M., and A. Kalyanasundaram. 2007. SERCA pump isoforms: Their role in calcium transport and disease. *Muscle Nerve.* 35:430-442.

Pessah, I.N., E.L. Durie, M.J. Schiedt, and I. Zimanyi. 1990. Anthraquinone-sensitized Ca2+ release channel from rat cardiac sarcoplasmic reticulum: possible receptor-mediated mechanism of doxorubicin cardiomyopathy. *Molecular pharmacology.* 37:503-514.

Pessah, I.N., K.H. Kim, and W. Feng. 2002. Redox sensing properties of the ryanodine receptor complex. *Front Biosci.* 7:a72-79.

Pfeffer, B., C. Tziros, and R.J. Katz. 2009. Current concepts of anthracycline cardiotoxicity: pathogenesis, diagnosis and prevention. *British journal of cardiology.* 16:85-89.

Philipson, K.D., and D.A. Nicoll. 2000. Sodium-calcium exchange: A molecular perspective. *Annu Rev Physiol.* 62:111-133.

Picht, E., A.V. Zima, T.R. Shannon, A.M. Duncan, L.A. Blatter, and D.M. Bers. 2011. Dynamic calcium movement inside cardiac sarcoplasmic reticulum during release. *Circ Res.* 108:847-856.

Pogwizd, S.M., and D.M. Bers. 2004. Cellular basis of triggered arrhythmias in heart failure. *Trends Cardiovasc Med.* 14:61-66.

Pogwizd, S.M., K. Schlotthauer, L. Li, W. Yuan, and D.M. Bers. 2001. Arrhythmogenesis and contractile dysfunction in heart failure: Roles of sodium-calcium exchange, inward rectifier potassium current, and residual beta-adrenergic responsiveness. *Circ Res.* 88:1159-1167.

Prestle, J., P.M. Janssen, A.P. Janssen, O. Zeitz, S.E. Lehnart, L. Bruce, G.L. Smith, and G. Hasenfuss. 2001. Overexpression of FK506-binding protein FKBP12.6 in cardiomyocytes reduces ryanodine receptor-mediated Ca(2+) leak from the sarcoplasmic reticulum and increases contractility. *Circ Res.* 88:188-194.

Qin, J., G. Valle, A. Nani, H. Chen, J. Ramos-Franco, A. Nori, P. Volpe, and M. Fill. 2009. Ryanodine receptor luminal Ca2+ regulation: swapping calsequestrin and channel isoforms. *Biophys J.* 97:1961-1970.

Qin, J., G. Valle, A. Nani, A. Nori, N. Rizzi, S.G. Priori, P. Volpe, and M. Fill. 2008. Luminal Ca2+ regulation of single cardiac ryanodine receptors: insights provided by calsequestrin and its mutants. *J Gen Physiol.* 131:325-334.

Radwanski, P.B., A.E. Belevych, L. Brunello, C.A. Carnes, and S. Gyorke. 2013. Store-dependent deactivation: cooling the chain-reaction of myocardial calcium signaling. *J Mol Cell Cardiol.* 58:77-83.

Regev, R., and G.D. Eytan. 1997. Flip-flop of doxorubicin across erythrocyte and lipid membranes. *Biochem Pharmacol.* 54:1151-1158.

Reid, M.B. 2008. Free radicals and muscle fatigue: Of ROS, canaries, and the IOC. *Free Radic Biol Med.* 44:169-179.

Richard, I., O. Broux, V. Allamand, F. Fougerousse, N. Chiannilkulchai, N. Bourg, L. Brenguier, C. Devaud, P. Pasturaud, C. Roudaut, and et al. 1995. Mutations in the proteolytic enzyme calpain 3 cause limb-girdle muscular dystrophy type 2A. *Cell.* 81:27-40.

Rios, E., and G. Brum. 1987. Involvement of dihydropyridine receptors in excitation-contraction coupling in skeletal muscle. *Nature.* 325:717-720.

Rizzi, N., N. Liu, C. Napolitano, A. Nori, F. Turcato, B. Colombi, S. Bicciato, D. Arcelli, A. Spedito, M. Scelsi, L. Villani, G. Esposito, S. Boncompagni, F. Protasi, P. Volpe, and S.G. Priori. 2008. Unexpected structural and functional consequences of the R33Q homozygous mutation in cardiac calsequestrin: a complex arrhythmogenic cascade in a knock in mouse model. *Circ Res.* 103:298-306.

Rossi, D., and V. Sorrentino. 2002. Molecular genetics of ryanodine receptors Ca2+-release channels. *Cell Calcium.* 32:307-319.

Roux-Buisson, N., M. Cacheux, A. Fourest-Lieuvin, J. Fauconnier, J. Brocard, I. Denjoy, P. Durand, P. Guicheney, F. Kyndt, A. Leenhardt, H. Le Marec, V. Lucet, P. Mabo, V. Probst, N. Monnier, P.F. Ray, E. Santoni, P. Tremeaux, A. Lacampagne, J. Faure, J. Lunardi, and I. Marty. 2012. Absence of triadin, a protein of the calcium release complex, is responsible for cardiac arrhythmia with sudden death in human. *Hum Mol Genet.* 21:2759-2767.

Sacco, G., R. Giampietro, E. Salvatorelli, P. Menna, N. Bertani, G. Graiani, F. Animati, C. Goso, C.A. Maggi, S. Manzini, and G. Minotti. 2003. Chronic cardiotoxicity of anticancer anthracyclines in the rat: role of secondary metabolites and reduced toxicity by a novel anthracycline with impaired metabolite formation and reactivity. *Br J Pharmacol.* 139:641-651.

Sag, C.M., A.C. Kohler, M.E. Anderson, J. Backs, and L.S. Maier. 2011. CaMKII-dependent SR Ca leak contributes to doxorubicin-induced impaired Ca handling in isolated cardiac myocytes. *J Mol Cell Cardiol.* 51:749-759.

Sakmann, B., and E. Neher. 2009. Single-channel recording. Springer.

Santiago, D.J., J.W. Curran, D.M. Bers, W.J. Lederer, M.D. Stern, E. Rios, and T.R. Shannon. 2010. Ca sparks do not explain all ryanodine receptor-mediated SR Ca leak in mouse ventricular myocytes. *Biophys J.* 98:2111-2120.

Santos, C.X., N. Anilkumar, M. Zhang, A.C. Brewer, and A.M. Shah. 2011. Redox signaling in cardiac myocytes. *Free Radic Biol Med.* 50:777-793.

Sawyer, D.B., X. Peng, B. Chen, L. Pentassuglia, and C.C. Lim. 2010. Mechanisms of anthracycline cardiac injury: can we identify strategies for cardioprotection? *Progress in cardiovascular diseases.* 53:105-113.

Schafer, F.Q., and G.R. Buettner. 2001. Redox environment of the cell as viewed through the redox state of the glutathione disulfide/glutathione couple. *Free Radic Biol Med.* 30:1191-1212.

Schmidt, U., R.J. Hajjar, P.A. Helm, C.S. Kim, A.A. Doye, and J.K. Gwathmey. 1998. Contribution of abnormal sarcoplasmic reticulum ATPase activity to systolic and diastolic dysfunction in human heart failure. *J Mol Cell Cardiol.* 30:1929-1937.

Schwinger, R.H., M. Bohm, U. Schmidt, P. Karczewski, U. Bavendiek, M. Flesch, E.G. Krause, and E. Erdmann. 1995. Unchanged protein levels of SERCA II and phospholamban but reduced Ca2+ uptake and Ca(2+)-ATPase activity of cardiac sarcoplasmic reticulum from dilated cardiomyopathy patients compared with patients with nonfailing hearts. *Circulation.* 92:3220-3228.

Shadle, S.E., B.P. Bammel, B.J. Cusack, R.A. Knighton, S.J. Olson, P.S. Mushlin, and R.D. Olson. 2000a. Daunorubicin cardiotoxicity: evidence for the importance of the quinone moiety in a free-radical-independent mechanism. *Biochemical pharmacology.* 60:1435-1444.

Shadle, S.E., B.P. Bammel, B.J. Cusack, R.A. Knighton, S.J. Olson, P.S. Mushlin, and R.D. Olson. 2000b. Daunorubicin cardiotoxicity: evidence for the importance of the quinone moiety in a free-radical-independent mechanism. *Biochem Pharmacol.* 60:1435-1444.

Shan, J., W. Xie, M. Betzenhauser, S. Reiken, B.X. Chen, A. Wronska, and A.R. Marks. 2012. Calcium leak through ryanodine receptors leads to atrial fibrillation in 3 mouse models of catecholaminergic polymorphic ventricular tachycardia. *Circ Res.* 111:708-717.

Shannon, T.R., K.S. Ginsburg, and D.M. Bers. 2000. Potentiation of fractional sarcoplasmic reticulum calcium release by total and free intra-sarcoplasmic reticulum calcium concentration. *Biophys J.* 78:334-343.

Shannon, T.R., K.S. Ginsburg, and D.M. Bers. 2002. Quantitative assessment of the SR Ca2+ leak-load relationship. *Circ Res.* 91:594-600.

Shannon, T.R., T. Guo, and D.M. Bers. 2003a. Ca2+ scraps: local depletions of free [Ca2+] in cardiac sarcoplasmic reticulum during contractions leave substantial Ca2+ reserve. *Circ Res.* 93:40-45.

Shannon, T.R., S.M. Pogwizd, and D.M. Bers. 2003b. Elevated sarcoplasmic reticulum Ca2+ leak in intact ventricular myocytes from rabbits in heart failure. *Circ Res.* 93:592-594.

Sharma, M.R., L.H. Jeyakumar, S. Fleischer, and T. Wagenknecht. 2006. Three-dimensional visualization of FKBP12.6 binding to an open conformation of cardiac ryanodine receptor. *Biophys J.* 90:164-172.

Sharma, M.R., P. Penczek, R. Grassucci, H.B. Xin, S. Fleischer, and T. Wagenknecht. 1998. Cryoelectron microscopy and image analysis of the cardiac ryanodine receptor. *J Biol Chem.* 273:18429-18434.

Sharov, V.S., E.S. Dremina, N.A. Galeva, T.D. Williams, and C. Schoneich. 2006. Quantitative mapping of oxidation-sensitive cysteine residues in SERCA in vivo and in vitro by HPLC-electrospray-tandem MS: selective protein oxidation during biological aging. *Biochem J.* 394:605-615.

Simunek, T., M. Sterba, O. Popelova, M. Adamcova, R. Hrdina, and V. Gersl. 2009. Anthracycline-induced cardiotoxicity: overview of studies examining the roles of oxidative stress and free cellular iron. *Pharmacol Rep.* 61:154-171.

Singal, P.K., T. Li, D. Kumar, I. Danelisen, and N. Iliskovic. 2000. Adriamycin-induced heart failure: mechanism and modulation. *Mol Cell Biochem.* 207:77-86.

Singh, N., A.K. Dhalla, C. Seneviratne, and P.K. Singal. 1995. Oxidative stress and heart failure. *Mol Cell Biochem.* 147:77-81.

Slupsky, J.R., M. Ohnishi, M.R. Carpenter, and R.A. Reithmeier. 1987. Characterization of cardiac calsequestrin. *Biochemistry-Us.* 26:6539-6544.

Smuder, A.J., A.N. Kavazis, K. Min, and S.K. Powers. 2011. Exercise protects against doxorubicin-induced oxidative stress and proteolysis in skeletal muscle. *J Appl Physiol.* 110:935-942.

Steinherz, L.J., P.G. Steinherz, C.T. Tan, G. Heller, and M.L. Murphy. 1991. Cardiac toxicity 4 to 20 years after completing anthracycline therapy. *Jama*. 266:1672-1677.

Stevens, S.C., D. Terentyev, A. Kalyanasundaram, M. Periasamy, and S. Gyorke. 2009. Intra-sarcoplasmic reticulum Ca2+ oscillations are driven by dynamic regulation of ryanodine receptor function by luminal Ca2+ in cardiomyocytes. *J Physiol*. 587:4863-4872.

Studer, R., H. Reinecke, J. Bilger, T. Eschenhagen, M. Bohm, G. Hasenfuss, H. Just, J. Holtz, and H. Drexler. 1994. Gene expression of the cardiac Na(+)-Ca2+ exchanger in end-stage human heart failure. *Circ Res*. 75:443-453.

Sun, J., L. Xu, J.P. Eu, J.S. Stamler, and G. Meissner. 2001. Classes of thiols that influence the activity of the skeletal muscle calcium release channel. *J Biol Chem*. 276:15625-15630.

Takenaka, H., P.N. Adler, and A.M. Katz. 1982. Calcium fluxes across the membrane of sarcoplasmic reticulum vesicles. *J Biol Chem*. 257:12649-12656.

Takeshima, H., S. Komazaki, K. Hirose, M. Nishi, T. Noda, and M. Iino. 1998. Embryonic lethality and abnormal cardiac myocytes in mice lacking ryanodine receptor type 2. *Embo J*. 17:3309-3316.

Takeshima, H., T. Yamazawa, T. Ikemoto, H. Takekura, M. Nishi, T. Noda, and M. Iino. 1995. Ca(2+)-induced Ca2+ release in myocytes from dyspedic mice lacking the type-1 ryanodine receptor. *Embo J*. 14:2999-3006.

Tateishi, H., M. Yano, M. Mochizuki, T. Suetomi, M. Ono, X. Xu, H. Uchinoumi, S. Okuda, T. Oda, S. Kobayashi, T. Yamamoto, Y. Ikeda, T. Ohkusa, N. Ikemoto, and M. Matsuzaki. 2009. Defective domain-domain interactions within the ryanodine receptor as a critical cause of diastolic Ca2+ leak in failing hearts. *Cardiovasc Res*. 81:536-545.

Tencerova, B., A. Zahradnikova, J. Gaburjakova, and M. Gaburjakova. 2012. Luminal Ca2+ controls activation of the cardiac ryanodine receptor by ATP. *The Journal of general physiology*. 140:93-108.

Terentyev, D., S.E. Cala, T.D. Houle, S. Viatchenko-Karpinski, I. Gyorke, R. Terentyeva, S.C. Williams, and S. Gyorke. 2005. Triadin overexpression stimulates excitation-contraction coupling and increases predisposition to cellular arrhythmia in cardiac myocytes. *Circulation research*. 96:651-658.

Terentyev, D., I. Gyorke, A.E. Belevych, R. Terentyeva, A. Sridhar, Y. Nishijima, E.C. de Blanco, S. Khanna, C.K. Sen, A.J. Cardounel, C.A. Carnes, and S. Gyorke. 2008. Redox modification of ryanodine receptors contributes to sarcoplasmic reticulum Ca2+ leak in chronic heart failure. *Circ Res*. 103:1466-1472.

Terentyev, D., S. Viatchenko-Karpinski, I. Gyorke, P. Volpe, S.C. Williams, and S. Gyorke. 2003. Calsequestrin determines the functional size and stability of cardiac intracellular calcium stores: Mechanism for hereditary arrhythmia. *Proc Natl Acad Sci U S A*. 100:11759-11764.

Thomas, N.L., C.H. George, and F.A. Lai. 2004. Functional heterogeneity of ryanodine receptor mutations associated with sudden cardiac death. *Cardiovasc Res*. 64:52-60.

Tidball, J.G., and M.J. Spencer. 2000. Calpains and muscular dystrophies. *Int J Biochem Cell B*. 32:1-5.

Timerman, A.P., E. Ogunbumni, E. Freund, G. Wiederrecht, A.R. Marks, and S. Fleischer. 1993. The calcium release channel of sarcoplasmic reticulum is modulated by FK-506-binding protein. Dissociation and reconstitution of FKBP-12 to the calcium release channel of skeletal muscle sarcoplasmic reticulum. *J Biol Chem*. 268:22992-22999.

Timerman, A.P., H. Onoue, H.B. Xin, S. Barg, J. Copello, G. Wiederrecht, and S. Fleischer. 1996. Selective binding of FKBP12.6 by the cardiac ryanodine receptor. *J Biol Chem*. 271:20385-20391.

Tinker, A., and A.J. Williams. 1992. Divalent cation conduction in the ryanodine receptor channel of sheep cardiac muscle sarcoplasmic reticulum. *The Journal of general physiology*. 100:479-493.

Tong, G.L., H.Y. Wu, T.H. Smith, and D.W. Henry. 1979. Adriamycin analogues. 3. Synthesis of N-alkylated anthracyclines with enhanced efficacy and reduced cardiotoxicity. *J Med Chem*. 22:912-918.

Towbin, H., T. Staehelin, and J. Gordon. 1992a. Electrophoretic transfer of proteins from polyacrylamide gels to nitrocellulose sheets: procedure and some applications. 1979. *Biotechnology*. 24:145-149.

Towbin, H., T. Staehelin, and J. Gordon. 1992b. Electrophoretic transfer of proteins from polyacrylamide gels to nitrocellulose sheets: procedure and some applications. 1979. *Biotechnology*. 24:145-149.

Toyoshima, C., M. Nakasako, H. Nomura, and H. Ogawa. 2000. Crystal structure of the calcium pump of sarcoplasmic reticulum at 2.6 A resolution. *Nature*. 405:647-655.

Trachtenberg, B.H., D.C. Landy, V.I. Franco, J.M. Henkel, E.J. Pearson, T.L. Miller, and S.E. Lipshultz. 2011. Anthracycline-associated cardiotoxicity in survivors of childhood cancer. *Pediatr Cardiol*. 32:342-353.

Trafford, A.W., M.E. Diaz, G.C. Sibbring, and D.A. Eisner. 2000. Modulation of CICR has no maintained effect on systolic Ca2+: simultaneous measurements of

sarcoplasmic reticulum and sarcolemmal Ca2+ fluxes in rat ventricular myocytes. *J Physiol-London.* 522:259-270.

Tu, Q., P. Velez, M. Cortes-Gutierrez, and M. Fill. 1994. Surface charge potentiates conduction through the cardiac ryanodine receptor channel. *The Journal of general physiology.* 103:853-867.

Tunwell, R.E., C. Wickenden, B.M. Bertrand, V.I. Shevchenko, M.B. Walsh, P.D. Allen, and F.A. Lai. 1996. The human cardiac muscle ryanodine receptor-calcium release channel: identification, primary structure and topological analysis. *Biochem J.* 318 (Pt 2):477-487.

van Dalen, E.C., H.J.H. van der Pal, W.E.M. Kok, H.N. Caron, and L.C.M. Kremer. 2006. Clinical heart failure in a cohort of children treated with anthracyclines: A long-term follow-up study. *Eur J Cancer.* 42:3191-3198.

van Norren, K., A. van Helvoort, J. Argilés, S. van Tuijl, K. Arts, M. Gorselink, A. Laviano, D. Kegler, H. Haagsman, and E. van der Beek. 2009. Direct effects of doxorubicin on skeletal muscle contribute to fatigue. *Br J Cancer.* 100:311-314.

Vasquez-Vivar, J., P. Martasek, N. Hogg, B.S. Masters, K.A. Pritchard, Jr., and B. Kalyanaraman. 1997. Endothelial nitric oxide synthase-dependent superoxide generation from adriamycin. *Biochemistry-Us.* 36:11293-11297.

Venetucci, L.A., A.W. Trafford, and D.A. Eisner. 2007. Increasing ryanodine receptor open probability alone does not produce arrhythmogenic calcium waves - Threshold sarcoplasmic reticulum calcium content is required. *Circ Res.* 100:105-111.

Vest, J.A., X.H. Wehrens, S.R. Reiken, S.E. Lehnart, D. Dobrev, P. Chandra, P. Danilo, U. Ravens, M.R. Rosen, and A.R. Marks. 2005. Defective cardiac ryanodine receptor regulation during atrial fibrillation. *Circulation.* 111:2025-2032.

Vinten-Johansen, J., Z.-Q. Zhao, and R.A. Guyton. 2004. Cardiac Surgery in the Adult. *In* L.H. Cohn, editor. HIghwire Press.

Wall, S.B., J.Y. Oh, A.R. Diers, and A. Landar. 2012. Oxidative modification of proteins: an emerging mechanism of cell signaling. *Front Physiol.* 3:369.

Wang, G.X., Y.X. Wang, X.B. Zhou, and M. Korth. 2001. Effects of doxorubicinol on excitation--contraction coupling in guinea pig ventricular myocytes. *Eur J Pharmacol.* 423:99-107.

Wang, R., W. Chen, S. Cai, J. Zhang, J. Bolstad, T. Wagenknecht, Z. Liu, and S.R. Chen. 2007. Localization of an NH(2)-terminal disease-causing mutation hot spot to the "clamp" region in the three-dimensional structure of the cardiac ryanodine receptor. *J Biol Chem.* 282:17785-17793.

Wang, S., W.R. Trumble, H. Liao, C.R. Wesson, A.K. Dunker, and C.H. Kang. 1998a. Crystal structure of calsequestrin from rabbit skeletal muscle sarcoplasmic reticulum. *Nature structural biology*. 5:476-483.

Wang, S., W.R. Trumble, H. Liao, C.R. Wesson, A.K. Dunker, and C.H. Kang. 1998b. Crystal structure of calsequestrin from rabbit skeletal muscle sarcoplasmic reticulum. *Nat Struct Biol*. 5:476-483.

Wegener, A.D., H.K. Simmerman, J.P. Lindemann, and L.R. Jones. 1989. Phospholamban phosphorylation in intact ventricles. Phosphorylation of serine 16 and threonine 17 in response to beta-adrenergic stimulation. *J Biol Chem*. 264:11468-11474.

Wehrens, X.H., S.E. Lehnart, F. Huang, J.A. Vest, S.R. Reiken, P.J. Mohler, J. Sun, S. Guatimosim, L.S. Song, N. Rosemblit, J.M. D'Armiento, C. Napolitano, M. Memmi, S.G. Priori, W.J. Lederer, and A.R. Marks. 2003. FKBP12.6 deficiency and defective calcium release channel (ryanodine receptor) function linked to exercise-induced sudden cardiac death. *Cell*. 113:829-840.

Wehrens, X.H., S.E. Lehnart, S. Reiken, R. van der Nagel, R. Morales, J. Sun, Z. Cheng, S.X. Deng, L.J. de Windt, D.W. Landry, and A.R. Marks. 2005. Enhancing calstabin binding to ryanodine receptors improves cardiac and skeletal muscle function in heart failure. *Proc Natl Acad Sci U S A*. 102:9607-9612.

Wehrens, X.H., S.E. Lehnart, S.R. Reiken, S.X. Deng, J.A. Vest, D. Cervantes, J. Coromilas, D.W. Landry, and A.R. Marks. 2004. Protection from cardiac arrhythmia through ryanodine receptor-stabilizing protein calstabin2. *Science*. 304:292-296.

Wei, L., E.M. Gallant, A.F. Dulhunty, and N.A. Beard. 2009a. Junctin and triadin each activate skeletal ryanodine receptors but junctin alone mediates functional interactions with calsequestrin. *Int J Biochem Cell Biol*. 41:2214-2224.

Wei, L., A.D. Hanna, N.A. Beard, and A.F. Dulhunty. 2009b. Unique isoform-specifc properties of calsequestrin in the heart and skeletal muscle. *Cell Calcium*.

Wei, L., M. Varsanyi, A.F. Dulhunty, and N.A. Beard. 2006. The conformation of calsequestrin determines its ability to regulate skeletal ryanodine receptors. *Biophys J*. 91:1288-1301.

Weinstein, D.M., M.J. Mihm, and J.A. Bauer. 2000. Cardiac peroxynitrite formation and left ventricular dysfunction following doxorubicin treatment in mice. *J Pharmacol Exp Ther*. 294:396-401.

Xia, R., T. Stangler, and J.J. Abramson. 2000. Skeletal muscle ryanodine receptor is a redox sensor with a well defined redox potential that is sensitive to channel modulators. *J Biol Chem*. 275:36556-36561.

Xiao, B., C. Sutherland, M.P. Walsh, and S.R. Chen. 2004. Protein kinase A phosphorylation at serine-2808 of the cardiac Ca2+-release channel (ryanodine receptor) does not dissociate 12.6-kDa FK506-binding protein (FKBP12.6). *Circ Res.* 94:487-495.

Xiao, R.P., H.H. Valdivia, K. Bogdanov, C. Valdivia, E.G. Lakatta, and H. Cheng. 1997. The immunophilin FK506-binding protein modulates Ca2+ release channel closure in rat heart. *J Physiol.* 500 (Pt 2):343-354.

Xie, Y., E. Grandi, J.L. Puglisi, D. Sato, and D.M. Bers. 2013. beta-adrenergic stimulation activates early afterdepolarizations transiently via kinetic mismatch of PKA targets. *J Mol Cell Cardiol.* 58:153-161.

Xin, H.B., T. Senbonmatsu, D.S. Cheng, Y.X. Wang, J.A. Copello, G.J. Ji, M.L. Collier, K.Y. Deng, L.H. Jeyakumar, M.A. Magnuson, T. Inagami, M.I. Kotlikoff, and S. Fleischer. 2002. Oestrogen protects FKBP12.6 null mice from cardiac hypertrophy. *Nature.* 416:334-338.

Xu, K.Y., J.L. Zweier, and L.C. Becker. 1997. Hydroxyl radical inhibits sarcoplasmic reticulum Ca(2+)-ATPase function by direct attack on the ATP binding site. *Circ Res.* 80:76-81.

Xu, L., J.P. Eu, G. Meissner, and J.S. Stamler. 1998. Activation of the cardiac calcium release channel (ryanodine receptor) by poly-S-nitrosylation. *Science.* 279:234-237.

Xu, L., A. Tripathy, D.A. Pasek, and G. Meissner. 1999. Ruthenium red modifies the cardiac and skeletal muscle Ca(2+) release channels (ryanodine receptors) by multiple mechanisms. *J Biol Chem.* 274:32680-32691.

Yamada, S., and N. Ikemoto. 1978. Distinction of Thiols Involved in Specific Reaction Steps of Purified Ca2+ Atpase of Sarcoplasmic-Reticulum. *Biophys J.* 21:A47-A47.

Yano, M., S. Okuda, T. Oda, T. Tokuhisa, H. Tateishi, M. Mochizuki, T. Noma, M. Doi, S. Kobayashi, T. Yamamoto, Y. Ikeda, T. Ohkusa, N. Ikemoto, and M. Matsuzaki. 2005a. Correction of defective interdomain interaction within ryanodine receptor by antioxidant is a new therapeutic strategy against heart failure. *Circulation.* 112:3633-3643.

Yano, M., K. Ono, T. Ohkusa, M. Suetsugu, M. Kohno, T. Hisaoka, S. Kobayashi, Y. Hisamatsu, T. Yamamoto, N. Noguchi, S. Takasawa, H. Okamoto, and M. Matsuzaki. 2000. Altered stoichiometry of FKBP12.6 versus ryanodine receptor as a cause of abnormal Ca(2+) leak through ryanodine receptor in heart failure. *Circulation.* 102:2131-2136.

Yano, M., T. Yamamoto, N. Ikemoto, and M. Matsuzaki. 2005b. Abnormal ryanodine receptor function in heart failure. *Pharmacol Ther.* 107:377-391.

Yoshida, H., and Y. Tonomura. 1976. Chemical modification of the Ca2+-dependent ATPase of sarcoplasmic reticulum from skeletal muscle. I. Binding of N-ethylmaleimide to sarcoplasmic reticulum: evidence for sulfhydryl groups in the active site of ATPase and for conformational changes induced by adenosine tri- and diphosphate. *J Biochem.* 79:649-654.

Yuan, Q., G.C. Fan, M. Dong, B. Altschafl, A. Diwan, X. Ren, H.H. Hahn, W. Zhao, J.R. Waggoner, L.R. Jones, W.K. Jones, D.M. Bers, G.W. Dorn, 2nd, H.S. Wang, H.H. Valdivia, G. Chu, and E.G. Kranias. 2007. Sarcoplasmic reticulum calcium overloading in junctin deficiency enhances cardiac contractility but increases ventricular automaticity. *Circulation.* 115:300-309.

Yuchi, Z., and F. Van Petegem. 2011. Common allosteric mechanisms between ryanodine and inositol-1,4,5-trisphosphate receptors. *Channels (Austin).* 5:120-123.

Zable, A.C., T.G. Favero, and J.J. Abramson. 1997. Glutathione modulates ryanodine receptor from skeletal muscle sarcoplasmic reticulum. Evidence for redox regulation of the Ca2+ release mechanism. *J Biol Chem.* 272:7069-7077.

Zaidi, N.F., C.F. Lagenaur, J.J. Abramson, I. Pessah, and G. Salama. 1989. Reactive disulfides trigger Ca2+ release from sarcoplasmic reticulum via an oxidation reaction. *J Biol Chem.* 264:21725-21736.

Zhang, J., Z. Liu, H. Masumiya, R. Wang, D. Jiang, F. Li, T. Wagenknecht, and S.R. Chen. 2003. Three-dimensional localization of divergent region 3 of the ryanodine receptor to the clamp-shaped structures adjacent to the FKBP binding sites. *J Biol Chem.* 278:14211-14218.

Zhang, L., J. Kelley, G. Schmeisser, Y.M. Kobayashi, and L.R. Jones. 1997. Complex formation between junctin, triadin, calsequestrin, and the ryanodine receptor. Proteins of the cardiac junctional sarcoplasmic reticulum membrane. *J Biol Chem.* 272:23389-23397.

Zima, A.V., and L.A. Blatter. 2006. Redox regulation of cardiac calcium channels and transporters. *Cardiovasc Res.* 71:310-321.

Zima, A.V., E. Bovo, D.M. Bers, and L.A. Blatter. 2010. Ca(2)+ spark-dependent and -independent sarcoplasmic reticulum Ca(2)+ leak in normal and failing rabbit ventricular myocytes. *J Physiol.* 588:4743-4757.

Zissimopoulos, S., and F.A. Lai. 2005. Interaction of FKBP12.6 with the cardiac ryanodine receptor C-terminal domain. *J Biol Chem.* 280:5475-5485.

Zissimopoulos, S., and F.A. Lai. 2006. Redox regulation of the ryanodine receptor/calcium release channel. *Biochem Soc Trans.* 34:919-921.

Zissimopoulos, S., S. Seifan, C. Maxwell, A.J. Williams, and F.A. Lai. 2012. Disparities in the association of the ryanodine receptor and the FK506-binding proteins in mammalian heart. *J Cell Sci.* 125:1759-1769.

Zorzato, F., G. Salviati, T. Facchinetti, and P. Volpe. 1985. Doxorubicin induces calcium release from terminal cisternae of skeletal muscle. A study on isolated sarcoplasmic reticulum and chemically skinned fibers. *J Biol Chem.* 260:7349-7355.

Zuhlke, R.D., G.S. Pitt, K. Deisseroth, R.W. Tsien, and H. Reuter. 1999. Calmodulin supports both inactivation and facilitation of L-type calcium channels. *Nature.* 399:159-162.